Modeling hydrological processes in a semi-arid mountainous catchment at the regional scale

Dissertation

zur Erlangung des Doktorgrades (Dr. rer. nat.)

der

Mathematisch-Naturwissenschaftlichen Fakultät

der

Rheinischen Friedrich-Wilhelms-Universität Bonn

vorgelegt von

Henning Georg Kaspar Busche

aus

Göttingen

Bonn, August 2012

Angefertigt mit Genehmigung der Mathematisch-Naturwissenschaftlichen Fakultät der Rheinischen Friedrich-Wilhelms-Universität Bonn

1. Gutachter: Prof. Dr. Bernd Diekkrüger

2. Gutachter: Prof. Dr. Barbara Reichert

Datum der Promotion: 14. Dezember 2012

Erscheinungsjahr: 2013

Acknowledgements

This work is conducted in the framework of the IMPETUS project, and was supported by the Federal German Ministry of Education and Research (BMBF) under grant No. 01 LW 06001B and by the Ministry of Innovation, Science, Research and Technology (MIWFT) of the federal state of Northrhine-Westfalia under grant No. 313-21200200.

This work was only possible because a lot of people supported me. First and foremost I express my gratitude to my supervisor Prof. Dr. B. Diekkrüger, who was always there for me to discuss the problems I encountered and assisted me in solving them. I would like to thank my co-supervisor Prof. Dr. B. Reichert for her interest in my work and for the good cooperation.

I would like to thank all my colleagues who provided data for this work, namely A. Klose, S. Klose, K. Born, M. Finckh, C. Heidecke, P. Fritzsche, H. Paeth, A. Roth, O. Schulz, G. Baumann, U. Kutsch and M. Petros.

I am grateful to our Moroccan partners who provided me with data and personal experience in the field, namely the Service Eau Ouarzazate, Direction Générale de l'Hydraulique and the Office Regionale de Mise en Valeur Agricole Ouarzazate. I further thank the IMPETUS head office for the support and cooperativeness.

During my stays in Morocco a lot of people contributed not only to my work, but also to making those stays precious memories. Representative of those I would like to mention J. Ait El Hadj, Abdallah, Abdessalam, Nour-Eddine, Fatima and Redouan; M. El Sabbar and A. Benbouziane; M. Ait Richa and L. Ait Ahmed.

Especially G. Steup, S. Klose, A. Klose and O. Schulz spend a lot of time on discussing my work. Their thoughts and objections improved this work substantially as well as their support and approval helped me finishing it! Furthermore A. Klose, G. Steup and S. Giertz spent a lot of time proof-reading this work, thank you for that!

I will not forget the time spent with the colleagues from the IMPETUS project and the Hydrology Research Group. Special thanks to A. Bossa, K. Born, P. Fritzsche, S. Giertz, C. Heidecke, C. Hiepe, B. Höllermann, H. Hölzel, A. Kebede Kassa, A. Klose, S. Klose, U. Kutsch, C. Rademacher-Schulz, A. Roth, O. Schulz, J. Sorge, G. Steup and A. Waidosch for the good time we had in Bonn and Morocco. I already miss that working atmosphere!

Last but not least, I express my deep gratitude to my parents, Günter and Elke Busche, and Flavia Castro for their patience and their unconditional support.

Abstract

In the Upper Drâa Valley (14,988 km²) on the southern slopes of the Moroccan High Atlas Mountains, a highly variable precipitation and large evaporation losses cause major water availability problems. The combined effect of projected increase in water demand and temperature and a decrease in precipitation poses a major challenge for water managers in the region. To assess the actual state of the hydrological system (1978-2007), but also the impacts of future changes (2000-2049) a conceptual model, adapted to the characteristics of a semi-arid mountainous environment, has been applied. A spatially explicit altitudinal representation, an oasis-irrigation routine, a second linear storage aquifer and a reservoir management module have been implemented in the SWAT model, extending it to SWAT-MAROC (SWAT-Mountainous and Arid Regions Oriented Concept).

During the validation period the model performs well on a monthly timescale at the basin outlet (CME: 0.89) and satisfactorily at the two main tributaries Oued Ouarzazate (CME: 0.69) and Oued Dades (CME: 0.62). Furthermore model results are in line with validation data obtained from groundwater, snow and irrigation studies. Nevertheless the model exhibits flaws in representing water availability in groundwater-fed oases and soil water dynamics.

Considering the variable sources of uncertainty, especially in arid and mountainous regions, a wide-ranging uncertainty assessment scheme, quantifying and comparing uncertainties with a signal-to-noise ratio, has been developed and applied. Uncertainties from the hydrological model are highest, followed by divergent signals from climate change ensembles, while the downscaling method has only minor effects on model results.

It has been shown that climate change effects for the period 2000-2029 are subject to considerable uncertainties and no clear trends could be identified. For the period 2020-2049 the following developments are “likely” according to the IPCC terminology. Despite a decrease in precipitation (-11%) and especially snowfall (-31%), irrigation water availability in the surface water dependent oasis remains high enough (-5%) to sustain agriculture to the current extent. In contrast, water availability at the reservoir is decreasing disproportionately high (-17%). Therefore the potential for riparian conflicts between the Upper Drâa and the Middle Drâa might augment. A further finding is that the reservoir Mansour-Eddahbi is likely to become inoperable due to siltation in the period 2030-2042, dependent on the assumed pathways of socio-economic development.

Zusammenfassung

Das südmarokkanische Obere Drâatal (14.988 km²), an der Südabdachung des Hohen Atlas gelegen, ist durch eine hohe Niederschlagsvariabilität und starke Verdunstung gekennzeichnet, die bereits heute die Wasserverfügbarkeit beeinträchtigen. Die kombinierte Wirkung des prognostizierten Anstiegs der Wassernachfrage und der Temperatur sowie des Rückgangs der Niederschläge stellen eine große Herausforderung für das Wassermanagement dar. Um den aktuellen Zustand des hydrologischen Systems (1978-2007) zu beurteilen und die Auswirkungen von zukünftigen Veränderungen (2000-2049) zu erfassen, wird ein konzeptionelles Modell verwendet, das an die Eigenschaften der semi-ariden gebirgigen Region angepasst wurde. Dafür ist das SWAT-Modell um eine räumlich explizite Darstellung der Höhengliederung, ein Oasen-Bewässerungs-Modul, einen zweiten Grundwasserleiter und ein Stausee-Management-Modul zu SWAT-MAROC (SWAT – Mountainous and Arid Regions Oriented Concept) erweitert worden.

Während der Validierungsphase erzielte das Modell auf monatlicher Zeitskala am Gebietsauslass (CME: 0,89) sowie an den beiden wichtigsten Zuflüssen Oued Ouarzazate (CME: 0,69) und Oued Dades (CME: 0,62) gute bis zufriedenstellende Ergebnisse. Darüber hinaus stehen Modellergebnisse im Einklang mit Validierungsdaten aus Grundwasser-, Schnee- und Bewässerungsstudien. Mängel zeigt das Modell bei der Simulation des Wasserdargebots in grundwassergespeisten Oasen und der Bodenwasserdynamik.

Um diversen Unsicherheitsquellen, vor allem in ariden und bergigen Regionen, gerecht zu werden, sind im Rahmen eines umfassenden Bewertungsschemas quantifizierbare Unsicherheiten mit einer Signal-to-Noise-Ratio verglichen worden. Unsicherheiten aus dem hydrologischen Modell sind am höchsten, gefolgt von divergenten Signalen aus den Klimaensembles, während das Downscaling nur geringe Auswirkungen auf die Trends zeigt.

Die Auswirkungen des Klimawandels für den Zeitraum 2000-2029 sind mit erheblichen Unsicherheiten behaftet und weisen keine eindeutigen Trends auf. Für den Zeitraum 2020-2049 sind folgende Entwicklungen „wahrscheinlich“ (entsprechend der IPCC-Terminologie). Trotz einer Abnahme des Niederschlag (-11%) und insbesondere des Schneefalls (-31%), ist die Bewässerungswasserverfügbarkeit an den Oberflächenwasseroasen hoch genug (-5%), um die Landwirtschaft im aktuellen Umfang aufrecht zu erhalten. Die Wasserverfügbarkeit am Stausee hingegen nimmt überproportional ab (-17%). Deshalb könnte das Konfliktpotenzial zwischen den Wassernutzern des Oberen und Mittleren Drâa zunehmen. Weitere Implikationen für das mittlere Drâatal beinhaltet der Sedimenteintrag in den Stausee Mansour-Eddahbi. Dieser wird voraussichtlich in der Periode 2030-2042 versandet sein.

Résumé

Dans la Haute Vallée du Drâa (14.988 km²) située au sud du Haut Atlas Marocain, une précipitation très variable et de grandes pertes d'évaporation causent des problèmes de disponibilité en eau. L'effet combiné projeté de l'augmentation de la demande en eau et la température et une diminution des précipitations prévues constitue un défi majeur pour les gestionnaires de l'eau dans la région. Pour évaluer l'état actuel du système hydrologique (1978-2007), mais aussi les impacts des changements futurs (2000-2049), un modèle conceptuel adapté aux caractéristiques d'un milieu semi-aride montagneuse, a été appliquée. Une représentation spatialement explicite d'altitude, une routine d'irrigation des oasis, un second aquifère et un module de gestion des réservoirs ont été mis en œuvre dans le modèle SWAT, en l'étendant à SWAT – MAROC (SWAT – Mountainous and Arid Regions Oriented Concept).

Dans la période de validation, le modèle simule qualitativement bien sur une échelle de temps mensuelle à l'exutoire du bassin (CME: 0,89) ainsi que dans les deux principaux affluents Oued Ouarzazate (CME: 0,69) et Oued Dades (CME: 0,62). En outre les résultats du modèle sont en accord avec les données de validation obtenues à partir d'études des eaux souterraines, de neige et d'irrigation. Néanmoins, le modèle présente des faiblesses dans la représentation de la disponibilité en eau dans les oasis alimentées par les eaux souterraines et de la dynamique de l'eau du sol.

Les sources variables d'incertitude, en particulier dans les régions arides et montagneuses, ont été comparées dans le cadre d'un système d'évaluation des incertitudes, avec un Signal-to-Noise-Ratio. Les incertitudes de la modélisation hydrologique sont les plus élevées suivies par des signaux divergents des ensembles de changement climatique, tandis que la méthode de downscaling n'a que des effets mineurs sur les résultats du modèle.

Il a été démontré, que les effets du changement climatique pour la période 2000-2029 sont sujets à des incertitudes considérables et aucune tendance claire n'a pu être identifiée. Pour la période 2020-2049 les développements suivants sont "probables" selon la terminologie du GIEC. Malgré une diminution des précipitations (-11%) et surtout des chutes de neige (-31%), la disponibilité en eau d'irrigation dans les oasis dépendant des eaux de surface reste assez élevée (-5%) pour soutenir l'agriculture dans la mesure actuelle. En contraste, la disponibilité en eau, au niveau du réservoir est anormalement en forte baisse (-17%). Par conséquent, le potentiel de conflits entre les riverains du Haute et Moyen Drâa pourrait augmenter. Une autre constatation est que le réservoir Mansour-Eddahbi est susceptible de devenir inutilisable en raison de l'envasement dans la période 2030-2042.

Content

Acknowledgements ..... **I**
Abstract ..... **III**
Zusammenfassung ..... **IV**
Résumé ..... **V**
Content ..... **VI**
Figures ..... **VIII**
Tables ..... **XI**
Abbreviations ..... **XIII**
1. Motivation and Context **1**
1.1 Research Context: The IMPETUS Project 2
1.2 Aim of Study 2
2. Hydrological Processes in Semi-Arid Mountainous Regions **5**
2.1 Precipitation 7
2.2 Snow 8
2.3 Infiltration and Surface Runoff 9
2.4 Evapotranspiration 11
2.5 Groundwater 12
2.6 Stream-Aquifer Interactions 14
3. Hydrology of the Upper Drâa Catchment **17**
3.1 Socio-economic Setting 18
3.2 Climate 21
3.3 Geology 26
3.4 Geomorphology 30
3.5 Pedology 32
3.6 Land Use and Land Cover 35
3.7 Hydrography 39
3.8 Perceptual Model: Hydrological Processes in the Upper Drâa Catchment 42
4. Modeling Process **45**
4.1 Theory of the Modeling Process 47
4.1.1 Model Structure 48
4.1.2 Model Sensitivity 52
4.1.3 Model Calibration 52
4.1.4 Model Validation 53
4.1.5 Scenario Development 54
4.1.6 Model Uncertainty 58
4.2 Metrics to evaluate Model Performance and Model Results 62
4.2.1 Goodness-of-fit Tests 62
4.2.2 Analysis of Scenario Effects 65
4.2.3 Drought Indicators 67
4.3 Modeling Hydrological Processes in Arid Mountainous Regions – State of the Art 69
5. Hydrological Model of the Upper Drâa Catchment **75**
5.1 The Conceptual Model 76
5.1.1 Basic Model: SWAT 77
5.1.2 Adaptations: SWAT-MAROC 81
5.2 Model Sensitivity 96
5.3 Model Data 98
5.3.1 Digital Elevation Model 98
5.3.2 Soil Data 100
5.3.3 Land Cover 104
5.3.4 Spatial Discretization 111
5.3.5 Geology 112

5.3.6 Climate Data ... 118
5.3.7 Discharge Data ... 121
5.3.8 Reservoir Water Balance Module ... 124
5.4 Model Calibration ... 126
5.4.1 Hydrological Model ... 126
5.4.2 Reservoir Water Balance ... 130
5.5 Model Validation ... 131
5.5.1 Discharge to Reservoir ... 131
5.5.2 Stream Gauges ... 132
5.5.3 Snow ... 134
5.5.4 Irrigation ... 135
5.5.5 Groundwater ... 136
5.5.6 Soil Water ... 137
5.5.7 Reservoir Water Balance ... 138
5.6 Scenario Setup ... 139
5.6.1 Climate Scenarios ... 139
5.6.2 Socio-economic Scenarios ... 143
5.6.3 DPSIR - Impact Indicators ... 145
5.7 Uncertainty Analysis ... 148
5.7.1 Uncertainty in Baseline Scenario ... 148
5.7.2 Uncertainty in Future Scenarios ... 150
5.8 Interim Summary: Model and Scenario Development ... 152
6. Discussion of Model Results and Uncertainties ... 153
6.1 Baseline Scenario Results and Uncertainties ... 154
6.1.1 Water Balance ... 154
6.1.2 Irrigation of Upstream Oases ... 159
6.1.3 Reservoir Inflow ... 162
6.2 Scenario Results and Uncertainties ... 165
6.2.1 Water Balance ... 165
6.2.2 Irrigation of Upstream Oases ... 170
6.2.3 Reservoir Inflow ... 173
6.2.4 Rangelands ... 175
6.2.5 Scenario impacts on the Middle Drâa Valley ... 177
7. Conclusions and Outlook ... 179
Bibliography ... 184
Appendix A ... 204
Appendix B ... 222

Figures

Figure 2-1: Different hydrological processes occurring on top soils containing rock fragments in various positions (Poesen & Lavee 1994) 10
Figure 3-1: Urban centers and irrigated perimeters in the Upper Drâa catchment. 19
Figure 3-2: Climate diagram of Ouarzazate 1961-1990 (GHCN 2; Peterson & Vose 1997) 21
Figure 3-3: Precipitation anomalies (Sep-Aug, 1900-2006) for the Atlantic region (ATL), Mediterranean region (MED) and the region south of the Atlas (SOA) (Fink et al. 2008) 22
Figure 3-4: Climate monitoring network in the Drâa region (modified after Schulz 2008). IMPETUS stations cover the period 2001-2009, SE Ouarzazate delivers long term records. Mean monthly precipitation and temperature is depicted for the IMPETUS stations only, to portray the gradient of aridity within the catchment. For measured variables and record lengths see 25
Figure 3-5: Geological setting of the Upper Drâa valley (El Harfi et al. 2001) 28
Figure 3-6: Geomorphologic processes along a fictional transect through the Upper Drâa catchment 31
Figure 3-7: Major WRB soil types in the Drâa catchment (Klose 2009) 32
Figure 3-8: Soils along a fictional transect through the Upper Drâa catchment 34
Figure 3-9: Natural potential vegetation in the High Atlas (Rauh 1952) 35
Figure 3-10: Degradation processes in Northern African highlands (Le Houérou 2001) 36
Figure 3-11: Land use and pasture types along a fictional transect through the Upper Drâa catchment 38
Figure 3-12: Annual and mean monthly (in dry and wet years) discharge of different tributaries to the reservoir Mansour-Eddahbi in the period 1982-1996 (Busche 2008b). See Figure 3-13 for locations of the gauges. Appendix 2 provides the delineated subcatchments and information on streamflow data availability for the gauges. 39
Figure 3-13: Hydrological setting of the Upper Drâa catchment (Busche 2008a) 41
Figure 3-14: Perceptual model of hydrological processes in the Upper Drâa catchment 42
Figure 4-1: Modeling process (modified after Beven 2003) 47
Figure 4-2: Main categories of hydrological models and their areal discretization schemes (modified after Becker & Serban 1990) 48
Figure 4-3: Hydrological processes at a range of characteristic space-time scales (Blöschl & Sivapalan 1995) 49
Figure 4-4: Data availability, model complexity and model performance (Grayson & Blöschl 2001) 50
Figure 4-5: Multi model averages and ranges for surface warming according to the IPCC-scenarios (Solomon et al. 2007). The grey bars at the right indicate the best estimate and the “likely” range of outcomes for each scenario (see section 4.2.2.2 for an explanation of likely). 56
Figure 4-6: The DPSIR-framework with regard to water availability 58
Figure 4-7: Increasing uncertainty in model chains (modified after Jones 2000) 60
Figure 5-1: Annual Rainfall-Runoff Relationship for the Upper Drâa catchment (15.000 km²). (Measured data: SE Ouarzazate) 76
Figure 5-2: Simplified schematic diagram of the water movement as simulated by SWAT (modified after Arnold et al. 1993) 77
Figure 5-3: Simplified schematic diagram of the water movement as simulated by SWAT-MAROC (new modules in grey) 81
Figure 5-4: Relative change in irrigated area for selected crops in the provinces Zagora and Ouarzazate (100% = Area of 1997/98) (Heidecke 2009) compared to the standardized reservoir inflow as a proxy measureof drought conditions (data: SE Ouarzazate) 85

Figure 5-5: The oasis effect on temperature, relative humidity and wind velocity (based on IMPETUS climate data) 86
Figure 5-6: Reference evapotranspiration (ETo), crop evapotranspiration under standard conditions (ETc) and inclusion of loss terms due to irrigation efficiency (modified after Allen et al. 1989b) 88
Figure 5-7: Hydrogeological setting of the Assif-Ait-Ahmed catchment (Cappy 2006) 89
Figure 5-8: Discharge into the reservoir Mansour-Eddahbi (logarithmic scale). Dominant baseflow components are exponentially approximated (Data: SE Ouarzazate) . 91
Figure 5-9: Scheme and equations of a baseflow system approximated by (a) one or (b) several linear reservoirs. 92
Figure 5-10: Aquifer conditions that can be represented by two linear storage reservoirs 92
Figure 5-11: Spatial model units of the Upper Drâa Catchment accounting for drainage system and elevation, prior to EHRU-discretization 99
Figure 5-12: Soil classification for SWAT-MAROC and naming scheme 102
Figure 5-13: Plant coverage in the Upper Drâa catchment. Median, error bars envelope the 2nd and 3rd quartile, i.e. the middle 50% of observations (Fritzsche 2011) 106
Figure 5-14: Quality of catchment representation using different sets of thresholds for EHRU classification 111
Figure 5-15: Aquifer types in the Upper Drâa valley (left side). Dominating aquifer type in simulation units (right side) 113
Figure 5-16: Daily flow recession measured at the reservoir Mansour-Eddahbi (15000 km²). Measured data provided SE Ouarzazate 114
Figure 5-17: Compilation of recession coefficients a) slow groundwater components for different lithologies in Germany (Schwarze 1999); b) French and Tunisian karstified regions (Brown et al. 1972); c) Upper cretaceous calcareous rock formations in Israel (Amit et al. 2002) 115
Figure 5-18: Precipitation gradients in the Upper Drâa catchment (2001-2007). (Data: IMPETUS and SE Ouarzazate). 119
Figure 5-19: Examples for low quality of discharge data compiled from different gauges: Replacement of the channel hampers low flow registration (photo a: Ait-Mouted gauge); Silted stilling well hampers flow registration after floods (photo b: Agouillal gauge); Hydrograph of the Ifre stream gauge (1.200 km²), with marked periods of questionable data. (data: SE Ouarzazate) 121
Figure 5-20: Sediment deposition in the reservoir Mansour-Eddahbi compared to an idealized profile (data: SE Ouarzazate) 124
Figure 5-21: Snow dynamics in the higher elevations of the Upper Drâa catchment 2001-2006. Measured: MODIS-based NDSI with courtesy of Oliver Schulz; Simulated: SWAT-MAROC 127
Figure 5-22: Monthly irrigation amounts for the Upper Drâa in 1995/96. (Measured data taken from DRPE 1998) 128
Figure 5-23: Simulated and measured annual discharge into the reservoir Mansour-Eddahbi (1978-2007) (14,988 km²). (Measured data: SE Ouarzazate) 129
Figure 5-24: Simulated and measured monthly discharge into the reservoir Mansour-Eddahbi (1978-2007) (14,988 km²). (Measured data: SE Ouarzazate) 129
Figure 5-25: Simulated and measured final annual stored volume and water release of the reservoir Mansour-Eddahbi (1973-2007) (14,988 km²). (Measured data: SE Ouarzazate) 130
Figure 5-26: Daily flow duration curve (smoothed by three day filter at the reservoir Mansour-Eddahbi (14,988 km²). Uncertainty range is twice the average daily irrigation. (Measured data: SE Ouarzazate) 131
Figure 5-27: Modeled monthly discharge compared to measured discharge for the stream gauges Ifre, Amane-n-Tini and Tamdroust, see Figure 3-13 for locations. (Measured data: SE Ouarzazate) 133

Figure 5-28: Proportion of snow to rain along the altitudinal gradient of the Upper Drâa catchment, snow measurements indicated by green bars. 135
Figure 5-29: Mean monthly soil water content [Vol%] derived from the model ARID at selected sites in the Upper Drâa Catchment: 12/2001-11/2003 (Weber 2004). 137
Figure 5-30: Soil water content modeled by SWAT-MAROC for two EHRUs 138
Figure 5-31: REMO-Bias variability in the Upper Drâa Catchment. modeled: 1970-2000, including range of 3 model realizations, measured: 1978-2007 141
Figure 5-32: 142
Figure 6-1: Mean annual water fluxes within the Upper Drâa catchment (1978-2007) 154
Figure 6-2: Limits of variation of water balance components due to parameter uncertainty; absolute (upper image), relative (lower image). Values are rounded. 155
Figure 6-3: Mean monthly precipitation and buffering effect of snow (1978-2007) in the Upper Drâa catchment (14,988 km²). 158
Figure 6-4: Mean monthly discharge components (1978-2007) in the Upper Drâa catchment (14,988 km²). 159
Figure 6-5: Annual flow duration curve including parameter uncertainty at the reservoir Mansour-Eddahbi (14,988 km²) indicating overlap between measured and simulated data (1978-2007). (Measured data: SE Ouarzazate) 162
Figure 6-6: Annual discharge including parameter uncertainty at the reservoir Mansour-Eddahbi (1978-2007) (14,988 km²). (Measured data: SE Ouarzazate) 163
Figure 6-7: Mean monthly discharge into the reservoir Mansour-Eddahbi (1978-2007) (14,988 km²). (Measured data: SE Ouarzazate) 164
Figure 6-8: Median changes in water balance components due climate change. The color indicates signal to noise ratio (SNR_m) for all considered sources of uncertainty; 2010s (top); 2030s (bottom) 166
Figure 6-9: Climate change effects on the mean monthly snowpack and –cover in different elevation zones of the Upper Drâa catchment in the Baseline and 2030s Scenario. 169
Figure 6-10: Mean monthly precipitation and buffering effect of snow in the Upper Drâa catchment (14,988 km²) for the 2030s scenario. 170
Figure 6-11: Fraction of years in which 70% of the irrigation demand of the Upper Drâa oases can be satisfied from surface water within the baseline and climate change scenarios. Bars represent median model results, error bars envelope the middle tercile of model results. 171
Figure 6-12: Mean monthly discharge at the surface water fed oases including all considered uncertainties during the scenario period 2030s 172
Figure 6-13: Annual flow duration curve including all considered uncertainties at the reservoir Mansour-Eddahbi (14,988 km²) during the scenario period 2030s ... 173
Figure 6-14: Mean monthly discharge to reservoir Mansour-Eddahbi in the scenario 2030s, considering a) all considered uncertainties (378 varieties); b) model uncertainty (21 varieties); c) downscaling uncertainty (3 varieties) and d) ensemble uncertainty (6 varieties) 174
Figure 6-15: Relative changes in annual upstream irrigation and reservoir inflow under climatic change; bubbles envelope eight deciles of model results parallel to the axes 177

Tables

Table 3-1: Aridity in the Drâa catchment (based on IMPETUS climate data (2001-2007), PET calculated after Penman-Monteith (Monteith 1965), Thresholds taken from (Kottek et al. 2006) [1] and (Middleton & Thomas 1992) [2]. For locations of the gauges see Figure 3-4. 23
Table 3-2: Summary of the geodynamic evolution of the Upper Drâa region (Michard et al. 2008); Time scale according to the International Commission on Stratigraphy (Walker & Geissman 2009) 26
Table 4-1: Likelihood defined as probability of a certain outcomes occurrence (Solomon et al. 2007). 67
Table 4-2: Drought conditions associated with SPI-Values (adapted from McKee et al. 1993) 68
Table 5-1: SWAT-routines and required parameters. Parameters are described in Appendix 3, values are determined in section 5.3. For details on the model routines see (Neitsch et al. 1999) 78
Table 5-2: Relative frequency of irrigation water sources in the Upper Drâa valley (Heidecke 2006) 84
Table 5-3: Parameters and ranges considered during the sensitivity analysis of the uncalibrated model (see Appendix 3 for details on parameters) 96
Table 5-4: Parameter sensitivities of the uncalibrated model. T- and p-values derived from Students t-Test. Abbreviations for further actions: MC: Manual calibration; AC: Autocalibration; UA: Uncertainty analysis 97
Table 5-5: Input data for the CORPT soil analysis (Klose 2008a) 102
Table 5-6: Thresholds for Hydrological Soil Group classification (Neitsch et al. 2004) 103
Table 5-7: Aggregation scheme for the LU/LC map used in SWAT-MAROC. Original data provided by Finckh (2008) 105
Table 5-8: Leaf area indices for the Upper Drâa catchment 107
Table 5-9: Runoff Curve Numbers Land Cover types in the research area (based on NRCS 1986) 108
Table 5-10: CropWat parameters for crops grown in the Upper Drâa catchment according to 1) Moroccan authorities (MTP 1998) and 2) CropWat Manual (Allen et al. 1989a) 110
Table 5-11: Irrigation efficiencies (Foster & Perry 2010) 110
Table 5-12: Selected thresholds for determination of EHRU s 111
Table 5-13: Spatial representation of different land covers in the EHRUs 112
Table 5-14: Baseflow recession coefficients in the Upper Drâa catchment 116
Table 5-15: Example hydraulic conductivity values for various river bed materials (Lane 1983) 116
Table 5-16: Parameters adapted during manual calibration (see Appendix 3 for details on parameters). 126
Table 5-17: Parameters adapted during autocalibration (see Appendix 3 for details on parameters). 128
Table 5-18: Uncertainty-considering Goodness-of-fit criteria for discharge for various stream gauges; green: good performance, yellow: acceptable performance, red: poor performance 134
Table 5-19: Irrigation requirement in the Upper Drâa valley 135
Table 5-20: Irrigation from surface water in the Upper Drâa catchment: Relative frequency of surface water irrigation (Heidecke 2006) and modeled covered irrigation demand 136
Table 5-21: Modeled soil water content of selected EHRUs, (Dec. 2001-Nov. 2003) 137
Table 5-22: Attributes and selected mean annual water balance components of the two EHRUs 138

Table 5-23: Temperature trend from REMO scenarios, for the period 1960-2000 compared to 2001-2049. Trend in rainfall indices (standard deviation units) from REMO scenarios, for the period 1960-2000 compared to 2001-2049.The range of uncertainty is given as the averaged deviation from the ensemble mean trend. Bold numbers indicate trends with error probabilities less than 1% for temperature and 10% for precipitation (Born et al. 2008). 140
Table 5-24: Temperature and precipitation trends from REMO scenarios, for the periods 2000-2029 and 2020-2049 compared to 1978-2007. 140
Table 5-25: Mean annual precipitation and variability in the Upper Drâa Catchment. modeled: 1970-2000, measured: 1978-2007 141
Table 5-26: Qualitative trend-matrix of socio-economic changes in the Upper Drâa Catchment ("+": increase of the considered variable; "0": no change of considered variable; "-": decrease of considered variable). The number of signs announces the intensity of change. 144
Table 5-27: Spatiotemporal extent of rangelands in the Upper Drâa Catchment (see section 3.6) 147
Table 5-28: Parameters and parameter ranges considered in the Uncertainty Analysis (see Appendix 3 for details on parameters). 149
Table 6-1: Effects of parameter changes on water balance components. Explained variability and magnitude of change (%); green: significant positive correlation; red: significant negative correlation (1% error probability: dark color, 5% error probability: light color) 157
Table 6-2: Annual coverage of irrigation demand by surface water in the Upper Drâa Catchment (15.000 km²) (1978-2007). Dry conditions (less than 70% of demand satisfied) are marked red, wet conditions (more than 70% of demand satisfied) are marked green. 160
Table 6-3: SNR_m-values for the scenarios 2010s and 2030s (green: $SNR_m>1$, sufficient suitability of model for scenario analysis; yellow: $0<SNR_m<1$, scenario effect larger than uncertainty; red: $SNR_m<0$, scenario effects not suitable to be assessed by model, thresholds are explained in detail in section 4.2.2.1) 165
Table 6-4: Likelihood and magnitude of changes in the hydrological cycle of the Upper Drâa Catchment in the 2030s scenario. The color indicates confidence in model result using the signal to noise ratio (SNR_m) for all considered sources of uncertainty: $SNR_m>1$ (green); $0<SNR_m<1$ (orange); $SNR_m<0$ (red) 167
Table 6-5: Future operation of the reservoir Mansour-Eddahbi as derived from the reservoir water balance model assuming the climate change scenario 2030s and different socio-economic scenarios. The middle tercile of 2030s discharge time series is used as boundary condition. [1)] In the baseline scenario the Water supply of Ouarzazate is only given for the year 2010, as drinking water has not been abstracted from the reservoir until 1998, therefore an average would be distorting. 175
Table 6-6: Precipitation changes in different rangeland domains within the Upper Drâa catchment under climate change conditions (median results): 3-monthly SPI compared to the Baseline scenario (green: drying below scenario median; red: drying above scenario median). Black rectangles indicate the respective grazing seasons. 176

Abbreviations

a	annum = year
ADCP	Acoustic Doppler Current Profiler
ATL	Atlantic region
BMBF	Bundesministerium für Bildung und Forschung German Federal Ministry of Education and Research
CIA	Central Intelligence Agency
CME	Coefficient of Model Efficiency
DEM	Digital Elevation Model
DIFGA	Differentielle Ganglinienanalyse Differential curves analysis
DPSIR	Driver-Pressure-State-Impact-Response
DREF	Direction nationale des eaux et forêts Moroccan Department of Water and Forests
DRPE	Direction de la Recherche et de la Planification de l'eau Moroccan Department of Water Research and Planning
EEA	European Environment Agency
EHRU	Elevation-Accounting HRU
ENSO	El Niño-Southern Oscillation
FAO	Food and Agriculture Organization
GCM	Global Circulation Model
GDP	Gross Domestic Product
GLOWA	Globaler Wandel des Wasserkreislaufes Global Change and the Hydrological Cycle
GLUE	Generalized Likelihood Uncertainty Estimation
GPS	Global Positioning System
GTOPO30	Global Topography 30 arc seconds
HRU	Hydrological Response Unit
IMPETUS	Integratives Management Projekt zum effizienten und tragfähigen Umgang mit Süßwasser in Westafrika An integrated approach to the efficient management of scarce water resources in Western Africa
IoA	Index of Agreement
IPCC	International Panel on Climate Change
LAI	Leaf Area Index
LU/LC	Land Use/ Land Cover
MAE	Mean Absolute Error
MED	Mediterranean region
MDG	Millennium Development Goal
Mm^3	Million cubic meters
mm	millimeter
MTP	Ministère des Travaux Publics Moroccan Ministry of Public Works
MYBP	Million years before Present
NDSI	Normalized Differentiated Snow Index
NAO	North Atlantic Oscillation
NRCS	US National Resource Conservation Service (former SCS)
ONEP	Organisation national d'eau potable National Drinking Water Organization
ORMVA	Organisation de Mise en Valeur Agricole Organization of Agricultural Development

ORMVAO	Organisation de Mise en Valeur Agricole Ouarzazate Organization of Agricultural Development Ouarzazate
ParaSol	Parameter Solution
PCP	Precipitation
PDSI	Palmer Drought Severity Index
PET	Potential Evapotranspiration
RAD	Radiation
RCM	Regional Climate Model
REMO	Regionalmodell Regional Model
RGPH	Recensement Général de la Population et de l'Habitat National Census Morocco
RH	Relative humidity
RMSE	Root Mean Square Error
SCS	Soil Conservation Service (now NRCS)
SD	Standard Deviation
SE	Service Eau Moroccan Water Service
SNR	Signal-to-Noise-Ratio
SNR_m	modified Signal-to-Noise-Ratio
SOA	Region south of the Atlas
SRES	Special Report on Emissions Scenarios
SPI	Standardized Precipitation Index
SRI	Standardized Runoff Index
SRTM	Shuttle Radar Topography Mission
SUFI2	Sequential Uncertainty Fitting Version 2
SWAT	Soil Water Assessment Tool
SWAT-CUP	SWAT - Calibration and Uncertainty Procedures
SWAT-MAROC	SWAT - Mountainous and Arid Region Oriented Concept
TMP	Temperature
UN	United Nations
UNEP	United Nations Environmental Program
WASA	Model of Water Availability in Semi-Arid Environments
WMO	World Meteorological Organization
WND	Wind speed
WRB	World Reference Base

Abbreviations and descriptions of model parameters are presented in Appendix 3

1. Motivation and Context

There is still enough water for all of us – but only so long as we keep it clean, use it more wisely, and share it fairly.

Ban Ki-Moon, 2008

In 2000 the United Nations member states agreed on the Millennium Development Goals (MDG, UN 2011). Two of the targets set were to halve the proportion of people who suffer from hunger and of those without sustainable access to safe drinking water by 2015. Especially in semi-arid areas sensible management of water resources is the key to both, as in these areas food production is dependent on irrigation to a vast extent.

Progress has been made to improve access to clean drinking water (coverage increased from 77% in 1990 to 87% in 2008) and it is very likely that the MDG drinking water target of 89% coverage will be met by 2015. Contrasting this success, the proportion of people in the developing world who are undernourished remained stable at 16% from 2000 through 2007 (UN 2011). Since these numbers are not yet accounting for the actual economic crisis and rising food prices, it is unlikely that the hunger-reduction target will be met, especially as demand is further rising. Although the global agriculture needs to provide more food for a growing and wealthier population in the future (Strzepek & Boehlert 2010), climatic conditions impend to become less favorable for agricultural activity in many regions of the world (Solomon et al. 2007). The combined effect of projected increase in water demand and decrease in water availability will be dramatic in northern Africa, where already today water resources are exploited beyond thresholds of sustainability (Strzepek & Boehlert 2010; Margat & Treyer 2004; Vörösmarty et al. 2000). These countries are facing an increased risk of political instability as consequence of climate change and decreasing water supply (Smith & Vivekananda 2007).

This is especially true for the Moroccan regions south of the High Atlas Mountains, upon the fringe of the Sahara, where the Drâa Valley is located. Here, a highly variable precipitation and large evaporation losses cause already today major water availability problems. Water was always a constraining factor for Morocco's economic development (Lybbert et al. 2009; Swearingen 1992). With renewable freshwater availability of only 917.5 m^3/person/year, Morocco is well below UNDP's scarcity criterion of 1,000 m^3/person/year (FAO 2011; Falkenmark 1989). Due to demographic and economic growth, 35 percent of the population might be below the absolute scarcity threshold of 500 m^3/person/year by 2020 (World Bank

2004). Despite prioritizing drinking water supply, water management has to focus on agricultural irrigation, as agriculture is by far the largest water consumer in Morocco (Ouassou et al. 2005). Morocco's irrigated cultures consume 87 % of available water resources, compared to 10 % domestic use and 3 % of resources used for industry (FAO 2011).

1.1 Research Context: The IMPETUS Project

In order to solve present and possible future problems with regard to freshwater supply, an interdisciplinary and holistic approach is clearly necessary. This was envisaged for the West African states of Morocco and Benin in the IMPETUS project (Integrated Approach to the Efficient Management of Scarce Water Resources in West Africa), a joint venture of the Universities of Cologne and Bonn, Germany (Speth et al. 2010). The work done within IMPETUS is part of a research program concerning the global water cycle (GLOWA), which is financed by the German Federal Ministry of Education and Research (BMBF). The aim of GLOWA is the development of strategies for sustainable future water management at a regional level while taking into account global environmental changes and socio-economic framework conditions. This work is incorporated into the IMPETUS subproject B2, which focused on soil water dynamics, surface runoff, groundwater recharge and soil degradation at the local and regional scale in the Upper and Middle Drâa catchment in Morocco.

Within the IMPETUS project the DPSIR-framework was adopted to provide indicators about future water availability to decision makers (Stanners & Bourdeau 1995). With regard to water availability the DPSIR framework can be considered as a causal chain starting with driving forces (climate, population, economic sectors, …) through pressures (climate and socio-economic changes) to states (water availability) and impacts on ecosystems and society, eventually leading to political or individual responses.

1.2 Aim of Study

A sustainable management of the resource can only be assured, if not only the actual state of the hydrological system is understood, but also the impacts of future climatic changes are assessed. Thus, it is imperative to understand the spatio-temporal variability of the hydrological cycle and to apply models, which are capable of quantifying the impacts of scenarios on the system.

Suitable model systems should consist of (simplified) physical rules, to perform robust scenario analyses (Beven 1989). Furthermore they should be spatially distributed to account for the different hydrological settings of the high- and lowlands, as mountain ranges are

known for relative high contributions to discharge especially in arid regions (Viviroli et al. 2003).

To provide assistance for water managers, the model should provide dependable estimates of surface water availability on a monthly to seasonal basis, also for future time periods. Estimates of other water balance components are desirable. Since conditions for modeling studies are in general unfavorable in arid regions (EI-Hames & Richards 1994), model results should not be presented without the associated uncertainties.

This work deals with the simulation of the water balance and in particular the surface water availability of the Upper Drâa Valley, South Morocco, during present and near future conditions (1978-2049). To do so the following approach has been chosen:

After a brief description of the hydrological processes within the region, the study area is presented in terms of climatology, geology, geomorphology, pedology, land use and land cover as well as hydrography. Based on this, as a prerequisite for successful model development, a perceptual model of the study areas hydrological behavior is developed. The following is a general notion on model structures; in particular the model SWAT2005 and the adjustments to the local, semi-arid and mountainous conditions of the Upper Drâa catchment are presented (SWAT-MAROC). Finally the model application for baseline and scenario conditions and the results together with the associated uncertainties are presented. Concluding, the following objectives have been derived:

- Objective 1: Identification of relevant hydrological processes in a semi-arid mountainous catchment
- Objective 2: Development of an appropriate model structure that accounts for the relevant processes and provides the required results
- Objective 3: Scenario Development
- Objective 4: Development of an uncertainty assessment scheme that allows quantifying and comparing uncertainties of different steps in the climate change impact assessment
- Objective 5: Quantitative assessment of the catchments water budget and the respective uncertainties on a monthly timescale
- Objective 6: Quantitative assessment of average climate change induced changes of the catchments water budget and the respective uncertainties on a monthly timescale

2. Hydrological Processes in Semi-Arid Mountainous Regions

Mountain regions represent, in practical terms, some of the blackest black boxes in the hydrological cycle.

Vit Klemeš, 1990

There are two easy ways to die in the desert: thirst and drowning

Craig Childs, 2001

The hydrological cycle is driven by the sun's energy, which evaporates water predominantly from the oceans. Water vapor is transported and returns to the earth's surface as precipitation (section 2.1), either rain or snow (section 2.2).

A part of the precipitation may be intercepted by vegetation and evaporate or reach the soil. If the soil is saturated or its infiltration capacity is exceeded, surface runoff is generated; otherwise the water infiltrates (section 2.3). In the soil, water can evaporate or be transpirated by plants (section 2.4). It can also distribute in the soil profile, leave the soil; either laterally, if horizontal conductivity suddenly decreases (interflow), or horizontally to become groundwater recharge (percolation, section 2.5 and 2.6). Surface runoff, interflow and baseflow can be aggregated to discharge, which eventually follows gravity to the ocean, closing the cycle. A very simple water balance is:

$$Precipitation = Runoff + Evaporation + Change\ in\ Storage$$

Precipitation equals the sum of discharge, evapotranspiration and change in storage. The latter is equal to zero if average values for long time periods are considered. In short periods changes in storage (soil moisture, groundwater, snow, etc.) can be immense. This equation can vary for different areas as well. The study area is dominated by the Central High Atlas mountain range on the one hand and a north-south gradient of increasing aridity on the other hand. As the introducing quotes suggest, the general conditions in these areas are unfavorable: Mountain areas are characterized by high spatial variability in terms of at least topography, soils and vegetation and highly variable weather conditions (Klemeš 1990). An even more pronounced spatial and temporal variability in terms of precipitation can be found in arid regions: Though drought conditions prevail, sudden flashfloods can occur after rare extreme events (Childs 2001). This simplifying outline will be followed by a deeper look at the dominant hydrological processes of the study area within this chapter.

A summary of arid regions hydrological features is presented by Wheater (2002):

- High levels of incoming solar radiation
- High diurnal and seasonal temperature variations
- Evaporation is prominent in the hydrological cycle
- Sporadic rainfall of high temporal and spatial variability
- Extreme variability of short-duration runoff events in ephemeral drainage systems
- High rates of infiltration losses in channel alluvium
- High sediment transport rates
- Relatively large groundwater and soil moisture storage changes
- Poorly developed soil profiles and low vegetation cover

A summary of mountainous regions hydrological features is presented by Gerrard (1990) and Weingartner et al. (2003):

- High radiation fluxes
- More frequent precipitation with greater total volume than in lowlands
- Susceptible to (convective) short-term heavy rainfall
- Discharge hydrographs influenced by snowmelt
- High available relief
- High sediment transport rates
- Poorly developed soil profiles and low vegetation cover

Since many of the presented studies focus either on drylands or on mountain areas, but only some on hydrological processes in arid mountain areas, it has to be kept in mind that some conditions are similar (high levels of solar radiation, high sediment transport rates, poorly developed soil profiles and low vegetation cover), whereas others superimpose (high evaporation rates in arid mountain ranges, perennial flow in arid basins[1]) or replace each other (increase of precipitation with altitude). Further general information can be found in Simmers (2003) for arid regions and Jong et al. (2005) for mountain areas. Several case studies from the Walnut Gulch experimental catchment (ephemeral) and the Reynolds Creek catchment (semi-arid, mountainous) are presented in Grayson & Blöschl (2001).

[1] In this study, the drainage area of a river is referred to as catchment, whereas the term basin is used in its geological sense, i.e. a low lying region that is being filled with sediments. The term basin is therefore used to differentiate between the more humid High Atlas (mountains) and the arid foreland (basin).

2.1 Precipitation

Precipitation is the process by which atmospheric water vapor condenses into liquid or solid water which then falls to the earth's surface under the action of gravity. This happens when air masses cool down to or below their dew point. Two precipitation-generating processes are most commonly acknowledged, advective uplift at orographic barriers or frontal boundaries, and convective uplift driven by thermal expansion of the air. Rainfall thus depends on synoptic-scale conditions (e.g. pressure systems) and several meso-scale effects (e.g. terrain orography, surface heating).

Precipitation is the only relevant water input to the mountain range. Contrasting, in the arid lowlands the water input by allochthonous rivers (from the mountains) gain importance. Considering variability, precipitation characteristics are similar in both regions. High temporal and spatial variability of precipitation has been recognized for arid catchments (e.g. Goodrich et al. 1995) as well as for mountainous catchments (e.g. Seyfried & Wilcox 1995).

According to Kalma & Franks (2003) precipitation in (semi-)arid regions is characterized by one or two short rainy seasons with short and unevenly scattered rain periods ($\leq$ 48 hours) that feature violent showers of high intensity and high spatial variability. Due to the orographic uplifting of air masses a distinct shift towards higher annual precipitation sums in the elevated regions can be observed in most mountainous regions of the world (Roe 2005). Besides the annual precipitation sum, more rain days occur, but no clear relationship could be identified for intensity or duration of rainfall in Saudi-Arabia and Yemen (Wheater 2002). However, a strong relationship was noted between the frequency of rain days and elevation. The author concludes that once rainfall occurs, its point properties are similar over the catchment, but occurrence is more likely at higher elevations. The precipitation regime undergoes a substantial change, when the air temperature is low and snow falls. In the elevated regions a substantial part of the annual precipitation can be in the form of snow, therefore further details on snow dynamics are presented in the following section 2.2.

Because of topographic complexity and elevation, precipitation varies markedly within the mountains and is difficult to measure. The measurement of precipitation is error-prone, losses due to wind turbulences at the gauge rim account for up to 10% (rain) or up to 50% (snow). Wetting of interior components of the gauge (2-10%), evaporation losses (0-4%) and splash-in/out effects (1-2%) are of secondary importance (McMillan et al. 2012; WMO 1994). When measuring snow, further difficulties arise due to wind drift.

The problem of measurement is exacerbated by a lack of precipitation gauges in mountains. The WMO (1994) provides guidelines for minimum densities of measurement networks. In

mountainous regions one gauge for 250 km² (≙ 60 gauges in the Upper Drâa catchment) is recommended. For arid regions one gauge for 10,000 km² (≙ 1.5 gauges in the Upper Drâa catchment) is suggested. Furthermore the necessity to cover vertical zonality by using gauges at high altitudes is stressed. Snow surveys should supplement the measurement network.

2.2 Snow

Snow constitutes a major water resource in many countries of the world, especially in mountain areas that sustain arid forelands. Shallow subsurface flow driven by snowmelt is the major source of streamflow in many high-elevation first-order catchments (Flerchinger et al. 1992). However, recharge mechanisms are strongly influenced by frozen soils. According to Bayard & Stähli (2005) the development of soil frost under snow cover is strongly dependent on the timing of snowfall and the thickness of the snow-cover. From the Alps the occurrence of snow packs on frozen as well as non-frozen soil is reported (Rößler 2011; Rößler & Löffler 2009).

As the soil frost layer develops, water in the soil pores freezes. This ice blocks the soil pores, producing a reduction in hydraulic conductivity and infiltration (Daniel & Staricka 2000; Male & Gray 1981). However, infiltration rates can vary depending on the initial soil water content before freezing. Infiltration is initially greater for dry frozen soil than for a wet frozen soil. Water has been found to infiltrate into a dry frozen soil; however, it may only reach a depths of not more than 30 cm before freezing (Granger et al. 1984). Though frozen soil can drastically diminish infiltration at the local scale, a considerable portion of melt water can usually infiltrate further downslope due to high spatial heterogeneity of soil frost.

When soils are thawing an increase in matrix flow can occur because of an increase in soil porosity. Volume expansion associated with the former ice formation will leave soil pores larger after the ice melts and thus, temporarily increase hydraulic conductivity of the soil (Daniel & Staricka 2000).

In mountainous catchments, snow distribution exhibits tremendous spatial heterogeneity, largely as a result of wind redistribution (Winstral & Marks 2002). Depending on the prevailing topography and vegetation distinct patterns of snow deposition, micro-climatic conditions and snowmelt can evolve (Marks et al. 2002). Consequently the melting of the seasonal snow cover can be highly variable in space and time as well.

Ice and snow sublimation is a naturally occurring process in which the solid ice changes state to become vapor without passing through the usual liquid stage (e.g. Law & Dijk 1994). This

process gains importance in high mountain areas and in arid regions, where low relative humidity, high radiation and high wind velocities can create high evaporative demand despite low temperatures. Despite its importance Lundberg (1993) diagnoses that evaporation, particularly from intercepted snow, is the least known term of the winter water balance. This is owed to difficulties in measuring evaporation (cf. following section 2.4) and high spatial heterogeneity of snow cover, as outlined above. Depending on the site and its climate characteristics, sublimation rates are likely to be in the magnitude of 0-1 mm/d (Jackson & Prowse 2009).

2.3 Infiltration and Surface Runoff

In the research area runoff is most commonly of the Hortonian type, i.e. precipitation intensity surpasses infiltration capacity (Horton 1933). The most important driving force for infiltration-excess runoff, the soil infiltration capacity, is characterized by high spatial variability related to soil properties such as structure, organic matter content and antecedent soil moisture (Arnau-Rosalén et al. 2008). In arid regions with weak soil structure and low organic carbon content surface crusts play an important role in reducing infiltration capacity (Casenave & Valentin 1992). Further factors affecting the infiltration capacity are faunal activity, vegetation cover and surface roughness. The high rock content of the barely developed soils in the catchment has tremendous impact on most of the aforementioned physical and hydrological properties of the soils (Brakensiek & Rawls 1994). While total bulk density increases with rock content the fine materials density decreases with increasing rock content. Poesen & Lavee (1994) expect maximum total density for rock contents ranging from 40-50%. Further implications for saturated conductivity and soil water content are given by Brakensiek & Rawls (1994): Assuming zero conductivity and water content for rocks, both parameter values decline with increasing rock content. Pedotransfer functions, established to estimate hydrological properties for soils based on soil texture, have been adapted by the authors accordingly. Nevertheless saturated conductivity in the field is often higher than estimates based on pedotransfer functions suggest. From arid brush lands in Spain infiltration rates of 30 mm/h have been reported in silty and clayey soils with high rock content, very likely to be caused by macropores of biogenic origin and seasonal effects (Archer et al. 2002; Cerdà 1996).

To what extent and in which direction rock content affects infiltration is widely discussed in the literature. Poesen & Lavee (1994) provide an overview. Main influences on infiltration and runoff-generation, are presented in Figure 2-1. Rock fragments covering the soil surface

have an ambivalent effect on the infiltration rate and the generation of overland flow. On the one hand, rocks prevent direct infiltration of water into the soil and eventually might produce rock flow resulting in an increase of overland flow. On the other hand, rock fragments cause an increase of infiltration rates by protecting the soil surface against raindrop impacts, preventing sealing and crusting. Field observations show that clay soils with medium to high coarse fragment contents are less compacted, have a more favorable structure and provide better physical condition for tree growth than similar soils containing small amounts of coarse fragments (Magier & Ravina 1983). Whether the total infiltration is increased or decreased by rock fragments depends on various factors, e.g. position and size of rock fragments (Yair & Lavee 1976; Brakensiek & Rawls 1994).

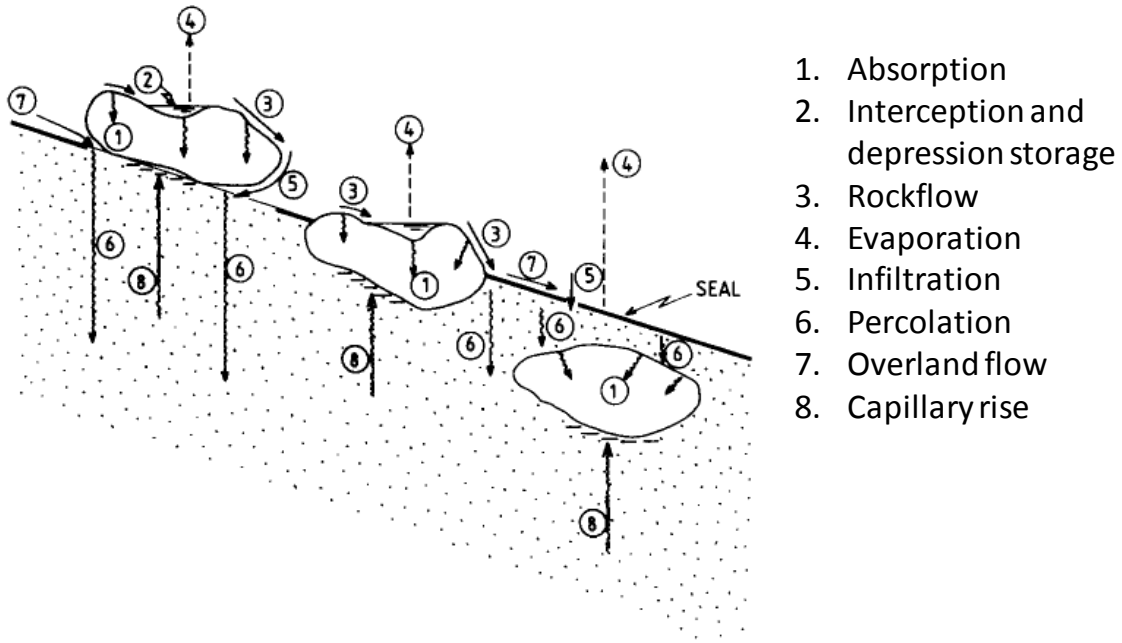

Figure 2-1: Different hydrological processes occurring on top soils containing rock fragments in various positions (Poesen & Lavee 1994)

Concluding, the extent of surface runoff generation is mainly dependent on the in-situ substratum:

- Thick unconsolidated sediment of fluvial/aeolian origin, favoring infiltration
- Debris-mantled slopes, favoring runoff

But not only the generation of overland flow is affected by the soils rock content. Stone covers influence also the velocity of surface runoff. In the Walnut Gulch catchment, surface runoff amount and velocity were measured on grassland and brushland (Abrahams et al. 1994). The latter featured high topsoil skeleton contents, as low vegetative cover provided little protection against sheet erosion. The experiments revealed that overland flow has higher

volume and velocity on brushland. The authors identified decreased infiltration capacity and decreased surface roughness as the main driving forces.

The role of antecedent soil moisture condition is ambivalent. The antecedent soil moisture condition plays a minor role for infiltration after high intensity, low frequency storms that are typical for arid regions (Castillo et al. 2003). On the other hand the authors state that the antecedent soil water content is an important factor controlling runoff during medium and low intensity storms. Hence the sensitivity of the runoff response to soil moisture depends on the predominant runoff mechanisms. When infiltration excess overland flow is predominant, as in the study area, the runoff response is more uniform and does not depend on initial soil moisture. Therefore water holding capacity and soil depth can be considered less important for the infiltration process.

2.4 Evapotranspiration

In dry environments, atmospheric water demand exceeds precipitation most of the year, causing characteristic hydrological stress that has an effect on most of the processes in the catchment, e.g. distribution of soil moisture and plant patterns (Wilcox 2002; Breshears & Barnes 1999). In these regions evapotranspiration is the catchments largest output flux at seasonal and yearly time scales, but it can be considered negligible on the event scale. Thus, in general evapotranspiration is rather limited by supply than by demand.

Plenty of methods exist to estimate actual evapotranspiration (e.g. sap-flow, soil water budget, eddy covariance, Bowen ratio, catchment water balance and models (Wilson et al. 2001; Kite & Droogers 2000)). Since most of these methods are either restricted to the local scale or difficult to conduct with scarce data, it is hard to determine evapotranspiration on a catchment scale. Therefore, evapotranspiration is perhaps one of the least well known hydrological processes for researchers that deal with catchment scale hydrology (Maneta et al. 2008). Especially in modeling studies, evapotranspiration is frequently used as closure term during calibration, i.e. imperfect boundary conditions (e.g. precipitation) or calibration data (e.g. discharge) lead to a distortion of modeled evapotranspiration.

A number of approaches to calculate evapotranspiration from climate data exist (e.g. Allen et al. 1989a; Hargreaves & Samani 1985; Priestley & Taylor 1972). Though potential evapotranspiration estimates vary considerably dependent on the approach chosen, Weiß & Menzel (2008) conclude that for the calculation of streamflow, the processes involved in the derivation of actual evapotranspiration from potential evapotranspiration are more relevant than the absolute value of the potential evapotranspiration itself.

Flerchinger & Cooley (2000) derived an evapotranspiration rate of 90% for the semi-arid mountainous Reynolds Creek catchment from Bowen ratio measurements. Due to little coverage degrees evaporation from soil is the dominant process in the brush-steppes.
Nevertheless, highly specialized plants can take up water from depths up to 50 m, depths of 15 m are likely to be reached by a variety of adapted species (de Vries & Simmers 2002; Haase et al. 1996).

2.5 Groundwater

Groundwater is the most reliable water resource in arid regions, as it stored widely protected against evapotranspiration losses and less variable in time compared to surface water. In these regions much of the groundwater abstracted from storage today was recharged during wetter conditions in the past (Alley et al. 2002), or is replenished from wadi streamflow originating from adjacent mountain ranges (Wilson & Guan 2004; Wheater & Al-Weshah 2002).
Groundwater recharge has been defined as "the entry into the saturated zone of water made available at the water-table surface, together with the associated flow away from the water table within the saturated zone" (Freeze & Cherry 1979). Groundwater recharge occurs to some extent in even the most arid regions (de Vries & Simmers 2002). Three different recharge mechanisms are commonly distinguished (Lerner et al. 1990):

- Direct recharge, originating from water that percolates vertically from the soil
- Indirect recharge, percolating through the beds of water courses
- Localized recharge, an intermediate form resulting from water concentration at the surface in absence of well-defined river beds.

Various techniques are used to quantify recharge (i.e. direct measurement, water-balance methods, Darcian approaches, tracer techniques, and empirical methods (Scanlon et al. 2006; Lerner et al. 1990). The water-table fluctuation method is a widely used technique; it requires knowledge of specific yield and changes in water levels over time. It is based on the assertion that rises in groundwater level in an unconfined aquifer are caused by recharge water arriving at the water table (Healy & Cook 2002). The resolution of regional water-balance studies in (semi-)arid areas is often too low to quantify the limited recharge component with sufficient precision (de Vries & Simmers 2002). Recharge, when estimated as a residual in water balance models, may be in error by an order of magnitude (Gee & Hillel 1988). This has serious implications for conducting modeling studies. As lined out for the evaporation component in the previous section 2.4, the groundwater recharge component of hydrological

models is seldom validated due to lack of data and groundwater recharge is frequently used as closure term during calibration.

A global synthesis of findings from 140 recharge studies in semiarid and arid regions concludes that 0.2 to 35 mm/year, representing 0.1–5% of long-term average annual precipitation, are groundwater recharge (Scanlon et al. 2006). However, locally these rates can vary to a large extent, due to different recharge mechanisms.

As aridity increases, direct recharge is likely to become less important than localized and indirect recharge (de Vries & Simmers 2002). This is due to little infiltration (see section 2.3), large depths to the groundwater tables and high evaporation rates. Conditions for direct groundwater recharge are more favorable in the mountains. Precipitation is higher than in the basin, with a significant fraction of snow (see section 2.1). Furthermore, potential evapotranspiration is lower due to lower temperatures and a larger surface albedo of snow covered areas. Besides the more favorable climatic boundary conditions mountains have thin soils that can store less water, reducing the amount potentially lost to evaporation. Fast flow along bedrock fractures or karstic conduits that underlie the thin soil may also limit water loss to evaporation.

The two principal mechanisms of indirect or localized recharge under (semi-)arid conditions are lateral affluxes from adjacent mountain systems and channel recharge (see following section 2.6). In recent literature the nomenclature of lateral affluxes is widely discussed. The terms *mountain front recharge* (Wilson & Guan 2004), formerly referred to as colluvial recharge, describes percolation in sedimentary fans or generally along the boundary of the mountain system, whereas *mountain block recharge* is referred to as water percolating into the mountain bedrock inside the mountains, reaching the basin via long deep flow paths. Both types are aggregated in the term mountain system recharge (e.g. Wahi et al. 2008). Thus it seems noteworthy that lateral affluxes should not be considered constant. They are rather a product of hydrological processes in the mountain system. This fact gains importance if model domains are restricted to basin floors (e.g. in groundwater models).

The question if, and to what extent, groundwater can evaporate is widely discussed, so called revaporation and/or transpiration of deep rooting plants have been reported to be an important part of the regional water balance in many semi-arid regions of the world. Inter-daily variations of streamflow in the River Limnatis (Cyprus) were reported to be caused by transpiration of water by trees in the river valley and direct evaporation from the water table of the alluvial aquifer (Boronina et al. 2005). Extrapolated to the whole catchment they account for evapotranspiration losses of 8 mm/year. In modeling studies revaporation rates of

1-22 mm/year have been derived for different model domains within the Nile Valley (Abdalla 2008). The importance of evaporation from groundwater has also been stressed by Christmann & Sonntag (1987) based on isotope analyses in Egypt. The previous authors assume extinction depths of evaporation of more than 20 m. Coudrain-Ribstein et al. (1998) derived an inverse power function by reviewing reported evaporation rates from phreatic aquifers in (semi-)arid regions. This empiric relationship depends on only on the depth to water table. Given a water table depth of 5 m revaporation rates of 2-16 mm/year can be concluded; from a 10 m deep water table up to 5 mm can evaporate per year.

2.6 Stream-Aquifer Interactions

Groundwater and surface water are not isolated components of the hydrological system, but interact in various ways (Sophocleous 2002). The terms indirect and localized recharge have been introduced in the last section 2.5. While groundwater usually contributes to streamflow in humid areas, the opposite occurs frequently in arid areas: surface water sustains disconnected alluvial aquifers. Therefore, in mountain regions with arid forelands, stream-aquifer interactions need to be studied carefully, as they may vary drastically between mountains and basin. Three different conditions of streams are generally acknowledged: *connected gaining stream*, *connected losing stream* and *disconnected stream* (Peterson & Wilson 1989). In the first case groundwater contributes to streamflow, whereas in the latter cases, surface water replenishes the aquifer underneath the streambed. This type of loss (also referred to as transmission loss) occurs in ephemeral or intermittent streams where the groundwater table is below the streambed for most of the year.

The importance of transmission losses (indirect recharge) as principal recharge mechanism in (semi-) arid regions has been stressed frequently (Scanlon et al. 2006; de Vries & Simmers 2002). Anyhow, the authors emphasize high spatial variability of hydrological properties of streambeds. Scanlon et al. (2006) report recharge rates beneath ephemeral streams and lakes to be highly variable, up to 720 m/year.

High variability of transmission losses is owed to the changing geometry and material of the streambed, but also to clogging effects. Fine sediments can be deposited during flood recession and eventually “clog” pore spaces in the uppermost layers of the channel bed when being suspended in percolating water. Clogging effects have been found to reduce riverbed infiltration during low flow events in many arid regions (Dunkerley 2008; Lange 2005). Anyhow, during floods the river stage may exceed clogged areas at the bottom of the riverbed. Furthermore adjacent plains may be flooded or the streambed can be reshaped,

breaking up clogging layers. Therefore infiltration rates are likely to be higher during flood events. The importance of floods for the recharge of alluvial aquifers has been denoted for ephemeral rivers in Namibia (Morin et al. 2009; Lange 2005; Lange et al. 2000).

As sediment dynamics and variable streambed conditions complicate the measurement and extrapolation of riverbed infiltration, many indirect recharge studies have to be considered site-specific; consequently the relationship between hydraulic properties of points and transmission losses of channel reaches demands further investigation (de Vries & Simmers 2002).

Practical approaches to estimate groundwater recharge in arid regions are either regional recharge studies (not accounting for different recharge mechanisms) or modeling studies, ranging from empirical (e.g. Lane 1983) to physically based (see section 4.3 for examples of physically based model studies).

Transmission losses gain importance, when water is routed over long distances, therefore they can be considered as a scale dependent phenomenon. Drainage-area to discharge plots reveal positive relationships up to drainage areas of ~1000 km², whereas the relationship turns negative for larger areas in Australia. On the one hand this is owed to small scale precipitation events; on the other hand the influence of transmission losses increases (Knighton & Nanson 2001). Goodrich et al. (1997) analyzed rainfall-runoff relationships for 29 subcatchments of Walnut Gulch and observed that the relationships become nonlinear when a threshold of 37-60 ha drainage area is exceeded. The authors also identified transmission losses and partial storm coverage as causes. Transmission loss rates for ephemeral flow are highly variable; values ranging from 8% to 75% have been compiled for a variety of arid rivers (Tooth 2000).

Besides the importance of transmission losses for aquifer recharge, the river bank may act as a temporary storage. Bank storage may considerably attenuate a flood wave, decrease peak discharge and extend the recession limb of the hydrograph. Furthermore it is noteworthy that bank-storage effects can cause interpretive difficulties in connection with hydrograph separation (Chen et al. 2006; Chen & Chen 2003).

3. Hydrology of the Upper Drâa Catchment

Come and rest in the shade, let me quench your thirst,
Shelter by my side from the sun's burning rays,
Comfort and solace will I provide, whatever the price!

Middle Atlas Berber poem (Peyron 1995)

The Upper Drâa Catchment (14,988 km²) is situated on the southern slopes of the High Atlas (5.5-8°W, 30-32°N, see Figure 3-1). It extends from the High Atlas summits (M'Goun: 4071 masl) to the catchments outlet at the reservoir Mansour-Eddahbi (1104 masl). Here the reservoirs main tributaries Dades and Ouarzazate converge to the name giving Drâa that drains in the Middle Drâa Valley.

In the Upper and Middle Drâa the traditional irrigated agriculture systems are not thinkable without the water provided by the High Atlas Mountains. Berber poetry refers to the life spending features of the mountain range and in everyday life the snow caps of the mountain peaks are used for water availability taxations by peasants. The interactions of different physiographic spheres and agricultural activities, characterized by discrepancies of high- and lowlands, are outlined in this chapter.

The first section 3.1 provides a brief overview of the socio-economic setting of Morocco and especially the Upper Drâa region, with a focus on water demand. The following physiographic setting of the research area is more detailed and represents the foundations of the perceptual model outlined in the final section 3.8.

3.1 Socio-economic Setting

Morocco is situated on the northwest coast of Africa (2-14°W, 27-36°N), bordering the Atlantic Ocean in the West, the Mediterranean Sea in the North, Algeria in the East, and West Sahara in the South. Morocco gained independence from France in 1956. From 1975 to 1979 Morocco occupied the former Spanish colony Western Sahara, considering it as a province since then, which has not been acknowledged by the United Nations[2].

Morocco had an estimated population of 31 million in 2007 (UN 2009)[3], with 44.3% living in rural areas. Annual population growth is 1.2% and decreasing. The population is predominantly Arab-Berber, an indigenous North African group that has adopted Arab customs. Therefore Arabic is the official language, but Berber dialects prevail in rural areas and French is the language of business, government and diplomacy and is taught in schools.

Most economic activity has centered in the fertile plains and major towns near the coast (Rabat, Casablanca and Agadir) whereas development elsewhere in Morocco has been slow, encouraging urban migration. The Gross Domestic Product (GDP) of Morocco and Western Sahara was estimated to be 73 billion $ (2316 $ per capita) in 2007. The GDPs annual growth rate is 2.2%. Primary Trade partners are the former colonial powers France and Spain; ties with the European Union have been further strengthened by an Association Agreement in 2000.

Economic output in 2008 was divided among sectors as follows: agriculture, 16%; industry, 20%; and services, 54% (CIA 2009). Even with a low contribution of agriculture to GDP, the sector still supports very large parts of the population, so that any reduction in output will have impacts on poverty and food security. Furthermore the sector is particularly sensitive to climate (Bates et al. 2008). This is portrayed by the proportion of the labor force occupied in the sectors: agriculture, 45%; industry, 20% and Services, 36% (CIA 2009). Especially in the marginalized rural areas, such as the Drâa valley, agriculture has the dominant share in economic activities. In the Drâa valley tourism is an important and growing driver of service-orientated economy.

The province of Ouarzazate has a population of 499,980 (RGPH 2004) and the annual population growth rate is 2.1% per year, being roughly twice as high than in northern

[2] Refers to Security Council Resolutions 2072(1963), 3292(1974), 3458(1975) and most recent 1754(2007). In this work Morocco is referred to as in the boundaries acknowledged by the United Nations and the Federal Republic of Germany. This does not imply any political statement of the author.

[3] If not stated differently, demographic, social and economic indicators are taken from the United Nations Data division: http://data.un.org (accessed: 03.12.2009)

Morocco (RGPH 2004; 1994). Due to high migration rates, lower fertility rates, longer birth intervals and a higher first marriage age the population growth is assumed to decline in the future (Rademacher 2010; Platt 2008a). Actual growth rates are 0.6% for rural and 4.1% for urban population in Ouarzazate, Skoura, Kelaat, Boulmalene and Taznakht (see Figure 3-1 for the locations of the cities). Hence the share of urban population is growing fast in the study area and with it the demand for drinking water. In 2010 a demand of 10 million cubic meters per year (Mm³/year) is assumed for the population in the urban centers. Additional 4.9 Mm³ are required by the rural population (DRPE 1998).

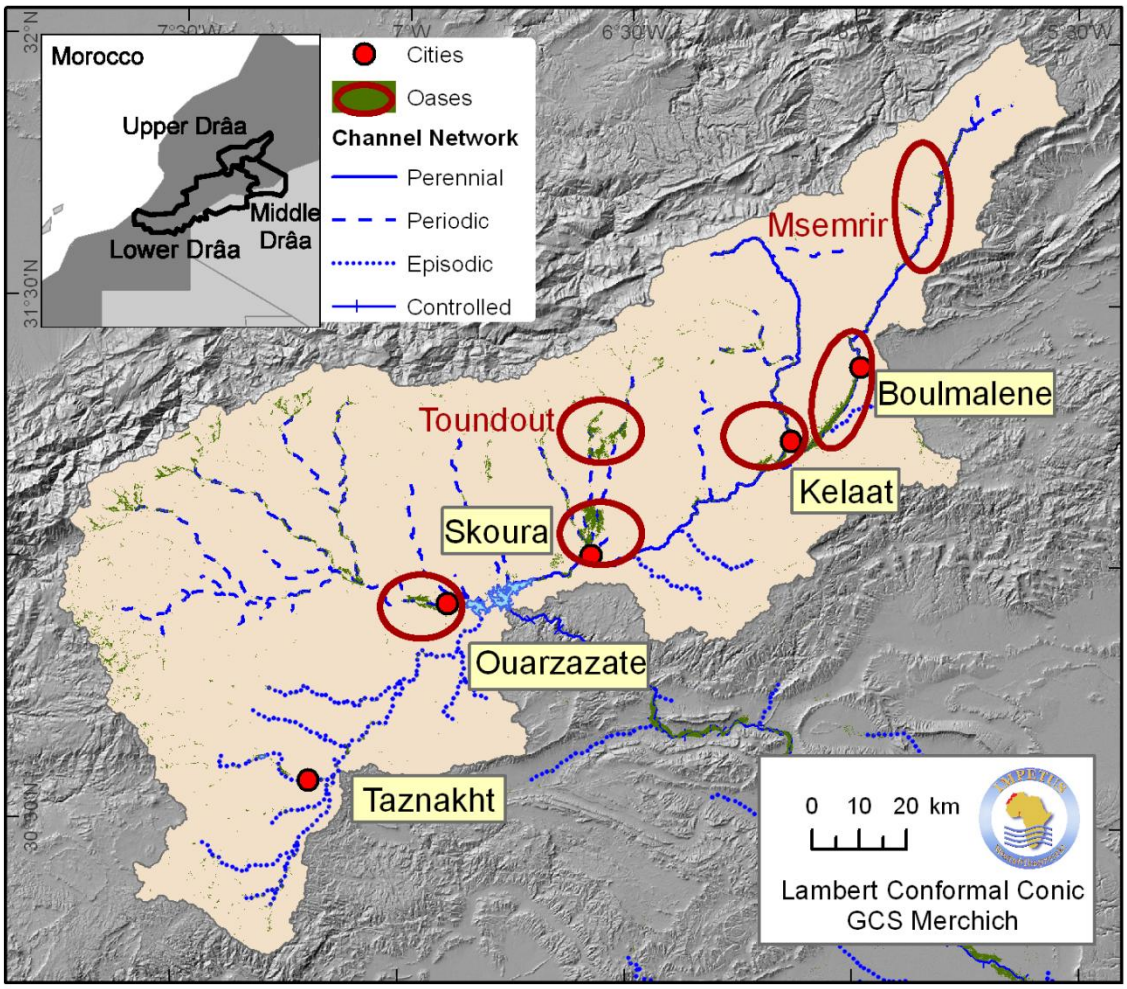

Figure 3-1: Urban centers and irrigated perimeters in the Upper Drâa catchment.

The primacy of drinking water to any other use is not questioned, but in terms of quantity the highest water demand in the Upper Drâa valley is that of irrigated agriculture. On average the oases of the Upper Drâa valley require 219 Mm³ of irrigation water per year (DREF Sud Ouest 2007). Irrigation water is taken from different sources: surface water and groundwater

(Heidecke 2006) as well as traditional groundwater harvesting systems, so-called *khettaras* (Faiz & Ruf 2010; Lightfoot 1996).

The irrigation water availability in the oases has always been variable. Traditionally agro-pastoralism, combining irrigation agriculture and transhumant livestock grazing, allows coping with low and variable precipitation (Freier et al. 2012; Barrow & Hicham 2000; Parish & Funnell 1999). First and foremost agro-pastoralism is by its definition a diversification of agricultural activities. By relying on husbandry and crop production, with consecutive diversification on different animals and crops, losses obtained in one field of activity can be balanced out or mitigated in another field of activity (hedging). Transhumant husbandry can mitigate drought impacts by (Hazell et al. 2001):

- carrying extra animals that can be liquidated during a drought, either for food or cash;
- maintaining reciprocal grazing arrangements with more distant communities for use in drought years, e. g. by truck transports of livestock (Baumann 2009) ;
- maintaining fodder reserves or purchasing supplementary fodder.

The crop producing sector mitigates drought impacts by (Heidecke 2009; Lybbert et al. 2009):

- stockpiling grain and fodder from good years;
- reducing land under cultivation;
- increasing groundwater irrigation;
- using fertilizers.

Furthermore labor migration, and nonagricultural labor diversification such as towards the touristic sector enables the rural population to make a living less dependent from agriculture and water availability (Rademacher 2010).

The institutional framework is actually being reshaped according to the 1995 Water Law (Ouassou et al. 2005). This law recognizes all water resources as public goods and foresees a unified water management agency for each basin, replacing parallel authorities established within the Water service (Service Eau, SE), Organization of Agricultural Development (Organisation regional de mise en valeur agricole, ORMVA) and National Drinking Water Organization (Organisation national d'eau potable, ONEP). Including participatory elements, the new structure is intended to be more decentralized and effective, once fully established. Furthermore the law envisages the implementation of water charges to rationalize water use (Doukkali 2005).

3.2 Climate

This section outlines the determinants of climate in the research area. The general weather situations dominating local climate vary considerably throughout Morocco, consequently a variety of climate zones can be identified (Kottek et al. 2006):

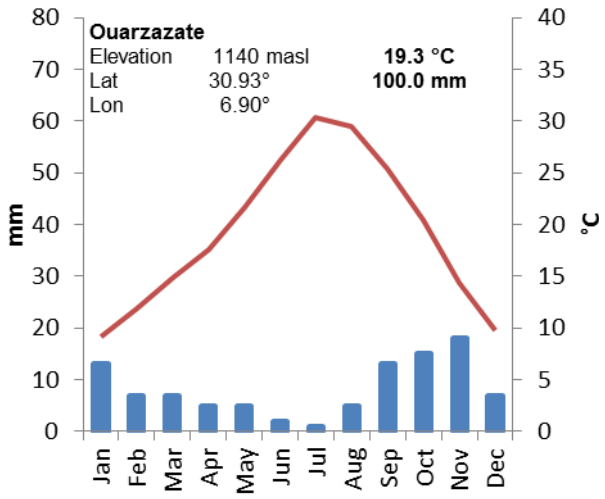

Figure 3-2: Climate diagram of Ouarzazate 1961-1990 (GHCN 2; Peterson & Vose 1997)

According to the Köppen-Geiger classification the Atlantic and the Mediterranean lowlands, as well as the northern slopes of the mountain ridges belong to the winter humid temperate zone, featuring hot summers (CSa). The southern slopes and the Sahara generally belong to the arid B climates. In the South hot desert climates (BWh, Figure 3-2) prevail, whereas in the elevated regions cold steppic climates dominate (BSk). Hot steppic climates (BSh) can be found in the southern coastal plains around Agadir, whereas cold desert climates (BWk) are hardly discovered.

The climatic zones exhibit strict margins along the mountain ridges, which are not only locally influencing climate through orographic effects (adiabatic rain, temperature), but also represent barriers for large scale air mass transport. Knippertz et al. (2003) distinguish three regions that are influenced by large scale circulation phenomena of different origin (see Figure 3-3). All three regions have in common that easterly winds, originating in continental Africa, and anticyclonal conditions bring rarely rain; whereas conditions that are associated with rain are different in those regions. The **Atlantic region** (ATL) is exposed towards westerly storms from the Atlantic Ocean; therefore precipitation in this region can be associated with westerly winds. The **Mediterranean region** (MED) is exposed towards the Mediterranean and rainfall is associated to northerly winds, especially northwesterly winter storms. In the **Region south of the Atlas** (SOA) southerly and southwesterly winds circumventing the High Atlas can be associated with rain, as they transport moisture from the Atlantic (Piecha 2009). Cyclones are related to rainfalls in the Atlantic region as well as in the region south of the Atlas. Cyclonal activity is increased in Morocco when the extratropical west wind zone is extended southwards. Therefore the pressure gradients over the Atlantic

Ocean are important determinants for precipitation in this region. An extension of the extratropical west wind zone comes along with the Azores high-pressure system moving southwards, i.e., a negative North Atlantic Oscillation index (NAO). This negative correlation (r^2=0.47) has been stressed by Lamb & Peppler (1987), and further enlightened by Knippertz et al. (2003). Influences of the El Niño/ Southern Oscillation (ENSO) are still subject to discussion (Nicholson & Kim 1997). Weak impacts such as an increased rainfall in autumns of El Niño years, followed by decreased rainfall in the following spring are assumed.

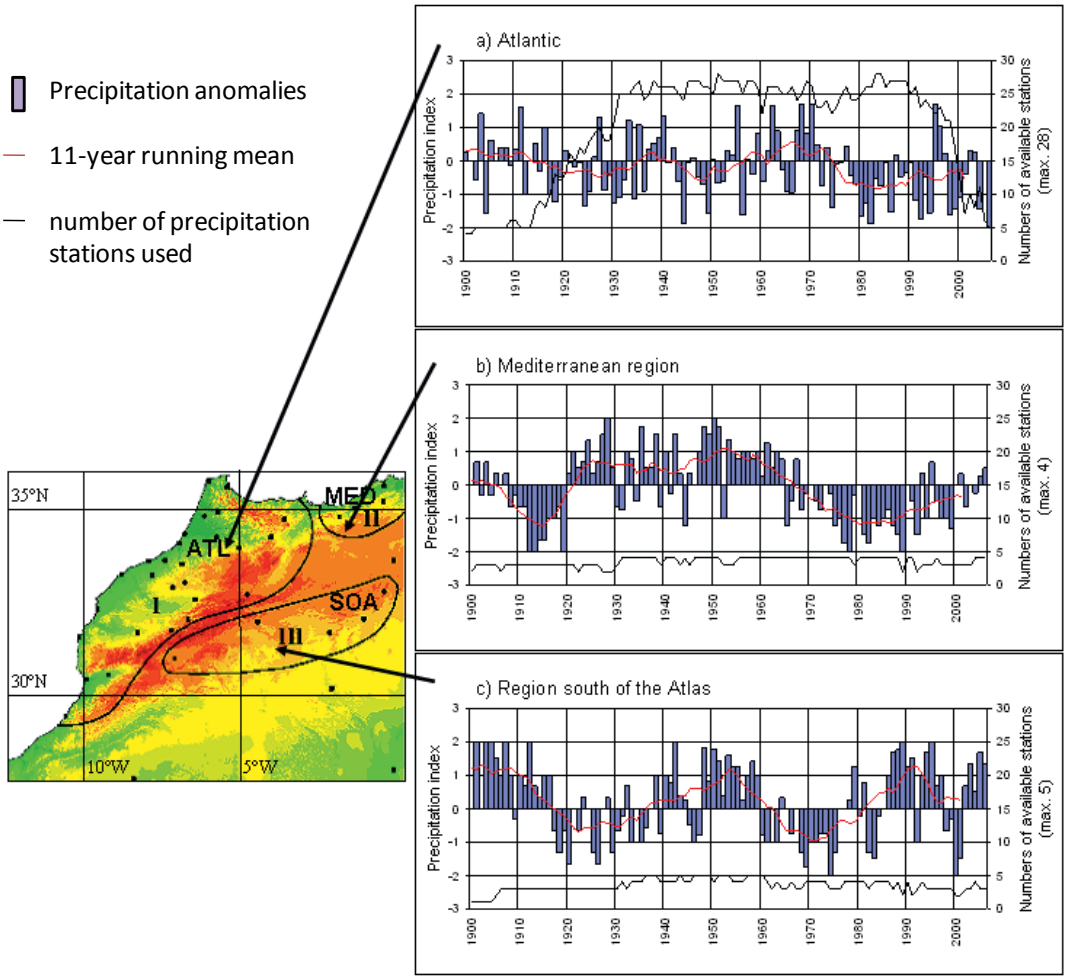

Figure 3-3: Precipitation anomalies (Sep-Aug, 1900-2006) for the Atlantic region (ATL), Mediterranean region (MED) and the region south of the Atlas (SOA) (Fink et al. 2008)

Beside these large-scale teleconnections, tropical-extratropical teleconnections are an important driver of extreme precipitation events in spring and autumn. Knippertz & Fink (2006) associated these events with a mid-tropospheric moisture transport from the tropics (tropical plume). The importance of different precipitation generating processes and associated circulating weather types explains the differences in time series of precipitation

anomalies for the three regions considered (see Figure 3-3). Decadal oscillations are out of phase for much of the last 30 years.

Due to data scarcity in the research area (5 synoptical stations in the SOA region, just the station of Ouarzazate (Figure 3-2) in the Upper Drâa valley) most regional assessments of long-term climate variability have a too low resolution to explicitly characterize the Drâa region. Anyhow, they allow a qualitative judgment on the importance of decadal variability and the impact of long-term trends such as climate change. Droughts as experienced from 1970 on are not unprecedented; a similar dry episode prevailed during most of the first half of the 20th century, but by mid-century, more normal conditions prevailed again (Nicholson 2001). These decadal "natural" oscillations are superimposed by trends of increasing temperature and decreasing rainfall in Northwestern Africa attributed to climate change (Hulme et al. 2001). Possible future developments of climate conditions in the research area will be outlined in section 5.6.1.

Table 3-1: Aridity in the Drâa catchment (based on IMPETUS climate data (2001-2007), PET calculated after Penman-Monteith (Monteith 1965), Thresholds taken from (Kottek et al. 2006) [1] and (Middleton & Thomas 1992) [2]. For locations of the gauges see Figure 3-4.

Climate station	Elevation [masl]	Latitude Decimal degree	Annual precipitation [mm/a]	Precipitation days (> 0 mm)	Average temperature [°C]	Annual PET [mm/a]	Aridity Köeppen-Geiger[1]	Aridity UNEP[2]
M'Goun	3850	31.51	613	101	0.0	1026	humid	Dry-sub-humid
Tichki	3260	31.54	443	100	4.9	1255	humid	semi-arid
Tizi-n-Tounza	2960	31.57	297	107	6.6	1331	humid	semi-arid
Imeskar	2250	31.50	291	72	12.8	1782	humid	arid
Taoujgalt	1870	31.39	210	58	14.2	1748	arid	arid
Bou Skour	1420	31.95	125	41	19.1	2325	arid	arid
Trab Labied	1380	31.17	139	32	19.0	2312	arid	arid

Having characterized the regional setting and long-term dynamics of climate in the research area, a closer look will be taken on local specifics. The IMPETUS project has set up a monitoring network in the Drâa catchment (Figure 3-4). An altitudinal/north-south gradient of aridity can be remarked throughout the catchment. Köppen and Geiger define dry climates as climates in which precipitation [cm] is lower than twice the average annual temperature [°C] (Kottek et al. 2006). A more recent definition of aridity can be taken from the UNEP (Middleton & Thomas 1992): According to the ratio of average annual rainfall to average annual potential evapotranspiration (PCP/PET), hyper-arid (PCP/PET <0.05), arid (PCP/PET

<0.2), semi-arid (PCP/PET <0.5) and dry sub-humid (PCP/PET <0.65) regions are distinguished. Accounting for these two definitions an increase in aridity with decreasing elevation/latitude can be stated (Table 3-1). Due to the dominant north-south orientation of the measuring network (see Figure 3-4) further gradients, such as increasing continentality, cannot be verified. Though its effects can be observed on larger scales (e.g. different vegetation types in western and eastern High Atlas; Rauh 1952), differences in continentality remain unresolved for the Upper Drâa.

Besides the absolute quantity of precipitation and the derived aridity indices, precipitation intensity varies considerably within the catchment. Fink & Knippertz (2003) report a severe rain event in April 2002 with intensities of more than 70 mm in 24 hours. Though intensities were higher in the Upper Drâa catchment than in the Middle Drâa catchment, no distinct altitudinal differentiation has been reported for the precipitation related to this tropical plume. Müller-Hohenstein & Popp (1990) report extreme rainfall events with intensities of about 50 mm per hour occur in the dry regions of southern Morocco.

In the lower and more arid parts of the catchment, such precipitation events represent the dominant rainfalls, whereas in the mountains a more balanced precipitation regime can be detected (see precipitation charts in Figure 3-4). The annual number of days with precipitation varies drastically within the catchment, from more than 100 days per year in the High Atlas to 17 in the Saharan Foreland (IMPETUS data: 2001-2007).

In the mountains an increasing fraction of precipitation falls in the form of snow. Snowfall occurs mainly from November to April but even in this period summit regions can become repeatedly devoid of snow cover. Snowfall is an important part of precipitation in altitudes of 2000-4000 m and becomes infrequent in lower altitudes. The presence of snow penitents at altitudes above 3000 m indicate that snow ablation is an important component of the high mountain areas water balance (Schulz & de Jong 2004). Modeling studies carried out with the Utah Energy Balance model (UEB; Tarboton et al. 1995) for the winter 2003/04 projected sublimation losses of 44% in the elevation of 3000 m. Decreasing importance of ablation in lower altitudes can be assumed (Schulz 2007; Schulz & de Jong 2004). Within the steppes evaporation is the dominant part of evapotranspiration. Weber (2004) reports annual transpiration/evaporation ratios of 0.5 to 15% for the Upper Drâa catchment. Due to increased water availability this ratio is different for the irrigated oases. In the Middle Drâa valley Gresens (2006) measured transpiration rates of 800 mm/year in date palm stands which is 9 times the annual precipitation.

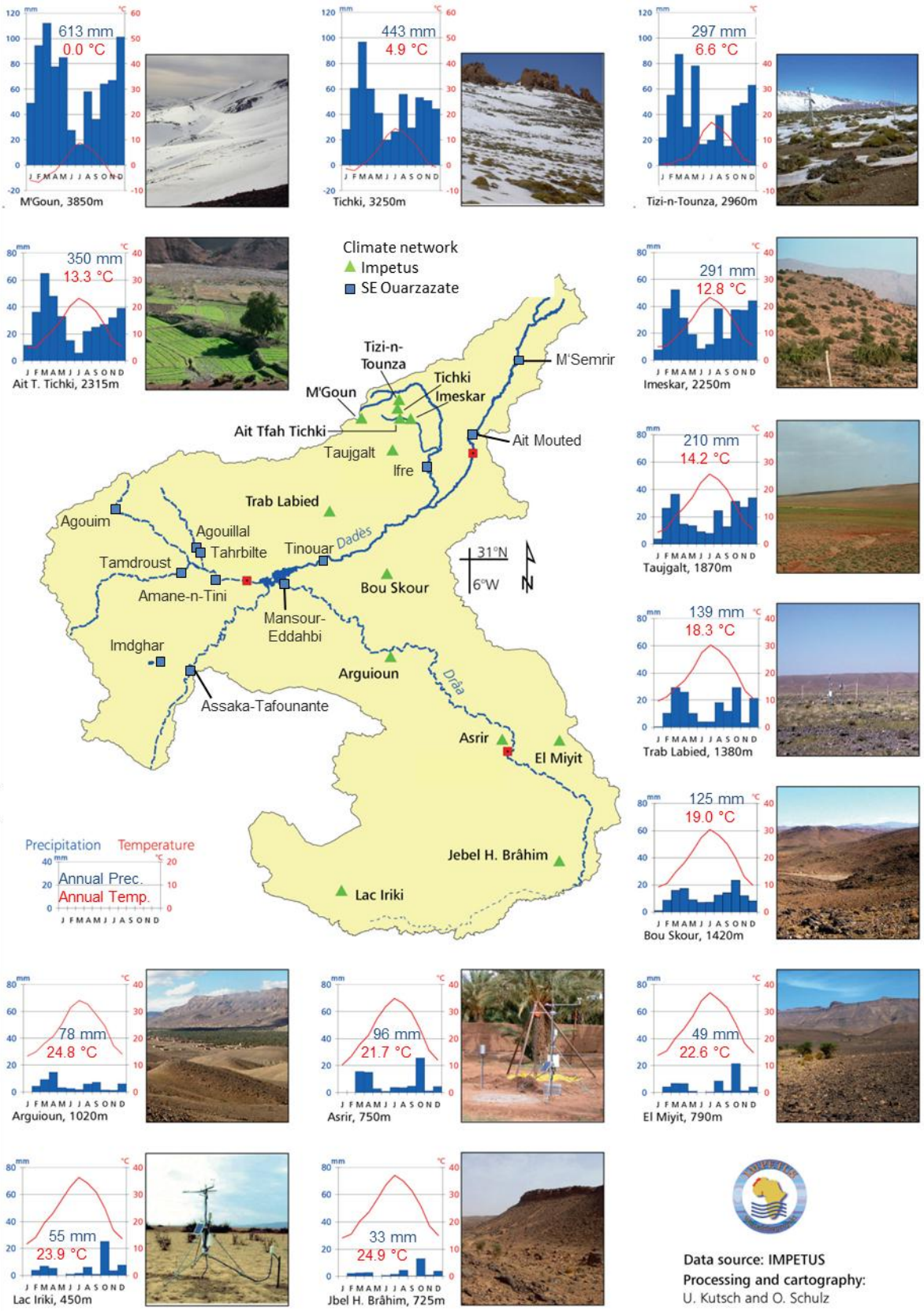

Figure 3-4: Climate monitoring network in the Drâa region (modified after Schulz 2008). IMPETUS stations cover the period 2001-2009, SE Ouarzazate delivers long term records. Mean monthly precipitation and temperature is depicted for the IMPETUS stations only, to portray the gradient of aridity within the catchment. For measured variables and record lengths see Appendix 1.

3.3 Geology

The Ouarzazate Basin and the Southern Atlas Marginal Zone lie in between the intra-continental High Atlas range to the North and the Anti-Atlas to the South. A detailed overview of the regions geological setting is provided by Michard et al. (2008), Piqué et al. (2002) and Stets & Wurster (1981). Table 3-2 provides a chronological overview.

Table 3-2: Summary of the geodynamic evolution of the Upper Drâa region (Michard et al. 2008); Time scale according to the International Commission on Stratigraphy (Walker & Geissman 2009)

Million years before present (MYBP)	Era	Period	Epoch	Dominant processes
0.01	Cenozoic	Quaternary	Holocene	↑ Ongoing erosion and sedimentation (alluvial terraces) ↓ ↑
2.3			Pleistocene	
5.3		Neogene	Pliocene	
23			Miocene	
34		Paleogene	Oligocene	
56			Eocene	
66			Paleocene	
100	Mesozoic	Cretaceous	Late	Discontinuous sedimentation conditions Influenced by eustatic changes and regional uplift (trough→shelf→intertidal→ lagoonal→continental)
146			Early	
161		Jurassic	Malm	
176			Dogger	↓ ~ 200 Climax of volcanic activity (basalt dykes and sills) ↑
202			Lias	
235		Triassic	Late	
245			Middle	Erosion and peneplation (red beds)
251			Early	
299	Paleozoic	Permian		↓ Hercyan orogeny: Folding and metamorphosis of basement
359		Carboniferous		
416		Devonian		
444		Silurian		
488		Ordovician		
570		Cambrian		
…	Precambrian			~685 Pan-African orogeny ~2000 West African Craton consolidates

Alpidian orogeny: Inversion and uplift of the Atlas rift domain

Rifting ↑ ↓

Minor rift

The Anti-Atlas represents the northern margin of the West African Craton, which consists of widely uncovered Precambrian rocks (~2000 MYBP, million years before present). The Anti-Atlas folded up when a Precambrian allochthonous terrane (Northern Morocco) collided with

the West African Craton during the Pan-African orogeny (~685 MYBP, Villeneuve & Cornée 1994) and has been only slightly reshaped since then.

The Meseta block, consisting mainly of the Western Meseta and the Western High Atlas, has been uplifted as result of the Hercyan orogeny (also referred to as Variscan orogeny), which resulted in the formation of Pangaea. During this orogeny a weak rift system developed, as the Meseta block sheared along a NE-SW axis. Small basins subsided in Permian and have been filled predominantly with red beds. During the Late Triassic another rifting event occurred in the Atlas domain, along with the breakup of Pangaea (Laville et al. 2004). The rift led to the development of half-grabens and volcanism; most basaltic sills or dykes in the region originate from this volcanic activity. Fault activity and volcanic activity gradually declined from Early Liassic times on. The first major marine incursion from the Tethys Sea occurred at approximately 200 MYBP and gave way to flooding of the rifted area. A progressive westward onlap of marine deposits took place onto the rift and onto its margins.

Throughout the Jurassic and Cretaceous the trough formed by the failed rift was filled with sediments. They attest to two major episodes of sedimentation: late Cretaceous to middle Eocene, where marine deposition was controlled primarily by eustatic changes and late Eocene to Quaternary, during which the Basin of Ouarzazate formed and filled with thick continental series largely through the uplift of the Central High Atlas.

The southern slopes of the western part of the Central High Atlas consist of the following structural units (El Harfi et al. 2001), see in Figure 3-5:

- Axial zone: This is the mountainous zone of the High Atlas, composed of a Hercyan basement and Mesozoic, mainly Liassic, limestone cover. Neogene deposits crop out in intra-montane basins.
- Subatlas Zone or Southern Atlas Marginal Zone: Compressional deformation of this zone, which is folded over a width of approximately 10 km. It includes very narrow anticlines and synclines. Deposits in this folded and thrusted zone are mostly Cretaceous and Tertiary.
- Ouarzazate Basin: An asymmetrical synclinorium of structural origin (~150*40 km) with Cenozoic continental formations locally up to 1200 m thick.
- Anti-Atlas: Stable domain of Precambrian basement, partly with Paleozoic cover.

This setting describes the actual geological framework that has to be accounted for in a hydrological simulation. In terms of porosity and hydraulic conductivity, the lithology and hydrogeological properties of the different zones can be summarized as follows (Klose 2008b; Cappy 2006):

Fractured and partly karstified Liassic formations have locally varying permeabilities. In general, these rocks act as aquifers. Due to the aquifer structure and morphology, many groundwater outcrops are contact springs emerging from Liassic aquifers overlying Triassic aquitards or aquicludes (e.g. basalts). Tritium ages younger than 10 years indicate an efficient recharge of the Liassic aquifer system in the High Atlas by recent precipitation. Recharge rates of 4% (Assif-n'-Ait Ahmed catchment: 100 km²) and 11% (Ifre catchment: 1,240 km²) have been computed in water balance studies (Cappy 2006). The isotopic signatures of most of the groundwater samples from the alluvial aquifers in the Basin of Ouarzazate reflect mean altitudes of the recharge area from 2,400 to 2,900 masl, locating these areas in the High Atlas Mountains.

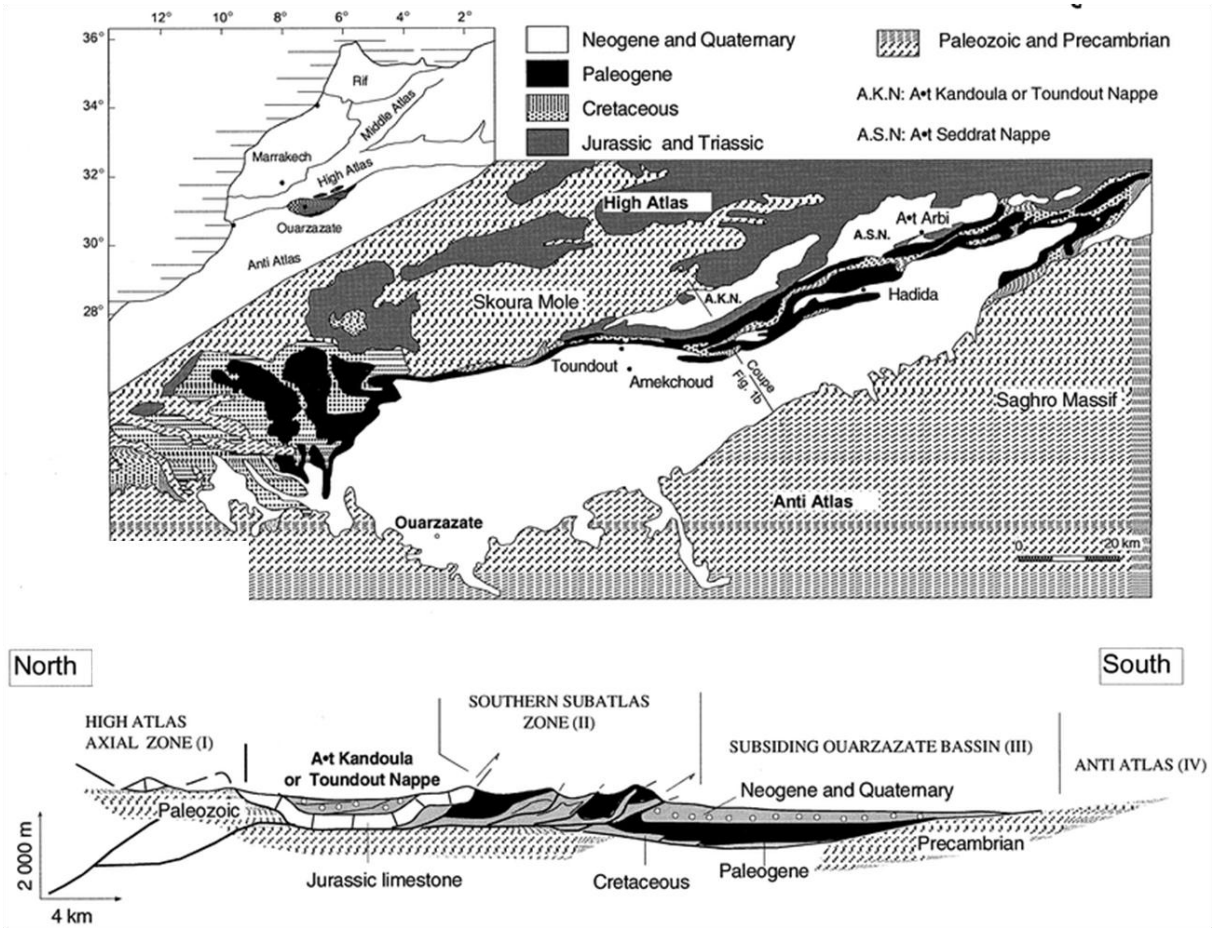

Figure 3-5: Geological setting of the Upper Drâa valley (El Harfi et al. 2001)

In the South Atlas Marginal Zone strong compressional deformations lead to narrow anticlines and synclines of Cretaceous and Tertiary rocks of different hydrogeological properties thus effectively blocking groundwater transfer from the mountains to the basin. Therefore Cappy (2006) assumes groundwater flow occurs only in the alluvial aquifers as

their porous quaternary deposits are highly permeable. These assumptions have been affirmed by MODFLOW simulations that resulted in a riverbed infiltration to total recharge ratio of 85% (Cappy 2006). Therefore direct recharge by precipitation within the basin is considered not significant. Older alluvial terraces, located mainly in the basin, are of rather variable permeability due to different degrees of consolidation and cementation.

The uncovered fractured basement is exposed in the Anti-Atlas and central parts of the High Atlas. These rocks are characterized by low to ultralow hydraulic conductivities and low water content.

Summarizing, the **Anti-Atlas** features poor groundwater storage capacity and renewability. The carbonate rocks of the **High Atlas** represent the main aquifer system in regard to its volume and its recharge. The recharge of this aquifer system by recent precipitation is efficient. A connection of this Aquifer and the basin via mountain-front discharge has to be neglected, as the Southern Atlas Marginal Zone acts as a decisive hydrogeological barrier between the aquifers of the High Atlas Mountains and the Basin of Ouarzazate. Therefore groundwater from the High Atlas is mainly transported via the wadis and the corresponding alluvial aquifers. The alluvial aquifers in the **Basin of Ouarzazate** are mainly fed by these wadis, as recharge by precipitation within the basin can be considered subordinate.

3.4 Geomorphology

As pointed out in the last section, processes associated with the uplifting of the High Atlas shape the region. These are in particular incision of the drainage system, erosion in the High Atlas and sedimentation in the basin of Ouarzazate. These processes are variable in time, as they intensify or weaken according to climatic fluctuations (Awad 1963), and they trace geological features (Sebrier et al. 2006; Stäblein 1988).

The creation of the drainage system is directly associated with the topography generated during the formation of the High Atlas system. During the uplift, the foreland basin of Ouarzazate was created, as the margins of the inverted rift mountain topography subsided. It was eventually filled with sediments until the drainage system cut through the Anti-Atlas, enabling the Drâa to drain the basin presumably 2.6 MYBP (Arboleya et al. 2008). The development of Quaternary alluvial fans and terraces along the northern margin of the Ouarzazate basin is strongly controlled by climate oscillations on glacial–interglacial time scales. Incision occurred during interglacial times, when the region was wetter, hillslopes were stabilized by wooded vegetation and streams were more pervasive. In contrast, during the more arid glacial times aggradation dominated, as increased hillslope erosion enhanced sediment supply and the hydrological regime was less effective at transporting sediment (Awad 1963; Arboleya et al. 2008). Fluvial incision rates for the late Quaternary are estimated to range between 0.3 and 1.0 mm/year, using surface exposure dating of abandoned fill-terraces (Arboleya et al. 2008).

The recent geomorphological processes exhibit characteristics of drylands and high-mountain systems. Gerrard (1992) provides detailed toposequences of drylands as well as of mountains. In the study area both of these conditions apply, therefore the described processes participate and superimpose. Figure 3-6 provides a brief overview of the geomorphological phenomena that dominate the research area. In the M'Goun area glacial and periglacial forms witness the latest glaciations. Cirques and moraines can be observed in the vicinity of the M'Goun. The actual snowline is estimated to be 4200 m, 800 m above the Pleistocene snowline (Hughes et al. 2006). Due to low temperatures weathering is mostly physical and debris is transported downward steep slopes either by gravity or torrential floods. Finer material is also transported by wind. Alluvial fans extend into the sedimentary filled basins, which are cleared by ephemeral rivers. High plateaus with flat slopes and wide intra-montane basins provide stable conditions for soil formation, whereas elsewhere erosion and transport are the dominant processes.

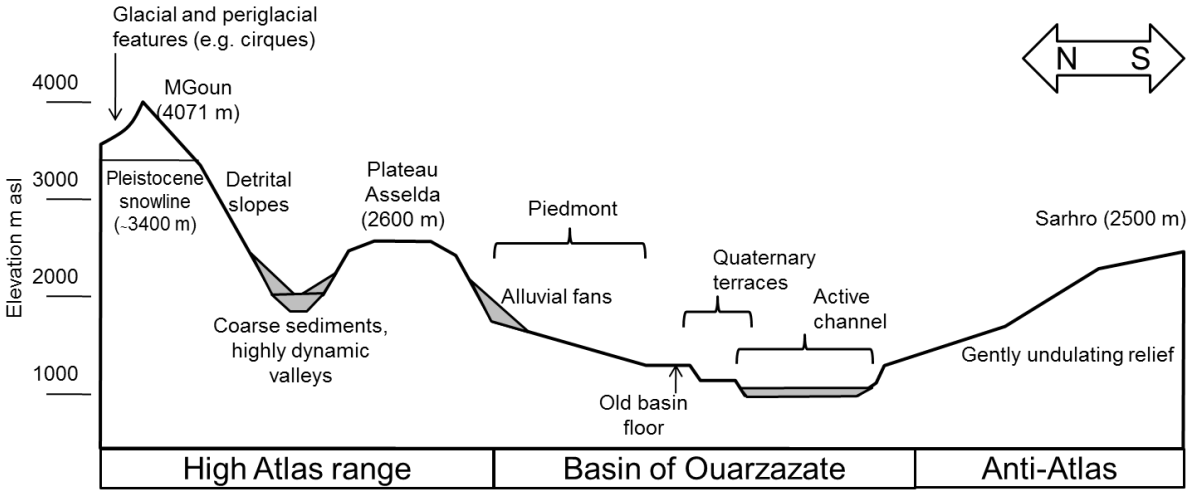

Figure 3-6: Geomorphologic processes along a fictional transect through the Upper Drâa catchment

Presently even the Ouarzazate Basin is dominated by erosion and sedimentation is restricted to the south-dipping alluvial fans, marking the edge of the High Atlas Mountains. Slopes are generally flat in the basin; therefore gravity is no more an important transporting agent, but sheet flow and intermittent stream flow erode the sparsely vegetated slopes. Erosion and deposition conditions changed frequently during the Quaternary; hence 6 different terraces could be identified in the basin by Arboleya et al. (2008). The Anti-Atlas features a gently undulating relief as it is far older than the High Atlas and has therefore already been denudated.

3.5 Pedology

Soil formation is dependent on climate, organisms, relief, parent material and time (Jenny 1941). In the specific context of the Upper Drâa catchment these factors can be addressed as the increasing aridity from sub-humid in the mountains to arid in the basin, along with adapted sparse vegetation (in different degrees of degradation). The relief generally exhibits high slopes in the Mountains, rather low ones in the basins, and gentle slopes in the Anti-Atlas as lined out in the previous section 3.4. Soils evolve on different parent materials (section 3.3), most dominantly exposed basement and Liassic limestone in the mountains, sedimentary deposits in the basins and again Precambrian basement in the Anti-Atlas. Cooke et al. (1993) noted that dry lands are generally set aside from more humid ones, by three points:

- A more sharply defined angle of slope instability
- Capillary rise of groundwater in low lying areas
- Heterogeneous composition of catenas in terms of age

Therefore steep slopes are expected to have the youngest and least developed soils, if any; whereas flat slopes have the oldest and possibly deepest soils. Furthermore alkaline soils should occur in the lower slope positions of the basin.

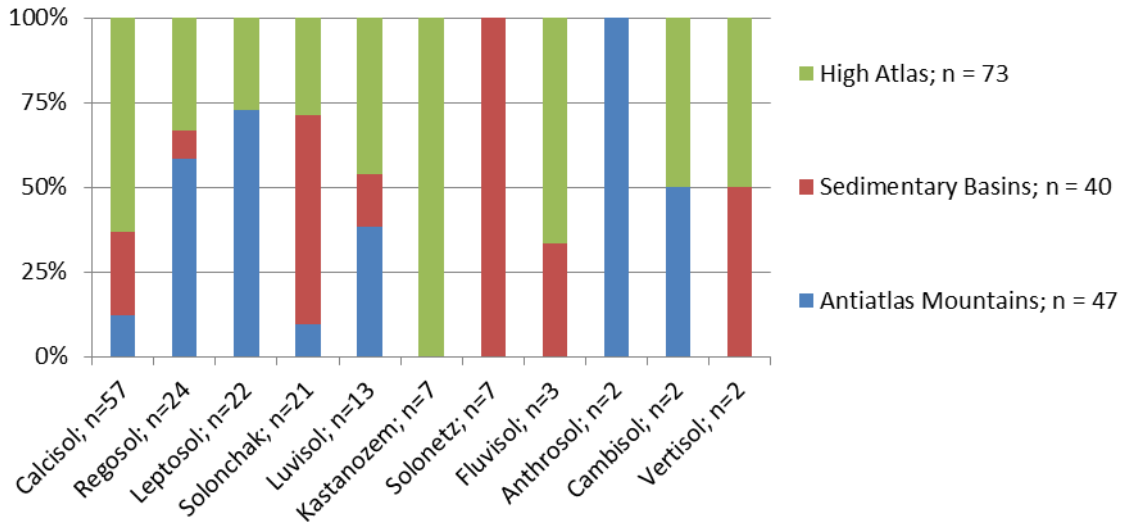

Figure 3-7: Major WRB soil types in the Drâa catchment (Klose 2009)

Soil information is rare in the Drâa catchment. Until recently the only soil map available was a scale 1: 1,500,000 map (Cavallar 1950). Soil types are described with respect to their genesis, but no information on soil properties is provided. Bryssine & Billaux (1967) provide

an overview of soil studies in the region; they further describe the most common soil types and depict their distribution. Recently, soils in the Drâa region have been portrayed by Klose (2009), who classified soils in the catchment according to the World Reference Base taxonomy (WRB; FAO 1998): Soil types identified in the Drâa catchment are in order of observed frequency: Calcisols, Regosols, Leptosols, Solonchaks, Luvisols, Kastanozems, Solonetz, Fluvisols, Anthrosols, Cambisols and Vertisols. Figure 3-7 gives an idea of the distribution of the different soil types and therefore helps identifying the governing processes of soil formation in the catchment.

Soils with accumulations of Calcium carbonate are referred to as **Calcisols**. They are identified in the High Atlas, on Liassic limestone as parent material. Furthermore calcaric material is widely distributed through Aeolian transportation, allowing Calcisols to evolve anywhere in the catchment, thus they represent the dominant soil type. **Regosols** are soils in an initial stage of development. They occur at the lower slope positions where ongoing disturbance by deposition of material eroded upslope prevents distinct profile development. Hence, these soils rarely occur in the flat basins. **Leptosols** are defined as very shallow or extremely gravelly soils. They are limited to the mountain ranges as well, as soil depth is generally higher in the sedimentary basins. They mainly occur at upper slope positions where skeleton content is high due to the selective removal of fine material by erosion. **Solonchaks** and **Solonetz** are soils with horizons of distinct salt enrichment. Due to the concentration of water and salts washed out from the upper slope parts, both soils are mainly found at lower slope positions of the sedimentary basins. The Solonchaks detected in the High Atlas are all situated within or adjacent to strata containing gypsum. **Luvisols** feature subsoil horizons of clay accumulation. As lessivage requires a certain amount of percolating water, these soils usually develop under (sub-) humid conditions. Water availability in the relatively humid High Atlas may be sufficient for the evolution of Luvisols, but in the basins water scarcity hampers recent evolution. Luvisols found here might be paleosols, witnessing more humid quaternary periods. The steppic **Kastanozems** are characterized by high organic matter content in the topsoil. Kastanozems evolve under sub-humid conditions and can sustain steppic grasslands. These soils are exclusively located in the High Atlas, restricted to areas that are not prone to overgrazing. Both **Fluvisols** and **Anthrosols** are mainly found in the low slope positions of the depth lines, on loamy deposits of the oases or the coarse gravels of alluvial fans and rivers. Fluvisols are defined as young soils on material transported by water and deposited in alluvial lowlands, whereas Anthrosols are further formed by human activity, in this case by irrigation. These soils have been portrayed in detail by Moroccan authorities

(Brancic 1968; Radanovic 1968). **Cambisols** are soils of beginning profile differentiation that differ from unweathered parent material in terms of aggregate structure, clay and carbonate content, hence color and other properties that give evidence of soil-forming processes. They rarely occur in the catchment. **Vertisols** are clay rich soils. Clay enrichment may occur in denudation plains or sedimentary lowlands. They cover minor areas in the Basin of Taznakht and inner-montane basins of the High Atlas. Figure 3-8 displays the distribution of the dominant soils along a fictional transect through the Upper Drâa valley.

In the study area terrain units can alternate quickly, even on the hillslope scale. Weber (2004) measured final infiltration rates ranging from less than 1 mm/h (bare rock surface) to 90 mm/h (ephemeral wadi beds). Further physical properties that are suggested to be common to many (semi-)arid soils are high erodibility, high runoff generating potential, crusting tendencies, poor water holding capacity, structural instability and high bulk density (Singer 1991). Generally low organic carbon contents have been measured in the study area, making the soils prone to aggregate instability, crusting and a reduction of infiltration capacity (Klose 2009).

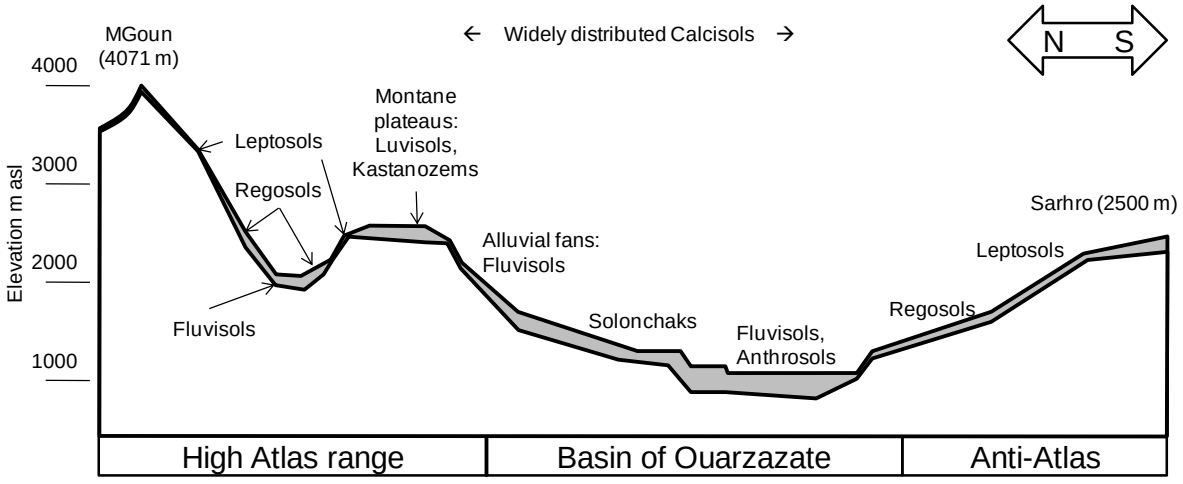

Figure 3-8: Soils along a fictional transect through the Upper Drâa catchment

3.6 Land Use and Land Cover

Potential natural vegetation follows the arid Mediterranean altitudinal zonation (Walther and Breckle 1999), which will be portrayed, before the actual anthropogenically influenced vegetation is described. Steppic plant communities dominate the semi-arid plains south of the High Atlas; according to edaphic conditions either sagebrushes (e.g. *Artemisia herba-alba*) or Halfa grass (*Stipa tenacissima*). They give way to open evergreen leaf forests (e.g. *Quercus ilex*, *Juniperus phoenicia*) in the submontane zones above 1500-2000 m. Unlike the vegetation of the humid Mediterranean type in Southern Europe deciduous trees do not establish themselves due to frequent drought conditions. In elevations from 2500 to 3000 m montane and subalpine conifers (e.g. *Juniperus thurifera*, *Cedrus atlantica*) prevail, interspersed with shrubs. Above the tree line (~3250 m; Troll 1973) mountain steppes are dominated by thorny cushion shrubs (e.g. *Bupleurum spinosum*). This general pattern deviates slightly due to increasing continentality, and slope exposition as described by Rauh (1952) (see Figure 3-9).

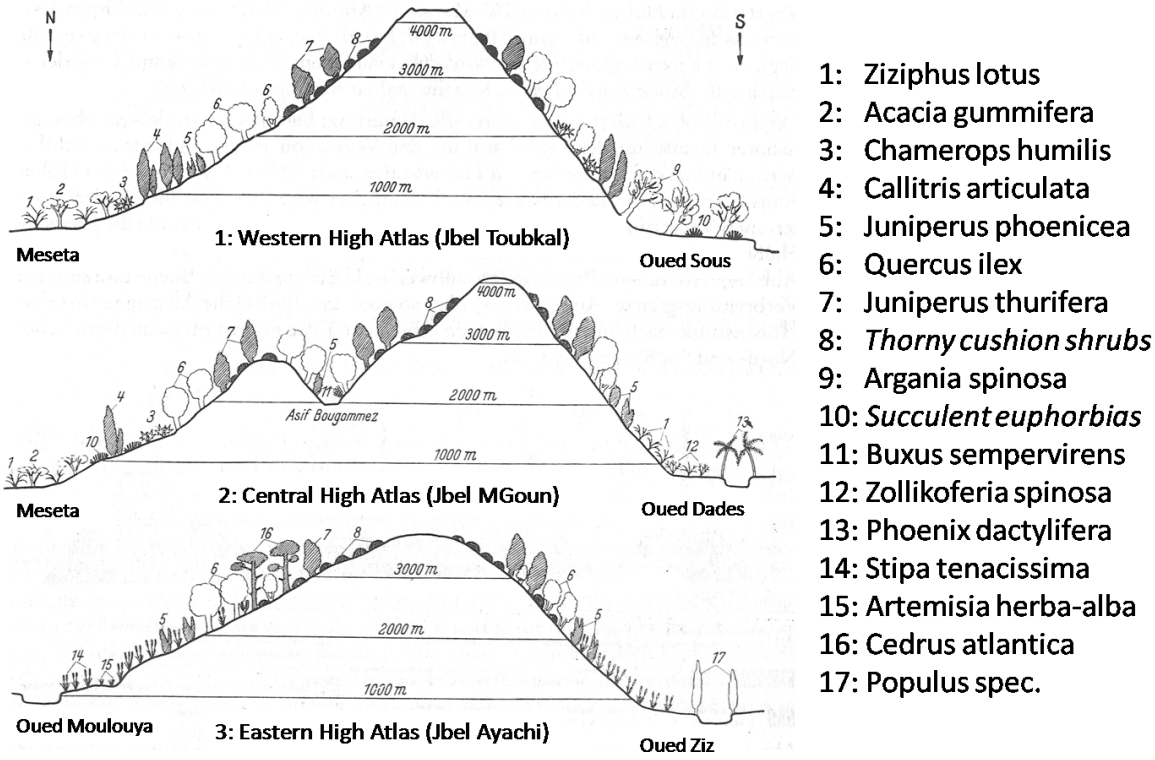

Figure 3-9: Natural potential vegetation in the High Atlas (Rauh 1952)

Contrasting this potential natural vegetation, the High Atlas and the Basin of Ouarzazate are dominated by arid steppes to a vast extent, even in altitudes where precipitation could sustain open forests. These secondary steppes are product of an increasingly intense anthropozoogenic impact on fragile and unstable ecosystems (Le Houérou 2001; Le Houérou 1996). Increased grazing and woodcutting has led to a degradation of vegetation and via redistribution of organic matter to a degradation of soils as well.

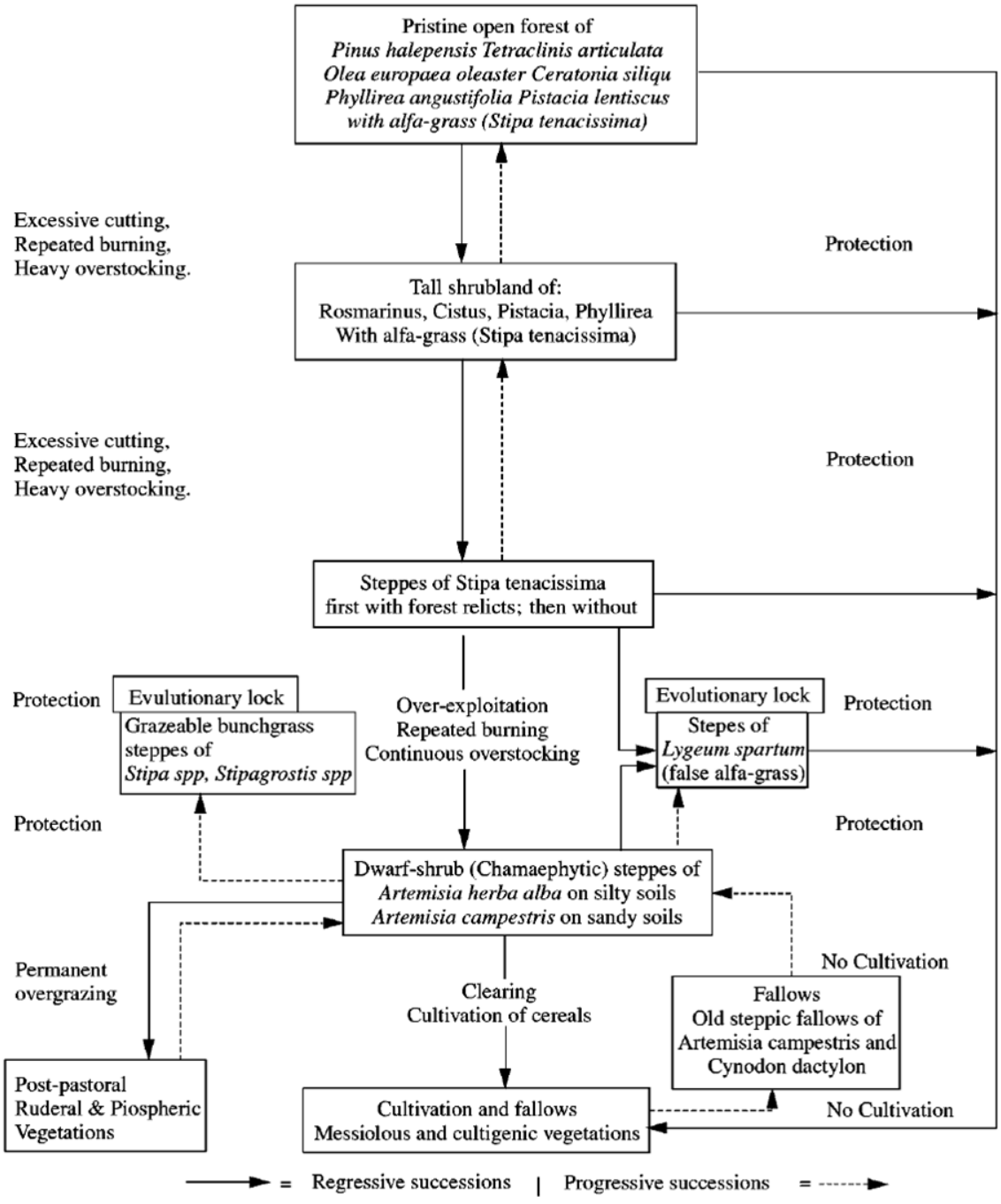

Figure 3-10: Degradation processes in Northern African highlands (Le Houérou 2001)

Furthermore Halfa grass can only regenerate sexually in the shades of trees. On the other hand pine trees (*Pinus halepensis*) find favorable growing conditions in tussocks of Halfa grass (Gasque and Garcia-Fayos 2004). Both species therefore encounter difficulties to reestablish themselves. Therefore these degradation processes are virtually irreversible, when Halfa grassland has been degraded to dwarf-shrub steppe (Puigdefabregas and Mendizabal 1998; Le Houérou 2001). Le Houérou (2001) provides an overview of this regressive succession (see Figure 3-10). Already under natural conditions high surface runoff rates are expected due to sparse vegetation cover. The outlined degradation goes along with loss of organic matter, crusting and soil loss, enhancing surface runoff.

However brush steppe and annual grasslands prove to be able to regenerate within short periods of time. Exclosure experiments, carried out by the ORMVAO in the basin of Ouarzazate, demonstrated that after only two years of protection, the vegetation was reconstituted in a remarkable manner (reports compiled by Davis 2005).

Pastoral activities in the Upper Drâa Valley follow a seasonal cycle, dependent on rainfall and fodder availability (Baumann 2009). During summer, rangelands in the High Atlas mountains, often above 2600 masl, are used. Access to these pastures is traditionally regulated by the *agdal*, a local assembly of stakeholders in the Atlas region (Ilahiane 1999), and usually granted from June through September. During winter, November through March, winter pastures below 2000 masl, such as the basin of Ouarzazate or the Anti-Atlas, are frequented. In between, intermediate mountain ranges serve as transition pastures. Since overstocking and grazing as well as woodcutting is strongly connected with population dynamics and economic structures, the degradation of vegetation is likely to continue within the area of investigation.

Concluding, actual land cover[4] patterns in the investigation area are product of natural boundary conditions (such as climate and topography) on the one hand and increased human influences on the other hand. Both factors vary in time and space. Therefore actual vegetation is not in equilibrium and represents only the actual state of the outlined interacting processes.

Finckh (2008) describes 3 different large floristic regions: Oromediterranean ecosystems of the high elevations (>2200 m), sagebrush steppes (1400-2200 m) and Pre-Saharan semi-deserts and rock steppes below 1400 m. The **Oromediterranean ecosystem** consists mainly of thorny cushion shrubs, showing microclimatic and anti-herbivore adaptations. The forests that form the transition zone towards the steppes, nowadays only exist as relicts due to overexploitation and degradation. Halfa grasslands are found in remote places (Oldeland

[4] Due to a better readability, in this work the term land cover refers to land use as well as land cover. If a further distinction between the two is required, it is provided in the text.

2004), but have widely been replaced by **sagebrush steppes**, which dominates the elevations 1400-2200 in varying degrees of degradation. Annual grasses flower in spring and contribute to floristic diversity of the steppes. In the basin **semi-desert- and rock steppe** (e.g. *Hamada scoparia, Farsetia occidentalis*) prevail as a result of limited water availability. In the depth lines these brushes are interspersed with deep-rooting *tamarix* species (Roth 2009). Seasonal grasses can flourish here during the rainy season in high spatial and temporal variability.

In vicinity of the wadis natural vegetation (*populous, salix*) have been widely replaced by orchards and croplands. Cultivated fruits vary with altitude due to differences in frost tolerance and growth period: apple, walnut, almond, olive, date palm and various field crops. Figure 3-11 depicts the main characteristics of the land cover within the research area.

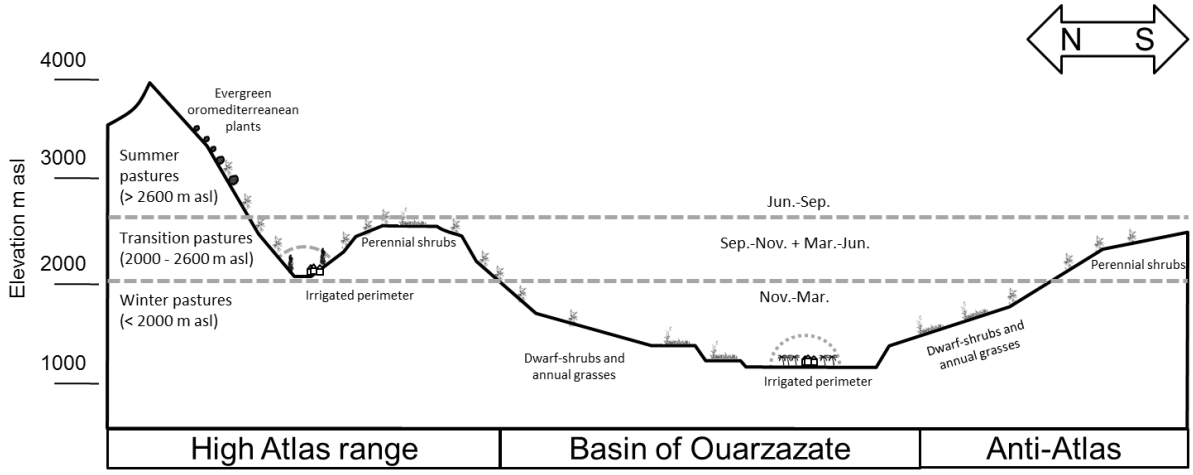

Figure 3-11: Land use and pasture types along a fictional transect through the Upper Drâa catchment

3.7 Hydrography

At the outlet of the basin of Ouarzazate the reservoir Mansour-Eddahbi has been constructed in 1972 with a capacity of 583 Mm³ (DREF 2007). In the period 1978-2007 an average inflow to the reservoir of 356 Mm³/a was registered. Before the construction runoff frequently reached Lac Iriqui during floods. This is the Drâa's endorheic lake, as the amount of water is not sufficient to overcome the last 750 kilometers toward the Atlantic Ocean (Lower Drâa Valley). Since the construction the reservoir assures irrigation, generates hydroelectric energy and reduces flood risks (DGH 1988). As a result the timing of irrigation has been improved (ORMVAO 1995), but evaporation losses and reservoir silting as well as eutrophication and algae blooms pose new challenges (Sadek et al. 1997; Lahlou 1988; Sadani et al. 2004; Douma et al. 2009). Until 1998, when the last bathymetry was conducted, the reservoirs capacity was reduced to 433 Mm³ (Klose 2009). To ensure irrigation to the oases of the Middle Drâa valley, 245 million m³ of water are needed each year, so that the ideal seven *lâchers*[5] (35 million m³ each) can be provided (ORMVAO 1995). Approximately an additional 55 million m³ of water are lost by evaporation and water supply for the city of Ouarzazate (Schulz et al. 2008).

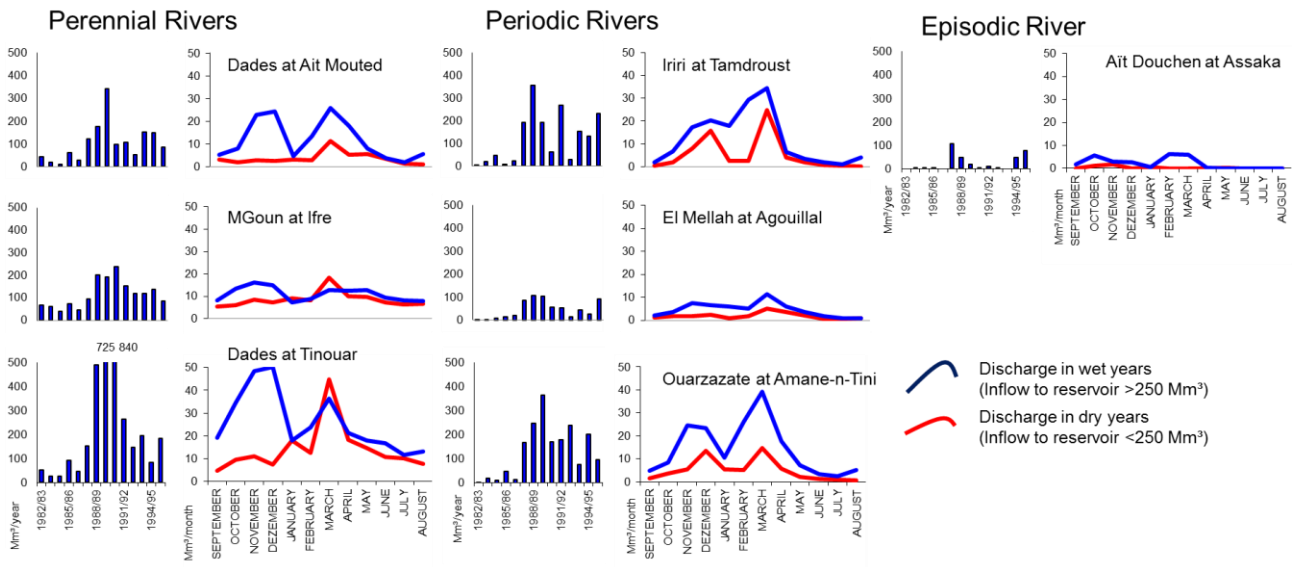

Figure 3-12: *Annual and mean monthly (in dry and wet years) discharge of different tributaries to the reservoir Mansour-Eddahbi in the period 1982-1996 (Busche 2008b). See Figure 3-13 for locations of the gauges. Appendix 2 provides the delineated subcatchments and information on streamflow data availability for the gauges.*

[5] Lâcher is a local expression for a period of water release from the reservoir for irrigation purposes.

Inflow into the reservoir depends on the perennial, periodical and episodical tributaries (see Figure 3-13 for locations of rivers and gauges and Figure 3-12 for hydrographs[6]).

The only **perennial** rivers in the research area, Oued[7] Dades (223 km long[8]) and its main tributary the Oued M'Goun (96 km), are fed by the karstic aquifers of the north-eastern High Atlas (Youbi 1990). This aquifer is replenished by melting snow and water infiltrating in the gravely and highly permeable beds of the tributary channels. Even in years of drought, the buffered groundwater driven system of the north-eastern regions provides baseflow, which constitutes a reliable base for irrigation in the Dades valley (Schulz et al. 2008). This baseflow from the High-Atlas is routed through the basin of Ouarzazate. Transmission losses are low, as the channel bed is naturally sealed to a large extent. These rivers drain the eastern half of the catchment (7,519 km³).

Oued Ouarzazate (26 km), draining the north western part of the catchment (4,552 km²), is the major **periodic** river that contributes from autumn to spring, due to seasonally increased storm activity and snowmelt. It has several periodic tributaries among which the Oued Iriri is the longest (54 km). The gauges Tamdroust, Agouillal and Amane-n-Tini represent this river type.

Rare extreme events make the whole basin **episodically** contribute to runoff. As the infiltration capacity of the rocky soils is exceeded fast during high intensity rainfalls, large areas generate surface runoff. In this case high amounts of water infiltrate through the permeable floodplains and the river bed and recharge the groundwater. This is when episodic tributaries as the Aït-Douchen (79 km, drainage area 2,911 km²; gauge Assaka) and the ungauged central basin, as well as the Anti-Atlas contribute to discharge. These events are important for the filling of the reservoir and hence the irrigation of the downstream oases (Schulz et al. 2008; Fink & Knippertz 2003).

[6] The Moroccan hydrological year starts in September and ends in August. If not stated differently the Moroccan hydrological year is used in this work. It is referred to either as "2001/02" or to ensure better readability just "2002"

[7] Oued is a local term for wadi. Unlike the usual limitation to ephemeral rivers, in francophone Northwestern Africa the term oued is used also for periodic and perennial rivers.

[8] Drainage areas and river lengths are taken from hydrographic analyses of topographic maps (1/1,000,000) conducted by the Direction Regionale des eaux et forets du sud oust (DREF 2007).

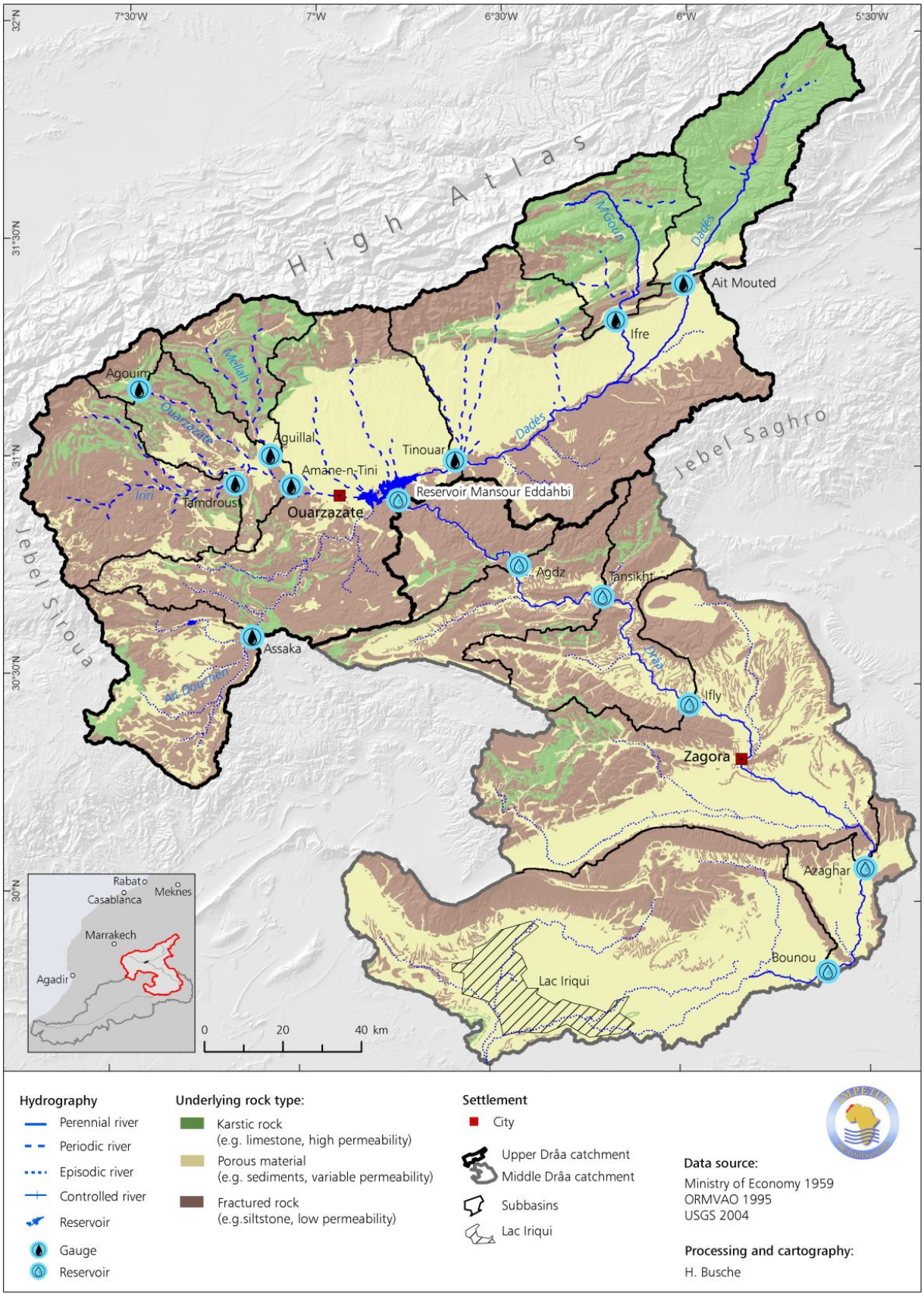

Figure 3-13: Hydrological setting of the Upper Drâa catchment (Busche 2008a)

3.8 Perceptual Model: Hydrological Processes in the Upper Drâa Catchment

A detailed overview of hydrological processes is provided in chapter 2. This section presents an outline of the hydrological setting of the study area and therefore presents the perceptual model that is the basis for the modeling process explained in the following chapter 4 and carried out in chapter 5. The Upper Drâa catchment experiences a hydrological regime of the semi-arid subtropics. High evaporation losses, infrequent precipitation events of partly high intensity and flash-floods accompanied with high transmission losses characterize the hydrological behavior of this catchment. Anyhow the potential water scarcity is compensated by the "water towers" of the High Atlas range. Hydrological processes addressed in this and the previous chapter and summarized in Figure 3-14 are of varying importance in different subregions of the catchment, according to elevation, geology, dominant soil type etc.

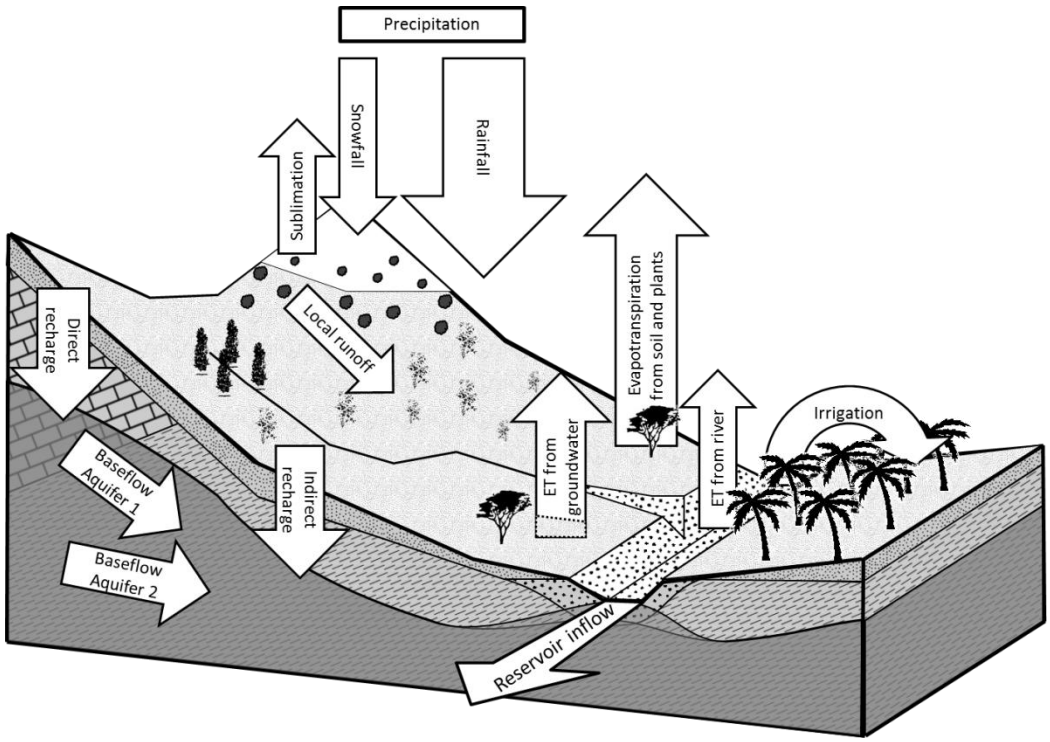

Figure 3-14: Perceptual model of hydrological processes in the Upper Drâa catchment

The present study seeks to develop a model that is capable of representing the hydrolological processes of the Upper Drâa catchment. Therefore the main characteristics of the hydrological behavior of the Upper Drâa catchment have been identified and associated with the processes described in chapter 2. The most striking feature of the catchment is the elevation dependency

of the vast majority of hydrological processes, especially of those related to climate, land cover and soil. Furthermore snow dynamics play an important role in the elevated regions.

The highly heterogeneous geological setting creates distinct baseflow regimes in different subcatchments, as well as superimposing baseflow responses in the same catchment. This is addressed by the two aquifers in Figure 3-14. Stream-aquifer interactions are dominated by transmission losses and therefore indirect recharge can occur even in regions with little precipitation. A large quantity of discharge is used for irrigation purposes in the basins oases, whereas in terms of quantities, drinking water supply is of minor importance.

4. Modeling Process

Essentially, all models are wrong, but some are useful.

George Box & Norman Draper, 1987

Within this chapter a brief and general introduction to models is given including an overview of the modeling process (section 4.1). Furthermore measures to describe model goodness or to evaluate model results are introduced (section 4.2). This chapter closes with a presentation of model applications in the study area or a similar environment (section 4.3).

Stachowiak (1973) gives a very general definition of models, stating that all „cognition is cognition in models and by models“. He further elucidates that recognition is “relative to certain subjects, intentional selecting, focusing and in temporal limitation of its relation to the original”. Based on these broad postulates three properties of all models are specified:

- **Representation**
  A model represents another system.
- **Simplification**
  This representation is always simplified, as a model never incorporates every aspect of the represented system.
- **Pragmatism**
  The extent of simplification, and the decision whether certain system components are included in the model or not, depends on the models purpose.

This general definition accounts for all types of models, ranging from technical sketches to cognitive patterns and as well for hydrological models. In this specific case the system considered is the hydrological cycle or a part of it. Hydrological models are used for a range of purposes from tools for testing hypotheses about the behavior of natural systems to practical applications such as flood-monitoring or Integrated Water Resource Management (IWRM) – in fact anything influenced by hydrological response. Grayson & Blöschl (2001) emphasize the use of models for the scientific gain of knowledge: We begin with a certain degree of process understanding and plan sampling campaigns accordingly, until we have enough understanding to develop a model. Ideally, the model improves our process understanding and provides ideas for new sampling campaigns which then promote the development of new models etc. At the best, process understanding and models co-evolve perpetuating in this loop.

Necessarily the required simplifications of the hydrological cycle depend on the purpose of the model. Therefore it is inevitable to formulate exact questions, the model is supposed to answer. Furthermore it has to be decided, what are the key processes that dominate the response at the scale of interest and therefore might answer the questions raised.

Therefore, even well adapted hydrological models might turn out to be completely useless for different purposes in the same catchment. This finding, has been summarized in the pointed remark, introducing this chapter that “essentially all models are wrong, but some are useful” (…for a given purpose, in a given area, at a given time and under given assumptions) (Box & Draper 1987).

4.1 Theory of the Modeling Process

This section will outline the modeling process as generally acknowledged in hydrological science and illustrated in Figure 4-1 (Refsgaard & Henriksen 2004; Beven 2003; Refsgaard 1997). Having decided on a models purpose, relevant processes and associated scales need to be identified and translated into an appropriate model structure, i.e. the conceptual model (section 4.1.1).

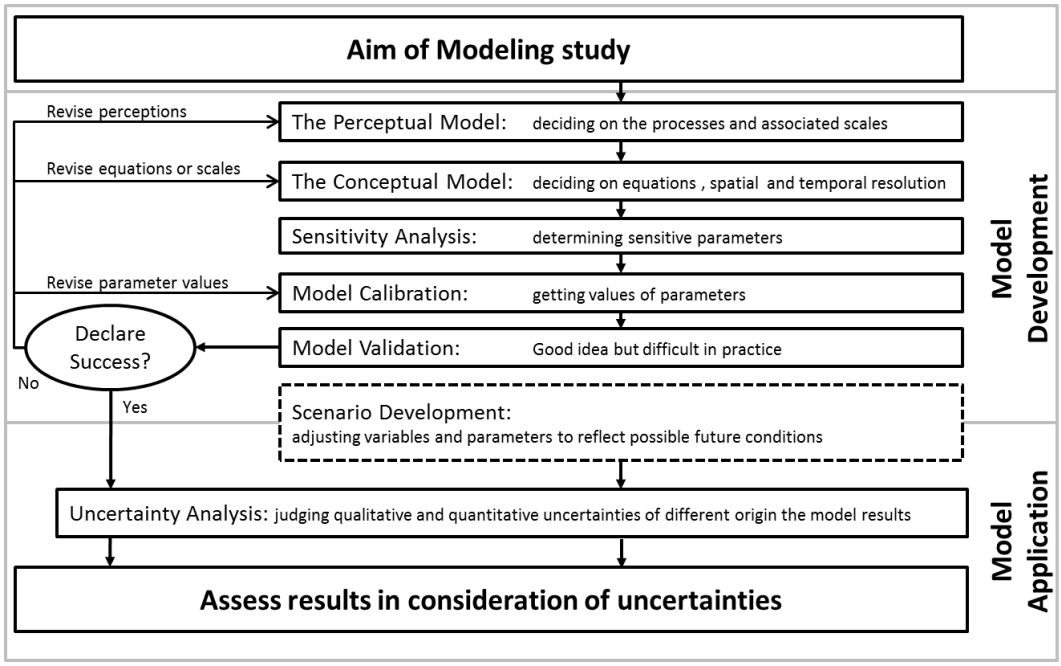

Figure 4-1: Modeling process (modified after Beven 2003)

Before parameterization and calibration are carried out, a sensitivity analysis is highly recommended. This allows the modeler to focus on sensible parameters[9] in the subsequent steps of model development (section 4.1.2). Depending on the model structure more or less parameters need to be adapted in the process of calibration (section 4.1.3). The last step of model development is the model validation (section 4.1.4). It is pointed out that true calibration and validation is hardly possible, as many different model structures and parameter sets can reasonably reproduce observed discharge data; the so-called problem of equifinality (Beven 2006; Beven 1993). This is one aspect of model uncertainty that has to be addressed in order to sensitively interpret the results provided by the model (section 4.1.6). One of the model applications presented in this study is the evaluation of climate change effects as prescribed in scenarios. A brief introduction to scenarios is provided in section 4.1.5.

[9] In this study constants representing intrinsic system characteristics (e.g. soil depth) are called parameters. Variables represent either boundary conditions (e.g. precipitation) or model fluxes (e.g. discharge).

4.1.1 Model Structure

A variety of model structures are available, suiting different modeling purposes. A commonly acknowledged classification scheme for hydrological models is provided by Becker & Serban (1990). The authors distinguish models according to its degree of causality and its spatial representation (see Figure 4-2). A first rough divide can be made between stochastic and deterministic models.

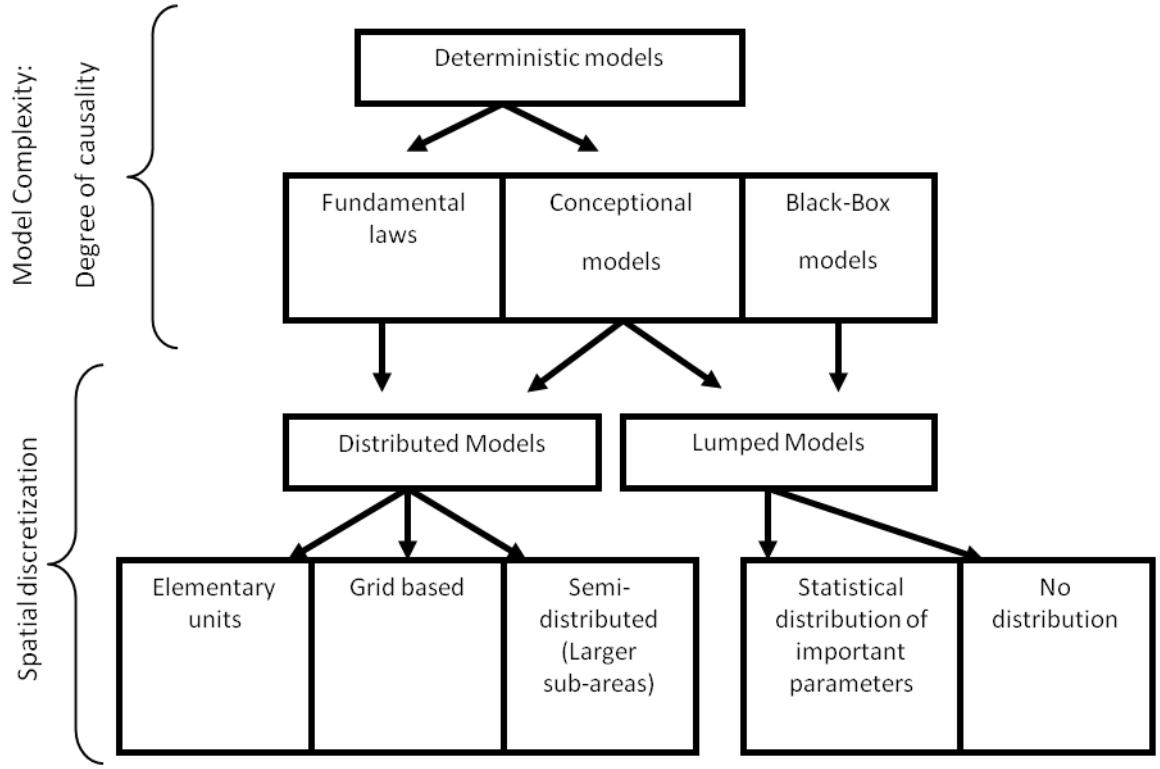

Figure 4-2: Main categories of hydrological models and their areal discretization schemes (modified after Becker & Serban 1990)

A model is called stochastic, when probabilistic laws are being used and stochastic elements, with known or estimated distributions, occur in the model. Therefore ranges of results are produced or model runs produce different output. This model type is not further explained here. A model is called deterministic when a given input always results in the same output. The relations between input and output may be described using physical laws (white box or physically-based), simplifications of these laws (grey-box or conceptual[10]) or empirical relationships (black box). The degree of process understanding associated with the model development should be corresponding to the modeling purpose (see previous section).

[10] In hydrological modeling "conceptual model" is an ambiguous term that refers to a stage in model development (previous section 4.1) and a specific type of model structure (this section). The ambiguity remains unresolved for this work; hence the appropriate connotation is determined by the context.

Obviously these different model types suit different tasks and varying spatial discretization can be associated with them. The following paragraphs provide general ideas of scales, model complexity and spatial regionalization schemes.

4.1.1.1 Scales

Characteristic space and time scales are associated with different hydrological processes (Blöschl & Sivapalan 1995). While shifting scales new processes might gain importance (emergence). For instance real-time flood-monitoring requires models that operate on sub-daily time steps, and focus on surface flow and channel processes (lower left center of Figure 4-3), whereas irrigation managers might use models operating on monthly time-scales, focusing on snow-melt or groundwater dynamics (top center of Figure 4-3). These requirements demand different models, with different simplifications.

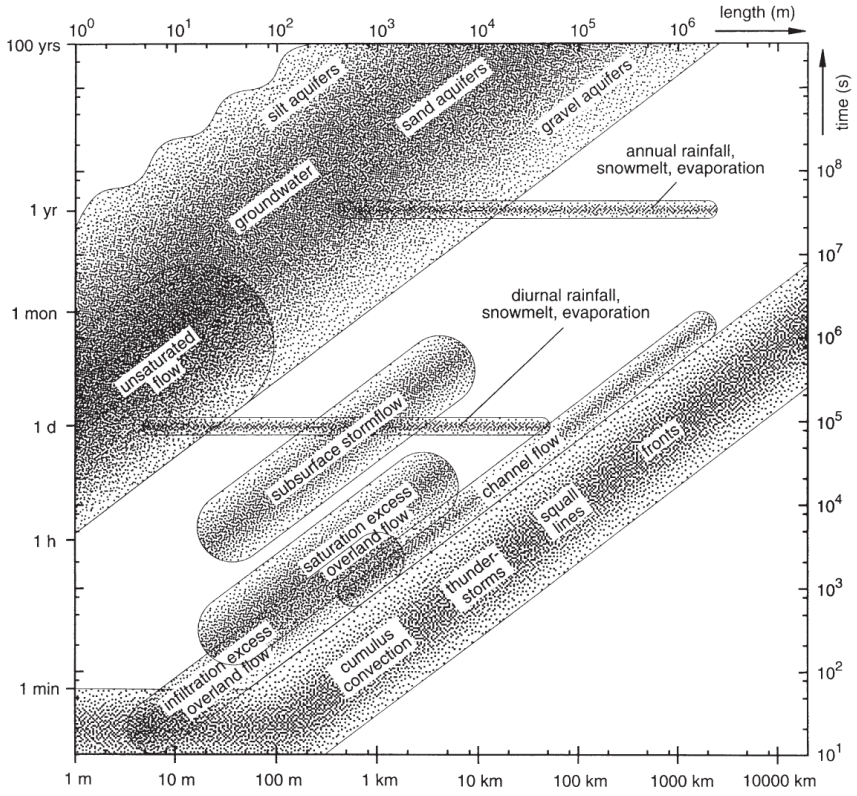

Figure 4-3: Hydrological processes at a range of characteristic space-time scales (Blöschl & Sivapalan 1995)

A modeling challenge associated with scales is that required data is available on different scales only (Beven 1995; Wood et al. 1988). As exemplary variables meteorological data can be considered. Generally measured climate data is site-specific, whereas modeled climate data refers to grid cells larger than 100 km². The same accounts to parameters that, though derived from local measurements, represent areal entities (Herbst et al. 2006).

4.1.1.2 Model complexity

A general trend in modeling is to use the most sophisticated scheme that can be practically applied, based on the assumption that, the more processes a model includes the better its results are (Bates & De Roo 2000). However the authors argue that ultimately the best model will be the simplest one that provides the information required by the user whilst reasonably fitting the available data. Grayson & Blöschl (2001) point out that model complexity needs to match the data available. Otherwise model parameters cannot be identified properly (model complexity > data availability) or the model is not able to fully exploit the data (data availability > model complexity, Figure 4-4).

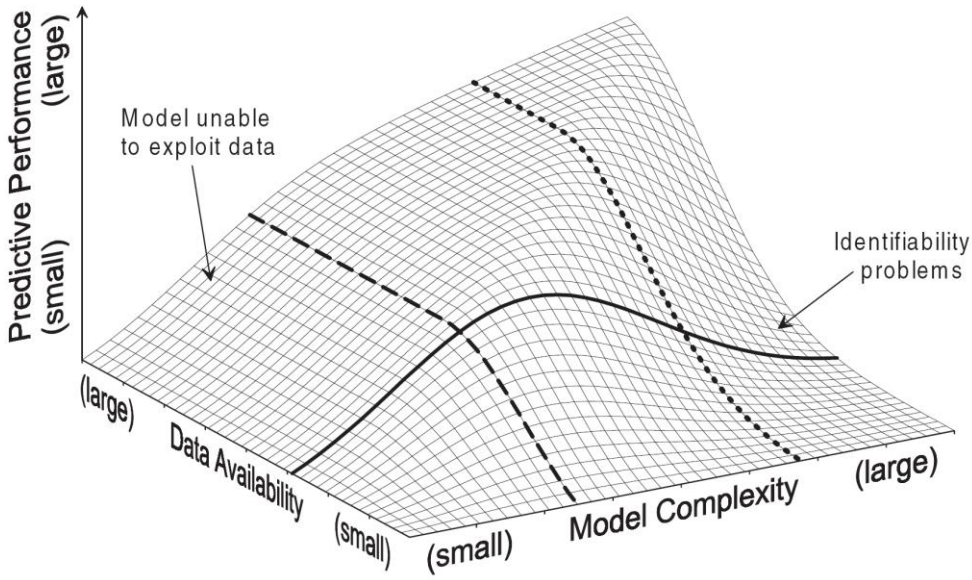

Figure 4-4: Data availability, model complexity and model performance (Grayson & Blöschl 2001)

Some input elements have a reduced or insignificant influence over the output; only the sensitive relations between input and output must be evaluated. From a practical point of view, this means that only a relatively reduced number of input elements are considered as proper input, being linked to the output through strong causal dependencies; the remaining input elements are neglected or considered perturbations, which produce deviations (or noise) from the system's deterministic behavior. If the deviations are too large, one should widen the focus of the investigation, as one or more significant inputs may have been neglected. Following this approach, the optimum model complexity can be obtained.

4.1.1.3 Spatial discretization

It has been shown in section 4.1.1 that the model structure is associated with its spatial representation. Therefore a variety of spatial representations exist. Several distributed hydrological models are based on regular grids, e.g. MIKESHE (Abbott et al. 1986a; Abbott et al. 1986b), ECOMAG (Motovilov et al. 1999), and TOPKAPI (Ciarapica & Todini 2002). The choice of the grid size is not always dependent on the processes that are represented, but rather a result of available data resolution (see the previous section 4.1.1.2 for associated problems). Instead of using square elements, some discretizations of irregular geometry are proposed as well: iso-contours of elevation in TOPOG (Vertessy et al. 1993) or Triangular Irregular Networks in tRIBS (Vivoni et al. 2005). The latter solutions pronounce already aspects of computational efficiency and "similarity" of mesh units, in terms of elevation, aspect, etc. Hydrological similarity of model units is a prerequisite for spatial aggregation beyond grid or mesh-size. Beven & Kirkby (1979) used the topographic index to derive units of hydrological similarity in TOPMODEL.

The Representative Elementary Area concept (REA; Wood et al. 1988) pronounces the existence of characteristic spatial scales for different hydrological processes. Therefore specific features can be assumed to be distributed statistically beyond related thresholds. This approach has been further developed by Reggiani et al. (1998), who propose the use of Representative Elementary Watersheds (REW), self-similar modeling units that are characterized by the same parameter sets, independent of the required scale (i.e., from the drainage area of a stream to that of a rill). Anyhow in the latter case relationships and fluxes between REWs have to be described for every scale considered.

Flügel (1995) propose to define Hydrological Response Units (HRU), based on topography, soils, geology, precipitation characteristics and land cover. SWAT utilizes HRUs based on soils, geology and land cover (Arnold et al. 1993) and most recently slope (Winchell et al. 2007). One of the drawbacks of the HRU mapping is the merging of smaller units into larger ones by applying thresholds or smoothing filters. The resulting loss of information might lead to the overlooking of major hydrological processes that are localized on small units, such as return flow above rock outcrops, transpiration of riparian vegetation, etc. This shortcoming is partly overcome by the development of pre-processing routines allowing to consider special land cover types or soils, even if their spatial extent is below the chosen thresholds (Di Luzio et al. 2004).

4.1.2 Model Sensitivity

While uncertainty analysis aims to characterize the empirical probability density function and the confidence bounds for a model output, sensitivity analysis aims to identify factors or groups of factors mostly responsible for the variation in the model results (Saltelli & Annoni 2010). Due to their mathematical and technical similarity, techniques to quantify both are introduced in section 4.1.6.

Sensitivity is a measure of the effect of change in one factor on another factor (McCuen 1973). A sensitivity analysis therefore determines the rate of change in model output with respect to changes in model parameters or model input, with the latter being rarely done. Consequently the analysis of parametric sensitivity is a vital part of most optimization techniques, as it can be used to identify key parameters and parameter precision required for calibration. A general distinction is made between local sensitivity (varying one factor at a time) and global sensitivity (varying all factors at the same time). It has been argued that the latter should be favored, since it does not impose the assumption of linearity on models and parameter correlations can be identified (Saltelli & Annoni 2010; Saltelli et al. 2006). Most of the available software solutions portrayed in section 4.1.6.3 therefore follow the global approach.

4.1.3 Model Calibration

Calibration is "a process of optimizing a model's parameter values to improve the fit between simulated and observed catchment responses" (Grayson & Blöschl 2001). Several techniques to measure the goodness-of-fit exist (see section 4.2.1). In practice calibration is fraught with the following difficulties (Beven 2006; Sorooshian & Gupta 1995):

- Correlation between parameters

  In complex models, different parameters may have a similar effect on the model result (i.e. the chosen goodness of fit indicator). In SWAT for example this is the case with soil depth and available water content (expressed as a fraction of the soil profile).

- Equifinality

  Due to parameter intercorrelation, plenty of "good" model results can be obtained if the model is calibrated against discharge only. Each of the "good" models may represent totally different parameter constellations, i.e. represent different hydrological behavior of the catchment. For the research area this issue has been explored in detail by Chaponnière et al. (2008), concluding that compensation effects seem to take place in the soil, the groundwater and the snow modules.

- Large number of parameters in complex models

  The problem of equifinality aggravates with an increased number of calibrated parameters. This is especially true for complex models with a variety of parameters. Therefore the calibrated parameters should be carefully chosen and set within physically meaningful ranges.

Key considerations for calibration should be the water balance overall amount and in detail, the distribution among runoff components (i.e. evapotranspiration, surface runoff, baseflow). The shape of the hydrograph is governed by peaks (i.e. time of concentration, travel time) and recession (i.e. baseflow, irrigation). Considering the primary objective of this study, to quantify surface water availability on a monthly to seasonal basis, the focus of the calibration is set on parameters affecting the overall water balance and its seasonal shift.

In general two approaches to calibrate a model exist, manual calibration and autocalibration. An automated approach to model calibration provides substantial labor savings compared to a manual approach, but values of the calibrated parameters may not realistically reflect catchment characteristics (van Liew et al. 2005). To overcome this drawback, a combination of manual calibration and autocalibration is generally recommended (Green & van Griensven 2008). Within the SWAT modeling framework different techniques of model calibration are provided. Recently the SWAT-CUP program has been released (Abbaspour et al. 2008)[11], which links the autocalibration procedures GLUE (Beven & Freer 2001), ParaSol (van Griensven et al. 2006), SUFI2 (Abbaspour et al. 2004) and Monte-Carlo procedures to SWAT.

4.1.4 Model Validation

Validation is the process of testing, whether a model is an accurate representation of the real world, bearing in mind the intended model use. This is usually done by evaluating goodness-of-fit metrics between model results and observation records that have not been used for calibration. Whether a hydrological model can be validated has been widely discussed in the recent literature (Beven 2006; Beven 1993; Konikow & Bredehoeft 1992). Oreskes et al. (1994) contrast the terms verification, i.e. the establishment of truth, stating this is not possible for numerical models, and validation, i.e. internal consistency and the absence of known or detectable flaws. The latter can be obtained for numerical models, anyhow Oreskes et al. (1994) conclude that models can only be evaluated in relative terms, and their predictive value is always open to question.

[11] Download: http://www.eawag.ch/organisation/abteilungen/siam/software/swat (accessed: 29.07.2010)

A particular problem in the use of distributed hydrological models is the disproportionate data availability. While spatial data such as soil and land cover is usually available as input data, spatial data is seldom used for validation. Validation is carried out most frequently against discharge data, which limits the explanatory power of distributed hydrological models. Only few model studies are reported in the literature, where a model has been validated against discharge data and field data on internal variables (e.g. Refsgaard 1997; Güntner et al. 1999; Cao et al. 2006). The more data is used for validation (different variables, longer records) with appropriate results, the higher is the chance of adequately reproducing the hydrological processes in the study area.

4.1.5 Scenario Development

The assessment of future changes in the hydrological cycle is a prominent application of hydrological models. The use of white-box or at least grey-box models, once validated under current conditions is the most promising approach (Beven 2003). Future conditions are often represented by so-called scenarios. These may be thought of as coherent and plausible stories about the possible co-evolutionary pathways of combined human and environmental systems (Swart et al. 2004). This includes a characterization of current conditions and driving forces changing the system in the future. Scenarios are neither predictions, nor prognoses nor forecasts, but they represent internally plausible futures. Scenario analysis has emerged as a key methodology for exploring alternative futures, identifying critical uncertainties, and guiding political action (Raskin 2005). Consequently the use of standardized scenarios serves as a common basis for climate change analyses as in the IPCC reports (e.g. Solomon et al. 2007). These SRES-scenarios (Special Report on Emissions Scenarios) are presented within the following section 4.1.5.1. Furthermore socio-economic scenarios for the Drâa region, developed within the IMPETUS project, are portrayed in section 4.1.5.2.

4.1.5.1 Climate change scenarios

The climate change scenarios that are used in this study, B1 and A1B, have the following storylines (Solomon et al. 2007):

- The **B1** scenario describes a convergent world with a global population that peaks in mid-century and declines thereafter. A rapid change in economic structures toward a service and information economy favors sustainable development, i.e. reduced material intensity and the introduction of clean and resource-efficient technologies.
- The **A1B** scenario describes a similar population development as B1, but the economic development is not focused on sustainable solutions. A balanced development, defined as not relying too heavily on one particular energy source, is assumed.

In order to assess the impact of future climate changes on the global scale, computational models of the climate system (GCMs, Global Circulation Models) have been developed during the past decades. They are based on physical principles of the Earth's atmosphere, represented by a set of differential equations that are numerically solved by the model. The recent trend in model development consists of an increasing reflection of other climate subsystems such as oceans, land-cover etc. (Solomon et al. 2007). GCMs project a continuation of the observed warming trend for the subtropical regions in the 21st century (Hulme et al. 2001; Nicholson 2001; Paeth et al. 2009). However, the detection of rainfall trends is more complex, since they are steered by teleconnections and local conditions as well (Born et al. 2008). For the Atlas region, these teleconnections have been highlighted in section 3.2.

Exemplary global surface temperature changes that are associated with these scenarios are portrayed in Figure 4-5, whereas the more complex precipitation signals are depicted within section 5.6. These scenarios describe global trends that are independent of local or regional developments, i.e. political decisions in Morocco affecting economic development, especially land-use, energy consumption and use of technology, do not have an effect on these pre-defined global boundary conditions.

One of the urgent issues of the latest IPCC assessment report (Solomon et al. 2007) was the downscaling of GCM results, since it is well known that local conditions may be very different from what is observed on the large scale. This is especially true for complex terrains such as mountainous catchments. Impact studies in general, among these hydrological modeling studies, require time series of daily meteorological parameters corresponding to the local scale. In contrast GCMs and Regional Climate Models (RCMs) provide circulation patterns for the Macro- or Mesoscale (Xu 1999). Mearns et al. (1995) conclude that especially

frequencies and intensities of daily precipitation are to be questioned, as model output rather represents averages for modeled grid boxes.

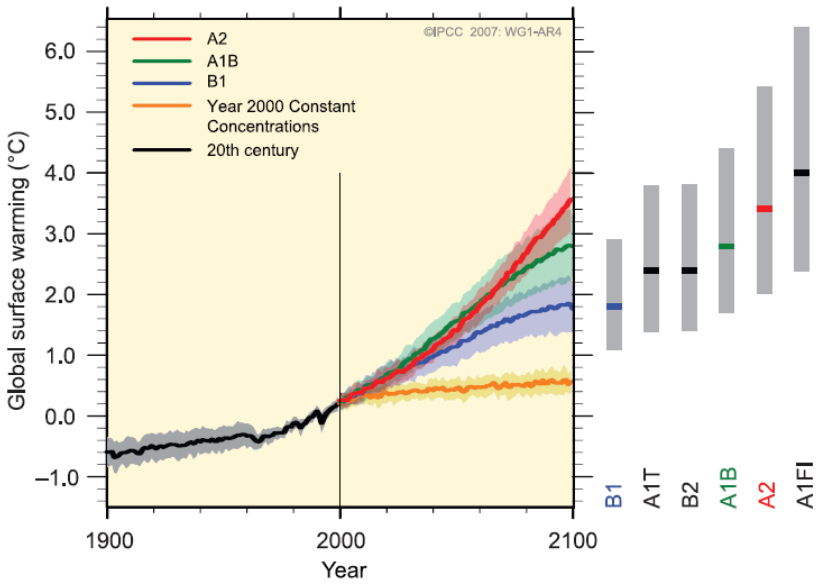

Figure 4-5: *Multi model averages and ranges for surface warming according to the IPCC-scenarios (Solomon et al. 2007). The grey bars at the right indicate the best estimate and the "likely" range of outcomes for each scenario (see section 4.2.2.2 for an explanation of likely).*

Three techniques exist to overcome the gap between the GCM and impact assessment, i. e. translating large scale climatic trends into site specific time series (Xu 1999):

1. Statistical downscaling, using statistical transfer functions between local observations and large scale patterns obtained from climate models. This computationally efficient approach is followed in so-called weather-generators, e.g. WGEN (Richardson & Wright 1984), which is incorporated in SWAT.
2. Dynamical downscaling, using embedded finer scale climate models, e.g. REMO nested in ECHAM5.
3. Statistical-dynamical downscaling, a mixture of both approaches.

4.1.5.2 Socio-economic scenarios

Beside climatic boundary conditions, governing natural water availability, human water consumption is a main driving force of water availability. Global scenarios are too coarse to describe changes in these patterns, therefore within the IMPETUS project local scenarios have been developed (Christoph et al. 2010b):

- Scenario **M1** "Marginalization – non-support of the Drâa-Region" portrays a withdrawal of governmental and international institutions support.

- Scenario **M2** "Rural development in the Drâa-Region through regional funds" is a constant economic growth scenario. Against the background of overall political stability and supported by governmental aid programs, the Drâa-Region experiences an improvement of living conditions and economic development.
- Scenario **M3** "Business as usual" extrapolates the dominant trends of past decades. The status as a marginalized region remains unchanged and only incremental improvements in the overall living conditions and economic development occur.

The parameterization of these scenarios is pointed out in section 5.6.2.

4.1.5.3 DPSIR – A framework to assess scenario impacts

Predictions on climate change impacts are still highly uncertain. Nevertheless water managers are dependent on reliable information about likely changes within the water providing natural system. Therefore the focus of research should be set on risk assessment rather than single predictions associated with extreme ranges of uncertainty (Pittock & Jones 2000). According to the authors, thresholds critical to the considered sector should be identified and expressed as functions of climatic variables.

Concerning scenario assessments and the description of human-nature systems in general the European Environment Agency (EEA) proposed the use of a framework, which distinguished driving forces, pressures, states, impacts and responses (Stanners & Bourdeau 1995), known as DPSIR. This framework has since then been widely adopted by the EEA, other agencies and research institutions (Jun et al. 2011; Hák & Moldan 2007; Kristensen 2004). Its main purpose is giving a structure in which to present system indicators to policy makers on environmental impacts and on impacts of political actions. In Morocco the use of the DPSIR framework is promoted as well. In the Ziz catchment, neighboring the Drâa catchment, an environmental risk assessment following the DPSIR framework is currently carried out (Messouli et al. 2009).

The DPSIR framework can be considered as a causal chain leading from driving forces through pressures to states and impacts on ecosystems and society, eventually leading to political or individual responses.

With regard to water quantities the following framework can be outlined for this study (Figure 4-6). Water availability problems occur when the demand for water exceeds the amount available during a certain period. Therefore they occur frequently in areas with low rainfall and in areas with intensive agricultural activity. The associated driving forces are climate, population and the economic structure. The derived pressures are changes in water availability

or water demand, as reflected in the outlined scenarios. Consequently these pressures lead to a new state of water availability, calculated by the model and presented in the form of indicators such as average discharge or irrigation volumes. Induced by a new state are impacts on the ecosystem and the society, such as freshwater shortage in the Upper Drâa valley due to reduced discharge or in the Middle Drâa valley due to reduced reservoir inflow. Consequently riparian conflicts may arise. Possible responses range from political actions (building of new reservoirs, water pricing, enhancing economic change) to the individual level (traditional risk reduction, more efficient water use).

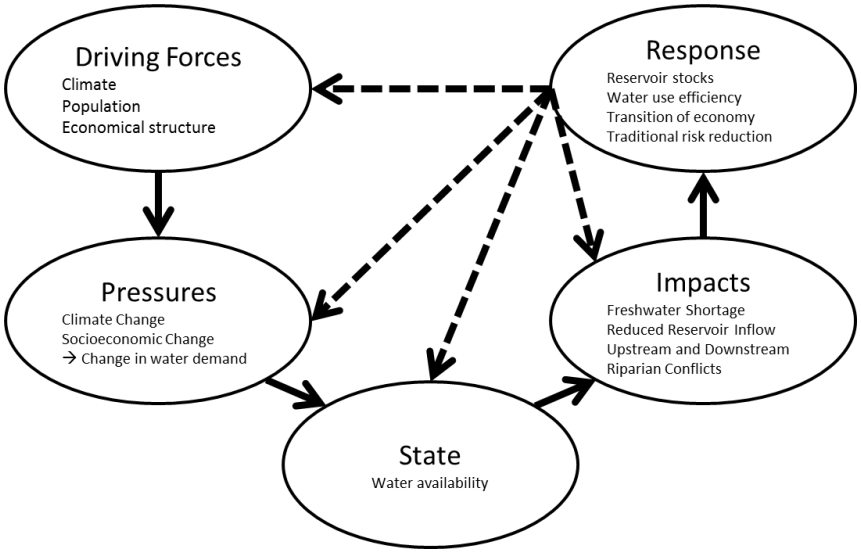

Figure 4-6: The DPSIR-framework with regard to water availability

4.1.6 Model Uncertainty

Hydrology is a science that is highly uncertain. The main reason for this is that too little is known of many hydrological processes. Additionally, we cannot observe and, consequently, cannot mathematically represent the geometry of hydrological control volumes (river beds, subsurface preferential flow paths, etc.), as well as most of the related initial and boundary conditions and biogeochemical processes (Montanari et al. 2009). Since uncertainties in hydrological modeling cannot be avoided, they have to be quantified, to enable the user to sensibly interpret model results or to point out further research directions.

4.1.6.1 Sources of Uncertainty

In general uncertainties in the **model structure** (or conceptual model), **input data** (measured data for model setup as well as for calibration and validation) and model **parameterization** are considered (Abbott & Refsgaard 1996). Inadequate conceptual models are assumed to result in uncertainties much larger than measurement errors in input data or an inadequate

choice of parameters (Beven 2002). Nevertheless uncertainty deriving from structural errors in the conceptual model is rarely addressed (Refsgaard et al. 2006). Conceptual model or structural uncertainty could be of the following categories (Abbaspour et al. 2008):

a. Model uncertainties due to simplifications in the conceptual model (e.g. Curve Number)
b. Model uncertainties due to processes occurring in the catchment but not included in the model (e.g. annual variability of irrigated areas)
c. Model uncertainties due to processes that are included in the model, but their occurrences or extent in the catchment are unknown to the modeler (e.g. complex aquifer settings)
d. Model uncertainties due to processes unknown to the modeler and not included in the model either

In addition to structural uncertainty, there are uncertainties due to errors in input variables like climate (rainfall and temperature, especially in mountainous environments), as point measurements have to be extrapolated to be used in distributed models. On the other hand spatial information (soil and land cover information) has to be aggregated to suit the spatial representation of the model. Uncertainties inherent to data used for calibration and validation (e.g. discharge data) need to be mentioned in this context as well. In ephemeral rivers these errors can be very high.

Parameter Uncertainty is closely related to equifinality, as an observed signal can be more or less reproduced with infinite equally good different parameter sets. This source of uncertainty is paid increased attention to, as inverse-modeling or autocalibration-structures are especially prone to it (Beven 2006; 2008). Consequently model structures that are dependent on calibration (grey-box or black-box) are in need of a proper parameter uncertainty assessment. The use of multiple equifinal parameter sets in so-called behavioral models is therefore recommended.

4.1.6.2 Uncertainty in Scenarios

In scenario analysis several further sources of uncertainty appear. Therefore, an analytic framework to deal with uncertainty propagation and the uncertainty cascades is clearly necessary (Rößler 2011). GCMs offer the most credible tools for estimating the future response of the climate system to the radiative forcing. These models largely agree on large-scale pattern of climatic change, but there are still essential uncertainties in regional projections (Carter et al. 1999). This uncertainty is reflected in different results of emission scenarios (varying boundary conditions) or ensemble members (varying initial conditions) or

in the use of different GCMs that the RCM is embedded in. Therefore uncertainty in regional climate model output can never be eliminated, but it can be quantified and communicated effectively (Foley 2010).

Different methods used to apply projections in an impact assessment can influence the model results of the study as much as differences between the projections themselves (Carter et al. 1999). These methods comprehend different downscaling methods or the choice of different hydrological models. By working with a range of models (GCMs, RCMs and hydrological models) and applying different downscaling techniques, general trends for a range of plausible futures can be identified. Rather than looking at a single model result that depends upon a trend, model results should be valid under a range of different conditions, especially if used to support decision-making (Foley 2010).

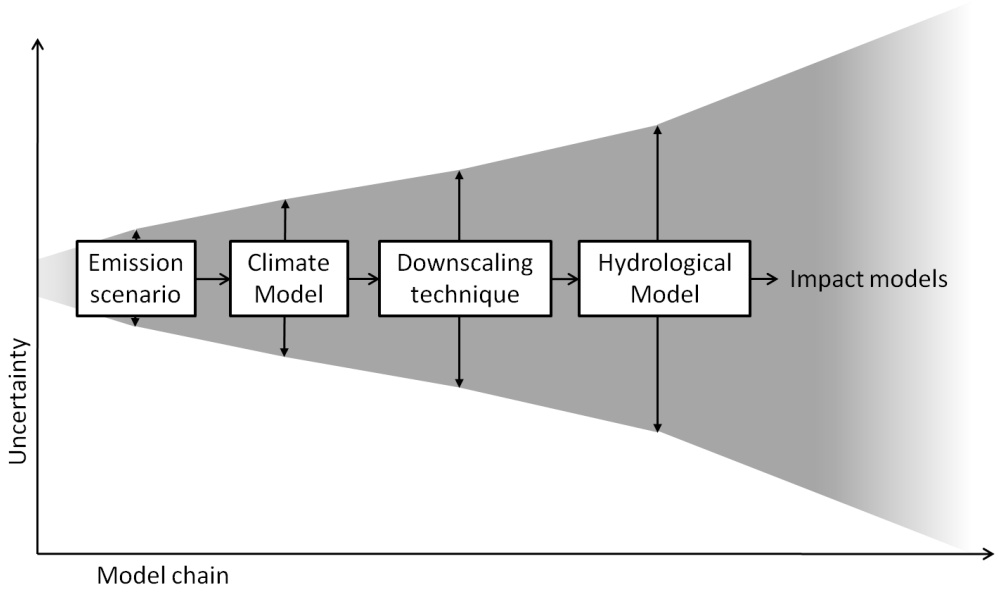

Figure 4-7: Increasing uncertainty in model chains (modified after Jones 2000)

On the one hand the full ranges of quantifiable uncertainty from all sources should be incorporated into climate change assessments wherever possible (Jones 2000; Carter et al. 1999). But on the other hand an "explosion of uncertainty" (Henderson-Sellers 1993; Jones 2000) should be avoided. The term refers to the accumulation of uncertainty throughout the process of climate change prediction and impact assessment. When the upper and lower limits of projected ranges of uncertainty are applied to impact models the range of possible impacts commonly becomes too large for recognizing general trends. This problem aggravates as more models are included in the model chain (see Figure 4-7).

4.1.6.3 Assessing Uncertainty

Knowing about the uncertainties involved in hydrological models, responsible modeling tries to quantify them. There exist several methodologies to do so for parametric uncertainty, but input data or model structure are difficult to assess in numbers. Therefore most methods assess parameter uncertainty. Beven (2008) gives an overview of techniques available and situations in which to use them. Some of the most commonly used approaches in hydrological modeling are Generalized Likelihood Uncertainty Estimation (GLUE; Beven & Binley 1992), Parameter Solution (ParaSol; van Griensven & Meixner 2007), Sequential Uncertainty Fitting (SUFI2; Abbaspour et al. 2004) and different varieties of Monte Carlo algorithms (e.g. Kuczera & Parent 1998; Vrugt et al. 2003).

Strategies to assess structural model uncertainty, e.g. by increasing parameter uncertainty margins to cover for structural errors, estimating structural terms or the use of multiple conceptual models, have drawbacks which are further elucidated by Refsgaard et al. (2006). Therefore the most common approach is to judge structural uncertainty rather qualitatively.

Within this study the SUFI2 algorithm (Sequential Uncertainty Fitting Version 2) has been used to quantify effects of parameter uncertainty on model results. Therefore numerous simulations are performed using parameters modified within physically meaningful ranges. Parameter values are chosen using the Latin-Hypercube algorithm (McKay et al. 1979). The spread in model results is assumed to reflect the model uncertainty. Assuming large parameter ranges, model results might spread beyond helpful ranges. Existing uncertainties are most likely covered, but the model turns out to be useless as results are unspecific. This problem is addressed by SUFI2, by introducing two measures: the P-factor, which is the percentage of measured data bracketed by a band displaying the 95% confidence interval of the performed simulations output and the R-factor, which is the average thickness of the band divided by the standard deviation of the measured data (Abbaspour et al. 2008). SUFI-2 starts by assuming a large parameter uncertainty, resulting in a large P- and R-factor. Sequentially parameter ranges are narrowed down, in order to maintain a large P-factor (i.e. measured data is still bracketed by the uncertainty band), while trying to minimize the R-factor (i.e. the band is getting less wide). Within each iteration the adapted parameter ranges have to be checked for physical plausibility.

4.2 Metrics to evaluate Model Performance and Model Results

In order to use model outputs for tasks ranging from research to decision support, models should be scientifically sound, robust, and defensible (Moriasi et al. 2007). In order to "prove" that a model provides sufficiently accurate results, so-called goodness-of-fit tests are useful (section 4.2.1). These are only applicable, when measured data is available, and they have to be judged in consideration of the uncertainties of the model. When it comes to scenario analyses no measured data is available, therefore other indicators are needed to communicate effectively confidence in and likelihood of specific future developments (section 4.2.2). Since the assessment of water availability is one of the prominent tasks of this study, drought measures are introduced in the final subsection 4.2.3. In the scenario analysis these will be used as impact indicators in order to quantify impacts within the DPSIR-framework.

4.2.1 Goodness-of-fit Tests

During model calibration and validation procedures statistical measures are required to declare success or failure. This section briefly portrays some of the most commonly used goodness-of-fit measures which are used in this study as well. Their strengths and weaknesses are outlined and commonly acknowledged ranges representing "good" model results are given, if available. Furthermore the possibilities of reflecting different model uncertainties in goodness-of-fit tests are reviewed. Though the need for commonly accepted guidance of model evaluation has been stressed (e.g. ASCE 1993), none has been established. Anyhow, an abundance of specific statistics and performance ratings has been developed and used for model evaluation (Moriasi et al. 2007; Janssen & Heuberger 1995). It is recommend to include at least one dimensionless statistic, one absolute error index and one graphical technique as well (Legates & McCabe 1999).

4.2.1.1 The Coefficient of Determination (r^2)

Linear regression is often used to compare predicted variables with observations. The coefficient of determination (r^2) is a statistical measure of how well the regression line approximates the observed data points. The coefficient of determination can also be interpreted as variance in the observed data explained by the model. It ranges between 0 and 1 with 1 indicating a perfect fit (and most probably a trivial model). Although r^2 is widely used for model evaluation, it is oversensitive to high extreme values (outliers) and insensitive to

additive and proportional differences between model predictions and measured data (Legates & McCabe 1999).

$$r^2 = \left(\frac{n * \left(\sum_{i=1}^{n} x_i - x_i'\right) - \left(\sum_{i=1}^{n} x_i\right) * \left(\sum_{i=1}^{n} x_i'\right)}{\sqrt{n * \sum_{i=1}^{n} x_i{}^2 - \left(\sum_{i=1}^{n} x_i\right)^2} * \sqrt{n * \sum_{i=1}^{n} x'_i{}^2 - \left(\sum_{i=1}^{n} x'_i\right)^2}} \right)^2$$

in which	n	=	number of observations
	x_i	=	observed variable
	x'_i	=	simulated variable

4.2.1.2 Coefficient of Model Efficiency (CME)

The coefficient of model efficiency (CME ; Nash & Sutcliffe 1970) is a normalized statistic that determines the relative magnitude of the residual variance compared to the measured data variance, i.e. the ratio of noise to information. It ranges between $-\infty$ and 1, with 1 indicating a perfect fit. Values less than zero indicate that the mean observed value is a better predictor than the simulated value.

$$CME = 1 - \frac{\sum_{i=1}^{n} (x_i - x'_i)^2}{\sum_{i=1}^{n} (x_i - \bar{x}_i)^2}$$

in which	n	=	number of observations
	x_i	=	observed variable
	$\bar{x}_i$	=	arithmetic mean of x_i (i = 1,...,n)
	x'_i	=	simulated variable

The CME is commonly used in hydrological modeling due to its recommendation by the American Society of Civil Engineers (ASCE 1993) and Legates & McCabe (1999). Therefore a variety of reported values are available. Since deviations of simulated to observed variables are squared, this goodness-of-fit indicator again is sensitive to outliers. Moriasi et al. (2007) reviewed reported values of CME for monthly time step hydrological models. Values of CME larger than 0.75 are considered being very good, 0.65 to 0.75 good, 0.5 to 0.65 satisfactory and values smaller than 0.5 unsatisfactory.

4.2.1.3 Index of Agreement (IoA)

The Index of agreement (IoA; Willmott 1981) is a standardized measure of the degree of model prediction error. It varies between 0 and 1, 1 indicating a perfect fit of measured and

predicted values and 0 indicating no agreement at all. The index of agreement represents the ratio between the mean square error and the "potential error", being the sum of the squared values of the distances from the predicted values to the mean observed value plus the distances from the observed values to the mean observed value. The index of agreement can detect additive and proportional differences in the observed and simulated means and variances; however, it is overly sensitive to extreme values.

$$IOA = 1 - \frac{\sum_{i=1}^{n} (x'_i - x_i)^2}{\sum_{i=1}^{n} \left(\left| x_i - \bar{x} \right| + \left| x'_i - \bar{x} \right| \right)^2}$$

in which	n	=	number of observations
	x_i	=	observed variable
	$\bar{x}_i$	=	arithmetic mean of x_i $(i = 1,...,n)$
	x'_i	=	simulated variable

4.2.1.4 Root Mean Square Error and Mean Absolute Error (RMSE, MAE)

The root mean square error, RMSE, and mean absolute error, MAE, are well-accepted absolute error indices. The latter, accounting for the deviations as absolute values, is less sensitive to outliers than the RMSE. Both do not allow for compensations of positive and negative discrepancies.

$$RMSE = \sqrt{\frac{\sum_{i=1}^{n} (x_i - x'_i)^2}{n}} \qquad MAE = \frac{\sum_{i=1}^{n} \left| x_i - x'_i \right|}{n}$$

in which	n	=	number of observations
	x_i	=	observed variable
	x'_i	=	simulated variable

Singh et al. (2005) state that RMSE and MAE values less than half the standard deviation of the measured data may be considered low, hence indicating good model performance.

4.2.1.5 Graphical Techniques

Graphical techniques provide possibilities for visual comparison of simulated and measured data and allow to judge model performance qualitatively in a first overview. Legates & McCabe (1999) underline the importance of graphical techniques for appropriate model evaluation. Two commonly used graphical techniques, hydrographs and exceedance probability curves, are frequently used (e.g. van Liew et al. 2005).

A hydrograph is a time series plot of simulated and measured flow throughout the calibration and validation periods. Hydrographs help identify differences in timing and magnitude of peak flows and the shape of recession curves. Percent exceedance probability curves for different time steps can illustrate how well the model reproduces the frequency of measured flows. A general agreement between observed and simulated frequencies indicates adequate model performance over a range of different conditions (e.g. dry and wet periods).

4.2.1.6 Uncertainty-considering Criteria

Harmel et al. (2006) showed that substantial cumulative uncertainty in hydrological data can result when individual errors from all procedural data collection categories are considered. Therefore, care needs to be taken while calibrating or validating models on basis of measured data. This accounts especially for water quality and sediment data, but discharge measurements in arid mountainous regions are hampered by considerable uncertainties as well (e.g. EI-Hames & Richards 1994).

Harmel & Smith (2007) propose to account for uncertainties using specialized goodness of fit tests. Basically the commonly used indicators are used, but a fit of simulated and measured data is assumed, when simulated data lies within the uncertainty range of the measured data. These indices are referred to as mCME, mIoA, mRMSE and mMAE (m for modified) in this study. A basic drawback, increasing model goodness with increasing measurement uncertainty, remains unresolved. Anyhow the focus on imperfect data used for model assessment is valuable.

4.2.2 Analysis of Scenario Effects

To express confidence in scenario results, indices that go beyond standard quality measures are required. Many model applications suffer from the fact that model suitability for scenario analysis is not addressed despite well-known sources of uncertainty within the modeling process (Bormann 2005). This topic is gaining increased attention within the IPCC-reports (Solomon et al. 2007). The authors distinguish (in analogy to uncertainties lined out in section 4.1.6) structural uncertainties and value uncertainties. Structural uncertainties can only be discussed qualitatively, but it needs to be considered in scenario analysis as well, representing experts' confidence in scenario results. Value uncertainties should generally be estimated using statistical techniques and expressed probabilistically. This section provides two methodologies to do so. While the SNR_m provides a measure of confidence in the model structure, scenario trends etc., the Likelihood terminology allows to formulate a relative probability of certain outcomes.

4.2.2.1 Signal-to-Noise-Ratio

Though uncertainty assessments have become widely applied in hydrological science, they are commonly performed separated from scenario assessment. However, as the model used for scenario computation is not free from uncertainties, they should be compared to the effect of the scenario itself. Therefore Bormann (2005) introduced the "Signal to noise ratio" (SNR) to determine the suitability of a model for scenario analysis.

$$\mathrm{SNR} = \left[\frac{\frac{|X_b - X_s|}{X_b}}{\frac{1}{n}\sum_{i=1}^{n} \frac{|X_b - X_{i,uc}|}{X_b}} \right] - 1$$

in which

SNR	=	"signal - to - noise ratio"
X_b	=	value of the reference scenario
X_s	=	value of the scenario
$X_{i,uc}$	=	values of the n realisations of the uncertainty analysis carried out fr the baseline scenario

The SNR is a comparative index between the uncertainty of a model and the change effects of scenario calculations. It enables the comparison of model uncertainty to the effects of scenarios as well as the comparison of particular uncertainty sources such as climate scenario ensembles or downscaling techniques.

Since in this study the effects of different uncertainty sources will be explicitly quantified for the scenarios (see section 5.7.2), a "modified Signal to Noise Ratio" (SNR_m) can be formulated, rather than assuming the model uncertainty of the baseline scenario perpetuating.

$$\mathrm{SNR_m} = \left[\frac{\frac{|X_b - X_{s,mean}|}{X_b}}{\frac{1}{n}\sum_{i=1}^{n} \frac{|X_{s,mean} - X_{s,i}|}{X_{s,mean}}} \right] - 1$$

in which

$\mathrm{SNR_m}$	=	modified "signal - to - noise ratio"
X_b	=	value of the baseline scenario
$X_{s,mean}$	=	average scenario value
$X_{s,i}$	=	values of the n realizations of the specific scenario

SNR_m indices should be interpreted as follows: positive SNR_m values indicate that scenario effects are larger than uncertainty effects. Values larger than 1 indicate that scenario effects at least double uncertainty effects (high SNR_m). Negative SNR_m values imply that uncertainties cover up scenario effects.

The SNR_m can be used for scenario analysis and furthermore to quantify and eventually rank sources of uncertainty within scenario analysis. In this study uncertainty ranges are attributed to different sources (all considered uncertainties, model uncertainties, downscaling and ensemble uncertainty) by averaging model results of each specification (i.e. hydrological model, downscaling approach or climate change scenario ensemble) and attributing the remaining spread in results to the source of uncertainty considered.

4.2.2.2 Likelihood

The IPCC proposed a terminology (Risbey & Kandlikar 2007; Solomon et al. 2007) that quantifies the likelihood of a specific outcomes occurrence by indicating their relative occurrence in model results (see Table 4-1). This common nomenclature facilitates the comparison of model results by decreasing arbitrariness of formulations. This relative measure of likelihood excludes any kind of subjective uncertainty (confidence in model structures, scenario development etc.), which therefore has to be addressed separately, e.g. by the SNR_m.

Table 4-1: Likelihood defined as probability of a certain outcomes occurrence (Solomon et al. 2007).

Terminology	Likelihood of occurrence
Virtually certain	> 99%
Extremely likely	> 95%
Very likely	> 90%
Likely	> 66%
More likely than not	> 50%
Unlikely	< 33%
Very unlikely	< 10%
Extremely unlikely	< 5%

4.2.3 Drought Indicators

Drought is usually defined in terms of a moisture deficit leading to ecological stress and eventually human distress. Most definitions are relative that is, the supply shortage of moisture is assessed in relation to the demand for that moisture, so that absolute drought thresholds will vary between regions (Wilhite 1996). The prevalence of drought is dependent of the system considered. Therefore drought is often classified into four types (Mishra & Singh 2010; Wilhite & Glantz 1985; Palmer 1965):

Meteorological drought is a period with precipitation below normal. It is often associated with above-normal temperatures, and precedes and causes the subsequent types of droughts. **Hydrological drought** occurs when streamflow and water storage (such as aquifers or reservoirs) fall below long-term mean levels. Hydrological drought develops more slowly

than meteorological drought, because storage systems buffer or delay the effect of little precipitation. **Agricultural drought** is a period in which soils dry out as a result of below-average precipitation or above-normal evaporation, leading to reduced crop production or crop failure. The term **socio-economic drought** refers to the failure of water management structures to cope with the conditions outlined above, which is the case when eventually water demand of the society exceeds supply.

Besides absolute drought thresholds that can be determined for water-dependent systems, a variety of relative drought indicators has been developed in recent decades, in order to detect the occurrence of a drought and to quantify intensity, duration, severity and spatial extent (Mishra & Singh 2010; Heim 2002).

The **standardized precipitation index** (McKee et al. 1993) for any location is calculated, based on the long-term precipitation record. This long-term record is fitted to a probability distribution (most common are log-normal or gamma), which is then transformed to a normal distribution of which average and standard deviation are determined. The success of fitting should be validated using an appropriate test (e.g. Kolmogorov-Smirnov or Mann-Whitley). The time series can now be normalized, so that the mean SPI for the location and desired period is zero, and the standard deviation is 1. Values of the SPI are associated with drought or wet conditions according to the following Table 4-2.

Table 4-2: Drought conditions associated with SPI-Values (adapted from McKee et al. 1993)

SPI Values	Drought Category	Time in category
≥ 2.00	Extremely wet	2.3%
1.50 to 1.99	Severely wet	4.4%
1.00 to 1.49	Moderately wet	9.2%
-0.99 to 0.99	Near normal	68.2%
-1.49 to -1.00	Moderately dry	9.2%
-1.99 to -1.50	Severely dry	4.4%
≤ -2.00	Extremely dry	2.3%

The **Standardized Runoff Index** (Shukla & Wood 2008) follows exactly the same methodology as the SPI, only that streamflow records are used instead of precipitation records. The **Palmer Drought Severity Index** (PDSI; Palmer 1965) is a more sophisticated index that accounts for the buffering effect of soil water storage.

Reaction times to the onset of a drought are different between the indices. The rainfall-driven SPI reacts fast, the soil-moisture considering PDSI has an intermediate reaction and the hydrology-considering SRI the longest reaction-time. All indices can be calculated for cumulated values of 1 to 12 months depending on the scale of interest.

4.3 Modeling Hydrological Processes in Arid Mountainous Regions – State of the Art

As outlined previously, description and modeling of hydrological phenomena is dependent on the purpose of the analysis on the one hand and the associated scale on the other hand. This section introduces some exemplary modeling studies conducted in (semi-)arid and/or mountainous regions.

Hydrological data are lacking in arid regions for a variety of reasons, making empirical methods of flood estimation unsatisfactory (EI-Hames & Richards 1994). Anyhow, since surface runoff results from storm intensity exceeding soil infiltration, similar flood frequency curves can be derived from different arid regions. Farquharson et al. (1992) compiled data from more than 160 discharge gauges from arid regions in Northwest Africa, Iran, Jordan, Saudi Arabia, Botswana, South Africa, Australia, southwest USA and Russia. The authors conclude that the combination of estimated mean annual floods and regional flood frequency curves permits flood magnitudes with a known risk of exceedance to be derived for arid zones of the world even where local flow data are unavailable. Knighton & Nanson (2001) successfully described relationships of annual discharge, the average number and length of zero-flow periods, and event duration as power functions of drainage area. Anyhow, flood flows cannot be described that easily, as transmission losses and soil moisture conditions gain importance. On the regional scale the required data is hardly available.

Physical based modeling offers a promising approach to overcome this data shortcoming. According to EI-Hames & Richards (1994) suitable models should consist of at least the following modules: infiltration and runoff production; overland flow routing; channel routing to propagate flood waves down wadis beyond runoff source areas and transmission losses into the wadi beds.

Hydrological modeling in arid regions has widely been focused on transmission losses, since they are known to be the dominant recharge mechanism in many arid regions (compare section 2.5 and 2.6). A broad variety of model structures exists (Cataldo et al. 2004). Regression techniques are most frequently used (e.g. Sharma & Murthy 1994). The empirical approach developed by Lane (1983) is incorporated in many actual modeling systems, including SWAT, using effective infiltration parameters and a variable channel bed area to compute transmission losses. Rao & Maurer (1996) coupled an infiltration function with a stage-discharge relationship. They integrate this relationship over the entire reach, creating a one parameter loss model that can be easily calibrated using stream gauge data. This approach retains a non-linear relationship between transmission losses and flow. More sophisticated

modules contain the coupling of St-Venants and Richards equation (e.g. EI-Hames & Richards 1994). The importance of transmission losses has to be further stressed, as modeling results from the arid Kuiseb river in Namibia indicate that transmission losses concentrate during high discharge peaks and are minor during small to medium flows (Lange 2005). This behavior is attributed mainly to enhanced water losses in flooded overbank areas.

It is denoted that seepage does not only represent a sink, but potentially forms bank storage that contributes to low flow after the flood wave has passed (Chen et al. 2006; Chen & Chen 2003). Using a numerical model for different idealized flood situations the authors pinpoint the differences between idealized linear-aquifer response and bank storage effects. Therefore they stress the general importance of incorporating bank storage effects in catchment models, at least if the considered time scale is days to weeks.

Gheith & Sultan (2002) adopted a model that estimated transmission losses in the Egypt desert. They developed an integrated model containing spatial rainfall distribution and appropriate effective infiltration parameters. Within 4 different catchments (7,000-15,000 km²), groundwater recharge rates through transmission losses from 21 to 33% of the precipitation have been determined for a 1994 storm event.

Lange (1999) developed a non-calibrated rainfall-runoff model for the 1400 km² Nahal-Zin catchment in Israel. Focusing on Hortonian surface runoff generation (spatially distributed, according to land-cover) and transmission losses, robust estimates of discharge volume during short-duration floods could be made.

In semi-arid areas, the lateral redistribution of surface runoff between adjacent landscape units is an important process. Therefore Güntner & Bronstert (2004) developed the WASA modeling system (Model of Water Availability in Semi-Arid Environments) that explicitly accounts for toposequences. By delineating areas characterized by a typical toposequence, organized and random variability of landscape characteristics is captured in the model, hence lateral surface and subsurface water fluxes between modeling units at the hillslope scale are represented. According to the authors re-infiltration of surface runoff and lateral redistribution processes between landscape patches cause a reduction of runoff volumes at the catchment scale and contribute to the amplification of variations in runoff volumes relative to variations in rainfall volumes for semi-arid areas.

Jothityangkoon et al. (2001) draw a more detailed image by analyzing governing processes on different time-scales (annual, monthly and daily) and spatial scales (13 to 2,545 km²) in semi-arid Western Australia. At the annual time scale, a simple water balance model including surface runoff and evaporation is found adequate, including spatial differentiation in soil

depth and precipitation. At the monthly time scale, additional processes such as subsurface runoff and differentiation of evapotranspiration in bare soil evaporation and fluctuating transpiration had to be considered. At the daily time scale further differentiation of groundwater had to be included to capture prolonged low flow. For larger catchments the authors included a routing module. This module helped the model to match measured discharge, but did not contain any aquifer interactions. The authors conclude that the spatial distribution of soil depths is the most important control on runoff variability at all time and space scales. A similar approach is chosen by Hughes (1994) who compares the performance of four different rainfall-runoff-models in a small (0.18 km^2) grassland catchment in South Africa. The models vary in complexity, ranging from a sub-daily to monthly time steps; two soil layers to a lumped soil module and SCS-Curve number procedure to Green-Ampt infiltration model. Channel and groundwater processes are not included in the models. Considering discharge, the performance of all four models is reasonably well, but measured soil moisture is captured only by the sub-daily model. These finding can hardly be extrapolated to larger scales, as the importance of channel and groundwater processes is increasing and therefore the effect of soil moisture loses relative importance. Consequently the monthly Pitman-model and the sub-daily VIT-model have been applied to the 28,000 km^2 catchment of the Sua-Pan in Botswana (Hughes 1995). The author concludes that two major errors hamper hydrological modelization in arid regions, the conceptual structure of the runoff generation processes and the extent to which the model input rainfall data is representative. The problems are interlinked, as high resolution rainfall data is a prerequisite for successful elaborate modeling of infiltration processes.

As these data are rarely available for large scale applications in arid regions, design storms (i.e. artificial precipitation records) are frequently used to model catchment response to severe storms or relative impacts of land-cover change.

Foody et al. (2004) use the HEC-HMS modeling system to predict peak discharge rates for design storms in the Eastern Desert of Egypt. The model is driven by information on land cover distribution (derived by satellite remote sensing) and soil properties (derived from field measurement). Design storm scenarios cannot be validated, but channel segments prone to high throughflow are identified. In this study corresponding places suffered flood damage during previous floods. The results indicate the potential to drive an integrated hydrological model from limited data to derive important and useful hydrological information in a region where data are scarce.

A variety of studies has been conducted in the semi-arid Walnut Gulch experimental catchment, Arizona. Process-studies have been highlighted in chapter 2. This section introduces some of the modeling studies carried out.

Goodrich et al. (1997) stress the impact of nonlinearity for regional model studies. Applying conceptual models to 29 subcatchments of the Walnut Gulch the authors denote that catchment response to rainfall becomes more nonlinear with increasing catchment scale, assuming a transition threshold of 37–60 ha. Again, increasing importance of transmission losses but also sub-scale storm coverage is considered as cause.

In the same catchment Hernandez et al. (2000) set up one event-based model with a one-minute time step (KINEROS), and one continuous model with a daily time step (SWAT). Noting that the lack of distributed rainfall data is a limiting factor in many arid regions, the authors point out the use of these models to assess relative impacts resulting from land cover change using design rainfall for input. They further stress the potential of commonly available datasets for the assessment of hydrological response to land cover change.

Reynolds Creek, another experimental catchment of USDA Agricultural Research Service, is located in the Rocky Mountains, Idaho, and represents semi-arid mountainous steppe. Process-studies carried out in Reynolds Creek have been presented in chapter 2. Flerchinger & Cooley (2000) conducted a long term assessment of the water balance of the Upper Sheep Creek Catchment (26 ha, subcatchment of the Reynolds Creek). Evapotranspiration was calculated, using the validated Simultaneous Heat and Water (SHAW) Model, to be 90% of the annual precipitation (450 mm). Compared to the measured discharge, a water balance error of 10% was detected, which has been attributed to deep percolation losses in fractured basalts. Simulated runoff was primarily fed by subsurface flow. In the simulation, above a threshold of 50 mm precipitation, approximately 67% of the water percolating beyond the root zone produces runoff.

Bathurst & Cooley (1996) developed a snow-melt routine for the physically based SHE model (Abbott et al. 1986a) that was tested in Reynolds Creek as well. As outlined earlier, one purpose of physically-based models may be to test different hypothesis about systems behavior (see section 4.1). In this case, four hypotheses of catchment response, based on different representations of the soil permeability and subsurface flow patterns were examined: (1) impermeable (frozen) ground surface; (2) fully permeable soil profile (3) reduced soil permeability away from the channel; (4) rapid, near-channel subsurface response. Hypothesis (4) could explain observed discharge best, providing ideas for the next field campaigns.

Most studies presented here denote the high levels of uncertainty associated with hydrological modeling in arid regions. Though these uncertainties can hardly be reduced one important modeling task is to quantify them. Therefore several techniques have been developed (see section 4.1.6).

McMichael et al. (2006) used the Generalized Likelihood Uncertainty Estimation (GLUE) methodology for calibration, testing and predictive uncertainty estimation of the MIKE-SHE hydrological model in a semi-arid shrubland catchment in central California. Monthly discharge has been modeled, and the 5% and 95% uncertainty bounds of reasonable parameter sets have been considered as model results. Though only spreads of results are presented differences to land-use scenarios were significant. A similar approach is incorporated in the Sequential Uncertainty Fitting program (SUFI-2) and has been tested in macro-scale applications of SWAT in Iran (Rostamian et al. 2008; Faramarzi et al. 2009) and Western Africa (Schuol et al. 2008).

In the High Atlas some modeling studies have been conducted as well. Chaponnière et al. (2008) applied SWAT in a small headwater catchment (227 km²) on the northern flank of the High Atlas. It was pointed out that conceptual models such as SWAT can hardly be validated on observed streamflow alone. Although necessary, this analysis is not sufficient to estimate the quality and realism of the modeling since all processes of the water cycle are integrated in measured streamflow. Many modeled processes can only be validated with appropriate data. In this study the authors identified superimposing groundwater, soil water and snow dynamics. They therefore conducted tracer studies und snow cover monitoring to quantify the respective processes. The authors identify several groundwater components concluding that an appropriate model should account for different aquifers.

Within the IMPETUS framework several modeling studies have been conducted in the Drâa catchment. Weber (2004) successfully applied the physically based model ARID to model soil water dynamics at the local scale. Model predictions on discharge could not be validated, as discharge data was not available. Anyhow, the understanding of infiltration processes along toposequences as obtained from measurements has been confirmed.

Kutsch (2008) applied the physically based model HYDRUS-1D to the Upper Drâa catchment to analyze soil water dynamics. The importance of local groundwater recharge mechanisms has been highlighted for elevated regions, whereas the importance of local recharge in the lowlands can be neglected.

Since the relevant processes vary, as the considered scale changes, different models are necessary for regional hydrological studies.

In the 1240 km² Ifre-catchment the Snowmelt Runoff Model (SRM) has been applied (Schulz 2007; Schulz & de Jong 2004). The importance of both, snowmelt and high intensity precipitation events as discharge generating processes has been accentuated by the model results. Lacking modules for irrigation and channel routing confine the applicability of the SRM to the montane regions.

The Modular Modeling System (MMS) has the potential to overcome these shortcomings. Feasibility studies have been carried out in the same catchment (de Jong et al. 2008; de Jong et al. 2006; de Jong et al. 2004).

5. Hydrological Model of the Upper Drâa Catchment

This section will follow the outline of the modeling process given in section 4.1. A perceptual model of the hydrological processes in the Upper Drâa region has been given in the section 3.8. The dominant hydrological processes in both, arid and mountainous regions have been outlined. The idealized concept of model development envisages a model that suits a specific demand and a specific site. This is often foiled by the broad availability of ready-to-use computer models on the one hand, and limited resources of the user. This is true for this study as well. The conceptual structure of the model SWAT has been considered as generally appropriate for this study, considering the aim of the study, data availability and the concluding degree of model complexity. Some modifications of the original model have been carried out (as described in section 5.1.2.) in order to adapt it to the local specifics of an arid mountainous catchment. The following sections present the subsequent steps of model development. The spatial discretization of the model is presented, and most parameters are set according to the reflections lined out in chapter 3. Calibration and validation are carried out and critically reviewed in section 5.4 and 5.5. As the assessment of surface water resources in the coming decades is one of the objectives of this study, the scenario development is lined out in the following section. The chapter concludes with the development of an uncertainty assessment scheme for the baseline model as well as the scenarios. Results are presented in the next chapter.

5.1 The Conceptual Model

A first approach to model the hydrological behavior of the catchment is a simple rainfall-runoff relationship. A suitable polynomial regression can be found for the mean annual precipitation of 12 precipitation gauges within the catchment and the discharge into the reservoir (Figure 5-1). For the Validation period an r^2-value of 0.76 indicates an adequate quality of the relationship. Regarding monthly or seasonal variations of runoff simple rainfall-runoff relationships come to their limits, as many processes delay or modify runoff. As pointed out in the previous chapters those processes are at least baseflow, transmission losses, snow dynamics and irrigation. Consequently a more complex model, incorporating more elaborate process representations, is clearly needed. Due to the high altitudinal and spatial variability a spatially distributed representation of the catchment is crucial as well. Considering the purpose of water availability assessment, monthly time steps seem appropriate (see section 4.1.1.1).

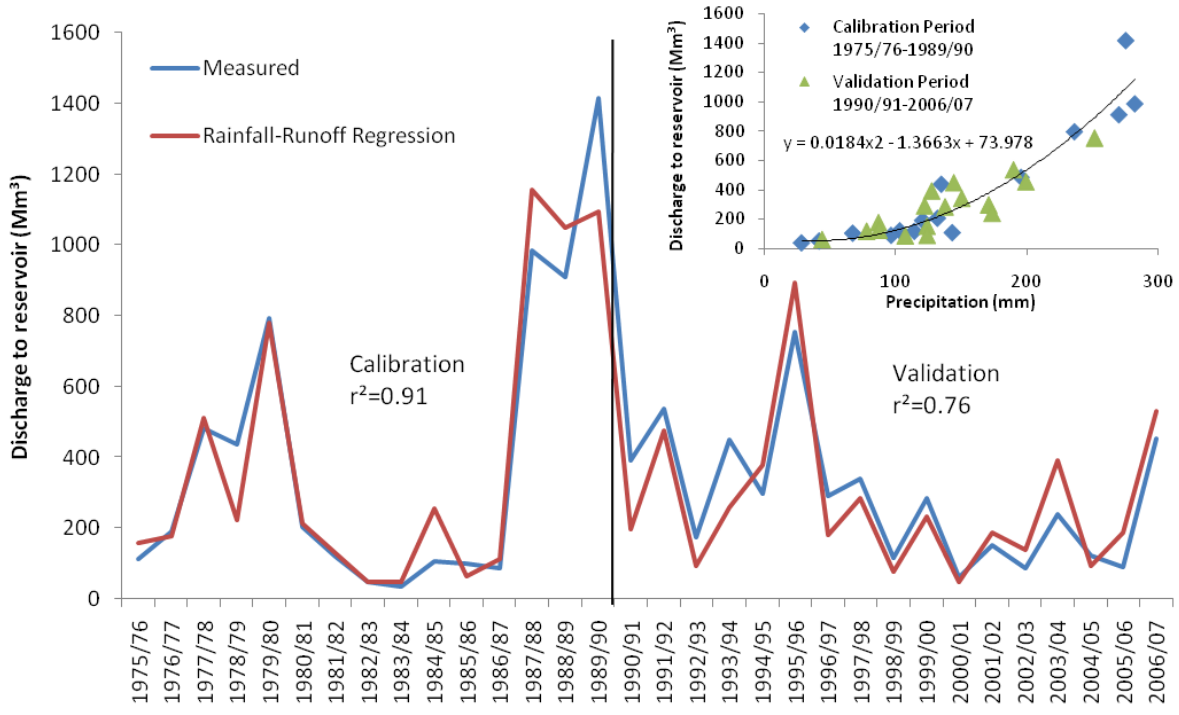

Figure 5-1: Annual Rainfall-Runoff relationship for the Upper Drâa catchment (15.000 km²). (Measured data: SE Ouarzazate)

5.1.1 Basic Model: SWAT

SWAT (Soil Water Assessment Tool, Version 2005; Arnold et al. 1993) accounts for most of hydrological processes relevant in the research area, including snow hydrology and channel processes, while maintaining simple approaches (Figure 5-2), so that hydrological complexity and data scarcity are considered at the same time. Selected equations are presented within this section, while others can be found in the manuals (Neitsch et al. 1999; Neitsch et al. 2004). SWAT2005 has proven capable of simulating hydrological processes in high mountain areas (Cao et al. 2006; Fontaine et al. 2002), as well as in semi-arid zones (Menking et al. 2003; Hernandez et al. 2000). SWAT has also been applied to a small headwater catchment in the High Atlas (Chaponnière et al. 2008).

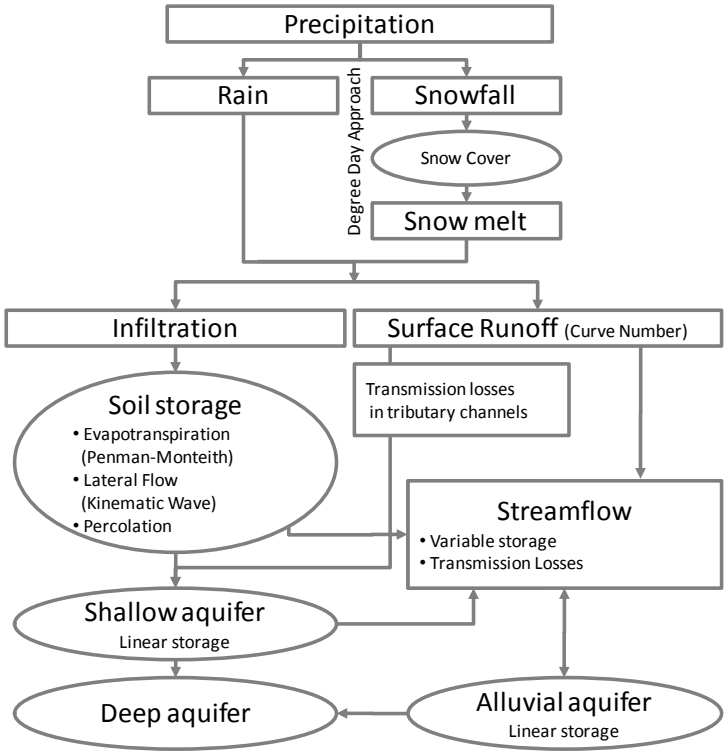

Figure 5-2: Simplified schematic diagram of the water movement as simulated by SWAT (modified after Arnold et al. 1993)

The following Table 5-1 provides an overview of the SWAT routines used in this study. Several other routines (sediment, nutrients) as well as parameters that regulate daily flow (surface runoff delay, etc.) have not been considered due to the scope of this study, which is to assess water availability on a monthly timescale. Therefore the respective parameters have been set to default values. The derivation of the parameters listed in Table 5-1 is lined out in section 5.3.

Table 5-1: SWAT-routines and required parameters. Parameters are described in Appendix 3, values are determined in section 5.3. For details on the model routines see (Neitsch et al. 1999)

SWAT routine	Process description	Associated parameters and variables
Interception	indirectly modeled as initial abstractions in Curve Number method	see Surface runoff
Surface runoff	NRCS Curve Number	climate data: PCP CN2, HYDGRP
Snow	Degree-Day-Approach	climate data: PCP, TMP SFTMP, SMFMN, SMTMP, SNO50COV, SNOCOVMX
Soil Water Percolation	Storage routing Transit time	SOL_AWC, SOL_BD and SOL_CLAY, SOL_K, GW_DELAY
Lateral flow	Kinematic storage model	SOL_K, HRU_SLOPE, SLSOIL
Groundwater flow	Linear storage model	RCHRG_DP, ALPHA_BF
Potential evapotranspiration	Penman-Monteith	climate data: PCP, TMP, WND, RH, RAD CHTMX, GSI, SOL_ALB, SOL_ZMAX, RDMAX
Actual evapotranspiration	Soil evaporation Plant transpiration Revaporation	SOL_Z, ESCO see potential evapotranspiration GW_REVAP
Transmission Losses	Effective conductivity	Channel width and channel length CH_K1, CH_K2, ALPHA_BNK
Crop growth	Heat units concept	climate data: TMP ALAI, BLAI, T_BASE, T_OPT→LAI

Within SWAT water fluxes are calculated on a daily basis for hydrological response units (HRU), elementary spatial units, considering land cover, soil type slope and indirectly elevation. Within each HRU precipitation occurs either as rain or snow, depending on temperature. Snowfall is added to the HRUs snowpack, which starts melting, when temperature rises. Snowmelt is quantified by a degree-day approach (Fontaine et al. 2002).
Snowmelt and precipitation either infiltrate or generate surface runoff according to the NRCS Curve Number method (US National Resource Conservation Service; NRCS 1986), an empiric rainfall-runoff relationship, taking into account land-cover and antecedent soil moisture condition. Hence infiltration is not directly modeled but regarded as rainfall minus surface runoff (Neitsch et al. 1999):

$$Q_{surf} = \frac{\left(R_{day} - 0.2 * 25.4 * \left(\frac{1000}{CN} - 10\right)\right)^2}{\left(R_{day} + 0.8 * 25.4 * \left(\frac{1000}{CN} - 10\right)\right)}$$

in which Q_{surf} = Daily surface runoff [mm]
R_{day} = Daily precipitation [mm]
CN = Curve Number [-]

Interception is calculated as a by-product of the Curve Number approach. It is therefore independent from the development of the vegetation. Due to the little vegetation cover in the study area, the error can be considered small. It has been noted that the Curve Number method gives a faulty representation when saturation-excess runoff is the dominant runoff type (Easton et al. 2008; Garen & Moore 2005). Since infiltration-excess of the Hortonian type is the dominant runoff-generating process in the catchment (see section 2.3), the procedure appears to be adequate.

Infiltrating water is distributed between the different soil layers according to saturated conductivity and soil water content. The permanent wilting point is calculated as:

$$WP = 0.4 * m_c * BD$$

in which	WP	=	Wilting point, expressed as a fraction of the total soil volume [%]
	BD	=	Bulk density [t/m³]
	m_c	=	Clay content [%]

As the available water capacity is provided as a model parameter, field capacity can be calculated as the sum of wilting point and available water capacity. Water volumes above field capacity are routed to lower soil layers, delayed according to the layers saturated hydraulic conductivity. If the saturated hydraulic conductivity of the lower layer is lower than that of the upper layer lateral subsurface flow is quantified by a kinematic wave approach accounting for slope, slope length and saturated conductivity (Sloan & Moore 1984).

Evapotranspiration is calculated using a modified Penman-Monteith approach (Allen et al. 1989a). The approach has been chosen as required data are available in a daily resolution and regional characteristics (aridity, frost, advective conditions) constrain the application of simpler approaches. Due to diurnal distributions of the required climatic variables, the daily calculation of evapotranspiration might result in faulty values, but given the data availability there exist no alternatives. Furthermore in the research area evapotranspiration is usually limited by water availability and not by evaporative demand; therefore the error should be small. While transpiration is calculated directly by the Penman-Monteith approach by using the respective plant parameters, potential evapotranspiration is determined by applying the Penman-Monteith approach to a fictional well-watered Alfalfa grass of 50 cm height. Based on the acquired values the plant specific actual transpiration, evaporation from interception storage and snow are satisfied. The remainder is the evaporative demand from the soil.

This is satisfied by calculating the evaporative demand for a given soil depth (Neitsch et al. 1999):

$$E_{soil,z} = E'_s * \frac{z}{z + \exp(2.374 - 0.00713 * z)}$$

in which	$E_{soil,z}$	=	Evaporative demand at depth z [mm]
	E'_s	=	Total evaporative demand from soil [mm]
	z	=	Soil depth [mm]

Then the evaporative demand for a soil layer is calculated (Neitsch et al. 1999):

$$E_{soil,layer} = E_{soil,zl} - E_{soil,zu} * esco$$

in which	$E_{soil,layer}$	=	Evaporative demand from soil layer [mm]
	$E_{soil,zl}$	=	Evaporative demand at lower layer boundary [mm]
	$E_{soil,zu}$	=	Evaporative demand at upper layer boundary [mm]
	$esco$	=	Evaporation from soil compensation factor [-]

ESCO represents a conceptual parameter that allows the user to calibrate soil evaporation. If the soil layers are above field capacity, water might as well leave the soil profile downwards, entering the shallow aquifer. Transfer through the vadose zone is simulated by a mean residence time. A fraction of the percolating water is diverted to a deep aquifer and permanently lost from the system. The shallow aquifer is represented by linear storage.

Lateral flow and baseflow directly enter the channel, whereas surface runoff is routed through tributary channels accounting for transmission losses via effective conductivity (Lane 1983). These transmission losses enter the shallow aquifer directly. The remaining surface runoff enters the primary channel as well. Discharge is then routed using the variable storage concept (Williams 1969), again accounting for transmission losses that are entering bank storage.

5.1.2 Adaptations: SWAT-MAROC

First test runs with SWAT2005 showed poor results and the following modules (Figure 5-3) had been added to the model in order to overcome the identified shortcomings: Spatially explicit elevation bands, an alternative irrigation module and a second linear storage aquifer. To avoid confusion with the original model the new version is referred to as SWAT-MAROC (Soil Water Assessment Tool – Mountainous and Arid Region Oriented Concept).

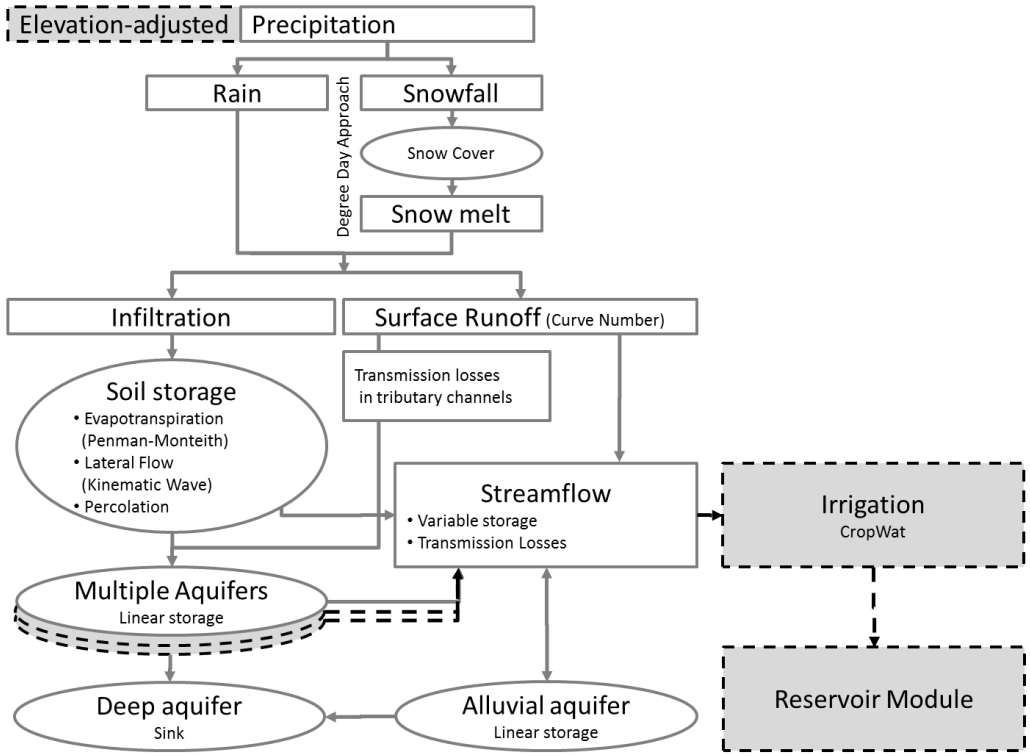

Figure 5-3: Simplified schematic diagram of the water movement as simulated by SWAT-MAROC (new modules in grey)

Furthermore a conceptual reservoir component has been added, in order to provide input data for subsequent modeling studies foreseen in the IMPETUS-project (Klose et al. 2010b), and to estimate siltation effects on the reservoir.

5.1.2.1 Elevation-accounting HRU

Hydrological Response units represent the smallest model unit within the original SWAT model, accounting for land-use, soil and slope. The proposed new type of HRU in SWAT-MAROC accounts spatially explicit for elevation as well.

Motivation

The subdivision of the catchment into model units enables the model to reflect varying importance of different hydrological processes in different environments. Within the original model, HRUs account for differences in soil, land cover and slope. So-called elevation bands have been introduced, to account for elevation as well (Fontaine et al. 2002). These elevation bands allow the user to work with precipitation and temperature gradients, but they are not spatially explicit. It has been shown that especially in arid mountainous regions not only precipitation sums vary with altitude, but also the number of precipitation days (see section 2.1). Therefore the use of elevation bands results in poor model performance in the Upper Drâa catchment (Petros 2009). The proposed model change is to implement spatially explicit elevation bands that can be modeled using different climate data series in each elevation. Therefore a new spatial model unit is introduced, the elevation accounting HRU or EHRU. This is expected to increase the models accuracy and give a better physical based representation of the water balance as most processes lined out in chapter 2 and 3 vary drastically with altitude.

Model Modification

Two modifications are addressed, the spatial derivation of the EHRU and the generation of elevation-adjusted time series of precipitation. Both steps have been taken as part of the preprocessing and they are not part of the model code.

As climate data is linked to subbasins rather than HRUs within SWAT, hydrological subbasins have to be intersected with elevation zones, before being further differentiated according to soil and land use. In this study this was done by resampling the DEM to a resolution of 1 km and then manually modifying the resulting coarse DEM to receive connected elevation bands within the subbasins (when possible). For next model versions this could be rendered obsolete by assigning elevations to HRUs and linking climate data to the HRUs.

Based on this change in regionalization of model units, elevation has been explicitly taken into account for the regionalization of climate data. Elevation accounting HRUs can now be

linked with elevation-specific climate data. As these data do not exist necessarily for all elevation zones it has to be extrapolated from precipitation gauges nearby.

The model uses semi-generated precipitation series for altitudes not covered by precipitation gauges. Semi-generated time series consist of two components: measured precipitation from adjacent gauges adjusted for altitude and a stochastic component. Adjustment for altitude is done adding some elevation specific amount to measured precipitation.

$$PCP1_{day,EHRU} = PCP_{day,Base} + plapse*(elevation_{EHRU} - elevation_{base})$$

in which	$PCP1_{day,EHRU}$	=	Daily precipitation adjusted to EHRU(mm)
	$PCP_{day,Base}$	=	Daily precipitation at gage (measured)
	$plapse$	=	Precipitation lapse rate (mm/km)
	$elevation_{EHRU}$	=	Mean elevation of the EHRU (km)
	$elevation_{base}$	=	Elevation of the gage (km)

This lapse rate can be derived from daily precipitation data as lined out in section 5.3.6.1. In addition random wet days need to be added, as the adjustment of measured precipitation does not suffice to meet expected annual sums. Therefore mean annual wet days and precipitation sums are estimated for a given EHRU and the deficits are determined. For each dry day in the time-series, a month-specific probability of additional rain occurrence can be calculated as:

$$p_{rain,\,month} = \frac{PCP_{days,lack}}{365.25} * \frac{\left(\frac{12*PCP_{month}}{PCP} + \frac{12*PCP_{days,month}}{PCP_{days}} \right)}{2}$$

in which	$p_{rain,\,month}$	=	Month-specific probability of additional rain occourence
	$PCP_{days,lack}$	=	Estimated annual number of wet days in EHRU minus number of wet days at adjacent gage
	PCP_{month}	=	Mean monthly precipitation in the catchment
	PCP	=	Mean annual precipitation in the catchment
	$PCP_{days,month}$	=	Mean monthly number of wet days in the catchment
	PCP_{days}	=	Mean annual number of wet days in the catchment

The first factor calculates the mean annual probability of additional rain occurrence, while the second factor imposes a monthly variation due to wet and dry seasons. If long time series of precipitation in elevated regions are available, this calculation might be replaced by robust monthly probabilities. Precipitation amount on these randomly added wet days can be calculated using an exponential distribution (Neitsch et al. 1999) as:

$$PCP2_{day,HRU} = \frac{PCP_{lack}}{PCP_{days,lack}} * \left(-\ln\left(rnd_1\right)\right)^{1.3}$$

in which	$PCP2_{day,HRU}$	=	Daily precipitation on randomly added day in HRU
	PCP_{lack}	=	Estimated annual precipitation in HRU minus adjusted precipitation from adjacent gage
	$PCP_{days,lack}$	=	Estimated annual number of wet days in HRU minus number of wet days at adjacent gage
	rnd_1	=	Random number [0 - 1]

Again, with robust time series of precipitation measurements, this approach might be replaced by a more sophisticated approach (Gamma- or mixed exponential distribution) that represents local characteristics in a better way (Wilks 1999). But so far, this procedure assures that within the basin, where most precipitation measurements take place, the generated time series match the measurements, whereas in the high elevations at least the characteristics of annual rainfall are represented satisfactorily.

A structural error is introduced into the model, as the routine allows only to add wet days, but not to add dry days in case the EHRU is located below the gauge. Since all gauges are located in depth lines, the effect is considered negligible for the study area.

5.1.2.2 Irrigation Module

Simplifying the original model concept, irrigation requirements are calculated on a monthly basis using CropWat (Allen et al. 1989b).

Motivation

Irrigation in the Upper Drâa valley relies predominantly on surface water, but dependent on surface water availability and tolerance of cultivated crops to water stress, groundwater can be applied additionally (Heidecke 2006). The amount of groundwater utilized for irrigation therefore varies in space (see Table 5-2) and time. SWAT has no routine implemented that changes the irrigation source, if water availability falls below certain thresholds.

Table 5-2: Relative frequency of irrigation water sources in the Upper Drâa valley (Heidecke 2006)

Irrigation water Source	Oasis			
	Ouarzazate	Skoura	Kelaat	Boulmalene
Wadi	50,0%	11.8%	86.5%	88.0%
Groundwater	3.8%	50.0%	1.9%	0.0%
Wadi and groundwater	46.2%	17.6%	9.6%	12.0%
Sources	0.0%	20.6%	1.9%	0.0%
n =	26	34	52	25

Furthermore a variety of farming strategies exist to cope with prolonged drought periods. Either irrigation from groundwater can be increased (if deep wells and pumping gear is available), or water demand is reduced, by growing drought tolerant plants or limiting the irrigated area.

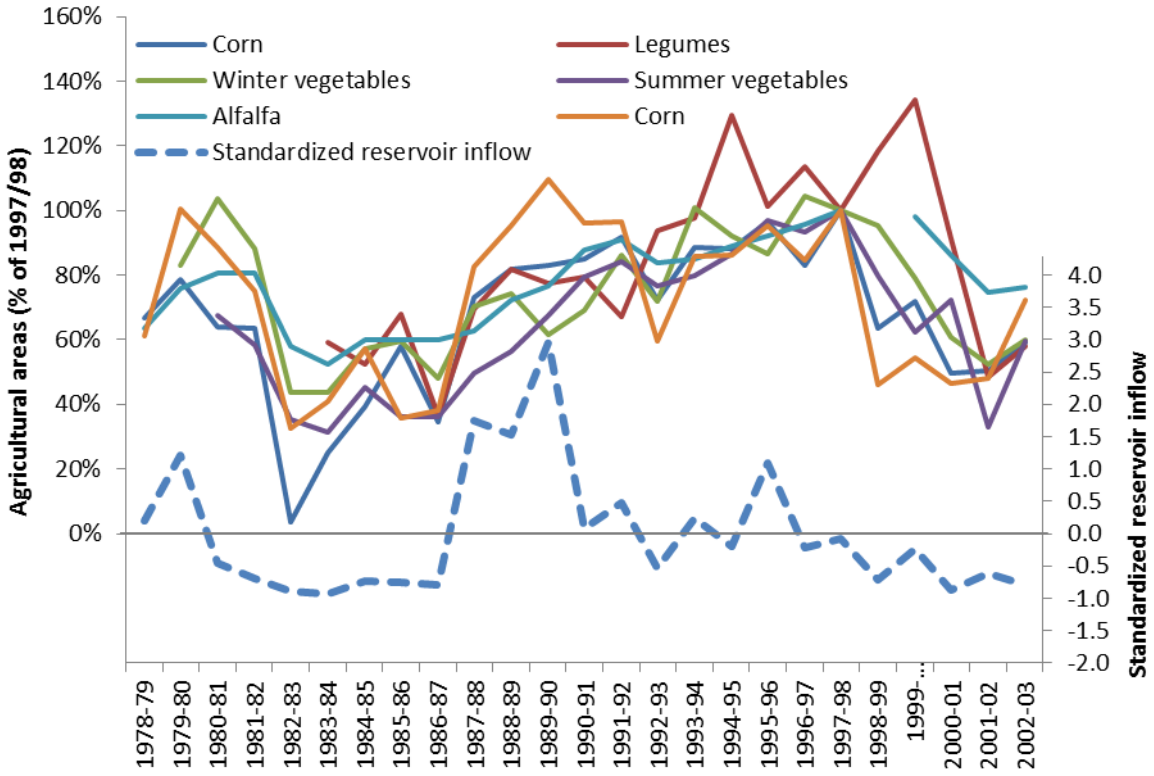

Figure 5-4: *Relative change in irrigated area for selected crops in the provinces Zagora and Ouarzazate (100% = Area of 1997/98) (Heidecke 2009) compared to the standardized reservoir inflow as a proxy measureof drought conditions (data: SE Ouarzazate)*

Agricultural statistics of the ORMVAO reveal strong shifts in irrigated area for dry and wet periods (Figure 5-4). These are lumped data for the provinces of Ouarzazate and Zagora, so that oscillations for the Upper Drâa valley might be superimposed by stronger oscillations in the Middle Drâa valley which is more drought-prone and therefore might tend to higher variations in irrigated area. Since irrigation sources, crop mix and extent of irrigated area and vary considerably on annual basis, the static crop model included within SWAT is not appropriate.

A separate treatment of the oases is furthermore reasonable as distinct microclimatic effects influence evapotranspiration in the oases. The climatic definitions of the desert ‘oasis effect’ generally refer to the phenomenon of a cooling effect: “Due to evaporation [or transpiration] cooling, an isolated moisture source is always cooler than its surroundings in an otherwise arid region” (Oke 1987).

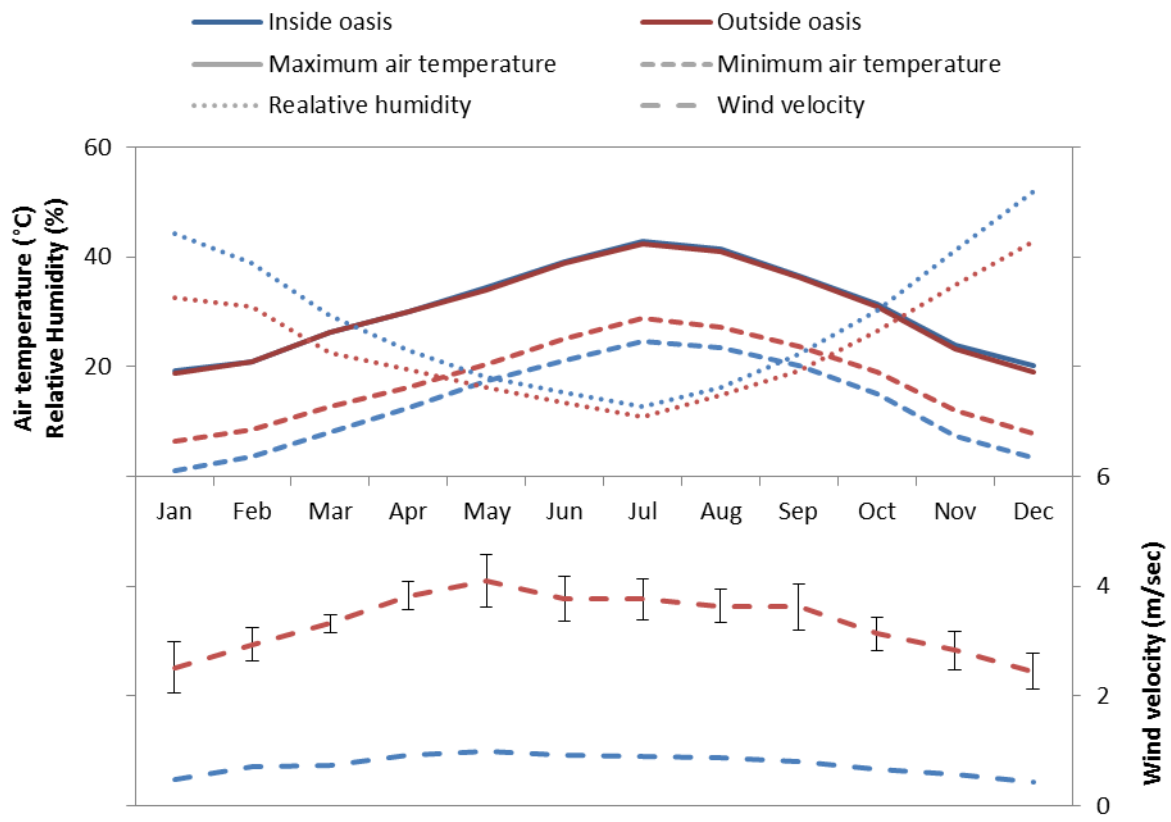

Figure 5-5: The oasis effect on temperature, relative humidity and wind velocity (based on IMPETUS climate data)

Pochter et al. (2008) draw a more detailed picture by pronouncing the decrease in wind velocity and incoming radiation. These effects are observed at the IMPETUS test sites as well (Klose et al. 2008a). Within the IMPETUS framework climate measurements have been conducted in the palm orchard Asrir (oasis Ternata, 750 masl). Measured climate data from the adjacent 4 climate stations (Bou Skour, 1400 masl; Arguioun, 1200 masl; El Miyit 790 masl, Jbel Hassan Brâhim, 725 m), has been linearly correlated with elevation on a monthly basis ($r^2 \geq 0.90$ for T_{max}, $r^2 \geq 0.97$ for T_{min}, $r^2 \geq 0.77$ for RH). These variables have then been estimated for the elevation of the Asrir station ("outside oasis" conditions) and compared to the Asrir measurements ("inside oasis" conditions). Wind velocity of the Asrir station has been compared to the average wind speed of the adjacent stations, as it is rather dependent on topographical features than on elevation. Results of this comparison are presented in Figure 5-5. It can be stated that minor differences in T_{max} (oasis +0.4°C) are contrasted by a strong difference in T_{min} (oasis -4.2°C), both with little deviation throughout the year. Relative humidity is 4.9% higher in the oasis (ranging from 11.5% in January to 1.4% in August). Wind velocity is decreased by 77% in the oasis. Radiation measurements are not available for

the Asrir station. Applying the modified Penman approach for calculating evapotranspiration should account for the differences in temperature, humidity, wind velocity and radiation. Within SWAT each vegetation unit in the same subbasin/simulation unit is assigned the same climate files. Therefore distinct microclimatic differences, as between oasis and steppe/desert cannot be handled adequately. Again this could be overcome by linking climate data to HRUs instead of subbasins.

Last but not least irrigation measurements in the Drâa catchment show that irrigation takes place in periods when water availability is high, irrespective of the plants water demand. Local authorities state that irrigation is twice the plant water demand in spring, but only half the demand in summer (MTP 1998). Hence the assumption of a simple soil storage seems to be appropriate to model this system. This storage is filled in autumn and more important in spring and depleted during summer.

Model Modification

Within this study irrigation requirements of agricultural areas are calculated on a monthly basis using CropWat[12] (Allen et al. 1989b). SWAT and CropWat are not directly coupled since management decisions (e.g. no second crop in summer, limitation of irrigated surface in dry years, increased groundwater pumping) vary on a yearly basis and data describing them is missing. Therefore water availability and irrigation demand are calculated separately for each oasis and the surface water deficit is determined, assuming that irrigation demand is satisfied from surface water, if available.

To compute irrigation requirements CropWat estimates reference evapotranspiration (ET_0) using the modified Penman approach, also referred to as Penman-Monteith, (Penman 1956; Monteith 1965). This evapotranspiration is multiplied with a crop-specific parameter (K_c). Furthermore a loss term is added to account for evaporation or percolation losses (see Figure 5-6). Bos & Nugteren (1990) provide an overview on irrigation efficiencies in different climate zones and under different irrigation practices. The water required by the plant is referred to as net irrigation, whereas the amount of water needed to fulfill this demand is referred to as gross irrigation. The lost water is considered to leave the system.

Irrigation is assumed to take place every time the soil storage is not completely filled. Hence the actual irrigation is either limited by insufficient discharge, the volume of the soil storage or the withdrawal capacity, which is set to a certain fraction of the channel discharge. For each oasis in the catchment, one reach is defined, where irrigation water is extracted.

[12] Download: http://www.fao.org/nr/water/infores_databases_cropwat.html (accessed: 05.07.2012)

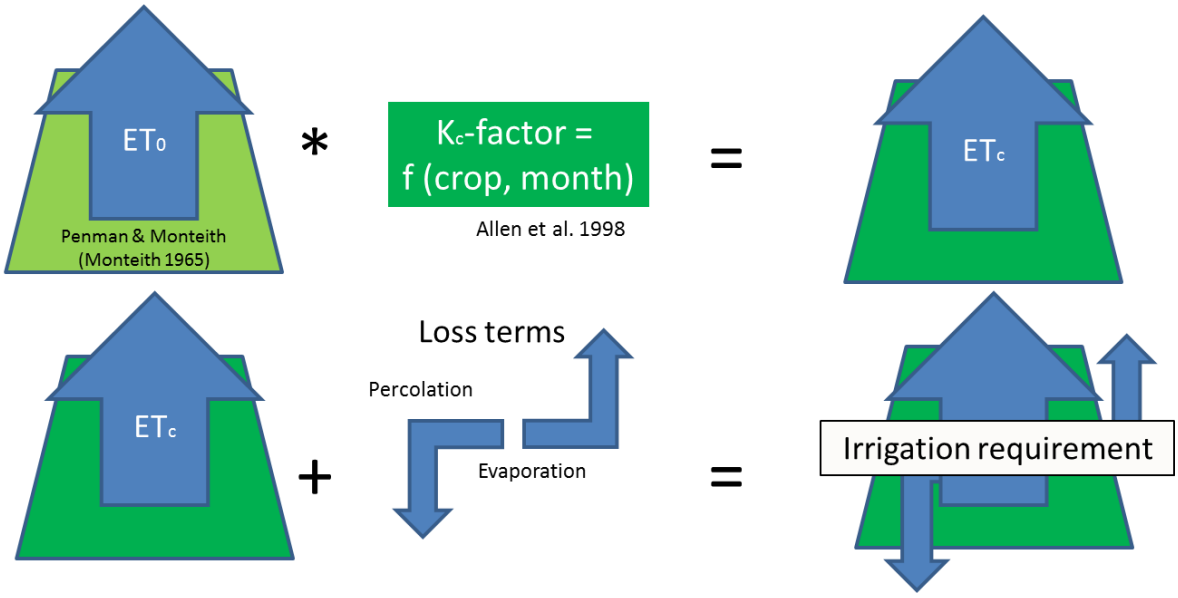

Figure 5-6: Reference evapotranspiration (ETo), crop evapotranspiration under standard conditions (ETc) and inclusion of loss terms due to irrigation efficiency (modified after Allen et al. 1989b)

A post-processing routine has been written for SWAT, reducing the discharge in each channel segment and its subordinated segments by the amount of irrigation determined. A slight error is introduced in this routine, as channel processes (such as transmission losses, channel evaporation etc.) are calculated on basis of the original, non-reduced values. Further model versions could imply a direct coupling, though different time-steps (daily for the hydrological model, monthly for the irrigation routine) need to be considered.

5.1.2.3 Second Linear Storage Aquifer

The original model concept accounts for two aquifer systems: shallow aquifer and bank storage. The so-called deep aquifer acts as a sink, permanently removing water from the system. Water that enters the deep aquifer is assumed to contribute to streamflow somewhere outside the catchment (Arnold et al. 1993). This section discusses the implementation of a second aquifer into the simulation model that can contribute to discharge and therefore represent heterogeneous aquifer settings as found in the study area.

Motivation

The horizontal distribution of different aquifer types can easily be reproduced via the spatially distributed approach of SWAT. But in geologically heterogeneous catchments as the Upper Drâa valley this is not sufficient.

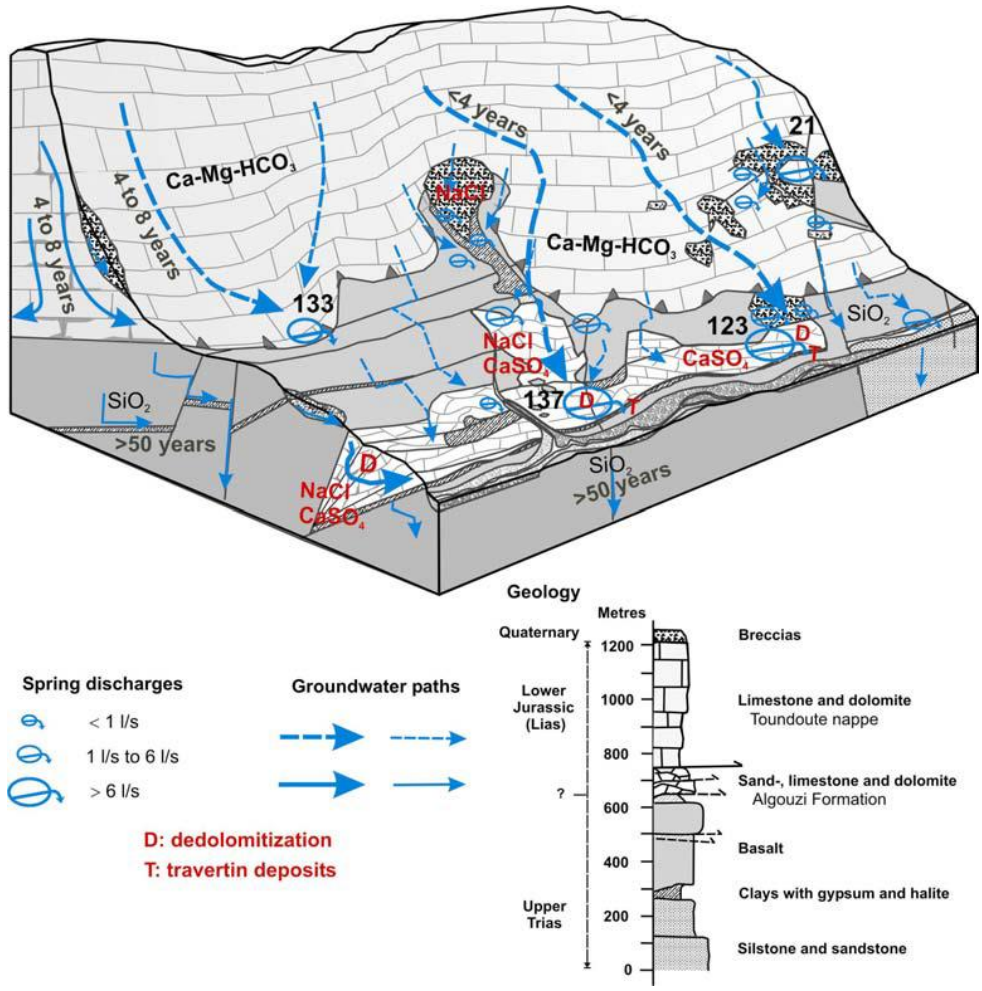

Figure 5-7: Hydrogeological setting of the Assif-Ait-Ahmed catchment (Cappy 2006)

As the conceptual model of the hydrogeological setting points out, distinct changes of the geological structure of the Toundout aquifer can be observed (see Figure 5-7 and chapter 3.3). Therefore aquifer properties do not only vary in the horizontal plane, but also vertically. Karstified limestone, sandstone and fissured basalt exhibit large varieties in hydraulic conductivity and storage capacity. As seen in Figure 5-7 these different aquifers contribute to streamflow with different reaction times.

Furthermore the Toundout aquifer, which sustains the perennial flow of the Dades, exhibits properties of karstified limestone that have been widely discussed in the literature. Within limestone porosity and permeability may be microscopic (pores, interstices, microfissures) or macroscopic (fissures, joints, channels) (Kovalevsky et al. 2004; White 2002). Therefore it is convenient to distinguish between the rock or intrinsic permeability (microscopic) of the rock mass and the regional or formational permeability (macroscopic). The latter includes the added permeability supplied by fissures, joints and channels. Consequently an initial high permeability and a decreased transient permeability may be recognized. This property of

limestone aquifers is generally referred to as "double porosity" (Freeze & Cherry 1979). Hence the representation of a limestone aquifer as a single linear storage module could result in poor process representation and model results. This has been explicitly stated for the applicability of the SWAT model in the High Atlas (Chaponnière et al. 2008).

Several studies recognize the postulated components in limestone aquifers: Atkinson (1977) concluded from an analysis of spring hydrographs in England that 50% of the spring discharge was by "quickflow" and 50% by "slowflow". Atkinson also concluded that 92% of the groundwater is stored in fractures or the matrix of the limestone rather than in caves or conduits. Amit et al. (2002) analyzed two years of discharge for five different springs in Israel and concluded ratios of quickflow to total flow greater than 80%. For limestone aquifers in France hydrological models consisting of three and two conceptual reservoirs obtained good results (Fleury et al. 2009; Fleury et al. 2007).

The outlined conditions seem to apply to the Upper Drâa catchment due to several reasons:

The Upper Drâa valley is drained by different river types (see section 3.7). Only the eastern tributaries Dades and M'Goun are perennial. Originating in the elevated areas of the northeastern catchment, these rivers sustain baseflow in the basin in summer. Even during prolonged droughts of several years (such as the 1982-1986) baseflow can be observed. Springs in the recharge areas have been sampled and Tritium analysis exhibit a large variety of residence times (Cappy 2006), ranging from less than 4 years to more than 50 years (Figure 5-7). Though these findings cannot directly be converted in aquifer parameters, they can be interpreted qualitatively: Several sources of groundwater exist in the High Atlas. Those sources exhibit different water ages and therefore might have different response times.

Analyses of baseflow recession registered at the reservoir Mansour-Eddahbi have been carried out (for details see section 5.3.5). Two superimposing recessions can be distinguished:

- Bank discharge: short-term interactions of the stream and the highly conductive alluvial aquifer. Recession times are in the magnitude of ~20 days per $\log_{10}$-cycle.
- Quick baseflow: intermediate baseflow with recession times of ~200 days per $\log_{10}$-cycle.

During droughts a third component, slow baseflow, gains importance. Which means for long recession periods a model consisting of bank storage and one aquifer tends to underestimate measured discharge. Recession times can hardly be quantified due to measurement uncertainty, effects of snowmelt and irrigation and the lack of long recession periods. Nevertheless discharge records indicate at least its presence (see Figure 5-8).

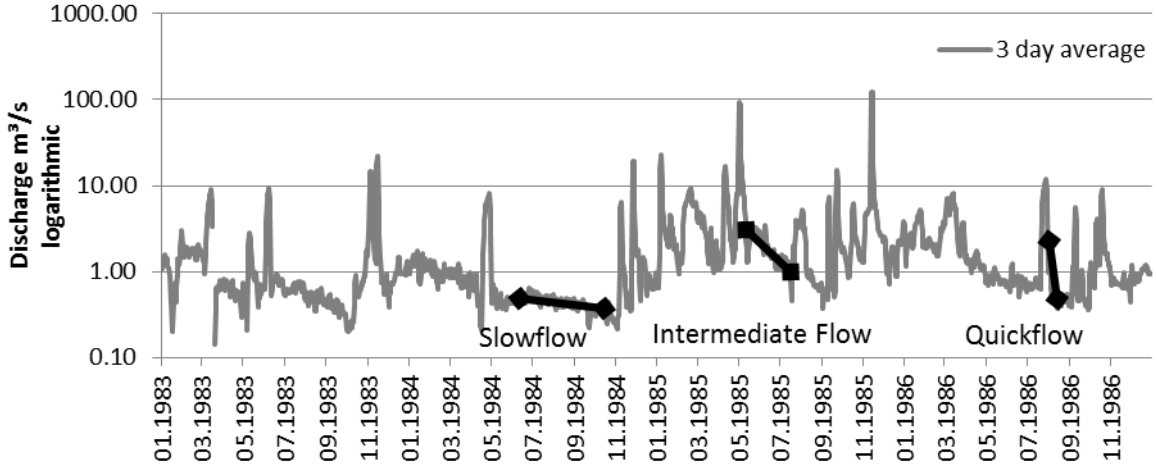

Figure 5-8: Discharge into the reservoir Mansour-Eddahbi (logarithmic scale). Dominant baseflow components are exponentially approximated (Data: SE Ouarzazate)

The derivation of recession coefficients and other groundwater related model parameters is presented in detail in section 5.3.5.

Model Modification

The first attempt to fit a quantitative expression to observed baseflow recession was probably made by Boussinesq (1903). Assuming a moderate hydraulic gradient, homogeneity, isotropy and one-dimensional flow, Boussinesq proposed a fitting of two exponential components to observed recession. Later this approach has been interpreted as the depletion of several different (linear) reservoirs (Tallaksen 1995; Mero 1964). The conceptual recession coefficient α can be interpreted physically (Hennig & Schwarze 2001), since it accounts for lumped aquifer properties, such as geometry, permeability and porosity. Further conceptual models of groundwater discharge have been developed (e.g. exponential and power-law storage). Moore (1997) and Tallaksen (1995) provide an overview and compare different approaches. Anyhow in conceptual hydrological models the linear storage approach is very common, not only for aquifers but for all kinds of storages (e.g. soil, Figure 5-9). Several numbers of reservoirs have been utilized in different simulation models:

- SWAT uses one linear storage reservoir (the "shallow aquifer") (Arnold et al. 1993; Smedema & Rycroft 1983)
- HBV uses 3 linear storage reservoirs (one represents soil storage) (Lindstrom et al. 1997)
- DIFGA (Differentielle Ganglinienanalyse) accounts for two and more linear subsurface reservoirs (Schwarze et al. 1995; Schwarze et al. 1989)

a)

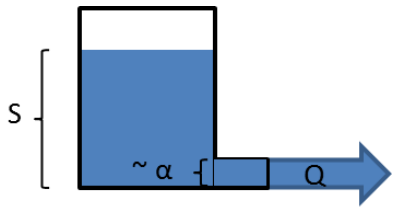

$$Q(t) = \frac{\delta}{\delta t} S(t) = -\alpha * S(t) \quad \rightarrow \quad S(t) = S_0 * e^{-\alpha * t} \quad \rightarrow$$

$$Q(t) = Q_0 * e^{-\alpha * t}$$

in which

$Q(t)$	=	Discharge at timestep t
$S(t)$	=	Reservoir storage at timestep t
S_0	=	Initial storage
Q_0	=	Initial discharge
α	=	Recession coefficient

b)

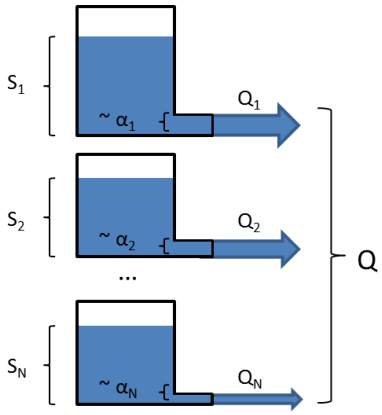

$$Q(t) = \sum_{i=1}^{N} Q_{0,i} * e^{-\alpha_i * t}$$

in which

$Q(t)$	=	Total discharge at timestep t
$Q_{0,i}$	=	Initial discharge of reservoir i
N	=	Number of reservoirs
α_i	=	Recession coefficient of reservoir i

Figure 5-9: Scheme and equations of a baseflow system approximated by (a) one or (b) several linear reservoirs.

In theory an arbitrary number of reservoirs can be included in the model, contributing to discharge or acting as a sink, in case surface and subsurface watersheds do not coincide.

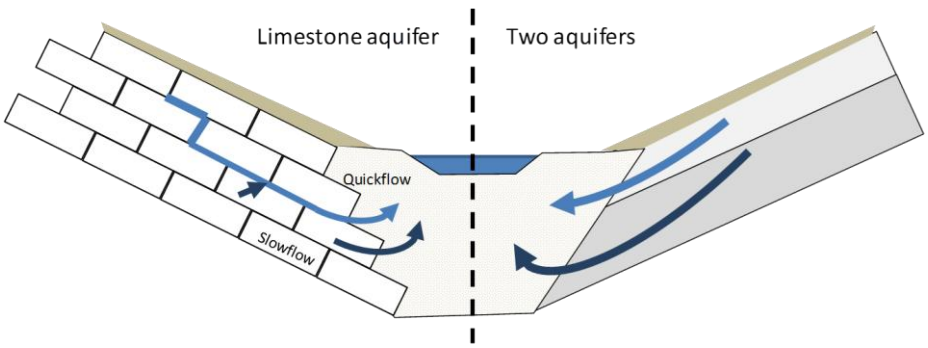

Figure 5-10: Aquifer conditions that can be represented by two linear storage reservoirs

For SWAT-MAROC two aquifers were chosen. Therefore the model can account for two types of aquifer conditions: Two aquifers exhibiting different discharge behavior (Figure 5-10, right side) or double permeability conditions of limestone aquifers (Figure 5-10, left side). There is no evidence that other noteworthy subsurface drainage than to the reservoir

exist (Cappy 2006). Therefore no sink was implemented. If required, the groundwater module can be extended by any number of additional reservoirs and the groundwater sink can be incorporated in the model. Bank storage is already included in the original SWAT channel model and has been used as well.

The groundwater recharge is diverted between the two aquifers by assuming a constant fraction. Discharge is then calculated by exponential decay functions for each aquifer:

$$Aq_{1,j} = Aq_{1,j-1} + recharge_{1,j} = Aq_{1,j-1} + recharge_{total,j} - recharge_{2,j}$$

$$recharge_{2,j} = recharge_{total,j} * fraction_{aq2}$$

$$Aq_{2,j} = Aq_{2,j-1} + recharge_{2,j}$$

$$gwq_{i,j} = gwq_{i,j-1} * e^{-\alpha_i} + recharge_{i,j} * (1 - e^{-\alpha_i})$$

in which	$Aq_{i,j}$	=	Storage of aquifer i at during timestep j [mm]
	$recharge_{total,j}$	=	Groundwater recharge in in timestep j [mm]
	$recharge_{i,j}$	=	Recharge of aquifer i in timestep j [mm]
	$fraction_{aq2}$	=	Fraction of groundwater recharge diverted to aquifer 2 [%]
	$gwq_{i,j}$	=	Discharge of aquifer i in timestep j [mm]
	α_i	=	Baseflow recession coefficient of aquifer i [mm]

5.1.2.4 Reservoir Module

A simple water balance model is added at the outlet of the catchment, representing the operation of the reservoir Mansour-Eddahbi.

Motivation

Beside drinking water supply, the release of irrigation water is one of the prominent objectives of the reservoir Mansour-Eddahbi. For planning purposes and management tools applied in the Middle Drâa catchment the amount of irrigation water released from the reservoir is the most important boundary condition as local runoff and groundwater recharge is small (Klose et al. 2008b). Therefore a conceptual model is needed to convert annual inflows into realistic time series of water releases, especially for the future scenarios. Furthermore ongoing siltation effects on the reservoir can be approximated. The reservoir routines included in SWAT are considered not appropriate as the options provided (target level or measured release data) do not represent the reservoir management experienced (target release) or cannot be used during scenario analysis (see Neitsch et al. 2004; Neitsch et al. 1999).

Model Modification

An annual time-step conceptual water balance model is developed as a post-processor of the results of the hydrological model. The water balance is computed as:

$V_{end} = V_{start} + Q_{in} - (V_{abstract} + V_{over} + V_{release} + V_{evap})$ [all in Mm³]

in which
- V_{end} = Stored Volume at the end of the hydrological year
- V_{start} = Stored Volume at the start of the hydrological year
- Q_{in} = Inflow to the reservoir during the hydrological year
- $V_{abstract}$ = Abstractions (Drinking water supply of the city of Ouarzazate)
- V_{over} = Overflow due to exceedance of the reservoirs storage capacity
- $V_{release}$ = Planned water release (lâcher)
- V_{evap} = Evaporation loss from reservoir

V_{end} and V_{start} are calculated by the reservoir module; Q_{in} is provided by the hydrological model. Time series of measured abstractions ($V_{abstract}$) are provided for the baseline scenario or assumed by future scenarios. The remaining volumes V_{over}, $V_{release}$ and V_{evap} are calculated, dependent on the reservoirs decreasing capacity (see section 3.7) and the dynamic surface area.

Assuming the recharge to occur in the first half of the hydrological year and the water release to occur in the second half along with the dominant part of evaporation, the order of calculations is the following: Calculate recharge and overflow, when necessary. Calculate water release. Subtract drinking water supply. Calculate evaporation, based on the average surface of the reservoir before and after water-release. The required volumes are calculated as follows. The decrease of the capacity of the reservoir is assumed to occur linearly with inflow:

$$Cap_n = Cap_{1972} - \sum_{i=1972}^{n-1972} sr_i * Q_{in,i}$$

in which
- Cap_n = Reservoir Capacity in Year n [Mm³]
- Cap_{1972} = Reservoir Capacity in 1972 [Mm³]
- sr_i = Sedimentation Ratio in Year i [%]
- $Q_{in,i}$ = Reservoir inflow in year i]Mm³]

The required sedimentation ratios can be determined from bathymetries and inflow records.

As soon as the inflow exceeds the remaining capacity, overflow occurs:

$$V_{over} = Q_{in}\text{-}(Cap\text{-}V_{start})$$

in which	V_{over}	=	Overflow from reservoir in a given year [Mm³]
	Q_{in}	=	Inflow to reservoir in a given year [Mm³]
	Cap	=	Capacity of reservoir in a given year [Mm³]
	V_{start}	=	Initial volume in reservoir in a given year [Mm³]

Dependent on the filling level of the reservoir, water releases for irrigation purposes can be determined. An optimum amount of irrigation water needs to be determined, as well as a residual volume of the reservoir that cannot be released for irrigation. An optional buffer coefficient allows reducing irrigation water amounts, when the reservoir volume approaches the residual volume.

$$V_{release} = \begin{cases} Max(0, V_{release,opt} - V_{over}) \; ; & \text{if } V_{start} + Q_{in} - Max(0, V_{release,opt} - V_{over}) > V_{\min} \\ (V_{start} + Q_{in} - V_{\min}) * c_{buffer}; & \text{if } V_{start} + Q_{in} - Max(0, V_{release,opt} - V_{over}) < V_{\min} \end{cases}$$

in which	$V_{release,opt}$	=	Optimum of water release [Mm³]
	$V_{\min}$	=	Reserve volume of reservoir [Mm³]
	c_{buffer}	=	Buffer coefficient [-]

A suitable polynomial regression for determining the reservoirs surface area, dependent on the water volume it contains, has to be determined from available bathymetries. By doing so annual evaporation losses can be determined. An evaporation coefficient between zero and one can account for microclimatic conditions that reduce evaporation, like e.g. evaporative cooling or thin saturated air layers above the water surface (Oke 1987):

$$V_{evap} = SA * E_0 * c_{evap}$$

in which	V_{evap}	=	Water loss due to evaporation [Mm³]
	SA	=	Surface Area of the reservoir [km²]
	E_0	=	Reference Evaportation at the reservoir [mm]
	c_{evap}	=	Evaporation coefficient [-]

Concluding, the complex management decisions that are related to the management of the reservoir Mansour-Eddahbi are reduced to a simple set of decision rules. While these rules will never be capable of reproducing actual management operations that are a result of many different processes (natural, political, etc.), they are essential to develop future scenarios. More sophisticated routines including fuzzy decision rules for vague operating objectives could be implemented in the future (Tilmant et al. 2002).

5.2 Model Sensitivity

Before model calibration, a global sensitivity analysis has been performed on the uncalibrated model[13], using the SUFI2 algorithm (Abbaspour et al. 2004; Abbaspour et al. 2007). 500 model runs are performed while varying the parameters given in Table 5-3 (see Appendix 3 or section 5.3 for details on the parameters). The effect of the parameter variations on the models CME has been evaluated, as other goodness-of-fit measures indicated no substantial deviations. Within the SUFI2 algorithm sensitivities are estimated by comparing the average changes in the objective function resulting from changes in each parameter, while all other parameters are changing. This is done by multi-linear regression of generated parameter values against the objective function. A t-Test is performed: the t-value represents the sensitivity of the models CME to changes in the parameter (high absolute values represent high sensitivity), while the p-value indicates the significance of the sensitivity (the closer to zero, the higher the significance). Further explications are provided by Abbaspour et al. (2008).

Table 5-3: Parameters and ranges considered during the sensitivity analysis of the uncalibrated model (see Appendix 3 for details on parameters)

Parameter	Type of change	lower bound	upper bound
CN2	absolute	-10	+10
ALPHA_BF	value	0	0.2
GW_DELAY	value	30	120
GW_REVAP	value	0	0.05
RCHRG_DP	value	0.2	0.8
CH_K1	value	0	200
CH_K2	value	0	25
ALPHA_BNK	value	0	1
SOL_AWC	relative	-30%	30%
SOL_K	relative	-30%	30%
SOL_Z	relative	-30%	30%
SOL_BD	relative	-30%	30%
SMTMP	value	0	5
SMFMN	value	3	10
SNOCOVMX	value	10	100
SNO50COV	value	0.1	0.5
IRR_FRAC	value	0.3	0.9
IRR_EFF	value	0.4	0.9

As presented in Table 5-4 soil-related parameters were most sensitive, along with parameters governing baseflow timing. Snow-related parameters are of minor importance. The derivation of parameters is outlined in the following section. In general physically meaningful parameters are determined, based on field data or literature reviews; whereas empirical parameters or parameters "meant" for calibration, only reasonable ranges are defined and final values were determined during calibration. Furthermore the most sensitive parameters and parameters that belong to newly developed model routines have been noted for uncertainty analysis.

[13] The sensitivity analysis has been performed after the discretization into EHRUs, i.e. default soil data and default land-use data have already been set. Further refinement of parameters has been carried out after the sensitivity analysis. Nevertheless the sensitivity analysis is presented here to preserve the structure lined out in section 4.1

Table 5-4: Parameter sensitivities of the uncalibrated model. T- and p-values derived from Students t-Test. Abbreviations for further actions: MC: Manual calibration; AC: Autocalibration; UA: Uncertainty analysis

Parameter	t-value	p-Value	Parameter determination (corresponding section)	Further actions
CN2	66.93	<0.01%	Literature review (5.3.3.1); Calibration	AC; UA
SOL_AWC	-20.48	<0.01%	Soil map (5.3.2) Correlates with SOL_Z	
SOL_Z	-15.38	<0.01%	Soil map (5.3.2) Correlates with SOL_AWC	UA
ALPHA_BNK	6.82	<0.01%	Determination based on baseflow separation (5.3.5)	
IRR_EFF	6.45	<0.01%	Literature review (5.3.3.2)	UA
SOL_BD	6.32	<0.01%	Soil map (5.3.2)	
CH_K2	-3.76	0.02%	Literature review (5.3.5)	
SNOCOVMX	-3.54	0.04%	SWAT Default values	MC
SMFMN	2.82	0.51%	SWAT Default values	MC
SOL_K	2.56	1.09%	Soil map (5.3.2)	
ALPHA_BF	2.38	1.79%	Determination based on baseflow separation (5.3.5)	
GW_DELAY	-2.32	2.05%	SWAT Default values	MC
SMTMP	-1.80	7.30%	SWAT Default values	MC
IRR_FRAC	1.76	7.83%	Estimation (5.3.3.2)	MC
RCHRG_DP	-1.58	11.49%	Literature review (5.3.5)	UA
GW_REVAP	-0.82	41.05%	Literature review (5.3.5)	AC, UA
CH_K1	0.69	49.14%	Literature review (5.3.5)	
SNO50COV	-0.12	90.26%	Estimation	MC

5.3 Model Data

The model setup has been done using the ArcSWAT graphical user interface (Winchell et al. 2007). This interface performs the delineation of (sub-) catchments from digital elevation data and the definition of HRUs based on soil, land cover and slope maps. Furthermore a database environment is provided for the model parameters (especially soil, land cover and climate). Via the interface parameters are written from the databases into the text files SWAT operates on. Parameter values are chosen as lined out in this section.

This section portrays the data requirement, data processing and parameter settings of the model outlined in the previous chapter. Basic datasets required to set up SWAT are a digital elevation model, soil map and land-cover classification, including databases of soil and land-cover parameters. Further, to exploit the model improvements addressed in section 5.1.2, geological data and CropWat values for local cultures are required. Subsequently, climate data, being the central boundary condition in a hydrological model, are presented. Discharge data, essential for calibration and validation of a hydrological model, are presented in the next section. In the final section the parameterization of the reservoir module is described. Every section comprises of a list of the required parameters, a description of the used datasets, and further information on parameter values chosen. The sections conclude with a consideration of uncertainties inherent to data.

5.3.1 Digital Elevation Model

A digital elevation model (DEM) is needed to delineate the catchment and to derive topographic properties as well as mean elevations of spatial model units. In this study the DEM of the Shuttle Radar Topographic Mission (SRTM, Farr & Kobrick 2000) has been used. The DEM is provided free of charge in a resolution of 3 arc seconds (~90 m)[14]. The dataset is provided in geographic coordinates (WGS84). Within the IMPETUS project, the 3 arc second SRTM data has been resampled to a resolution of 30 m. To be consistent with research results obtained within the IMPETUS framework, the resampled dataset is used in this study as well.

Based on the SRTM-data the following spatial discretization has been created: Seventeen hydrological subbasins have been created on basis of the gauges available (see Figure 3-13 and section 5.3.7.1). Those have been intersected with 5 elevation zones (<1500, 1500-2000, 2000-2500, 2500-3000, >3000), resulting in 60 units, as not every elevation zone is present within each subbasin (see section 5.1.2.1 and Figure 5-11).

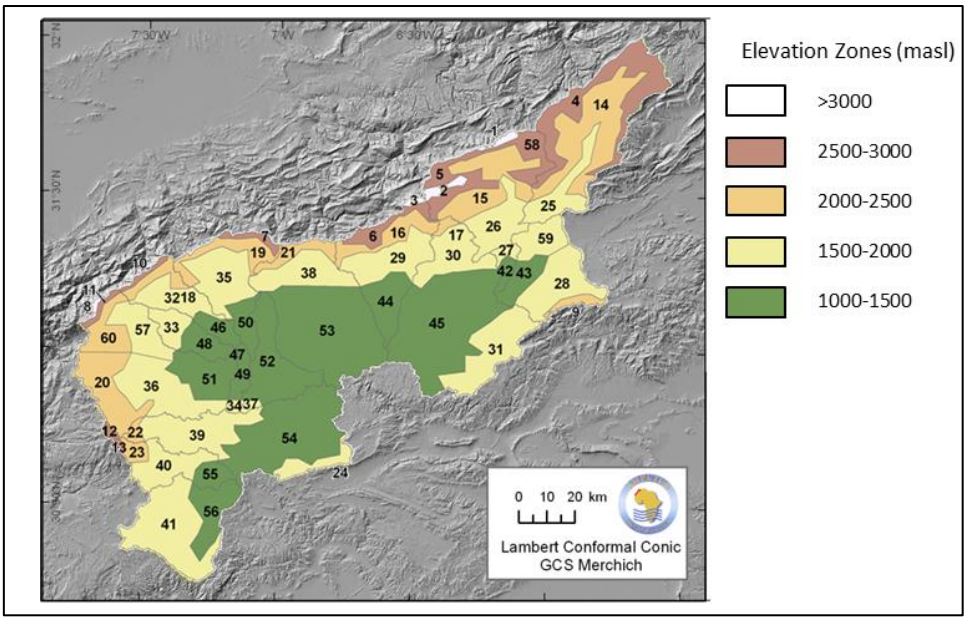

Figure 5-11: Spatial model units of the Upper Drâa Catchment accounting for drainage system and elevation, prior to EHRU-discretization

The units average size is 247 km² (standard deviation: 253 km², min: 1 km², max: 1145km²). Errors in the SRTM data have been assessed for different regions of the world (Rodriguez et al. 2006). In Africa the horizontal error is less than 11.9 m (at 90% confidence) and the vertical error is less than 5.6 m (at 90% confidence). The performance of SRTM data for hydrological applications has been discussed by Jarvis et al. (2004). The authors conclude that the SRTM-DEM clearly outperforms previous global elevation datasets (e.g. GTOPO30). At the catchment-scale topographic maps (scale 1:10,000) produce more detailed DEMs, but little difference was found between hydrological features, such as stream network, catchment boundaries and wetness index. Recently the ASTER-GDEM has been published, providing elevation data with a resolution of 1 arc second[15]. Usability assessments for hydrological applications are not yet published.

The effect of the DEM resolution depends on the catchment response of interest. Serious effects on physically based models with high spatio-temporal resolution are reported (Thieken et al. 1999). However conceptual models with low spatio-temporal resolution are less affected. Sensitivity studies of the SWAT model using different DEM resolutions in a semi-arid US catchment indicated that DEMs with a resolution of 100 to 200 m produce only slight deviations in output compared to high resolution DEMs, and can therefore be considered appropriate for reliable daily flow and nutrient predictions.

[14] Download: http://srtm.csi.cgiar.org/ (accessed: 03.12.2009)
[15] Download: http://www.gdem.aster.ersdac.or.jp/ (accessed: 03.12.2009)

In the research area A. Klose (2009) evaluated the RMSE of the ASTER-DEM compared to 194 DGPS points and concluded sufficient accuracy. Consequently the 30 m DEM used in this study can be considered suitable for modeling a monthly water balance.

Beside the size of the modeling units the following topographic parameters are required by SWAT, they were determined using the topographic routines included in the ArcSWAT tool:

- **Average Slope and Average Slope Length:** HRU_SLOPE [m/m], SL_SOIL [m]
  These parameters are required to calculate lateral flow within the EHRUs.
- **Average Elevation:** ELEV [m]
  Elevation-dependent processes (lapse rates etc.) require this parameter.
- **Channel Width and Channel length:** CH_W [m], CH_L [m]
  The channel profile is required to calculate transmission losses.

5.3.2 Soil Data

For setting up SWAT-MAROC the following physical and empirical soil-related parameters are determined. Optional parameters considering chemical and biological properties as well as erodibility have not been determined.

- **Available Soil Water Capacity:** SOL_AWC [%]
  This parameter can also be referred to as plant available water. While wilting point and field capacity are calculated by SWAT, available soil water capacity is a user input. Soil water saturation, and hence the related processes of evaporation and percolation, are strongly influenced by this factor.
- **Clay, Silt, Sand and Rock:** SOL_CLAY, SOL_SILT, SOL_SAND [%]
  The volumetric contents of the different particle classes are used to calculate the wilting point.
- **Soil Depth:** SOL_Z [mm]
  Soil depth governs the size of the soil storage for water, thereby it strongly influences evaporation, plant growth and direct groundwater recharge (percolation).
- **Soil Hydrological Group:** HYDGRP[A-D]
  The NRCS classifies soils in four Soil Hydrological Groups, based on their infiltration capacities. This classification is needed, as the SCS Curve Number infiltration routine is used.
- **Saturated Hydraulic Conductivity:** SOL_K [mm/h]
  This parameter is used for the determination of the conceptual hydrological soil groups. Further uses are the calculation of percolation and interflow.

- **Bulk Density**: SOL_BD [g/cm³]

  Bulk density mainly affects the temperature distribution within the soil and therefore evaporation rates.

- **Albedo:** SOL_ALB [%]

  Albedo affects the energy balance of the soil, as incoming short-wave radiation is partly reflected.

- **Depth Distribution of Evaporative Demand:** ESCO [-]

  This conceptual compensation factor adapts the depth distribution that is used to meet the evaporative demand from the soil.

Available soil data in the research area is limited to agricultural areas, where detailed investigations have been carried out but results are not representative for the whole catchment (e.g. Brancic 1968; Radanovic 1968). The soil map of Morocco (Cavallar 1950) is on the one hand rather coarse (1:1,500,000), on the other hand soil units are not attributed with the properties required to set up a hydrological model. Global datasets are available as well, but their resolution is too coarse and local conditions are not considered (e.g. the Harmonized World Soil database; FAO 2009).

Within the IMPETUS project a soil database has been established which includes data from 211 soil profiles within the Drâa Catchment (Klose 2008a). For each of these soil profiles skeleton content, texture, carbonate, organic carbon, nitrogen content and pH have been determined. In order to derive soil hydraulic properties which could not be measured in situ due to high skeleton contents, pedotransfer functions were applied including a correction for skeleton content (Rawls et al. 1982).

To derive continuous maps of soil properties Klose (2008a) used the CORPT approach. The CORPT approach is based on analyzing the relationships between soil properties and the five factors of soil formation Climate, Organisms, Relief, Parent material and Time (Jenny 1941). Except time each of these factors is represented by adequate datasets as shown in Table 5-5.

Multiple linear regressions including dummy variables accounting for nominal parameters are used to evaluate the relationship of soil parameters and soil formation factors statistically. The regression equations were used to generate maps of soil properties. An idealized soil profile consisting of two layers had to be assumed in order to carry out the regionalization.

Since the results are continuous maps for every parameter and SWAT-MAROC works on discrete soil types, a classification is required. Two parameters have been determined to base the classification on: **Available water capacity** of the profile (AWC, [mm]) and **saturated hydraulic conductivity** (Ks, [mm/h]) for each layer. The former is an integral measure of the

parameters soil depth and porosity which in combination most prominently influence evaporation; the latter determines the runoff composition, as the Curve-Number is dependent on saturated hydraulic conductivity and interflow is simulated only when a sudden decrease in saturated conductivity occurs between two soil layers. Consequently these parameters are among the most sensitive in SWAT simulations (see section 5.2).

Table 5-5: Input data for the CORPT soil analysis (Klose 2008a)

Factor	Dataset	Source
Climate	temperature and precipitation	(Schulz 2007)
Organisms	dominant vegetation type	(Finckh 2008)
Relief	various terrain analyses using the SRTM digital elevation model	(Global Land Cover Facility 2006)
Parent material	Geological map 1:500,000	(ME 1959; Klose 2008b)
Time	No data available	

Quartiles of AWC and Ks for the upper soil layer have been determined; whereas subsoil Ks has been split in only two classes (see Figure 5-12). The resulting 32 soil classes cover similar areas (0.92 – 7.62% of the catchment), hence distortion during model discretization is less likely to occur than by using a more detailed map.

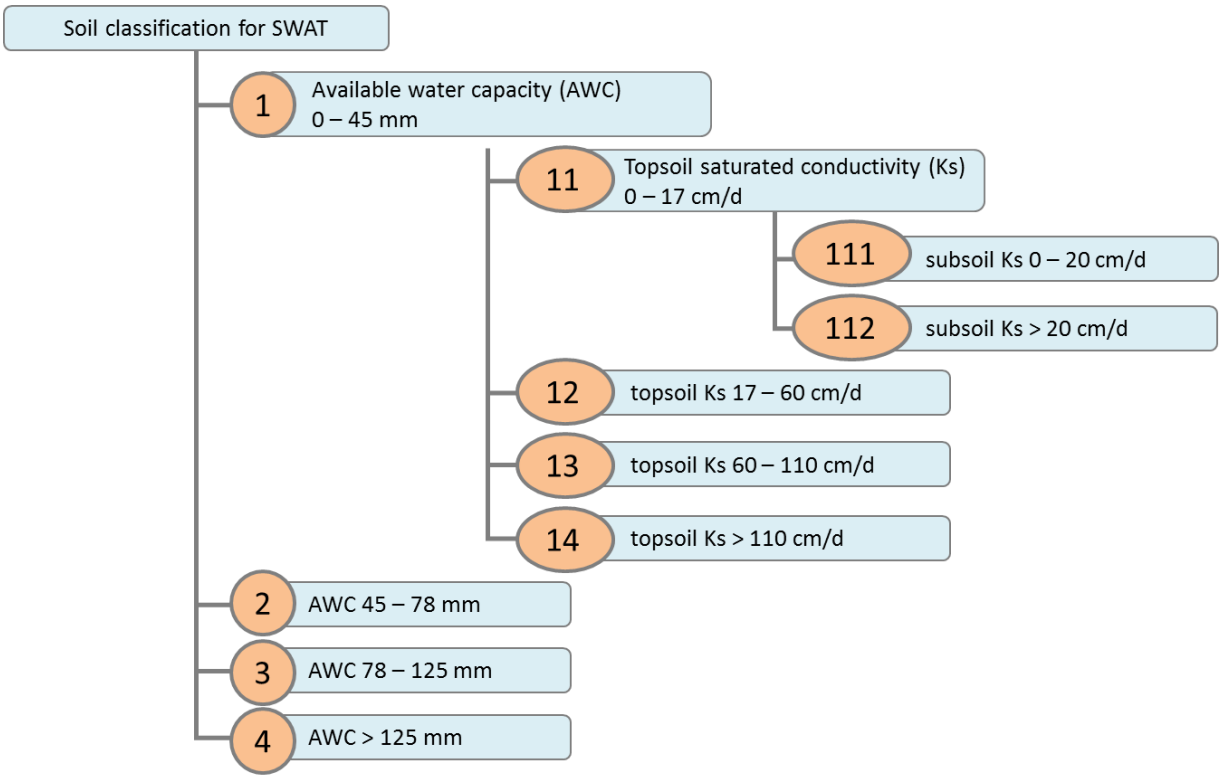

Figure 5-12: Soil classification for SWAT-MAROC and naming scheme

All required parameters have been taken from the soil property maps (see Appendix 4). Since the soil classification is based on the parameters that are required to determine the hydrological soil groups, the determination of these classes can be considered rather certain.

The **Hydrological Soil Groups** have been determined according to the USDA Soil Survey Guidelines (Neitsch et al. 2004). Class A soils are characterized by a high infiltration potential (see Table 5-6), whereas class D soil are characterized by a high runoff potential. Other thresholds considering cemented horizons or depth to an impermeable bedrock have not been considered, due to a lack of data. The catchment is dominated by class D soils.

Table 5-6: Thresholds for Hydrological Soil Group classification (Neitsch et al. 2004)

	Hydrological Soil Group			
	A	**B**	**C**	**D**
Saturated hydraulic conductivity of the most restrictive soil layer to a depth of 100 cm [mm/h]	>254.0	84.9 - 254.0	8.4 - 84.0	<8.4

The **Bulk density** has been estimated according to the sand content as proposed by Kemp et al. (1997):

$$BD = 1.009 + 0.835 * \frac{m_s}{100}$$

in which BD = Bulk density [t/m]

m_s = Sand content [%]

Albedo of moist soil has been set to 20% according to Garratt (1993), who compiled albedo measurements for different climate zones. Albedo for desert soils ranged from 10-20%.

The global parameter **ESCO** modifies the depth distribution to meet the evaporative demand from the soil; this conceptual dimensionless parameter is adapted during calibration, as it cannot be determined from measured data.

The regionalization of soil data, i. e. the construction of a large scale soil map, based on 211 soil profiles is highly uncertain. In this study this is especially true for soil depth, as a generally idealized two layer profile had to be assumed. Therefore, the depth representation of the created soil map only weakly represents the measured depths (r^2=.47). A more detailed statistical evaluation of the regionalization quality is provided by Klose (2008a). Furthermore the determination of the soils lower boundary, separating soil from unprocessed parent material is difficult, especially in arid regions, where already the soil itself is virtually devoid of any signs of biological activity (Klose 2009). In other studies the lower boundary is often set arbitrarily (e.g. 2 m; NRCS 1999). Therefore the soil depth is one of the most prominent factors examined in the uncertainty analysis.

5.3.3 Land Cover

The model used in this study is set up using two different land-cover related modules. Non-irrigated vegetation is modeled using the more physically based routines originally incorporated in SWAT, whereas irrigated agricultural areas are modeled using the more conceptually based CropWat approach (see section 5.1.2.2). Therefore the required input data is presented in the following distinct sections.

5.3.3.1 Non-irrigated Areas

The following parameters have been determined in field studies conducted within the IMPETUS framework or by literature review, as described in the following paragraphs:

- **Minimum and Optimal Growing Temperature:** T_BASE, T_OPT[°C]
  These temperatures determine the plants growth and its seasonal variation of other plant related parameters.
- **Minimum and Maximum Leaf Area Index:** ALAI, BLAI [m²/m²]
  These parameters govern transpiration and interception and its seasonal variation.
- **Canopy Height:** CHTMX [m]
  The Canopy height affects wind speed at the ground level, hence evapotranspiration.
- **Maximum stomata conductance** GSI [m/s]
  Stomatal conductance is a driver of transpiration.
- **Rooting depth:** SOL_ZMAX, RDMAX [m]
  The rooting depth affects the plants ability to extract water from the soil.
- **Curve Number:** CN2 [-]
  The Curve Number determines the surface runoff as a fraction of precipitation that reaches the ground. It is set based on land cover and the hydrological soil group determined in the last section 5.3.2.

Arid and semi-arid regions are under-represented in the SWAT crop database. Arid rangelands, grass and brush steppes are all represented by little bluestem (*Schizachyrium scoparium*) a North American prairie grass; they differ by varying Leaf Area Index (LAI) only. SWAT applications in arid regions have rarely been conducted; therefore only little information on required plant parameters exists and specifics of contrasting biomes are not captured by the actual database. Nevertheless, the remaining parameters, which are predominantly necessary for modeling the plants nutrient cycle and provide results that are not considered within this study, have been taken from the original SWAT model database (*Schizachyrium scoparium*, for details see Neitsch et al. 1999).

Within the IMPETUS project a vegetation map has been developed (Finckh 2008). The classification bases on elevation, climate data and soil data (sources, as described in section 5.3.2), Landsat ETM+ satellite imagery (NASA 2003) and a habitat model (Staudinger & Finckh 2005). 26 different land cover types have been classified. Since this classification is too detailed for a direct use in SWAT-MAROC, the land use map has been simplified according to Table 5-6. The following features have been dropped and resulting gaps have been filled using the Euclidian Allocation routine from ArcGIS:

- Agricultural areas, because they are modeled separately as described in the following section 5.3.3.2
- Linear features linked to streams such as stream beds, meadows and swamps, due to their minor areal extent
- The reservoirs, as small reservoirs are not considered in this study and the reservoir Mansour-Eddahbi is modeled separately as described in section 5.3.8

Table 5-7: Aggregation scheme for the LU/LC map used in SWAT-MAROC. Original data provided by Finckh (2008)

	Biome	Area [km²]	Simplified class
1	Date palm oases	33	-
2	Mediterranean Oases	199	-
3	Sub-Mediterranean Oases	59	-
4	Rain-fed agriculture	101	Hamada steppe, degraded
5	Swamps	7	-
6	Debris	57	Mountainous vegetation, degraded
7	Dense thorny cushion shrubs	797	Mountainous vegetation
8	Clear thorny cushion shrubs	1289	Mountainous vegetation, degraded
9	Dense thorny cushion shrubs, lowland	225	Mountainous vegetation
10	Clear thorny cushion shrubs, lowland	300	Mountainous vegetation, degraded
11	Juniper trees	67	Mountainous vegetation
12	Woody artemisia steppe	203	Brush steppe
13	Dense artemisia steppe	1998	Brush steppe
14	Degraded artemisia steppe	2313	Brush steppe, degraded
15	Dense rocky Hamada	6	Hamada steppe
16	Dense Hamada	1619	Hamada steppe
17	Degraded Hamada	4376	Hamada steppe, degraded
18	Arid Hamada	105	Hamada steppe, degraded
19	Saharan rock communities	900	Hamada steppe, degraded
20	Meadows (*Oleander*)	65	-
21	Meadows (*Atriplex Glauca*)	3	-
22	Active wadis	15	-
23	Reservoirs	29	-
24	Mountain wadis	22	-
25	Sealed surface	19	-
26	Mining site	1	-

The remaining classes have been aggregated to 6 major classes accounting for the most dominant factors that affect land cover in the research area: altitudinal zonation and human interference (Finckh 2008). The three altitudinal zones (mountainous vegetation, brush steppe and Hamada steppe) have been split in degraded and non-degraded conditions, thus resulting in 6 classes.

Temperatures that affect plant growth in a semi-arid to arid environment have been compiled by White et al. (2008). Along an altitudinal gradient in the Northern Chihuahuan desert, grass and brush steppe as well as mountainous vegetation have been characterized. Minimum growing temperature is set to 5°C; optimum growing temperature is 27°C for the steppes and 22°C for the mountainous vegetation.

Leaf Area Index (LAI) may be most simply described as leaf area (m^2) divided by ground area (m^2). This interpretation is also adopted by the SWAT model. Several other definitions exist; Asner et al. (2003) provide an overview. LAI can be determined using different methods: measurement (e.g. Asner et al. 2003), estimation based on the degree of ground cover (e.g. Diekkrüger 1996) or remote sensing techniques (e.g. Baret et al. 2007). All of these techniques except remote sensing have been applied in this study (Table 5-8 provides an overview). Baumann (2009) determined specific leaf areas (leaf area/leaf mass [m^2/ kg]) for dominant plant types and then harvested and weighed leaves of 120 sample plots in the research area. Within the catchment plant coverage degrees have been estimated for all vegetation units as displayed in Figure 5-13 (Fritzsche 2011).

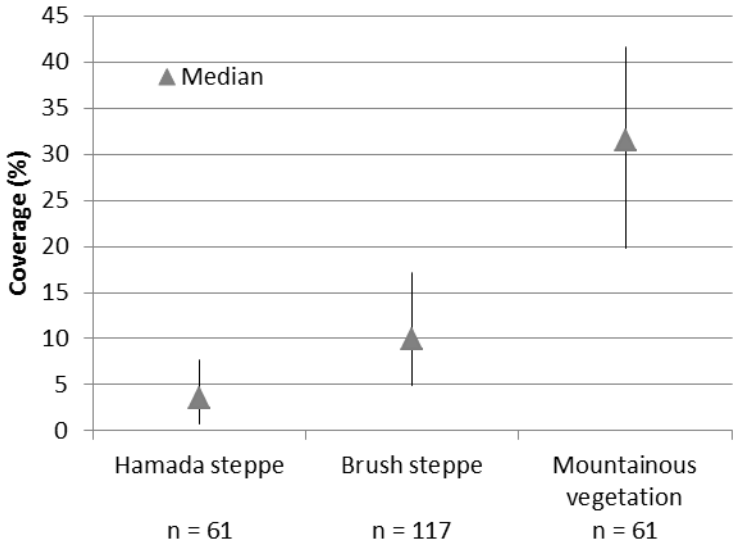

Figure 5-13: Plant coverage in the Upper Drâa catchment. Median, error bars envelope the 2nd and 3rd quartile, i.e. the middle 50% of observations (Fritzsche 2011)

Though these values are highly variable, a clear increase of coverage with altitude can be stated. To account for dense or degraded conditions, the 75th percentile has been assumed as dense vegetation cover and the 25th percentile as degraded vegetation cover. Based on these coverage degrees LAI has been calculated using an empirical relationship, as proposed by Diekkrüger (1996):

$$LAI = \frac{\ln\left(1 - \frac{CV}{100}\right)}{-0.4}$$

in which LAI = Leaf Area Index [m²/m²]
CV = Coverage degree [%]

Furthermore LAIs from a global synthesis report have been obtained (desert: 1.3, brush steppe: 2.1; Asner et al. 2003). Since Asner et al. define LAI as the leaf area per area covered by the plant (LAI_c); the given values have to be multiplied with the coverage degrees as well. The minimum LAI has been estimated according to the dominant plant types in each vegetation unit. Mountainous vegetation and shrub steppe are dominated by shrubs, their minimum LAI is estimated to 75% of the maximum LAI. Hamada steppes are dominated by annual grasses, therefore the minimum LAI is assumed to be 0.

Plant heights are generally low, not accounting for dispersed trees. Since vegetation degradation affects coverage stronger than height of particular plants (Baumann 2009), the same height has been assumed for dense and degraded conditions. These are in particular 50 cm for mountainous vegetation and 30 cm for dwarf-shrub steppe and the Hamada grasses.

Table 5-8: Leaf area indices for the Upper Drâa catchment

	Baumann (2009)	Fritzsche (2011)	Asner et al. (2003)	Based on Diekkrüger (1996)	SWAT parameters (Max/Min)
Mountainous vegetation	-	0.42	0.87	1.35	0.8 / 0.6
Mountainous vegetation, degraded	-	0.20	0.42	0.55	0.4 / 0.3
Brush steppe	0.23	0.17	0.36	0.47	0.3 / 0.225
Brush steppe, degraded	0.04	0.05	0.10	0.13	0.1 / 0.075
Hamada steppe	0.22	0.08	0.10	0.20	0.1 / 0.0
Hamada steppe, degraded	0.01-0.05	0.01	0.01	0.02	0.05 / 0.0

Maximum stomatal conductance represents the plants ability to minimize water losses through evaporation. In the mountains, where water availability is generally higher, a value of 0.004 m/s has been assumed (White et al. 2008). In the brush-steppe water-saving

mechanisms are more distinct; a value of 0.002 m/s has been assumed (White et al. 2008). The Hamada's annuals grow and blossom quickly after sufficient rain, therefore water-saving mechanisms are not required and a value of 0.005 m/s has been assumed (White et al. 2008).

Rooting depth is the essential parameter for determining to what extent plants can benefit from soil water storage. Haase et al. (1996) conducted tracer experiments with *Retama Sphaerocarpa* in semi-arid Southeastern Spain, concluding that their rooting depth exceeded 28 m. Excavated roots of *Prosopis juliflora* in Southern Arizona exceeded 50 m in length (Phillips 1963). Canadell et al. (1996) provide a comprehensive review of rooting depths for all terrestrial biomes, among these deserts (mean rooting depth 9.5 m) and sclerophyllous shrublands (mean rooting depth 5.2 m). *Tamarix* species, prevailing in the study area develop roots lengths of 20 m. Hence it can be assumed that roots are generally capable to penetrate the whole soil profile in the study area. In some cases they might as well reach the aquifer which gains importance considering the process of revaporation. Appendix 5 provides an overview on the plant parameterization used.

The **Curve Number** procedure is used in this model to calculate surface runoff. The Natural Resources Conservation Service provides Curve number values for a variety of semi-arid land cover types (NRCS 1986). The values have been chosen according to the following Table 5-9, accounting for land cover and soil properties. According to these values the tendency to produce surface runoff decreases with altitude, i.e. increase in vegetation cover. Due to the generally low coverage degrees, most parameters related to plant growth and plant cover introduced in this section can be assumed to be rather insensitive. The Curve Number instead, governing the discharge processes in this model, generally is the most sensitive parameter of the model (Veith et al. 2010).

Table 5-9: Runoff Curve Numbers Land Cover types in the research area (based on NRCS 1986)

Land cover SWAT-MAROC (Land cover NRCS)	**Hydrological Soil Group**			
	A	**B**	**C**	**D**
Mountainous vegetation (juniper steppe, good condition)	50	58	73	80
Mountainous vegetation, degraded (juniper steppe, fair condition)	60	75	80	89
Brush steppe (sagebrush steppe, fair condition)	40	51	63	70
Brush steppe, degraded (sagebrush steppe, poor condition)	60	67	80	85
Hamada steppe (desert shrub, fair condition)	60	71	81	89
Hamada steppe, degraded (desert shrub, poor condition)	70	80	87	93

Common ranges as provided by the NRCS give only an idea of reasonable values (NRCS 1986), but appropriate parameter values in a specific catchment depend on different variables, such as subcatchment size, climatology and others (Veith et al. 2010; Simanton et al. 1996; Hawkins et al. 2009). Therefore the adaptation of the values listed above during calibration is clearly needed. Furthermore the conceptual character of the Curve Number and the uncertainty already associated with the soil data needed to determine Soil Hydrological Groups and Curve Number make a further treatment of the Curve Number in the uncertainty analysis compulsory.

5.3.3.2 Irrigated Areas

For the irrigation subroutine the following parameters are required:

- **Evaporation coefficient:** K_c [-]
  A factor converting reference evapotranspiration into the actual plant water demand
- **Soil Storage:** SOL_STOR [mm]
  Pore space within the soil profile that can store water available to plants
- **Irrigation efficiency:** IRR_EFF [%]
  The fraction of irrigation water that is actually consumed by the irrigated plants
- **Fraction of Discharge available for irrigation:** IRR_FRAC[%]
  The fraction of discharge that can be diverted for irrigation purposes

Plant water requirement is calculated using the reference evapotranspiration (ET_0, calculated using the Penman-Monteith approach as described in section 5.1.1 and 5.1.2.2), which is calculated using the climate data introduced in section 5.3.6.1, which are adapted to the oasis conditions. Furthermore the area of each oasis and the respective crop mix are required. The values are set according to the agricultural census of 1997/98 (MTP 1998). The surface areas of the oases are: M'Semrir 1200 ha, Boulmalene 2553 ha, Kelaat 2673 ha, Skoura 1725 ha, Toundout 2635 ha and Ouarzazate 5215 ha. The crop mix is presented in Appendix 6. The locations of the oasis can be seen from Figure 3-1. The following

Table 5-10 gives an overview on the CropWat parameters used within the simulation. The **K_c-values** of each culture vary according to the seasonal plant growth cycle. The following perennial (p) or seasonal (s) crops are grown in the catchment: Alfalfa (p), Barley (s), Pulses (s), Vegetables (p), Wheat (s) and Corn (s) as second crop in summer. Furthermore date palms, fruit trees (Apple, Apricot, Almond) and olive trees are grown. A density of 300 per ha is assumed for palms and 400 per ha for other trees (Siebert et al. 2007).

Table 5-10: CropWat parameters for crops grown in the Upper Drâa catchment according to 1) Moroccan authorities (MTP 1998) and 2) CropWat Manual (Allen et al. 1989a)

	Stage [days]				K_c Value [-]			Planting Day
	I	II	III	IV	I	II	III	
Alfafa[1]	30	120	30	185	0.60	1.15	0.65	1
Barley[1]	30	90	50	40	0.55	1.00	0.20	270
Corn[1]	20	20	30	30	0.50	1.00	0.80	150
Date Palm[2]	140	30	150	45	0.90	0.95	0.90	1
Fruit tree[2]	140	30	150	45	0.40	1.00	0.85	1
Olive tree[2]	50	110	90	115	0.65	0.45	0.65	1
Pulses[1]	30	60	60	30	0.55	1.00	0.40	300
Vegetables[1]	30	150	150	35	0.35	0.35	0.35	1
Wheat[1]	30	90	60	30	0.45	1.00	0.60	270

Since oases are located close to the wadi beds, in general deep alluvial soils can be assumed (Klose 2009). Therefore **soil storage** is set to 500 mm. This relatively high value also accounts for deep rooting palm trees and groundwater storage that is accessed by pumping, hence not only water stored in the soil profile.

In this study, **irrigation efficiency** is defined as the fraction of applied irrigation water that is not lost to evaporation. Percolating water is not actually lost from the system, but can be pumped or consumed by deep-rooting plants. A range of reasonable values is given by Bos & Nugteren (1990) and Foster & Perry (2010). Since flood irrigation in basins is the dominant irrigation type in the study area, an irrigation efficiency of 75% has been assumed (cf. Table 5-11). This value is rather high compared to other studies conducted in the study area (Klose et al. 2010b), but lines in with values estimated by local authorities (ORMVAO 1995). A further parameter required in the irrigation module is the **fraction of runoff that can actually be abstracted**; it is set during calibration. This fraction reflects difficulties to fully exploit low flow, as the river stage might fall below irrigation channels, and high flow as the irrigation systems capacity might be surpassed.

Table 5-11: Irrigation efficiencies (Foster & Perry 2010)

Irrigation technology	Consumed fraction		Percolation
	Beneficial transpiration	Non-beneficial evaporation	
Gravity flow to Basin/furrows	Moderate-to-high (40-80%)	Moderate but variable	Moderate (20–30%)

Both latter parameters have to be considered in the uncertainty analysis, as they represent rather conceptual parameters and their effect on total irrigation volumes is high. The site-specific K_c-values have been adapted from local sources (MTP 1998) and their auditability is assumed.

5.3.4 Spatial Discretization

As lined out in 5.1.2.1 and 5.3.1 the subcatchments have been intersected with elevation zones. These spatial units have been further subdivided according to soil, land cover and slope to create the EHRUs, using the ArcSWAT-Interface. Considering slope, two slope classes have been created, steeper or flatter than 13% (the catchments median slope). Therefore geomorphological conditions on mountainous slopes, in the basin and on plateaus (as described in sections 3.4 and 3.5) are reflected by the model setup.

The areal thresholds that need to be exceeded by a soil- slope land cover or slope class in order to be represented in the model are given in Table 5-12.

Table 5-12: Selected thresholds for determination of EHRU s

	Elevation range	Soil	Land cover	Slope
Classes	5	32	6	2
Threshold	-	2000 ha	2000 ha	10000 ha

For the land cover the effect of different thresholds has been assessed. The deviation from the original distribution is given by the mean absolute error of land cover in the EHRUs compared to the original map, divided by the standard deviation. Values below a quotient of 50% are considered as good representations (see section 4.2.1).

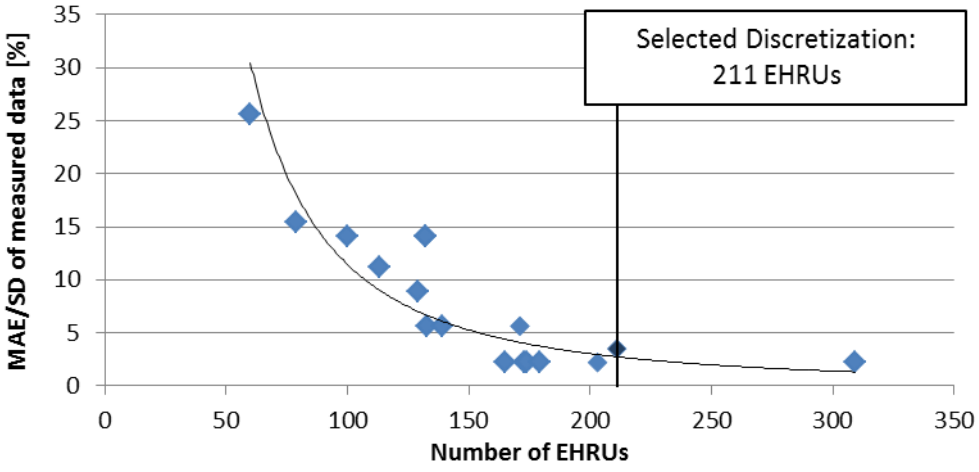

Figure 5-14: Quality of catchment representation using different sets of thresholds for EHRU classification

As it can be seen from Figure 5-14, the quality of the spatial representation does not improve considerably if smaller thresholds, hence larger numbers of EHRUs and computational power required for model runs, are applied. On the other hand areal representation decreases noteworthy, if larger thresholds are applied. Therefore the chosen thresholds can be considered as adequate in terms of areal representation and computational efficiency.

The final EHRUs average size is 70 km² (standard deviation: 45 km², min: 1 km², max: 217 km²). The representation of different land cover types is provided by Table 5-13. The MAE is 3% of the original spatial extends standard deviation, whereas soil representation performs poor (MEA equals 94% of the standard deviation, see Appendix 7 for areal extents).

Table 5-13: Spatial representation of different land covers in the EHRUs

Spatial extent in km²	Mountainous vegetation		Brush steppe		Hamada steppe	
	Dense	Degraded	Dense	Degraded	Dense	Degraded
EHRU	1227	1680	2326	2349	1803	5582
Land cover map	1207	1688	2349	2273	1679	5631

5.3.5 Geology

For setting up the SWAT-MAROC model eight groundwater-related parameters are determined:

- **Recession Coefficients:** ALPHA1_BF, ALPHA2_BF and ALPHA_BNK [-]
  The recession coefficients of the two aquifers and the bank storage control temporal baseflow dynamics.
- **Recharge coefficient of the second aquifer:** RCHRG_DP [%]
  This parameter diverts a fraction of percolating water to the second aquifer.
- **Effective hydraulic conductivity:** CH_K1 and CH_K2 [mm/h]
  The effective hydraulic conductivity represents the steady-state conductivity of the tributary channel beds and main channel beds.
- **Revaporation coefficient:** GW_REVAP [%]
  Water may move from the shallow aquifer into the overlying unsaturated zone by capillary rise or be consumed by deep rooting plants. GW_REVAP determines the fraction of evaporative demand that may be satisfied by groundwater from the shallow aquifer.
- **Delay coefficient of direct groundwater recharge:** GW_DELAY [-]
  Direct recharge does not occur instantaneously but is delayed using an exponential delay function. This represents the travel time of percolating water in the unsaturated zone.

Based on the official geological map; hydrogeological properties of the geological formations in the Upper Drâa valley have been determined (Klose 2008b; ME 1959). For this study a simplified map, distinguishing fractured, porous and karstified aquifers, is used (Figure 5-15). Each simulation unit is assigned the dominant aquifer type and consists of two linear

reservoirs (see section 5.1.2.3). In the karstic regions these two aquifers represent the "double porosity" phenomenon of karstified limestone. Both are recharged by direct and indirect recharge. In the porous and fractured simulation units, the second aquifer is considered to be a deep aquifer that is only fed by indirect recharge. The dominance of indirect recharge in arid regions has been pointed out in general (de Vries & Simmers 2002), and for the Upper Drâa catchment in particular (Cappy 2006).

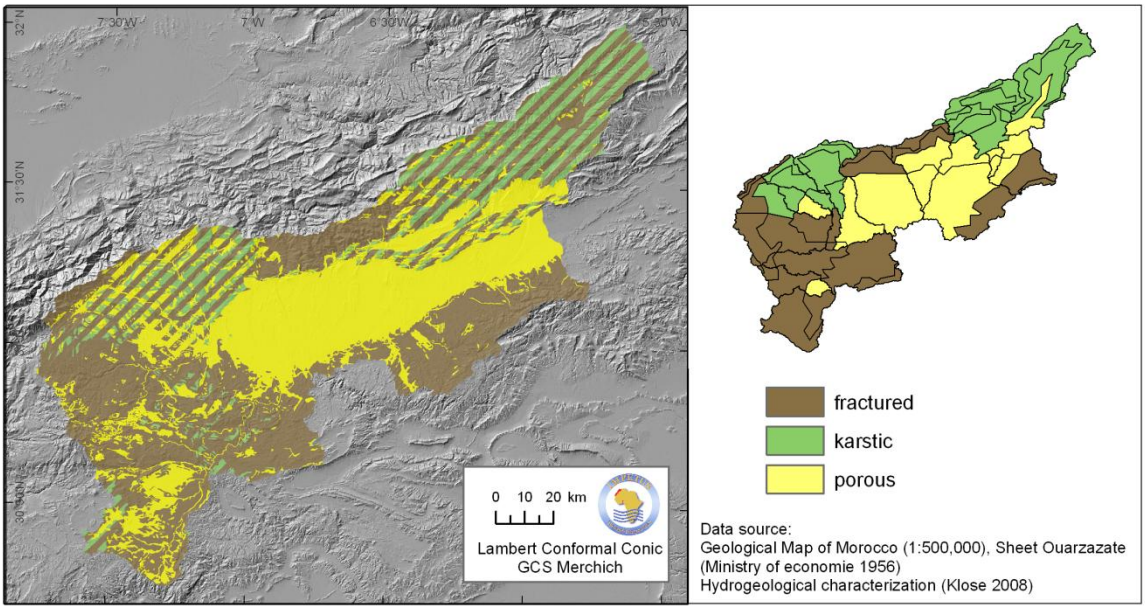

Figure 5-15: Aquifer types in the Upper Drâa valley (left side). Dominating aquifer type in simulation units (right side)

Recession coefficients are usually determined by the analysis of discharge data (Tallaksen 1995; Smakhtin 2001). However, in the Upper Drâa catchment reliable discharge data is hardly available (see chapter 5.3.7). Especially low flow data is not reliable, which is why recession coefficients cannot be derived from these data. At the reservoir Mansour-Eddahbi the filling level is measured daily and uncertainties are considerably smaller. Anyhow a robust master recession curve cannot be established and therefore a manual regression has been established for one event (calibration) and validated for six further events (see Figure 5-16). Performing a recession analysis one has to keep in mind that observed recession is a product of different superimposing processes, at least surface runoff, interflow, different baseflow components, snow melt and bank discharge (Griffiths & Clausen 1997).

The methodology developed can be outlined as follows. Three aquifers are postulated of which the first two are detectable and coefficients can be determined by the means of a recession analysis:

- Fast: alluvial, fracture drainage
- Intermediate: karstic quickflow, porous
- Slow: karstic slowflow

Measured discharge is smoothed by a three-day filter, to account for measurement uncertainties at the reservoir. Surface runoff and lateral flow are not considered in the analysis by not including the first five days after peak discharge. The contribution of the fast aquifer is assumed to be negligible after two months and the recession of the intermediate aquifer is approximated exponentially, from that day on. This exponential function is extrapolated back in time and the residual is assumed to be the fast aquifers contribution, which again is approximated exponentially.

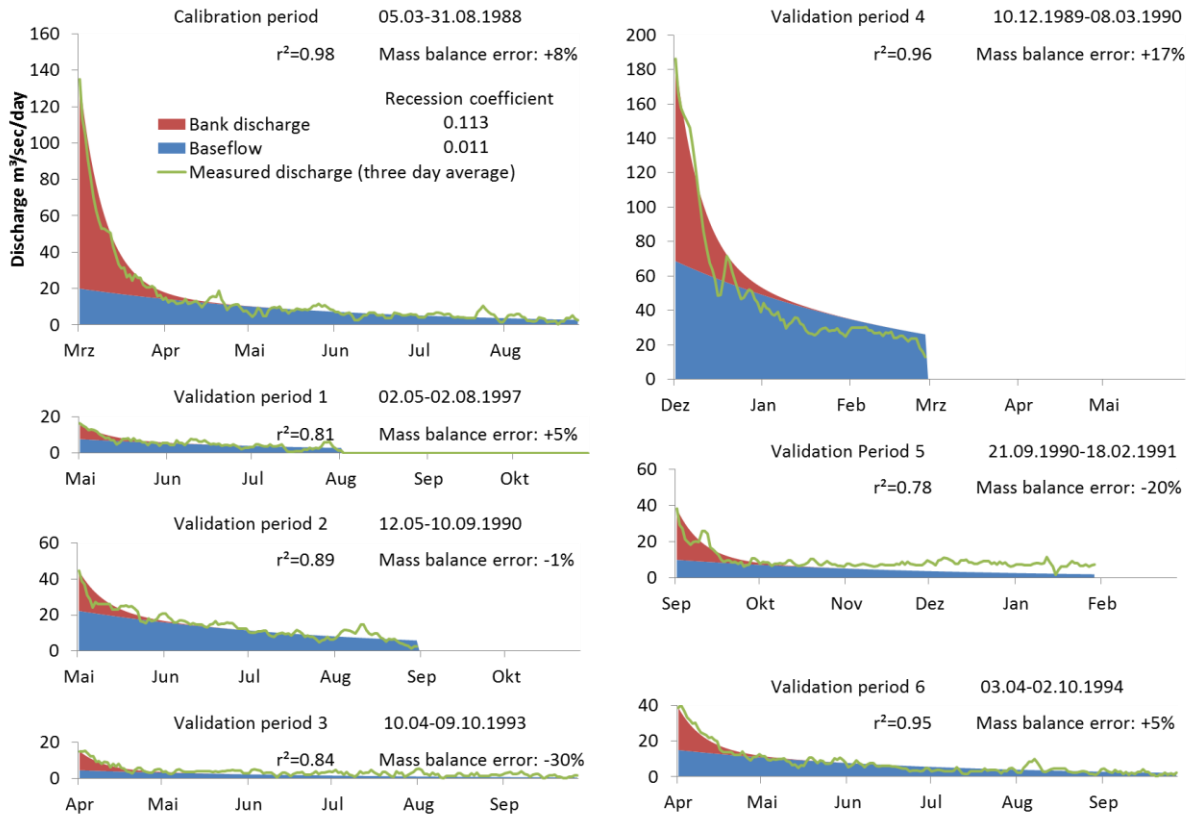

Figure 5-16: Daily flow recession measured at the reservoir Mansour-Eddahbi (15000 km²). Measured data provided SE Ouarzazate

During calibration and validation simulated recession flow matches observed recession flow reasonably well (r^2=0.98 and 0.78-0.96, respectively). Due to the fact that the reservoir displays only a lumped behavior of the catchment, some assumptions have to be made. The fast aquifer is assumed to represent the alluvial aquifer and fast discharge from fractures in the Precambrian basement (recession coefficient of 0.11). The intermediate response is driven by the draining of the karstic and porous aquifers (recession coefficient of 0.011). The postulated

slow aquifer can only be recognized qualitatively by the general trend of the model to underestimate baseflow in the long run. This is assumed to be the second component of the limestone areas. Since its flow recession cannot be measured, literature is reviewed to obtain reasonable values for this aquifer. Recession coefficients vary within a broad range for the lithologies considered (Figure 5-17): Anyhow, values for karstic quickflow center around 0.0125 for a variety of karst springs in Tunisia and France (Brown et al. 1972). Values from upper cretaceous calcareous rock formations in Israel are about 0.0465, but still envelope the value derived in this study. Furthermore slow components have been analyzed and values of 0.0016 (France/Tunisia) and 0.0039 (Israel) are obtained. Schwarze (1999) attributed German hydrogeological units that also prevail in the Central High Atlas: limestone/dolomites, conglomerates, cretaceous sandstone and new red sandstone with their slowest baseflow recessions. Average values for these units range from 0.0013 to 0.0056.

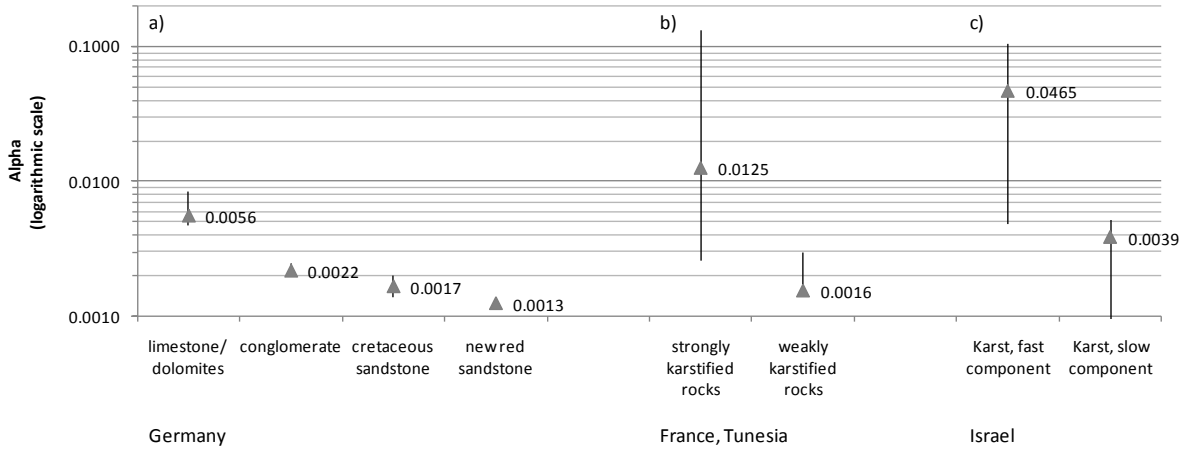

Figure 5-17: Compilation of recession coefficients a) slow groundwater components for different lithologies in Germany (Schwarze 1999); b) French and Tunisian karstified regions (Brown et al. 1972); c) Upper cretaceous calcareous rock formations in Israel (Amit et al. 2002)

Therefore the derived quickflow recession (0.0113) seems plausible, and the slow flow recession is set to 0.0015. Eventually, the derived baseflow recession coefficients are listed in Table 5-14.

Table 5-14: Baseflow recession coefficients in the Upper Drâa catchment

	fractured	**porous**	**karstic**
ALPHA1_BF	Fast flow in fractures, negligible flow through matrix → 0.113	Intermediate flow from conduits or fissures in limestone and or porous sediments of varying conductivity → 0.011	
ALPHA2_BF	No double porosity		Slow component from limestone matrix or embedded sandstones matrix →0.0015
ALPHA_BNK	Fast flow in alluvial aquifers → 0.113		

The **recharge coefficient of the second aquifer** can hardly be measured. In the Upper Drâa valley Liassic and Triassic limestone aquifers exhibit exclusive properties, due to varying sedimentation conditions (e.g. reef or peritidal facies) or tectonic faulting and shifting (Hofmann 2002). Detailed studies from regions with similar lithologies therefore reveal a wide range of plausible parameter values. Atkinson (1977) concluded from an analysis of spring hydrographs in England that 50% of the spring discharge was by "quickflow" and 50% by "slowflow". Amit et al. (2002) concluded ratios of quickflow to total flow greater than 80% for karst sources in Israel. Triassic sandstone formations as in the Central High Atlas occur also in Eastern Thuringia; here 70% "quickflow" and 30% slowflow have been acknowledged (Rödiger et al. 2009). In this study the fraction is set 50%.

Transmission losses are an important factor in the water balance of arid regions (EI-Hames & Richards 1994). Losing streams prevail in the research area; their effective infiltration rate varies according to discharge, stage height, flooded perimeter and clogging effects (Dunkerley 2008). Lane (1983) provides an overview of effective conductivities for different types of channel beds (Table 5-15). Effective conductivity represents the steady-state conductivity of the channel bed material under field conditions (entrapped air, sediment laden flow, etc.). Therefore, it can be an order of magnitude less than saturated conductivity measurements made with infiltrometers using clear water.

Table 5-15: Example hydraulic conductivity values for various river bed materials (Lane 1983)

Bed material group	**Bed material characteristics**	**Effective hydraulic conductivity**
Very high loss rate	Very clean gravel and large sand	> 127 mm/h
High loss rate	Clean sand and gravel, field conditions	51-127 mm/h
Moderately high loss rate	Sand and gravel mixture with low silt-clay content	25-76 mm/h
Moderate loss rate	Sand and gravel mixture with high silt-clay content	6-25 mm/h
Insignificant to low loss rate	Consolidated bed material; high silt-clay content	0.025-2.5 mm/h

Since the main channels exhibit silty beds and even little discharge is routed through to the reservoir during the dry season, the **effective hydraulic conductivity** of the main channel has been set to 10 mm/h. Due to minor clogging effects in tributary channels their effective hydraulic conductivity is set to 100 mm/h. This goes along with in-situ measurements conducted in the Upper Drâa catchment. Weber (2004) measured final infiltration rates (K_s) of up to 266 mm/h in first-order depth lines.

The process of **revaporation** (capillary rise or consumption by deep rooting plants) has been included in the model owing to several reasons.

- Contrasting low water tables in the regional aquifers, the dominant alluvial aquifers are characterized by relatively high water tables.
- Deep rooting plants, which are not included in the land-use map due to their minor spatial extent, prevail in the vicinity of the wadis (e.g. *populous, salix, tamarix*). They can easily access alluvial aquifers and account for substantial water losses from the aquifer.
- In the basin of Ouarzazate widespread salinization outside agricultural perimeters can be observed. The occurrence of gypsic strata is known, but this might also hint to high water-tables, enabling capillary rise to occur.

This parameter is adapted during calibration, the revaporation rates given in section 2.5 equaling a GW_REVAP coefficient of 0.0075 are considered as upper limits of revaporation. No threshold, i.e. minimum filling level of the aquifer, required for revaporation to occur, is set.

The exponential **delay of direct recharge** representing travel time through the unsaturated zone can hardly be measured or vary widely according to the depth of the water table. Therefore this parameter is determined during calibration.

Since recession coefficients and hydraulic conductivities are based on measurements or plausible literature values, they are not considered in the uncertainty analysis. The revaporation coefficient and the partition fraction between the two aquifers represent highly conceptual model components affecting evaporation rates as well as long term timing of discharge; therefore they are further analyzed in the uncertainty analysis.

5.3.6 Climate Data

Climate data are the dominating boundary condition in hydrological modeling. In more sophisticated models numerous climate variables have to be considered, besides precipitation. In SWAT, using the Penman-Monteith evapotranspiration module and the Curve-Number procedure, the following variables are required at daily time resolution:

- Precipitation [mm]
- Maximum temperature [°C]
- Minimum temperature [°C]
- Wind velocity [m/s]
- Relative humidity [%]
- Solar radiation [MJ/m²]

The following sections describe the sources and the climate data used in the simulation. Furthermore parameters derived from climate data are presented.

5.3.6.1 Measured Data

To set up a hydrological model capable of performing long term water availability assessment long time series of climate data are required. Climate data are registered at the meteorological station Ouarzazate since the 1920ies, but sufficient spatial coverage is not guaranteed until the 1970ies. Therefore only climate data from 1975 on is used within this study (see
Appendix 1, for locations of the stations see Figure 3-4). These data are complemented by climate measurements that have been conducted within the IMPETUS-project.

For the generation of semi-synthetic precipitation time series (refer to section 5.1.2.1), mean annual precipitation sums, average number of rain days and a precipitation lapse rate for daily precipitation have to be determined. Based on precipitation data form 19 gauges (SE and IMPETUS) for the period 2001-2007, reasonably robust linear relationships of elevation and annual precipitation sums/ average number of rain days can be established (see Figure 5-18). Though Schulz (2007) proposed a second-order polynomial regression fort the Middle and Upper Drâa catchment, a linear relationship seems sufficient for the Upper Drâa alone.

A mean precipitation lapse rate of 3.6 mm/ km has been determined comparing daily precipitation rates of the 7 IMPETUS gauges and 12 SE/DRPE gauges located in the Upper Drâa catchment. For this comparison only days with at least 12 out of 19 gauges indicating rain have been used, so the impact of small scale events could be diminished. In total 87 events have been evaluated.

Temperature data has been adapted to elevation by using linear lapse rates derived from IMPETUS-measurements as proposed by Dodson & Marks (1997). Linear regressions have been established for mean monthly maximum and minimum temperatures and the regression slopes were taken as the lapse rates. Lapse rates range from -5.3°/km in January to -8.1°C/km in July; associated coefficients of determination range from 0.79-0.90 (see Appendix 8 for details). The remaining variables (wind velocity, relative humidity and solar radiation) have been estimated using the WXGen weather generator incorporated in SWAT (Richardson & Wright 1984). The required values are obtained from IMPETUS measurements dating from 2000-2007, these data have been elevation adjusted by linear regression (see Appendix 8 for further details).

Having determined these parameters, missing values in the measured time series have been filled by using elevation adjusted values from neighboring gauges. Since temperature data are lacking from 2006 on, temperature data had to be generated for the period 2006-2007, based on a weakly stationary generating process as described by Richardson & Wright (1984). Assuming constant serial correlations and cross-correlations of the variables, plausible time series of temperature and radiation can be generated.

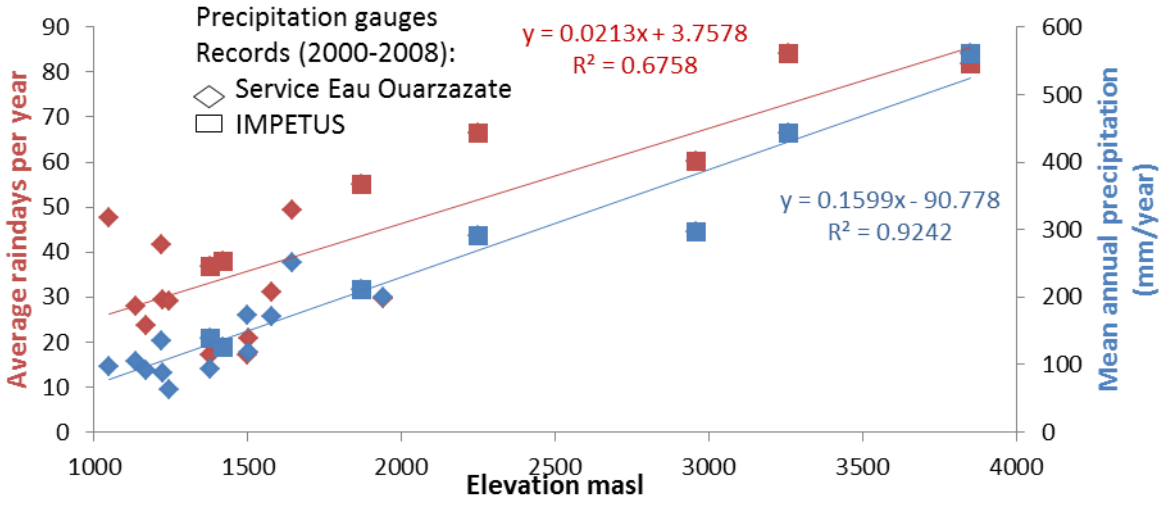

Figure 5-18: Precipitation gradients in the Upper Drâa catchment (2001-2007). (Data: IMPETUS and SE Ouarzazate).

Climate data used for the evapotranspiration estimates in irrigated areas are treated as follows. For each oasis climate data is adjusted by applying altitudinal gradients to climate data obtained from climate stations outside the oasis. Besides, the oasis effect is accounted for by decreasing T_{min} by 4.2°C and increasing T_{max} by 0.4°C. Wind speed is decreased by 77% and relative humidity is increased by 4.9-11.5% depending on the month. The derivation of these parameters is lined out in detail in section 5.1.2.2. To account for shading of palm and fruit

trees and since agricultural areas are located at valley bottoms, measured radiation is decreased by 20%. A decrease of 20% has also been reported from oases in southern Israel (Potchter et al. 2008).

5.3.6.2 Snow-related Parameters

SWAT-MAROC further requires data for the snow module (Fontaine et al. 2002). In this section parameters are briefly explained, and reasonable ranges are presented. All parameters are lumped, i.e. applied to the whole catchment. The parameters have been determined during manual calibration, since adapted parameters need to be evaluated carefully with regard to the lumped model approach.

- **Snow Fall Temperature:** SFTMP [ºC]

  Mean air temperature below which precipitation is falling as snow. This factor governs the accumulation of snow. A reasonable range is 0-5°C, as snow might form in higher and colder elevations before reaching the ground.

- **Snow Melt Temperature:** SMTP [ºC]

  This is the snow pack temperature above which snow starts melting. This parameter along with the melt factor SMF governs the melt of snow. A reasonable range is similar to that of SFTMP.

- **Snowmelt Factor:** SMF [mm/ºC/day]

  This is the melt factor for snow. The parameter is a factor of proportionality between melt rate temperatures surpassing SMTP. It accounts for the impact of snow pack density, albedo and radiation on snow melt. In rural areas, ranging from 1000 to 4000 masl, melt factor ranging from 2.7 to 5.9 mm/day-°C are reported (Hock 2003).

- **Minimum Snowpack at 100% Cover:** SNOCOV100 [mm]

  This is the minimum snow water content that corresponds to 100% snow cover; it governs the areal distribution of snow and the snowmelt. Drifting, shading and topography influence the snow accumulation in a catchment, therefore the parameter is higher the more rugged the catchment is. A reasonable range goes up to 300 mm.

- **Snowpack at 50% Cover:** SNOCOV50 [%]

  This is the fraction of SNOCOV100 corresponding to 50% snow cover. SWAT can assume a nonlinear correlation of snow volume to cover. In case this is not desired, this parameter should be set to 50%.

5.3.7 Discharge Data

Within the research area several stream gauges are installed. Their positions have been used to delineate the subbasins as described in section 5.3.4. At the basin outlet the reservoirs water balance can be used to quantify discharge. Both measurements are prone to different sources of uncertainty that are presented and concluding the data quality is discussed.

5.3.7.1 Stream Gauges

Within the Upper Drâa catchment eight discharge gauging stations are operated by the Service Eau (see Appendix 2, locations are provided in Figure 3-13). The stations are equipped with graduated vertical staff gauges that are read daily by the operating personnel. Furthermore the stations are equipped with a recording device. A float is connected to a wheel on the recording device via a thread. The float itself is located inside a stilling well connected to the stream. The quality of data from these gauges can be considered low. On the one hand harsh environmental surroundings (unstable channel bed, flash floods, low baseflow etc.) hamper measurements; on the other hand personnel and equipment is lacking. These phenomena have been denoted especially in arid or mountainous regions (EI-Hames & Richards 1994).

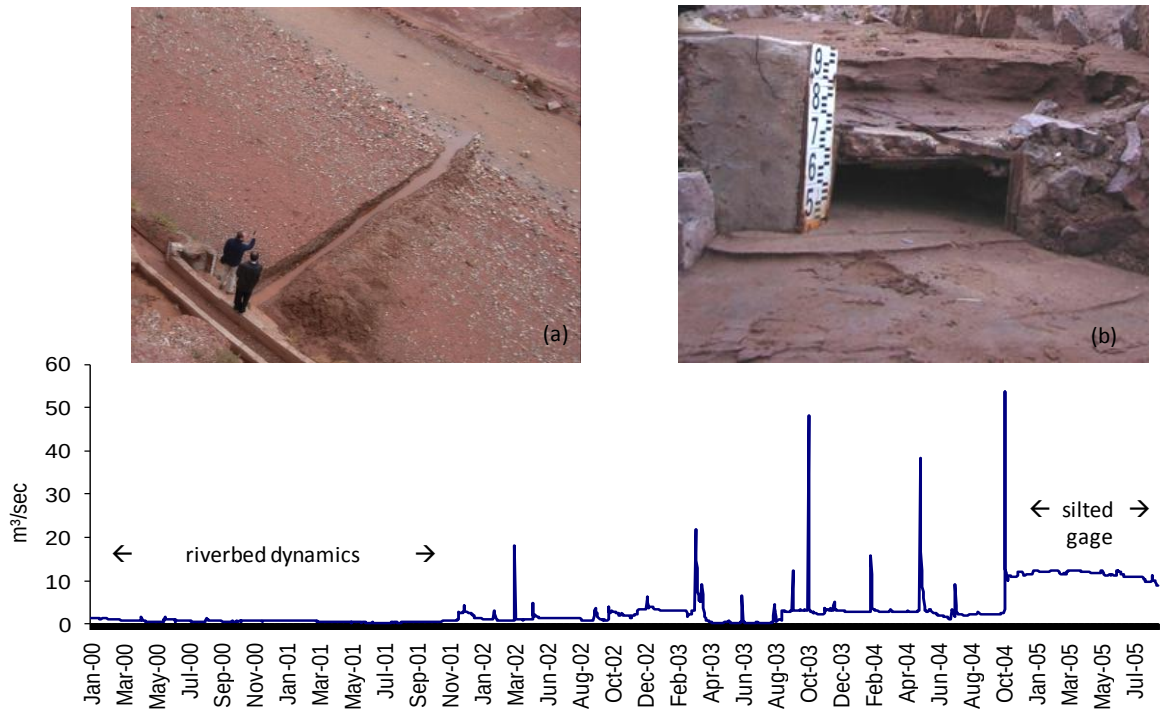

Figure 5-19: Examples for low quality of discharge data compiled from different gauges: Replacement of the channel hampers low flow registration (photo a: Ait-Mouted gauge); Silted stilling well hampers flow registration after floods (photo b: Agouillal gauge); Hydrograph of the Ifre stream gauge (1.200 km²), with marked periods of questionable data. (data: SE Ouarzazate)

These errors can hardly be quantified. Reviews on measurement uncertainty in the United States give a range of ±20% for velocity-area measurements under "poor" conditions. Shifting channels impede the establishment of robust stage-discharge relationships (±20%), unstable beds are associated with another ±10% (Harmel & Smith 2007; Harmel et al. 2006). Following the approach of Topping (1972) a cumulative uncertainty of 30% can be stated for the outlined conditions. Assessing different sources of uncertainty, an average measurement error of 26% has been estimated for the mountainous headwater catchment of the river Po in Italy (Di Baldassarre & Montanari 2009). This range can be considered as a lower boundary since environmental conditions in Southern Morocco are extreme, and stage-discharge relationships are updated infrequently. Figure 5-19 exemplifies the conditions experienced in the research area, where due to shifting channels gauges are frequently isolated from the stream, or clogged stilling wells inhibit measurements at all. Therefore these data can hardly be used for a quantitative assessment of model goodness. Nevertheless the occurrence or timing of flood peaks can be judged qualitatively.

Improving the quality of discharge measurements is one of the most prominent aspects to consider, when planning new measurement campaigns. In recent years a variety of promising new approaches has been developed (Mishra & Coulibaly 2009). Acoustic Doppler Current Profilers (ADCPs) for example measure the shift in the frequency of emitted acoustic signals reflected from suspended materials in the river and accordingly the velocity of the water, throughout the whole channel profile. Ultrasonic probes attached to bridges or cableways provide undisturbed stage measurements. The combination of both techniques has the potential to provide robust stage-discharge-relationships even under the harsh environmental conditions of the research area.

5.3.7.2 Reservoir

To overcome these shortcomings, the water balance of the reservoir Mansour-Eddahbi at the basins outlet is used for model calibration and validation. The water balance of the reservoir is calculated since its initial operation in 1973 by the SE. Abstractions can be either measured (downstream releases, drinking water supply) or estimated (seepage, evaporation); hence time series of inflow can be calculated:

$$Q_{in} = \frac{\partial V}{\partial t} + Q_{out} + Evap + Seep + DW - Sed \qquad \text{[all in M m³/timestep]}$$

in which

Q_{in}	=	Inflow during timstep t
$\frac{\partial V}{\partial t}$	=	Change of reservoir Volume during timstep t
Q_{out}	=	Water relase from reservoir during timstep t
$Evap$	=	Evaporation from reservoir during timstep t
$Seep$	=	Seepage through reservoir floor during timstep t
DW	=	Drinking water abstractions during timstep t
Sed	=	Sediment entry into the reservoir during timstep t

The calculations accuracy strongly depends on the precise assessment of the reservoirs volume. Bathymetries have been carried out in 1972, 1982, 1988, 1994 and 1998. As presented in Figure 5-20 the distribution of sediments follows roughly an idealized scheme as proposed by the (USACE 1997).

To account for the deposition of sediments in the time intervals between the bathymetries sediment entry was assumed to happen at a constant rate of inflow. The known volumes have been correlated to the associated reservoir stage level by 3rd order polynomials (r^2>0.99 for every bathymetry, see Appendix 9). In between the bathymetries the reservoirs volume was assumed to decrease linearly with cumulative inflow; hence volume was calculated as a linear combination of enveloping polynomial regressions.

Since 1998 no further bathymetries have been carried out, therefore the simplifying assumption that further sediment delivered into the reservoir is deposited at the bottom of the reservoir has been made. An average sediment delivery ratio of 1.6% (±0.6% standard derivation) could be derived from the bathymetries.

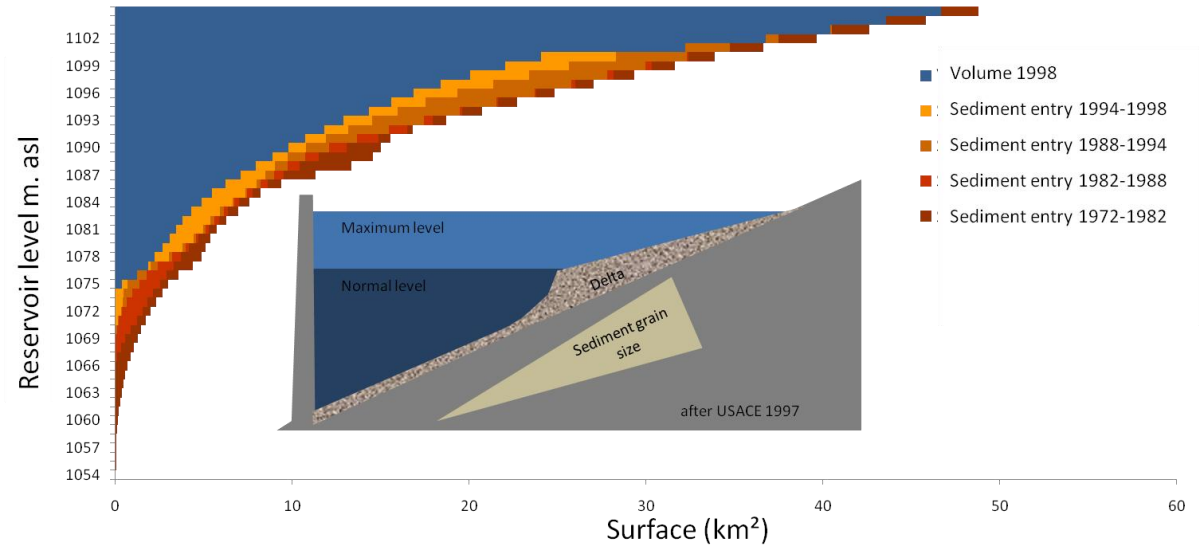

Figure 5-20: Sediment deposition in the reservoir Mansour-Eddahbi compared to an idealized profile (data: SE Ouarzazate)

Though uncertainties are considerable smaller compared to the stream gauges, they have to be accounted for. The quality of the bathymetries is the most important aspect to name; unfortunately neither a quality assessment has been performed, nor are original data available (sampling grid, technology used etc.). Data on water abstractions for irrigation and drinking water supply are rather certain and seepage can be considered negligible. Considering the sediment entry, the variance of the measured sediment delivery ratios has been taken for an appropriate uncertainty range (± 35.9%).

5.3.8 Reservoir Water Balance Module

The water balance module requires the following parameters and variables:

- **Abstractions:** $V_{abstract}$ [Mm³]

  As outlined in the previous section 5.3.7.2, the SE Ouarzazate provides series of drinking water abstractions from the reservoir. This time series is used in the baseline scenario and replaced by scenario values in the future scenarios.

- **Optimum amount of irrigation water:** $V_{release,\ opt}$ [Mm³]

  The quantity of irrigation water needed by the oases in the Middle Drâa valley is app. 250 Mm³ as lined out in section 3.1.

- **Residual reservoir volume:** V_{min} [Mm³]

  The residual water volume is the amount of water that should remain in the reservoir to sustain the lakes fauna and to supply drinking water to the city of Ouarzazate, even during prolonged droughts. This parameter is determined during calibration.

- **Buffer coefficient:** C_{buffer} [-]

  This parameter steers the reduction of water release, when storage is running low. It is determined during calibration.

- **Evaporation coefficient:** C_{evap} [-]

  This parameter is set to 0.6 according to similar routines in the SWAT model (Neitsch et al. 1999)

A bilinear regression for the surface area at a given filling volume and a given sediment body in the reservoir has been developed.

$$SA = (0.0001187 * SED + 0.07877335) * VOL - 0.0094835 * SED + 4.30631479$$

in which	SA	=	Surface of reservoir water body [km²]
	SED	=	Sediment body in Reservoir [M m³]
	VOL	=	Volume of water in reservoir [M m³]

Compared to the measured values obtained from bathymetries this equation reveals a good performance (r^2=0.98, MAE= 1.4 compared to a standard deviation of 12.1), and is therefore considered to approximate well the reservoirs surface in the scenarios.

5.4 Model Calibration

In this study a combined approach of manual calibration and autocalibration has been chosen. Therefore the available discharge record has been used for a split sample test: The observed inflows to the reservoir (1995-2007) have been used to calibrate the model. This period has been chosen, due to three reasons. The calibration period is dominated by intermediate flows, wet and dry years, therefore all relevant hydrological processes can be assumed to occur in the calibration period. In contrast the mid-eighties are very dry, exhibiting very little discharge at all and the late eighties/early nineties are very wet, exhibiting frequent floods. Furthermore the irrigated areas used within the CropWat-module represent the mid-nineties conditions. Finally snow dynamics have only been studied since the year 2000 within the IMPETUS project.

5.4.1 Hydrological Model

During the first manual calibration phase, the parameters presented in Table 5-16 have been adapted and a rough match of model results with the observed seasonal flow, observed snow cover and applied irrigation water was obtained. Besides the matching with flow records as presented in Figure 5-23 and Figure 5-24, irrigation records and snow cover measurements have been used to calibrate the snow parameters and the irrigation parameter IRR_FRAC.

Table 5-16: Parameters adapted during manual calibration (see Appendix 3 for details on parameters).

Parameter	Value
GW_DELAY [days]	90
SFTMP [°C]	1
SMTMP [°C]	3
SMFMX [mm/°C*Day]	5
SNOCOVMX [mm]	80
SNO50COV [%]	20
IRR_FRAC [%]	50

To compare innerannual dynamics of the **snow cover**, TERRA-MODIS (Moderate Resolution Imaging Spectroradiometer) image products (MOD09 GHK) have been used by Schulz (2007). The Normalized Difference Snow Index (NDSI; Salomonson & Appel 2004) classification method was applied to a time series of 500 images, with about 100 for each snow cover period for the years 2001 to 2006 that last from October to June. Analysis of the NDSI data shows that snow cover is present for only short periods in altitudes below 2000 masl. In elevations above 3000 masl snow cover is present from October through May (~ 150 days), exhibiting two distinct peaks in the early and the late rainy season. The annual variability of snow cover days is below 20% in altitudes above 3,000 masl, but rises with decreasing altitude towards the basin (Klose et al. 2010a).

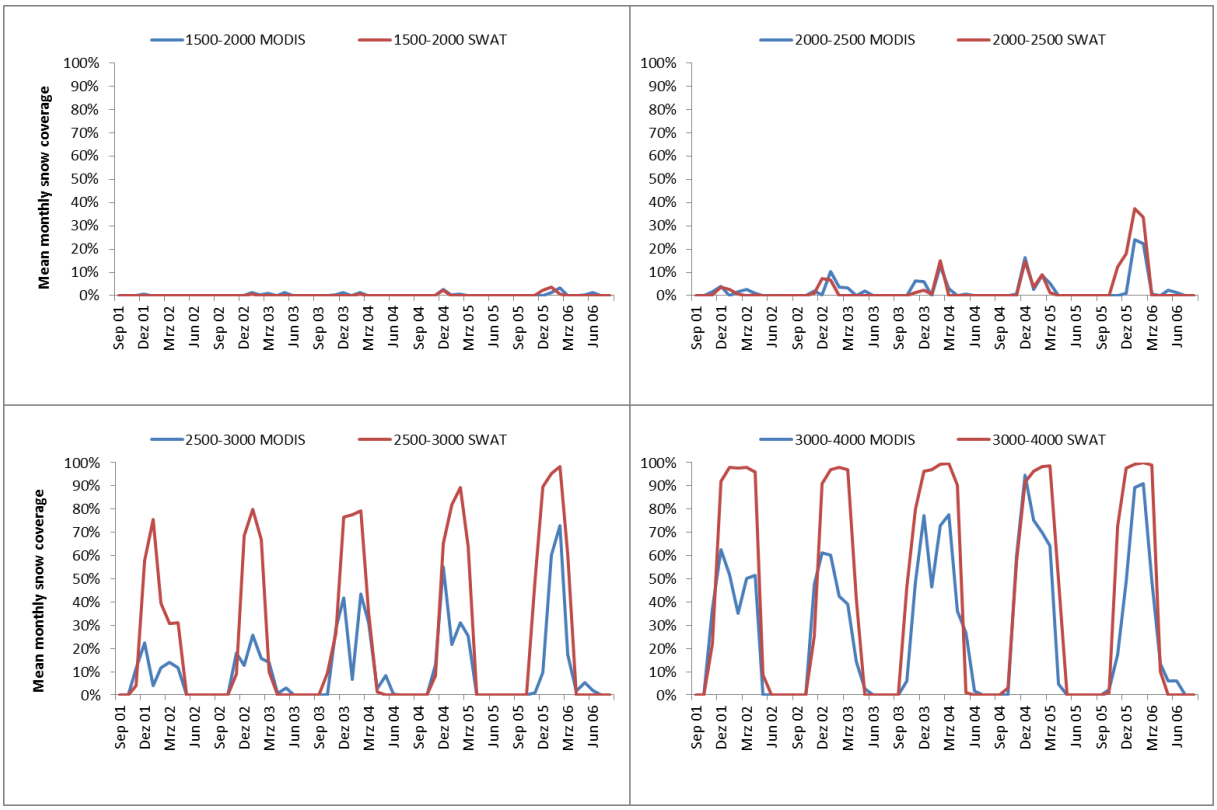

Figure 5-21: Snow dynamics in the higher elevations of the Upper Drâa catchment 2001- 2006. Measured: MODIS-based NDSI with courtesy of Oliver Schulz; Simulated: SWAT-MAROC

Figure 5-21 shows the comparison of measured and simulated snow covers for the period 2001-2006. Though absolute coverage differs in the elevated regions, the temporal extents of measured and simulated snow cover are similar in all elevation zones. Overestimations of absolute cover may derive from the simple degree-day-approach, which does not account for slope, exposition, wind deposition and other factors. Furthermore SWAT-MAROC uses only lumped parameters for snow-related processes; therefore it does not reflect topographic differences between high-montane and intermediate regions. For the future it should be tested whether the lumped snow module parameterization could be improved by spatially distributed parameters, for instance by relating snow cover thresholds to topographic features such as slope or terrain roughness that could easily be derived from the DEM.

However SWAT-MAROC modeling of interseasonal snow-melt is imperfect, as the distinct peaks in December and March/ snow melt in February, as identified in the satellite imagery are not reproduced by the model. The elevation zones 4 and 5 (2500-3000 masl and >3000 masl) represent only 1% and 8% of the catchment but roughly half the snow falls in these zones. The other half falls in elevation zone 2 and 3 (1500-2000 masl and 2000-2500 masl), which exhibit lower snow depths but a larger areal extent. In the latter two

zones snow dynamics are adequately covered by the model. The model also represents the two peaks of the snow cover in the elevated regions badly.

Concerning irrigation, a good match of the seasonal cycle, as well as the total volume of measured and simulated irrigation has been obtained for the hydrological year 1995/96, which is the only monthly irrigation time series available (Figure 5-22).

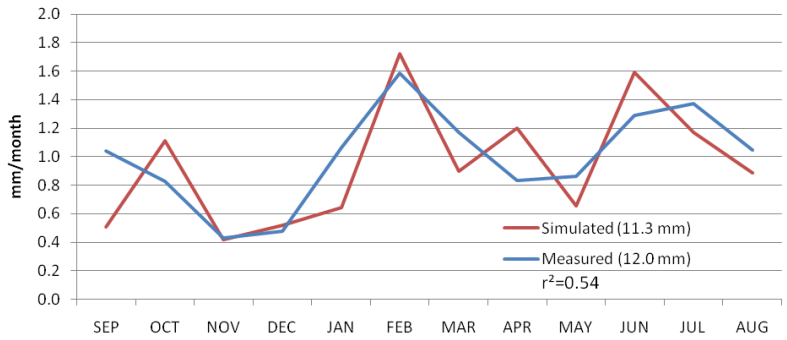

Figure 5-22: Monthly irrigation amounts for the Upper Drâa in 1995/96. (Measured data taken from DRPE 1998)

In the autocalibration phase, the SUFI-2 algorithm has been used. According to Refsgaard (1997) the number of real calibration parameters should be kept low, hence only three parameters have been chosen for calibration. All three are explicitly intended for calibration and have no or little physical meaning (Table 5-17).

Table 5-17: Parameters adapted during autocalibration (see Appendix 3 for details on parameters).

Parameter	Initial range	Calibrated Value
GW_REVAP[%]	0 – 1	0. 47
ESCO[-]	0 – 1	0.78
CN2[-]	-3 – 3	-0.3

To assess the model goodness at the reservoir measured inflow (calculated from the reservoir stage as presented in section 5.3.7.2) has been compared to simulated inflow. On an annual basis the dimensionless criteria are within an acceptable range: Nash-Sutcliffe Coefficient of Model Efficiency (CME) is 0.81 and the Index of Agreement (IoA) is 0.95. Absolute error indices do well likewise: The Root Mean Square Error (RMSE) is 79.36 Mm³/year (≙ 41% of measured values SD (Standard Deviation)) and the Mean Absolute Error (MAE) is 57.72 Mm³/year (≙ 33% SD) as displayed in Figure 5-23. During the calibration period goodness of fit criteria are within a good range for monthly values as well: (CME: 0.83; IoA: 0.96; RMSE: 13.89 Mm³/month (≙42% SD); MAE: 8.44 Mm³/month (≙26% SD); Figure 5-24).

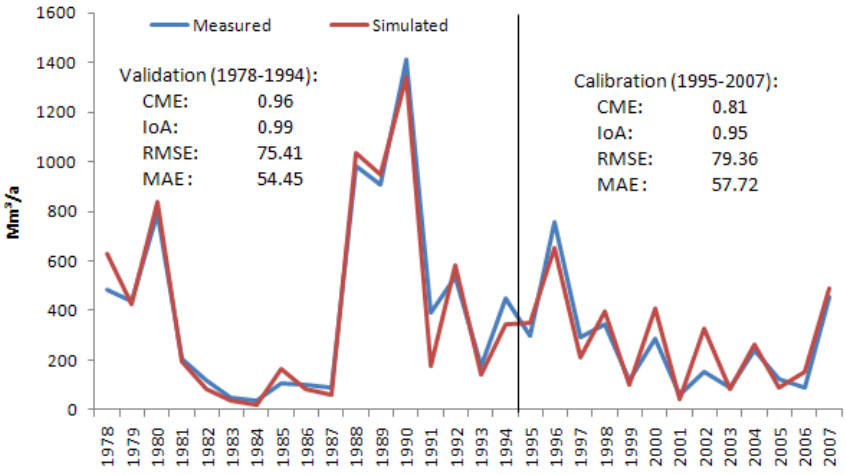

Figure 5-23: Simulated and measured annual discharge into the reservoir Mansour-Eddahbi (1978-2007) (14,988 km²). (Measured data: SE Ouarzazate)

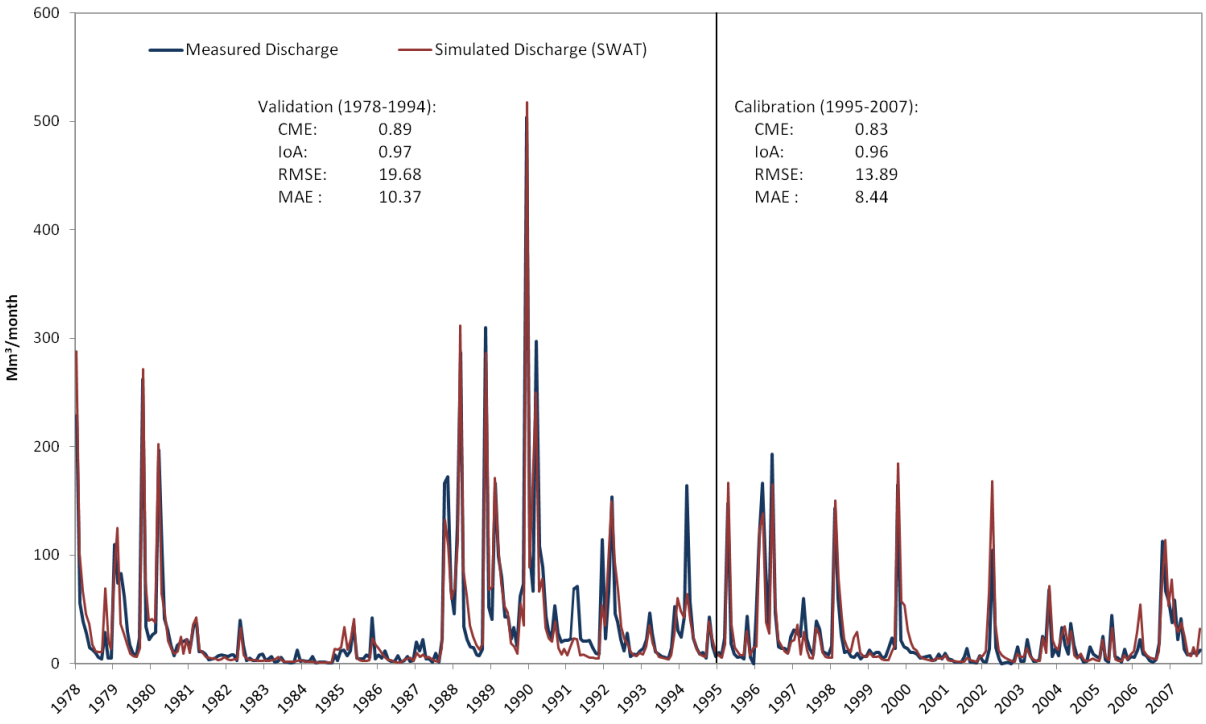

Figure 5-24: Simulated and measured monthly discharge into the reservoir Mansour-Eddahbi (1978-2007) (14,988 km²). (Measured data: SE Ouarzazate)

Within the model structure developed and using the input data available, calibration results can hardly be improved. As indicated in Figure 5-23 and Figure 5-24 no general bias can be detected, peak discharge as well as recession periods are overestimated and underestimated to the same extent. Deviations are therefore most likely results of measurement errors (climate or discharge), or incorrect process representation by the model. Further parameter adjustments would imply the trial to compensate for errors in the model or in the data (Abbott & Refsgaard 1996), and should therefore be avoided.

5.4.2 Reservoir Water Balance

The main purpose of reservoirs water balance module is the use within the scenarios, it has been driven with simulated discharge data. The module has been calibrated and validated for the same years as the hydrological model. Adapted parameters are the residual volume of the reservoir (50 Mm³) and the buffer coefficient that governs water releases in low storage periods (0.5).

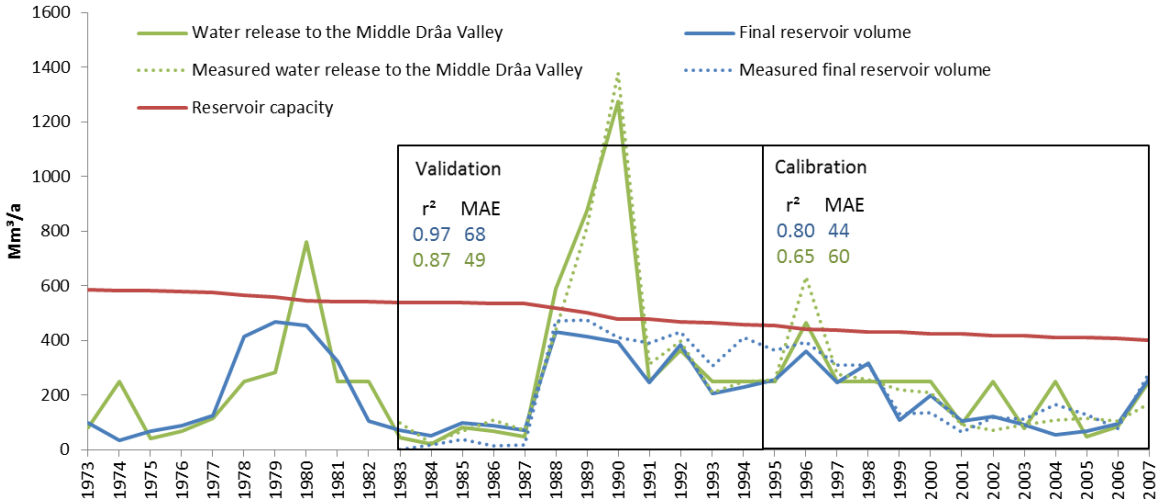

Figure 5-25: Simulated and measured final annual stored volume and water release of the reservoir Mansour-Eddahbi (1973-2007) (14,988 km²). (Measured data: SE Ouarzazate)

The simulated reservoir volume and water release are in synchronicity with measured values, as indicated by high r² values (0.80 for the reservoir filling level and 0.65 for the water release). MAE is well below 50% of the measured values standard deviation (38% for the reservoir filling level and 41% for the water release); hence calibration results can be considered good. Nevertheless an additive error can be stated, as the modeled reservoir storage is below the measured one throughout the 90ies (see Figure 5-25). As outlined in section 5.1.2.4 evaporation losses are subtracted from the reservoir at the end of the calculation step, therefore the volume at the end of the year can never equal the capacity of the reservoir.

5.5 Model Validation

In this study model results are validated using a variety of available data, ranging from more robust analyses, using goodness-of-fit criteria, to mere plausibility checks in terms of qualitative analyses, literature reviews and inter-model comparisons. Different aspects of the terrestric water cycle are covered to exploit all model results that contain informative value.

5.5.1 Discharge to Reservoir

A split sample test has been performed on the measured discharge records at the catchment outlet, the calibration results have been presented in the previous section 5.4. Also during the validation period (1978-1994) goodness of fit criteria are within acceptable ranges. Annual indices are very good (CME: 0.96; IoA: 0.99; RMSE: 75.41 Mm³/year (≙19% SD); MAE: 54.45 Mm³/year (≙14% SD); Figure 5-23). For monthly values dimensionless criteria perform better than during calibration (CME: 0.89; IoA: 0.97). Whereas absolute error indices are higher than during calibration (RMSE: 19.68 Mm³/month (≙32% SD); MAE: 10.37 Mm³/month (≙19% SD); Figure 5-24). No general bias of the model could be detected in the hydrograph.

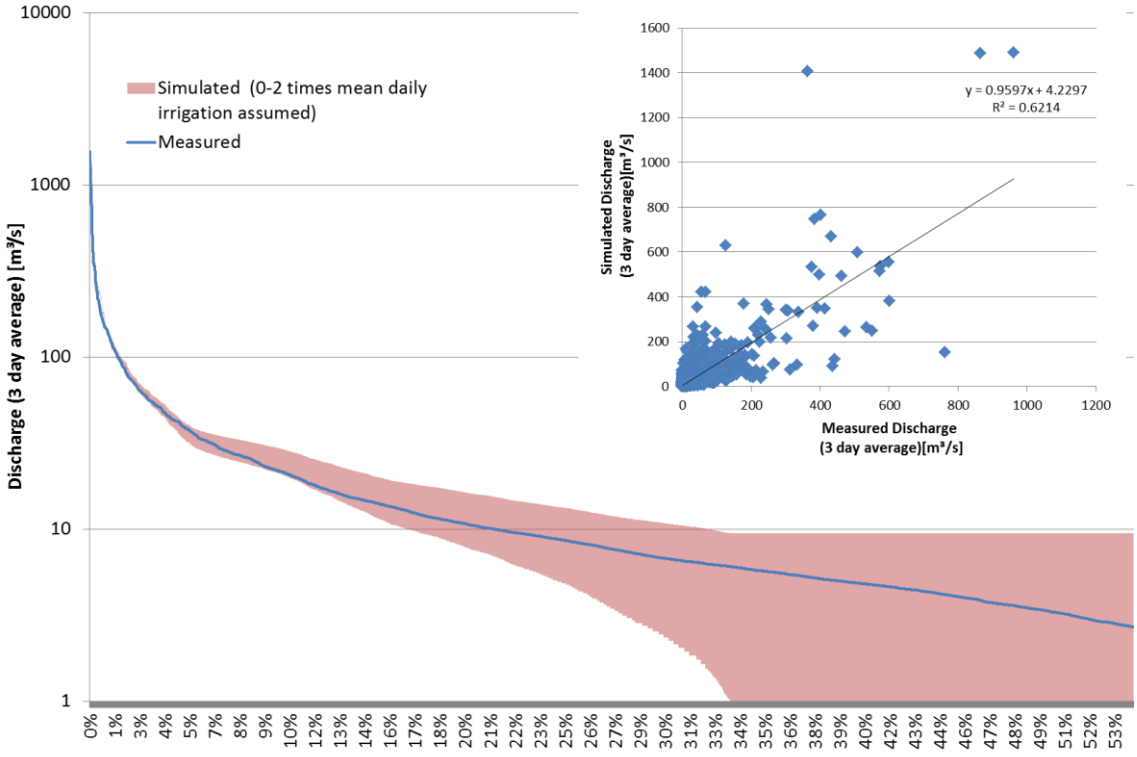

Figure 5-26: Daily flow duration curve (smoothed by three day filter at the reservoir Mansour-Eddahbi (14,988 km²). Uncertainty range is twice the average daily irrigation. (Measured data: SE Ouarzazate)

Daily flow at the reservoir (i.e. the catchments outlet) is available since 1983. These data have been compared to daily simulated flow (r^2: 0.36). To minimize the effect of measurement errors at the reservoir and to account for the lack of calibration of parameters affecting short-term dynamics (time of concentration, surface-runoff/ lateral flow delay, etc.), three-day average values have been considered as well. (r^2:0.62; see Figure 5-26). This analysis is hampered by the fact that the model calculates irrigation on a monthly basis only.

Therefore a mean annual irrigation amount has been determined based on model results (~4.23 m^3/s, see 5.5.4). Assuming actual daily irrigation ranges between zero and twice the average, flow duration curves have been compared, indicating that simulated daily discharge, despite not being calibrated, is within a reasonable range (Figure 5-26).

5.5.2 Stream Gauges

As outlined in section 5.3.7.1 the quality of discharge measurements at stream gauges is too low for a reliable quantitative assessment of model goodness. Nevertheless uncertainty-considering goodness-of-fit criteria have been used to assess the model performance for different subcatchments within the Drâa catchment. An uncertainty range of ±30% or at least 5 Mm^3/month (≙ 2 m^3/sec) has been assumed for the measured data. The hydrographs of the gauges are presented in Figure 3-12 and Appendix 10. The gauges Ait-Mouted, Tinouar, Amane-n-Tini and Ifre seem to be well represented by the model, whereas the gauges Assaka, Tamdroust and Agouillal are badly represented in terms of both discharge volumes and timing of peaks. The poor performance of the model at the gauges Assaka and Agouillal should not affect the overall model performance due to the little total runoff volumes.

This view is supported by the goodness-of-fit indices as presented in Table 5-18. According to thresholds outlined in section 4.2.1 green represents a good performance, yellow an acceptable performance and red a poor performance. The modified IoA and MAE provide only limited assistance, as they exhibit good model performance for every gauge, whereas the modified CME and RSME support the conclusion that only Ait-Mouted, Tinouar, Amane-n-Tini and Ifre are well represented by the model. Again Assaka, Tamdroust and Agouillal display bad performance for both discharge volumes and dynamics.

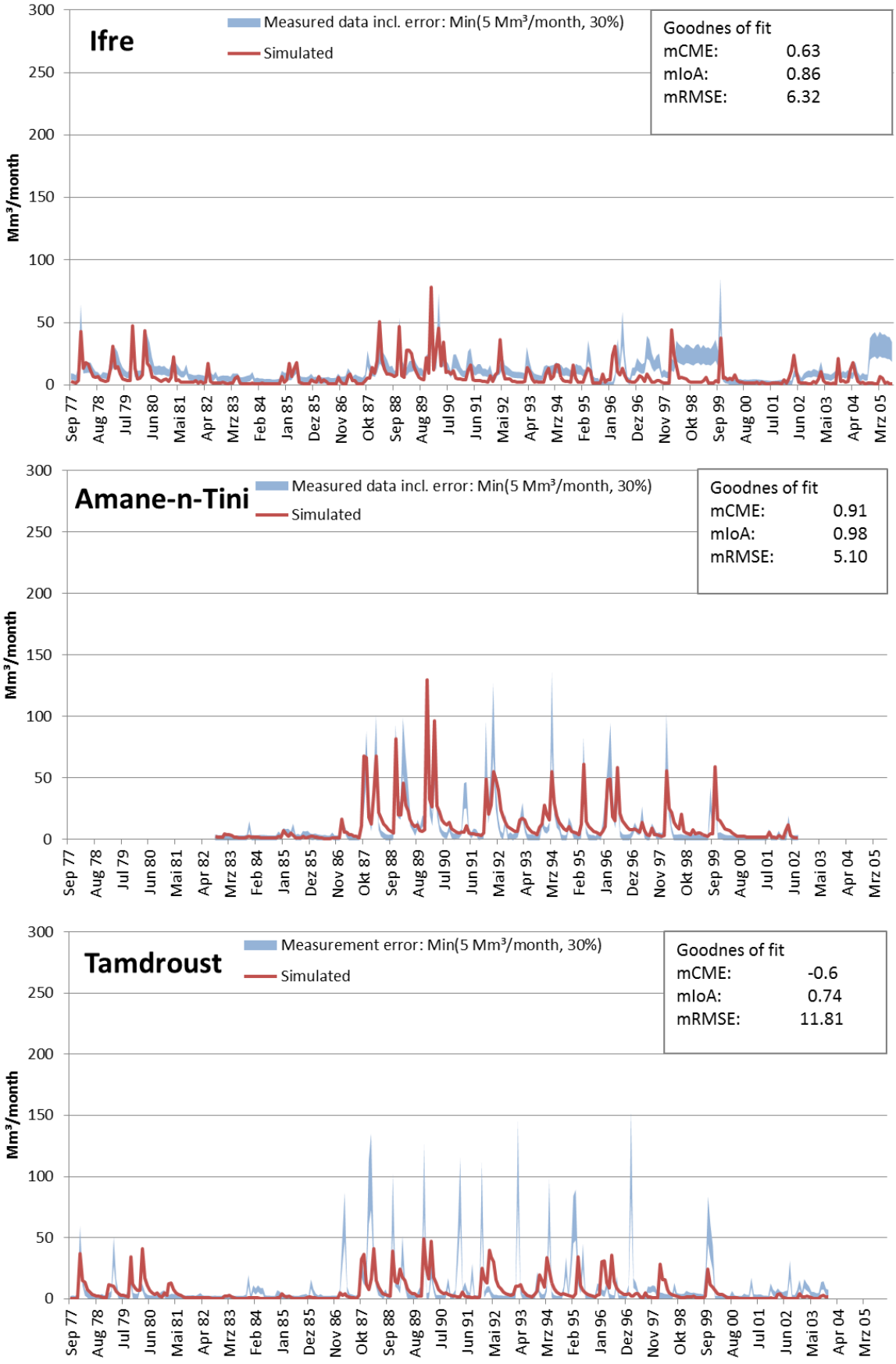

Figure 5-27: Modeled monthly discharge compared to measured discharge for the stream gauges Ifre, Amane-n-Tini and Tamdroust, see Figure 3-13 for locations. (Measured data: SE Ouarzazate)

The latter three subbasins (covering 26% of the catchment) might be badly represented due to several reasons. All of them are located in the western part of the catchment (cf. Figure 3-13), where no detailed information on altitudinal lapse rates is available (IMPETUS gauges cover only the eastern part of the catchment). Timing and magnitude of discharge peaks at Assaka, Tamdroust and Agouillal hint at a generally poor representation of areal rainfall. Geological case studies have been focused on the eastern part as well, i.e. the baseflow parameterization reflects conditions in the eastern catchment. Especially mismatched peak flow and flow recession at the gauge Tamdroust support this view. Furthermore agricultural activity is centered in the eastern part, only lumped data exists for irrigated areas west of Ouarzazate. The effect of irrigation water abstractions is not considered within the subbasins. Nevertheless the main tributaries to the reservoir Mansour-Eddahbi, Oued Dades at Tinouar and Oued Ouarzazate at Amane-n-Tini, as well as the main source regions of the Dades (M'Goun at Ifre and Dades at Ait-Mouted) seem to be reasonably well represented by the model. Since these four gauges do also surround the core room of agricultural activity, the Dades valley and the oasis of Ouarzazate, model results can be considered appropriate.

Table 5-18: Uncertainty-considering Goodness-of-fit criteria for discharge for various stream gauges; green: good performance, yellow: acceptable performance, red: poor performance

Gauge	Mean Q [Mm³/month]	SD Q [Mm³/month]	% of simulated values bracketed	CME	mCME	IA	mIoA	RMSE	mRMSE	MAE	mMAE
Ait-Mouted	8.23	12.24	55%	0.21	0.54	0.80	0.83	12.92	9.79	6.40	5.30
Tinouar	21.03	30.47	48%	0.62	0.84	0.90	0.95	19.90	12.74	10.96	7.10
Amane-n-Tini	10.11	18.86	52%	0.69	0.91	0.92	0.98	9.56	5.10	5.71	5.01
Ifre	11.37	9.38	31%	0.08	0.63	0.77	0.86	10.02	6.32	7.10	4.47
Assaka	2.06	5.43	75%	-4.11	-1.05	-0.28	0.75	5.15	3.26	2.35	1.58
Tamdroust	8.08	18.20	47%	-2.52	-0.63	0.12	0.74	17.36	11.81	8.06	6.39
Agouillal	3.38	5.19	70%	-1.63	-0.09	0.34	0.76	5.23	3.36	2.72	1.47

5.5.3 Snow

Based on the digital elevation model SRTM, a mean annual **precipitation** of 203.7 mm for the period 2001-2008 can be calculated for the basin using the elevation dependency lined out earlier (section 5.3.6.1). Schulz (2007) measured the proportion of snowfall to rainfall at three altitudes (2,250, 3,260 and 3,850 masl) during the years 2001-2005. A linear relationship can be established (r^2=0.99), as temperature decreases linearly with altitude.

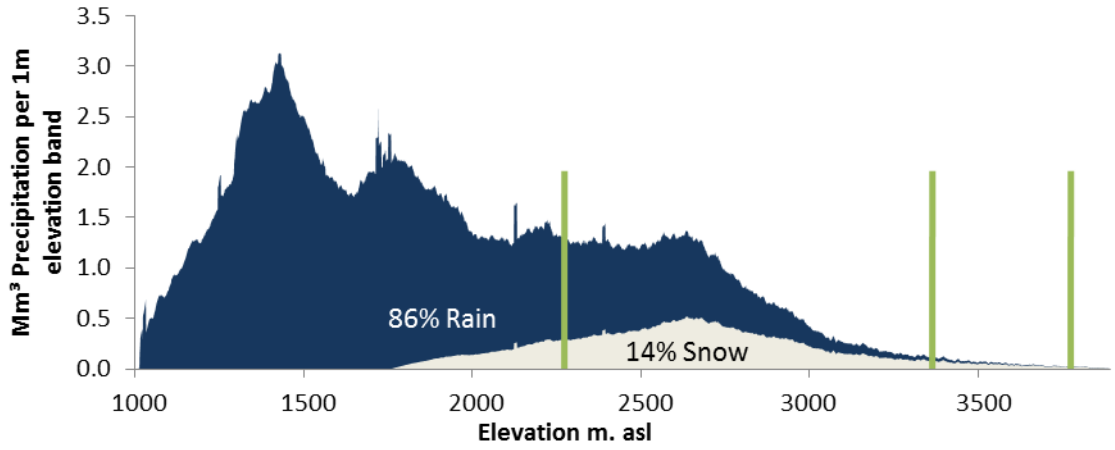

Figure 5-28: Proportion of snow to rain along the altitudinal gradient of the Upper Drâa catchment, snow measurements indicated by green bars.

Knowing the amount of precipitation and the fraction of snow for a given altitude, a precipitation fraction of 14% can be assumed to be snow (see Figure 5-28). The model calculates a fraction of 12.2% (1978-2007). The modeled snow-cover has been used for calibration and model deficiencies have been discussed in the corresponding section 5.4.1. along with problems in representing the measured snow cover goes an underestimation of sublimation: From field measurements and physical based modeling sublimation rates of up to 44% are reported for elevations of 3000 masl (Schulz & de Jong 2004), whereas the model estimates sublimation rates of 13% only for the corresponding elevation zone.

5.5.4 Irrigation

The Irrigation amounts calculated by the model have been compared to measured data and survey records, in terms of annual volume and the seasonal cycle. The model estimates a mean annual net irrigation requirement of 171 Mm³ or a gross annual irrigation requirement of 204 Mm³, assuming an irrigation efficiency of 75%. Irrigation requirement estimations of local authorities are provided in Table 5-19. The figures correspond well, since the demand was calculated using almost the same data. Irrigation amounts calculated by SWAT are by 10% lower than official figures, which can be considered appropriate.

Table 5-19: Irrigation requirement in the Upper Drâa valley

Irrigation requirement (Mm³/a)	Irrigation applied from surface water (Mm³/a)	Covered irrigation demand (%)	Source
204	125	61	SWAT-MAROC (1978-2007)
219	139	65	(DREF Sud Ouest 2007)

Spatial patterns of irrigation from surface water are well reproduced. Survey information, pointing out oases that rely predominantly on surface water for irrigation and model results are alike (Table 5-20). It has to be noted that that the survey did not consider irrigation amounts but only the relative frequency of irrigation from different sources.

Table 5-20: Irrigation from surface water in the Upper Drâa catchment: Relative frequency of surface water irrigation (Heidecke 2006) and modeled covered irrigation demand

Oasis	**Irrigation from surface water**	
	Survey (Heidecke 2006)	**SWAT-MAROC**
M'Semrir	No data	97%
Toundout	No data	35%
Kelaat	86.5%	79%
Boulmalene	88.0%	74%
Skoura	11.8%	16%
Ouarzazate	88.5%	76%

5.5.5 Groundwater

Groundwater recharge rates for arid and semi-arid regions have been reviewed by Scanlon et al. (2006) and presented in section 2.5. Annual **groundwater recharge** (recharge to both aquifers) ranges between 0.1-5% of annual precipitation or 0.2-35 mm. The model delivers a recharge rate of 6% or 14 mm. Differentiated after sub-regions (see Appendix 6) recharge rates of 3% (5 mm/year) for the arid basin, 8% (21 mm/year) for the more humid High Atlas and 5% (10 mm/year) for the Anti-Atlas can be derived. All of these values are within a reasonable range.

The dominant recharge mechanism in the basin is **riverbed infiltration**. Cappy (2006) used the model MODFLOW (Harbaugh et al. 2000) including the river package, designed to model the behavior of losing streams, and estimated annual riverbed infiltration in the river segments between Toundout, Ifre, Ait-Mouted and Tinouar (for locations see Figure 3-13). Dependent on the riverbed conductance (C_{riv}), infiltration rates ranging from 84.65 to 209.29 Mm^3/year were obtained. River bank infiltration calculated by SWAT-MAROC sums up to 208.3 Mm^3/year for this part of the model domain.

Regions of increased recharge have been identified by Cappy (2006) using stable isotope analysis. The estimated mean recharge altitude of the Basin of Ouarzazate ranges between 2,400 m and 2,900 m. As the maximum elevation of the Basin of Ouarzazate is about 1,800 m the results clarify that there is no significant groundwater recharge within the basin. The model calculates 50% of recharge generated in elevations above 2000 masl (EZ 3-5) which sum up to 26% of the catchment.

5.5.6 Soil Water

Soil water measurements and physical based modeling have been conducted in the research area (model ARID; Weber 2004). The seasonal variation of mean monthly soil water content is presented in Figure 5-29. Dependent on the season, prevailing soils and altitude, soil water content ranges from 15 to 30%. For the selected period (Dec. 2001-Nov. 2003), SWAT results of the respective EHRUs have been evaluated in Table 5-21. The most striking difference is that in some EHRUs there is no residual water content in the soil. This seems to be the case with EHRUs that cover 5349 km² or 36% of the catchment. Bad representation of soil moisture and/or interflow within the SWAT-model has been reported (e.g. Li et al. 2010; Hiepe 2008; Busche 2005; Eckhardt et al. 2002). Nevertheless relative seasonal changes seem to be in the right magnitude.

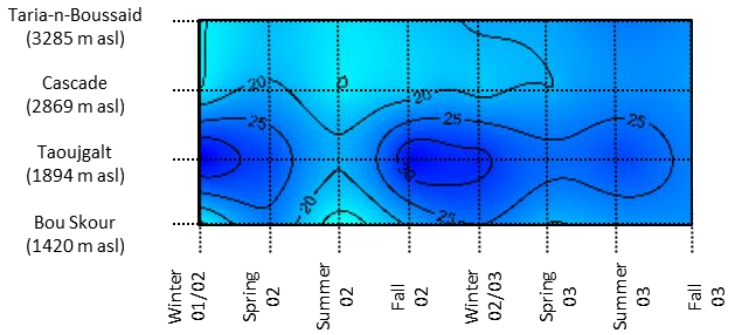

Figure 5-29: Mean monthly soil water content [Vol%] derived from the model ARID at selected sites in the Upper Drâa Catchment: 12/2001-11/2003 (Weber 2004)

Table 5-21: Modeled soil water content of selected EHRUs, (Dec. 2001-Nov. 2003)

	Soil Water Content [Vol%]	
	Min	**Max**
Taria	9%	25%
Cascade	0%	18%
Taoujgalt	16%	25%
Bou Skour	0%	27%

Soils that dry below any reasonable residual water content occur in every elevation zone, climatic regime and land cover. But all of the soils are characterized by low K_{sat} values of the second soil layer. Saturated conductivity calculated by pedotransfer functions might underestimate actual conductivity, as measured values from clayey soils are often reported to be higher than estimated by pedotransfer functions (see section 2.3). On the other hand a low K_{sat} value does not imply that the soil dries out completely. Two EHRUs featuring the same soil type have been compared (Figure 5-30 and Table 5-22). The steeper-sloped EHRU A exhibits higher soil-moisture, so the process of interflow does not seem reponsible for variations. Again it can be seen that the dominant seasonal change in soil moisture is reproduced by the model whereas long-term-trends such as the early-80ies drought ore drier conditions from 2000-2004 are not reflected by the model. The inaccurate representation of soil water content might also be a result of the rather conceptual soil evaporation components in SWAT (Neitsch et al. 1999) and the rather coarse vertical soil discretization.

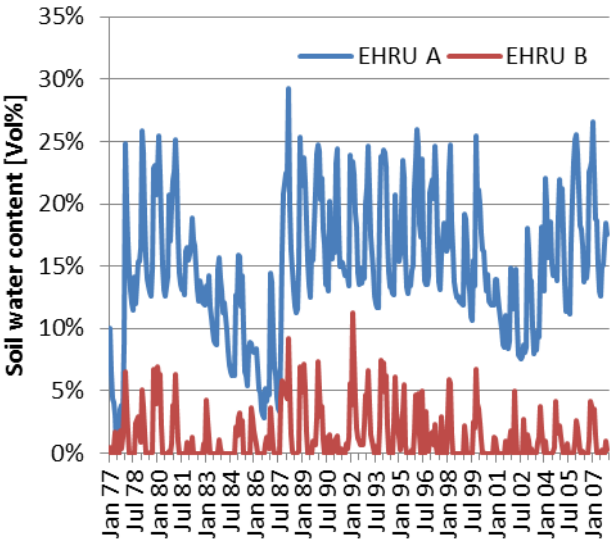

Figure 5-30: Soil water content modeled by SWAT-MAROC for two EHRUs

Table 5-22: Attributes and selected mean annual water balance components of the two EHRUs

EHRU	A	B
Land cover	Brush steppe	Hamada steppe
Soil code (see Appendix 4)	421	421
Slope [%]	22.5	4.2
Elevation [masl]	2163	1434
Precipitation [mm]	347.2	144.3
Average Soil Water Content [mm]	114.8	10.8
Percolation [mm]	39.2	0.0
Surface Runoff [mm]	23.1	7.2
Interflow [mm]	2.2	0.1

It is generally recommended to have a fine vertical resolution of the upper soil layer, since these are essential to compute evaporation properly (Downer & Ogden 2004; Zhang 2007). Similar studies performed in semi-arid parts of China showed that SWAT performed quite unsatisfactorily in soil-water estimation under dry soil-profile conditions (Luo et al. 2008).

It has been pointed out that antecedent moisture conditions are of subordinate importance for the prevailing infiltration-excess runoff generation (see section 2.3), as top-layers dry out fast under arid conditions with infrequent rainfall. Since absolute changes due to the seasonal wetting and drying of the soil are in a reasonable range, the overall informative value of the model does not seem to be compromised, though applications concerning soil water content have to be neglected. The model improvement regarding its soil moisture component is the most prominent work ahead.

5.5.7 Reservoir Water Balance

The time series of model results is displayed in Figure 5-25. In the validation period the model performs even better than in the calibration period. The r^2-values indicate a good to very good model performance (0.87 for the annual water release, 0.97 for the reservoir volume). The MAE is low: 49 Mm^3/year for the annual water release (≙ 13% of the measured values standard deviation) and 68 Mm^3/year for the reservoir volume (≙ 33% SD). Concluding, the water balance model performance can be considered as good to very good, especially bearing in mind the simplifications it contains.

5.6 Scenario Setup

Scenarios considered in this study are the 2010s (2000-2029) and the 2030s (2020-2049). These scenarios are developed based on the IPCC-SRES scenarios B1 and A1B (see section 4.1.5). Furthermore rather qualitative socio-economic scenarios are described (section 5.6.2) and impact indicators are developed (section 5.6.3).

5.6.1 Climate Scenarios

In this study the Regional Climate Model REMO (Regional Model) has been used to assess climate trends for the period 1960-2049 (Paeth et al. 2009). REMO (v5.7) is a hydrostatic limited-area model that has been designed for applications at the synoptic scale (Jacob et al. 2007). The model used within IMPETUS is centered over tropical and northern Africa (30°W to 60°E, 15°S to 45°N) with a horizontal resolution of 0.5°(≈50 km). It is nested into the ECHAM5/MPI-OM GCM (Roeckner et al. 1996) which is driven by greenhouse gas forcing according to the IPCC SRES A1B and B1 scenarios and has been published in the Fourth assessment report of the IPCC (Paeth et al. 2009). The use of REMO-scenarios has advantages compared to GCM model results (Paeth et al. 2009):

- A regional climate model features a six times higher resolution than most present-day global simulations.
- Spatially detailed patterns of future land-use change and increasing GHG concentrations are considered.

The model has been run for the period 1960 to 2049. During the 1960-2000 period increasing GHGs and constant land cover from the early 1990s are assumed (Baseline scenario), whereas from 2001 to 2049 increasing greenhouse gas concentrations and changing land cover according to the IPCC SRES A1B and B1 scenarios has been prescribed (Solomon et al. 2007). For each scenario (baseline and future) three ensemble members have been created to account for the uncertainty due to different boundary/initial conditions. Since no significant difference between the scenarios could be stated, all six ensembles are treated as if representing one scenario (Born et al. 2008). The authors conclude that the RCM results show a trustworthy and acceptable range of uncertainty for the research area. They further point out that the most prominent change is a shift of all climates towards warmer and dryer conditions Therefore, a further increase in the existing water stress is expected, especially south of the Atlas Mountains (Table 5-23).

Table 5-23: Temperature trend from REMO scenarios, for the period 1960-2000 compared to 2001-2049. Trend in rainfall indices (standard deviation units) from REMO scenarios, for the period 1960-2000 compared to 2001-2049.The range of uncertainty is given as the averaged deviation from the ensemble mean trend. Bold numbers indicate trends with error probabilities less than 1% for temperature and 10% for precipitation (Born et al. 2008).

	Winter	Summer	Year
Temperature trend	**1.27 ± 0.18 °C**	**2.02 ± 0.52°C**	**1.64 ± 0.29°C**
Rainfall Index Trend	-0.71±0.37	-0.63±0.41	**-0.83±0.26**

The single climate change scenarios feature the following climatic trends for the time periods 2000-2029 (referred to as 2010s) and 2020-2049 (referred to as 2030s) compared to the baseline period. Temperature increases 0.7°C (2010s) and 1.3°C (2030s), whereas precipitation decreases by 8% (2010s) and 12% (2030s), as depicted in Table 5-24.

Table 5-24: Temperature and precipitation trends from REMO scenarios, for the periods 2000-2029 and 2020-2049 compared to 1978-2007.

Climate scenario and ensemble		**2010s**		**2030s**	
		Temperature	**Precipitation**	**Temperature**	**Precipitation**
A1B	**Ensemble 1**	+0.7 °C	-11%	+1.5 °C	-16%
	Ensemble 2	+0.8 °C	-17%	+1.6 °C	-14%
	Ensemble 3	+0.5 °C	+2%	+1.3 °C	-10%
B1	**Ensemble 1**	+0.6 °C	-6%	+1.2 °C	-11%
	Ensemble 2	+0.6 °C	-5%	+1.2 °C	-11%
	Ensemble 3	+0.9 °C	-9%	+1.2 °C	-10%
Average		**+0.7 °C**	**-8%**	**+1.3 °C**	**-12%**

Despite the models ability to project trends in general, two flaws inhibit the direct use of REMO data in hydrological models: The coarse data resolution and a bias in precipitation compared to observed data for the baseline-period, a general problem in hydrological climate change modeling (Bates et al. 2008).

In this study, a statistical downscaling of climate scenarios has been used for preparing REMO-data for hydrological model studies in the Drâa region (Christoph et al. 2010a). The objective of the downscaling was to create time series of rainfall and temperature for the near-surface layer (2 m-height) with daily resolution from REMO climate model data, accounting for sub-scale features not resolved in REMO (the NW-SE gradient of rainfall, elevation and aspect of the surface). In the statistical downscaling approach used here, these data have been aggregated on a 1-km grid.

Then a transfer matrix has been estimated, based on multiple regression methods and the correction of statistical properties of rainfall. Regression coefficients of sufficient predictors with parameters taken from observing stations (climatic stations Ouarzazate, Agouim, Ifre, and Ait-Mouted and IMPETUS stations) are calculated in a multiple regression. Predictors are

climate model data and the above mentioned topographic characteristics. Temperature and precipitation data generated in this manner suit the surroundings and reflect altitude, aspect etc. The processing is presented in detail by Christoph et al. (2010a).

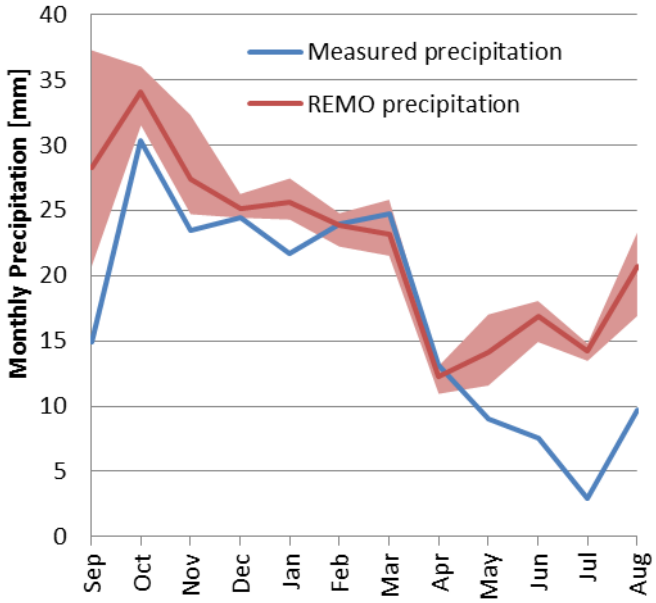

Table 5-25: Mean annual precipitation and variability in the Upper Drâa Catchment. modeled: 1970-2000, measured: 1978-2007

	Measured	REMO mean
AVG (mm)	213	265
SD (mm)	78	55
Variance	38%	21%

Figure 5-31: REMO-Bias variability in the Upper Drâa Catchment. modeled: 1970-2000, including range of 3 model realizations, measured: 1978-2007

Since GCM results are primarily analyzed in terms of relative or absolute changes, model biases can be neglected to a certain degree, as long as magnitude and seasonal variations are still within a reasonable range. Applied in impact studies the absolute values (temperature and precipitation), gain importance. Comparing measured data (mean monthly data based on measurements and the altitudinal lapse rates taken from section 5.3.6.1), the processed REMO data exhibits an overestimation of precipitation by more than 20% (see Figure 5-31). The annual dynamic of modeled precipitation matches roughly the observed dynamic (r^2=0.65), but summer precipitation is overestimated by REMO. Hence a direct use of the climate scenarios in the hydrological model is not possible. Furthermore the interannual and decadal variability of observed annual precipitation is underestimated by the baseline scenario as displayed in Table 5-25 (Born et al. 2008).

Therefore climate change signals have been computed with observed climate data to preserve reasonable absolute values and interannual variability. The use of different downscaling methods is recommended as generated time series are uncertain (e.g. Rößler 2011). Consequently three different downscaling techniques have been used to generate usable time series. Absolute changes in temperature have been added to measured temperature time series, whereas precipitation data has been treated in three different ways:

A) A relative decrease in precipitation has been converted into a decrease of wet days, i.e. random deleting of rain days from the record, whereas a relative increase has been added to events in the respective month, resulting in a scenario with rainfall intensities comparable or higher than in the baseline.

B) The second approach converted relative changes into relative changes of each event, resulting in decreased intensity of the events.

C) Within the third approach absolute changes of monthly precipitation have been added to single events, leading to (a slightly decreased) intensity comparable to the baseline scenario.

Knowing about the deficiencies of every single approach, the spread of results using different downscaling techniques is assumed to at least confine the range of reasonable results. It has to be stressed that using these downscaling approaches, the climate change scenarios do not account for possible changes in precipitation variability, i.e. the distribution of wet and dry years is exactly as in the baseline scenario.

The derived precipitation changes are depicted in the following Figure 5-32. It can be stated that the signal is rather weak for the 2010s scenario, but the decrease in precipitation becomes evident for the 2030s. Fall and spring are characterized by the highest decrease, whereas precipitation in summer remains quite stable. This pattern is similar throughout all the elevation zones.

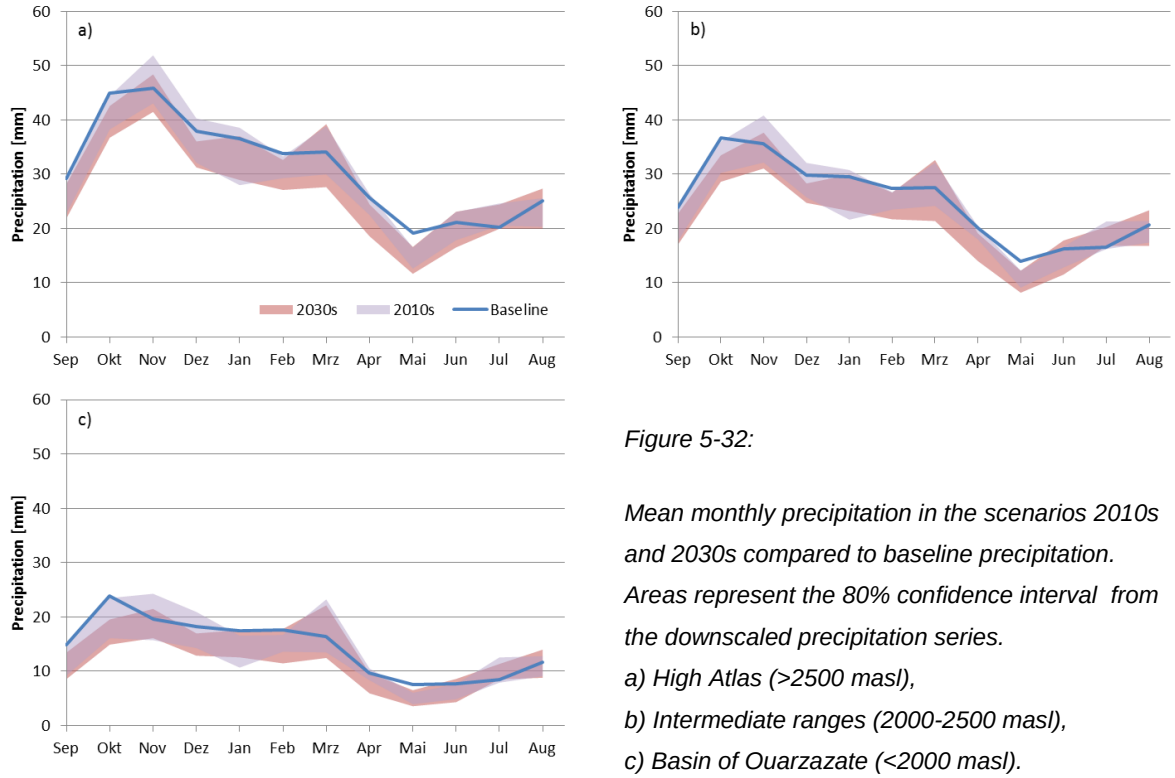

Figure 5-32:

Mean monthly precipitation in the scenarios 2010s and 2030s compared to baseline precipitation. Areas represent the 80% confidence interval from the downscaled precipitation series.
a) High Atlas (>2500 masl),
b) Intermediate ranges (2000-2500 masl),
c) Basin of Ouarzazate (<2000 masl).

5.6.2 Socio-economic Scenarios

Within the IMPETUS project the following socio-economic storylines have been developed:

- Scenario **M1** "Marginalization – non-support of the Drâa-Region" portrays a withdrawal of governmental and international institutions support. As a result, the marginalization of the region and the impoverishment of the local population accelerate.
- Scenario **M2** "Rural development in the Drâa-Region through regional funds" is a constant economic growth scenario. Against the background of overall political stability and supported by governmental aid programs, the Drâa-Region experiences an improvement of living conditions and economic development. As results, migration declines and the population increases.
- Scenario **M3** "Business as usual" extrapolates the dominant trends of past decades. The status as a marginalized region remains unchanged and only incremental improvements in the overall living conditions and economic development occur.

These storylines are not incorporated into the hydrological model due to the following reasons: Predicted relative changes in drinking water demand are immense (2010-2020: +27%, DREF Sud Ouest 2007; DRPE 1998). Nevertheless their absolute quantity (+3.6 Mm^3) is far below uncertainties of the hydrological model lined out in the previous chapter. Furthermore drinking water for the city of Ouarzazate (accounting for 69% of the total demand) is abstracted from the reservoir, i.e. it does not have to be incorporated in the hydrological model, as the model domain does not include the reservoir itself. Besides the primacy of drinking water supply over agricultural use is not questioned. Agricultural water demand is not subject to any decadal trends (apart from climate induced ones). Therefore only a "business-as-usual"-scenario is considered in the hydrological model, keeping the agricultural areas and crop-mix as in the baseline-scenario. Nevertheless the population growth and drinking water demand might along with other socio-economic factors affect the society's ability of coping and mitigating climate change induced impacts. Therefore relevant socio-economic changes according to the storylines are depicted in the trend-matrix Table 5-26. They will be referred to rather qualitatively in the results section 6.

Table 5-26: Qualitative trend-matrix of socio-economic changes in the Upper Drâa Catchment ("+": increase of the considered variable; "0": no change of considered variable; "-": decrease of considered variable). The number of signs announces the intensity of change.

Variable		M1 Marginalization		M2 Development		M3 Business as usual	
		Mountains	Basin	Mountains	Basin	Mountains	Basin
Population	Absolute population	0	+	+	++	+	++
	Emigration	++	++	0	0	+	+
	Urban population	n.a.	+++	n.a.	+++	n.a.	++
	Living standard	--	-	+	++	+	+
Economy	Irrigated area	0	0	0	0	0	0
	Productivity	0	-	+	++	0	+
	Livestock density	+	0	-	-	0	0
	Tourism	0	0	++	++ "Lake City"	+	+
Institutions	Traditional water management	0	--	+	+	0	--
	Public water management	n.a.	-	+	++	n.a.	0
Erosion (Klose 2009)		++	+	--	+	0	0

The reservoirs water balance model assumes the following changes in the scenario period 2030s. The figures from 2010 and 2020 are taken from scenarios developed by Moroccan authorities (DREF Sud Ouest 2007; DRPE 1998):

- Scenario **M1** "Marginalization – non-support of the Drâa-Region"
  Average sediment delivery increases by 103%, as the extraction of firewood expands and livestock gains importance (Klose 2009). A population growth rate of 1.5% in the City of Ouarzazate is assumed, as fewer people move to the city compared to other scenarios. The per capita water consumption in the city of Ouarzazate remains stable at 221 l/day (DREF Sud Ouest 2007; DRPE 1998). These figures are higher than average figures of domestic use (Rademacher 2010; Klose et al. 2008a), as they include water demand of all sectors excluding agriculture (e.g. tourism).
- Scenario **M2** "Rural development in the Drâa-Region through regional funds"
  Average sediment delivery decreases by 36%, as more sustainable practices are adopted in pastoral systems and afforestation schemes are implemented (Klose 2009). A population growth rate of 3% in the City of Ouarzazate is assumed; as the trend

towards a more service oriented economy (e.g. tourism) creates jobs in the centers (Platt 2008b). The per capita water consumption in the city of Ouarzazate increases from 227 l/day in 2020 to 247 l/day in 2049, extrapolating the trend from 2010 to 2020. Furthermore the Ouarzazate Lake City is included in the scenario (Ministry of Tourism 2011). This project, supported by the Moroccan government, includes a 18 hole golf course, a convention center and 8 hotels with 3600 beds. The water demand of these facilities is estimated to be 3 Mm^3/year[16].

- Scenario **M3** "Business as usual"
  Within this scenario the sedimentation rate remains stable; population growth and drinking water demand are the same as in the scenario M2. The Ouarzazate Lake City is not included in this scenario.

The reservoir water balance module is driven by the middle tercile of 2030s annual discharge time series, i.e. only for the scenario 2030s (2020-2049), i.e. the discharge is likely to be neither higher nor lower according to the IPCC terminology (section 4.2.2.2). The gap between the end of measured records and the first year of the scenario (2020) the mean annual inflow of the 2010s scenario is assumed. Since the climate scenarios do not include information about the occurrence of future wet and dry periods, five model versions are set up, using the annual discharge series generated by the hydrological model starting from year 1, 6, 12, 18 and 24. Once year 30 is reached, the record continues with year one. Thereby model results are independent from the dynamic of the measured records and model results reflect general trends regardless of the timing of wet and dry periods.

5.6.3 DPSIR - Impact Indicators

While the scenario setup describes the pressures on the hydrological cycle in the Upper Drâa region for the coming decades, the model results are indicating the concluding state of the system. As foreseen by the DPSIR-framework, the impacts on the natural and socio-economic system should be quantified by using adequate state or impact indicators. Only then responses (according to the socio-economic scenarios) can be anticipated. Within the Upper Drâa Catchment three economically meaningful dimensions of water availability can be identified:

1. in the upstream oases
2. at the reservoir Mansour-Eddahbi
3. on the rangelands

[16] Data available from the investors (available at http://www.ouarzazate-lake-city.com/ [last access 09.05.2009]).

Within the following sections appropriate indicators are chosen in order to describe the scenarios impacts on these domains.

5.6.3.1 Irrigation of Upstream Oases

Most oases in the Upper Drâa Valley are dependent on surface water for the irrigation of cropland and orchards. The use of the Standardized Runoff Index (SRI, see section 4.2.3) is discarded, since the procedure defines drought based on a probability distribution, independent from demand and supply. For example the upstream oasis of M'Semrir never experiences water scarcity, whereas the SRI indicates drought as soon as discharge falls below a certain threshold. Therefore an absolute indicator is preferred. The fraction of years in which 70 % of the irrigation demand calculated can be satisfied by surface water seems as an adequate indicator, since the irrigation demand is calculated based on the crop mix in a wet year. As the variability of the climate scenarios equals that of the baseline scenario (see section 5.6.1) no assessment of distribution and length of dry spells can be made.

5.6.3.2 Reservoir Inflow

Water released from the reservoir Mansour-Eddahbi is the main irrigation source for irrigated agriculture in the Middle Drâa Valley. Furthermore the drinking water for the city of Ouarzazate is abstracted from the reservoir. In the Upper Drâa Valley one of the most considered variables is the discharge to the reservoir. Due to the buffering function of the reservoir, the seasonal variation of the inflows does not inhibit the provision of irrigation water to the Middle Drâa catchment when needed; hence the assessment of annual discharge seems adequate.

In order to compare the changes in runoff to changes in water availability in other domains, the use of the annual SRI has been considered. But due to the normalization involved only little deviations were obtained and again the use of absolute metrics is favored.

An annual discharge to the reservoir of 300 Mm^3 is required to sustain irrigation in the Middle Drâa valley and drinking water supply, furthermore it compensates for evaporation losses from the reservoir (see section 3.1). Therefore the exceedance probability of an annual discharge of 300 Mm^3 is chosen as an essential impact indicator. Furthermore the average annual discharge is considered, as the reservoir can buffer short-term variations of annual discharge. Within the reservoirs water balance module a threshold of reservoir operation ability has been set, by comparing the reservoir storage capacity with the water demand of the Middle Drâa Valley plus the water demand of the city of Ouarzazate. This threshold is arbitrary, but can easily be replaced by more meaningful thresholds, e.g. considering

biological processes in the reservoir, such as eutrophication and algae growth (Douma et al. 2009; Sadani et al. 2004). Furthermore the water release, which includes water release when storage capacity is exceeded, is considered.

5.6.3.3 Rangelands

In the agropastoral system of the Upper Drâa Valley rangelands in different elevation zones sustain livestock throughout the year. On these pastures fodder availability is dependent on seasonal rainfalls. As pointed out in the model validation section (5.5.6), the imperfect modeling of soil water disallows the use of soil water data to assess rangeland condition. Furthermore biomass development and yield have neither been calibrated nor validated and grazing pressure is not considered in the model. Since plant growth, especially that of brushes and grasses, in the Upper Drâa Catchment is highly dependent on precipitation (Baumann 2009; Roth 2009), the assessment of rangeland conditions in the scenarios is carried out by using the climate data and climate scenario data only. The hydrological model is not used for the assessment. Nevertheless the results are presented as a by-product to cover the whole sphere of agricultural activity in the research area. For a more detailed assessments of rangeland productivity in the Upper Drâa valley under the pressure of global change see Baumann (2009) and Roth (2009) as well as Fritzsche (2011)

Table 5-27: Spatiotemporal extent of rangelands in the Upper Drâa Catchment (see section 3.6)

Season	Elevation Zone [masl]	Spatial Extent [km²]	Months
Spring	2000-2500	2496	March-May
Summer	>2500	1353	June-August
Fall	2000-2500	2496	September-November
Winter	<2000	10978	December-February

Due to the shallow soils in the research area and the exceedance of precipitation by potential evaporation throughout the year, no additional benefit of the PDSI compared to the SPI could be stated, as the soil storage is almost always empty. Therefore the SPI is considered as an appropriate proxy for rangeland condition. Precipitation data is aggregated spatially for the different season's ranges and temporally for three month averages to reflect the spatiotemporal change in rangeland use (section 3.6 and Table 5-27).

5.7 Uncertainty Analysis

For the baseline scenario a parameter-uncertainty analysis is conducted, while for the future scenarios additionally effects of climate change scenario uncertainty have been considered.

5.7.1 Uncertainty in Baseline Scenario

In this study, uncertainties of the conceptual model were diminished, by developing SWAT to SWAT-MAROC, reflecting process understanding of a semi-arid mountainous hydrological system. Uncertainties of the model structure have been addressed in section 5.1 and uncertainties of the input data have been addressed in section 5.3 and during the validation (section 5.5). Both subjects have been addressed rather qualitatively, but some uncertainties can be converted into parameter values. For example a wide array of recharge rates of the deep aquifer will be assumed to account for a lack of process studies and consequently weak knowledge of water distribution in complex aquifer systems. On the other hand the standard deviation of the soil depth distribution (input data) can be easily converted into parameter ranges and can therefore be considered in a parameter uncertainty analysis.

Therefore the parameter uncertainty analysis conducted in the following section partly accounts for other sources of uncertainty. These uncertainties are quantified using the SUFI2-algorithm (Abbaspour et al. 2004) as introduced in section 4.1.6.3. As this study aims to provide dependable estimates of surface water availability on a monthly to annual basis, for time periods until 2049, the focus of the uncertainty analysis is set on the runoff/rainfall-ratio and the irrigation module.

Consequently the effects of seven parameters have been addressed in this study (see Table 5-28). The Curve Number (**CN2**), as an empirical parameter used for approximating the amount of direct runoff from a rainfall event, is always open to question (Hawkins et al. 2009). CN2 has been calibrated, but many intermediate- or short-term effects on land use and soils, such as drought and changing stocking densities as well as effects of varying storm intensities etc. can be covered by moderate variations of the Curve Number only.

The revaporation coefficient (**GW_REVAP**) is the conceptual representation of the complex process of evapotranspiration from groundwater. As pointed out earlier (section 5.3.5) plausible ranges can be estimated, but exact values can neither be measured, nor be assumed to be constant. GW_REVAP has been calibrated, but allowing variations within the bounds outlined earlier is imperative.

Groundwater is represented via conceptual storage modules within SWAT-MAROC. The distribution of percolating water among the two aquifers (**RCHRG_DA**) is done according to literature values (section 5.3.5). The distribution has a minor effect on total water availability, but

due to different recession coefficients effects on seasonal water availability, hence irrigation volumes can be assumed. Plausible ranges have been discussed earlier.

Soil depth (**SOL_Z**) has the most pronounced effects on discharge composition and discharge volume among all soil parameters. Though soil depth can be assumed to be constant, even over time horizons covered by the scenarios, it can be measured only locally and regionalization is difficult, hence it is the most uncertain parameter from the soil database (Klose 2008a). Therefore possible deviations have to be considered in the uncertainty analysis. The depth up to which evaporative demand from the soil can be satisfied depends strongly on the conceptual **ESCO**-factor. This factor cannot be measured and has been adapted during calibration. Within the irrigation module two factors qualify for uncertainty analysis. The fraction of streamflow that is available for irrigation (**IRR_FRAC**) and the irrigation efficiency (**IRR_EFF**). IRR_FRAC has been adapted during calibration; the irrigation efficiency has been set according to literature values (section 5.3.3.2).

Table 5-28: Parameters and parameter ranges considered in the Uncertainty Analysis (see Appendix 3 for details on parameters).

Parameter	Lower Bound	Upper Bound
CN2[-]	-2.0	+2.0
GW_REVAP [%]	0.3	0.7
RCHRG_DP [%]	25	75
SOL_Z [mm]	-20%	+20%
ESCO [-]	0.71	0.85
IRR_FRAC [%]	25	75
IRR_EFF [%]	70	80

Both parameters are held constant by the model (due to a lack of data), but given the variability of irrigated areas and crops on the one hand and the different management strategies dependent on water availability on the other hand, parameter variations have to be accounted for by the uncertainty analysis.

Three runs of the SUFI2-algorythm have been performed, with 500 model parameterizations each. In the final run (parameter ranges given in Table 5-28) a P-value of 0.56 (i.e. modeled data brackets 56% of measured data) and an R-Value of 0.26 (i.e. average uncertainty range is 26% of the standard deviation of measured data) have been obtained (for details of the algorithm see section 4.1.6.3). Given the uncertainties not covered by SUFI2 (e.g. conceptual model, precipitation, discharge; see previous sections), these results are satisfying. Given our inability to represent exactly how the system works in a hydrological model, there will always be different models and equifinal parameter sets that represent equally well an observed variable (e.g. discharge). Such equally acceptable models are called behavioral (Beven 2008). Within the final parameter range a set of 20 behavioral models has been chosen according to their Nash-Sutcliffe Efficiency (NSE). Since the 20 behavioral models on average reproduce well the measured annual discharge (deviation of the average model discharge to the measured discharge: 1.7%), no further selection criterion has been used. Mean annual discharge of the selected models

ranges from 272 Mm³ to 424 Mm³ and NSE ranges from 0.82 to 0.89 (see Appendix 11). The results from all these models are evaluated and the spread in results is assumed to reflect the uncertainty in the hydrological system, i.e. the "real" systems response is assumed to be bracketed by the spread of results from the behavioral models.

5.7.2 Uncertainty in Future Scenarios

Uncertainties in scenario analysis are considered in this study as follows: Two emission scenarios have been used (IPCC SRES A1b and B2). These scenarios envelope an array of possible future developments based on low to medium emissions (see section 4.1.5). Three ensemble members with varying initial conditions for each model were generated. These ensembles are considered to reflect model uncertainties of the Climate Model. Furthermore three downscaling approaches for the climate data have been used (see section 5.6.1) and 21 behavioral parameterizations of the hydrological model have been used (see section 5.7.1). This results in 378 model realizations for the period 2000-2029 and 2020-2049:

2		*3*		*3*		*21*		*378*
emission scenarios	*x*	*ensembles*	*x*	*downscaling approaches*	*x*	*hydrological parameterizations*	=	*model realizations*

Different sources of uncertainty can now be quantified by averaging all model results of e.g. each downscaling approach. The remaining spread in results can then be attributed to the downscaling approach. For the SNR_m (section 4.2.2.1), the average scenario result compared to the baseline scenario result is the signal, while the spread in scenario results is the noise.

Nevertheless some sources of uncertainty have not been covered by this approach. The recent growth rate of atmospheric carbon dioxide is larger than assumed in all IPCC scenarios (Canadell et al. 2007), but this shortcoming can only be dealt with after revision of the official emission scenarios in upcoming IPCC reports (Moss et al. 2010). Both scenarios have been calculated with the model REMO (nested in the ECHAM5/MPI-OM, see section 5.6.2). The comparison of different RCM/GCM-data is desirable, but the warming and decrease in precipitation in Northern Africa has been identified as a robust trend within 15 different GCMs (Bates et al. 2008). Climate simulations with REMO are so far the only ones available for Western Africa that have a spatial resolution of 0.5° and that include land cover changes as a driving force. These features are available in regional models of Europe or Northern America, but in the study area no equivalent models exist. Therefore the effect of structural uncertainties within the climate model had not been assessed.

For the reservoirs water balance model three time series of annual inflows (1st tercile, median and 3rd tercile) have been used as input. Since these time series feature the exact variability as

in the baseline scenario each has been converted into five time series that start in the 1, 7, 13, 19 and 25 year and goes back to year one, when the end of the record is reached. By this approach a reasonable interannual variability is assured, while the impression of projecting future dry or wet periods can be avoided, as those cannot be derived from the climate change scenarios.

5.8 Interim Summary: Model and Scenario Development

In order to quantify the catchments water balance under present and future conditions the hydrological model SWAT has been successfully further developed to SWAT-MAROC, a regional version specifically reflecting hydrological conditions of the Upper-Drâa catchment. As outlined in section 3.8 the catchment is characterized by high altitudinal and geological heterogeneity. Baseflow, snow and irrigation processes were not adequately represented in the original model; therefore model components have been adapted or new model components have been developed. These were the spatially explicit elevation bands, a second linear storage aquifer, the loose coupling with CropWat and a reservoir module. The scarce data availability enforced the usage of rather conceptual approaches.

The new model produces reasonable results in quantitative and qualitative regards. Volumes and seasonal dynamics of different subsystems, especially groundwater and snow, are reproduced satisfactorily by the model and subsequently quantities of reservoir inflow and irrigation volumes match observed values. The model can therefore be considered as valid for the purpose of estimating surface water availability on a monthly to seasonal scale.

Climate change scenarios have been developed for the IPCC-SRES scenarios A1B and B2. Due to the orographic setting and scarce climate data availability, rather simple downscaling approaches had to be chosen.

An uncertainty assessment scheme has been outlined to quantify uncertainties associated with the climate model, the downscaling and the hydrological model itself.

6. Discussion of Model Results and Uncertainties

> *As we know, there are known knowns. There are things we know we know. We also know there are known unknowns. That is to say we know there are some things we do not know. But there are also unknown unknowns, the ones we don't know we don't know.*
>
> Donald Rumsfeld, 2002

> *A known mistake is better than an unknown truth.*
>
> Arabic proverb

Within this chapter model results from the baseline scenario covering the period 1978-2007 and from the future scenarios are presented. The use of the model results is twofold, on the one hand they are used as a research aid, quantifying immeasurable water balance components (section 6.1), and on the other hand it can be used to predict the systems behavior in the close future under climatic conditions that differ from the past (section 6.2). For both purposes the model uncertainties need to be addressed and as far as possible quantified. The scenario impacts on the agriculturally dominated economy of the Drâa region are analyzed and possible responses are outlined.

6.1 Baseline Scenario Results and Uncertainties

Within this section results from the Baseline scenario, i.e. the model run based on and compared to measured data, are presented. The model covers the time period 1978-2007. This model represents the actual state of the Upper Drâa's hydrological system and serves as reference for the future scenarios.

6.1.1 Water Balance

In the previous sections model results that have measured equivalents have been exploited to calibrate and validate the model. But as the model represents the whole water cycle within the catchment a closer look on non-measurable water balance components is presented. Among other results the perceptual model (lined out in section 3.8) can now be quantified for the period 1978-2007 (Figure 6-1).

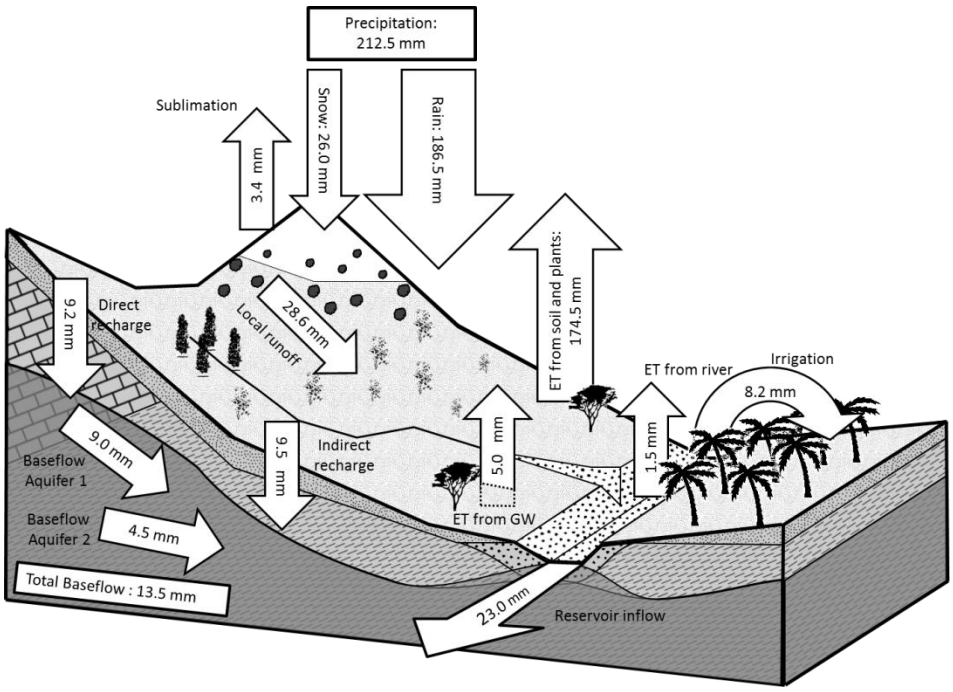

Figure 6-1: Mean annual water fluxes within the Upper Drâa catchment (1978-2007)

Within the catchment an annual average of 212.5 mm of precipitation can be assumed (measured and elevation-adjusted boundary condition of the model). Snow accounts for 26.0 mm or 12.2% of precipitation. Evaporation from different sources (excluding irrigated agriculture) sums to 181.0 mm (85.2%) resulting in a gross discharge coefficient of 14.8%. After the abstraction of 8.2 mm (3.9%) for irrigation purposes, a net discharge to the reservoir of 23.0 mm (11.0%) is obtained.

The parameter uncertainty[17] of the different components of the water balance has been analyzed on mean annual basis. Arbitrary relative and absolute thresholds have been set for different levels of uncertainty: below 25% (or 2.5 mm) for low uncertainty, between 25 and 50% (or 2.5-5 mm) for medium uncertainty and above 50% (or 5 mm) for high uncertainty.

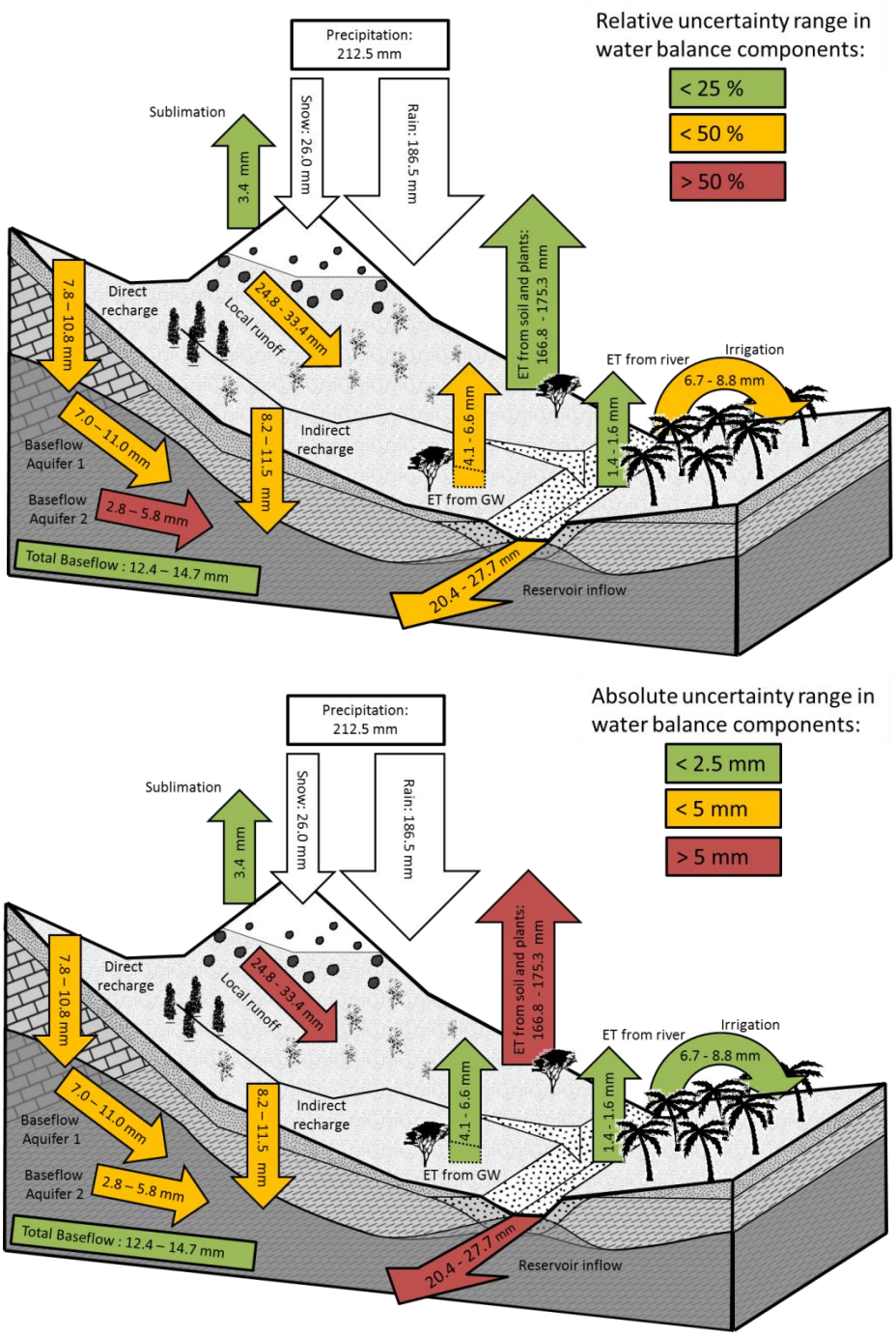

Figure 6-2: Limits of variation of water balance components due to parameter uncertainty; absolute (upper image), relative (lower image). Values are rounded.

[17] In general, uncertainty ranges for results are 80% confidence intervals unless stated otherwise. That is, there is an estimated 10% likelihood that the value could be above the range given and 10% likelihood that the value could be below that range.

Relative uncertainty is high (>50%) for the contribution of the second aquifer (see Figure 6-2). Measured data is hardly available and consequently the respective model module is rather conceptual (see section 5.1.2.3), with one parameter explicitly meant for calibration (RCHRG_DP). Due to the limited spatial extent of regions having a second aquifer, this does not affect total baseflow which has a low uncertainty range (<25%). Furthermore evaporation (from soil, snow, rivers and transpiration) exhibits low relative uncertainties, as it is largely dependent on climate data, which have not been assessed in terms of uncertainty.

The remaining components are within an average uncertainty range (25-50%). Absolute values draw a slightly different picture. Evaporation from soil and plants, local discharge and reservoir inflow are subject to high uncertainty ranges (> 5 mm). These are the three major components, so even slight relative changes might have large absolute implications. All groundwater related components (direct and indirect recharge, and baseflow contributions from both aquifers) have uncertainties below 5 mm. Since these partly derive from the partition of baseflow between the aquifers, total baseflow only exhibits low uncertainties (< 2.5 mm). Furthermore evaporation from rivers, snow and groundwater, as well as irrigation indicates small absolute uncertainties.

The uncertainties in single water balance components can easily be attributed to specific model parameters in a global sensitivity analysis performed on the output of the uncertainty analysis (Table 6-1). Changes in specific water balance components and parameter changes have been linearly correlated and checked for significance (t-Test: 1% and 5% error probability). Furthermore the relative change in water balance components caused by the parameter change is presented (slope of the regression line).

As assumed from the sensitivity analysis of the uncalibrated model (section 5.2), soil depth and Curve-Number are influencing most water balance components highly significant and to high degrees. The effects can be interpreted as follows. An Increased Curve Number (CN2) increases the fraction of surface runoff to total runoff. This change propagates in reduced evaporation losses. Along with surface runoff, indirect recharge and baseflow increase.

Increased CN2 therefore leads to an augmented discharge to the reservoir. Irrigation in the catchment does not benefit (no significant trend), as water availability is increased predominantly in months with already above-average water availability. Changes of soil depth (SOL_Z) show opposite effects, as the soil-storage is increased, evaporation losses rise and consequently all discharge components decrease. The partitioning of groundwater between the two aquifers is only governed by the partition rate (RCHRG_DP). As more water is diverted

to the second (slow responding) aquifer, more water is available in summer, enhancing irrigation, thus reducing discharge.

Having in mind the structure of the irrigation module, in which irrigation occurs, when water is available, not when it is required by the plant (see section 5.1.2.2), it is evident that irrigation efficiency (IRR_EFF) has rarely any effect on the result unlike the fraction of streamflow available for irrigation (IRR_FRAC); an augmentation of which leads to higher irrigation and consequently lower streamflow.

Table 6-1: Effects of parameter changes on water balance components. Explained variability and magnitude of change (%); green: significant positive correlation; red: significant negative correlation (1% error probability: dark color, 5% error probability: light color)

Water Budget (mm)	181.0	5.0	174.5	1.5	28.6	26.3	2.3	18.7	9.2	9.5	13.5	9.0	4.5	32.7	8.3	23.3
Explained variability (%) **relative change (%)**	**ET**	**from GW**	**from soil/plants**	**from rivers**	**Local runoff**	**Q_{surf}**	**Q_{lat}**	**Recharge**	**direct**	**indirect**	**Baseflow**	**Aquifer 1**	**Aquifer 2**	**Discharge**	**Irrigation**	**Reservoir Inflow**
CN2 **per point**	62 -1	12 5	58 -1	36 3	87 9	88 10	42 -1	16 3	14 -4	93 11	17 3	16 7	3 -4	61 6	8 3	53 7
GW_REVAP **per 0.1%**	<1 <1	73 14	4 <1	1 -1	1 1	1 1	6 <1	7 -2	14 4	<1 <1	7 -2	4 -3	<1 1	<1 <1	<1 -1	<1 <1
RCHRG_DP **per 10%**	6 <1	11 -4	9 <1	2 -1	6 -2	6 -2	3 <1	2 -1	4 -2	4 -2	3 -1	69 -11	95 19	7 -2	15 3	18 -3
SOL_Z **per 10%**	41 1	40 -10	53 1	50 -4	24 -5	23 -5	33 -1	45 -5	62 -9	14 -4	46 -5	41 -11	6 6	44 -5	2 -1	42 -6
ESCO **per 0.01**	9 <1	<1 <1	6 <1	12 1	4 1	5 1	3 <1	15 1	1 <1	5 1	14 1	<1 <1	12 2	8 1	<1 <1	8 1
IRR_FRAC **per 10%**	These parameters only affect the irrigation routine														69 7	19 -3
IRR_EFF **per 10%**															1 -3	<1 -1

Key findings of the model contain a quantification of so far only qualitative knowledge. The buffering effect of snow can be made visible, by using the concept of effective precipitation:

Effective Precipitation = Precipitation –Snowfall + Snow melt

While the snow buffer receives a net recharge from October through January, a net release can be observed from March through May (Figure 6-3). The snow melts share of effective precipitation is 24% in March, 12% in April and 7% in May. Thereby the unimodal precipitation regime with a maximum precipitation of 28 mm in October is transformed into a bimodal regime with two distinct peaks in October (27 mm) and in March (22 mm), i.e. in the main irrigation season.

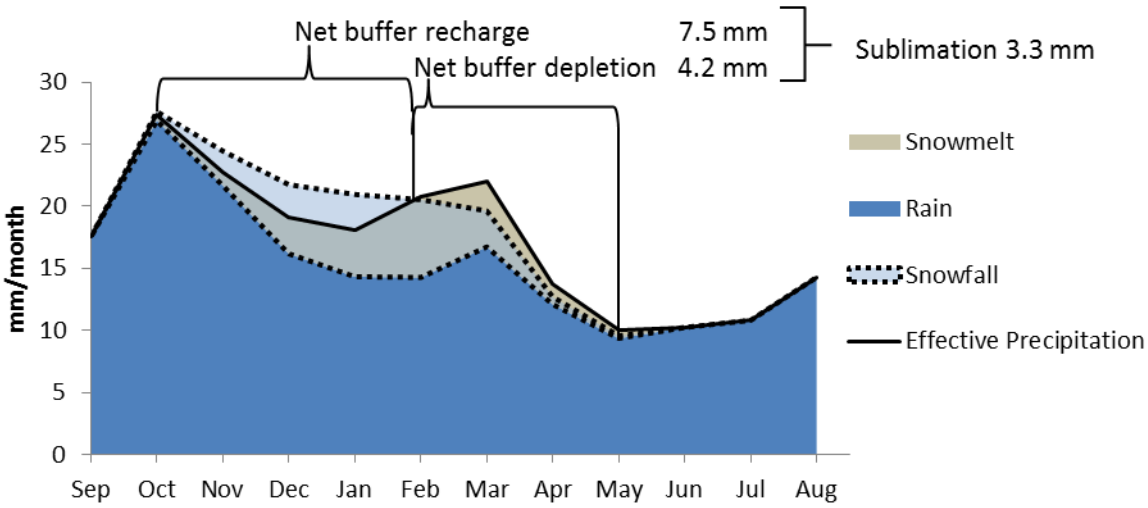

Figure 6-3: Mean monthly precipitation and buffering effect of snow (1978-2007) in the Upper Drâa catchment (14,988 km²).

Using a distributed model water balances for different sub-regions can easily be presented (see Appendix 12 and Appendix 13). The function of the High Atlas as "water towers" can be quantified: In elevations above 2000 masl (~1/4 of the catchment) 40% of the precipitation occurs and 57% of the discharge is generated. The important snow buffers are located in the elevation zones 2000-2500 masl (35%) and 2500-3000 masl (46%). Elevations above 3000 masl are of minor importance (9%) due to their minor spatial extent. Below 2000 masl no noteworthy amounts of snow occur, due to high temperatures (11% of total snow amount).

The relative importance of different tributaries to the reservoir can be determined: 42% of the discharge within the catchment is generated in the sub-catchments of Ifre and Ait-Mouted that account for only 18% of the surface. The Oued Ouarzazate at gauge Amane-n-Tini (24% of the catchment) accounts for 27% of the discharge. Hence the remaining areas (58%) contribution is below average (33%).

6.1.2 Irrigation of Upstream Oases

The importance of different hydrological subsystems for sustaining irrigated agriculture can be highlighted. As it can be seen from Figure 6-4 baseflow contribution to streamflow generally can sustain the irrigated agriculture in the catchment for most of the year.

Already from this lumped depiction it is evident that corn, planted from May through June, can only be grown in years with above average precipitation and discharge or in places that benefit from above average discharge. This is pronounced in annual time series of irrigation amounts.

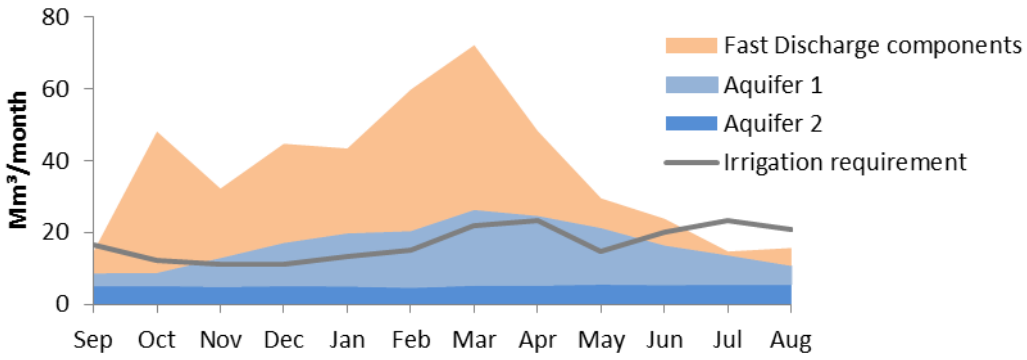

Figure 6-4: Mean monthly discharge components (1978-2007) in the Upper Drâa catchment (14,988 km²).

Assuming the crop mix from 1997/98 being constant, the coverage of irrigation requirement from surface water in the period 1978-2007 is given in Table 6-2. Due to the high variability of precipitation and discharge in the catchment on the one hand, and due to more or less privileged positions of the oases on the other hand an uneven picture is drawn (see Figure 3-1 for the locations of the oases).

It can be seen from fraction of satisfied water demand that the oasis of Toundout and Skoura cannot be irrigated using surface water alone. To what extent alternative water sources are used in these oases is uncertain, but qualitative surveys presented in section 5.1.2.2 indicate that only 10-20% of irrigation requirements are fulfilled by using surface water.

The oasis M'Semrir, Boulmalene and Kelaat, at the banks of the perennial oueds Dades and M'Goun, fed by the karstic aquifers in the North-East of the catchment, receive enough water to sustain agriculture most of the time. Only prolonged droughts as in the mid-80ies or 2001-2005 decrease water availability in these oases.

As water demand is calculated on basis of the year 1998 (see Figure 5-4), at the end of a relatively wet period, the assumed demand is rather high and a variety of options to reduce water demand (e.g. decrease in irrigated area, no spring grains) was not adopted in that year.

Despite the little parameter uncertainty in irrigation volume, great structural uncertainties are associated with the irrigation components of the model. It has to be acknowledged that the model provides only limited insight in irrigation from groundwater.

Table 6-2: Annual coverage of irrigation demand by surface water in the Upper Drâa Catchment (15.000 km²) (1978-2007). Dry conditions (less than 70% of demand satisfied) are marked red, wet conditions (more than 70% of demand satisfied) are marked green.

	M'Semrir	Toundout	Kelaat	Boulmalene	Skoura	Ouarzazate	Total
Gross annual Irrigation Requirement (mm)	**1346**	**1085**	**1293**	**2109**	**1380**	**1016**	**1274**
Area (km²)	**12**	**26**	**27**	**17**	**26**	**52**	**160**
Gross Irrigation Requirement (Mm³)	**16**	**28**	**35**	**36**	**36**	**53**	**204**
1978	100%	71%	88%	88%	32%	82%	75%
1979	100%	45%	100%	97%	20%	100%	78%
1980	100%	93%	100%	95%	41%	100%	89%
1981	100%	11%	100%	83%	4%	100%	68%
1982	100%	14%	59%	42%	6%	70%	48%
1983	100%	3%	36%	20%	1%	23%	24%
1984	40%	2%	15%	10%	1%	14%	12%
1985	93%	9%	85%	82%	4%	28%	41%
1986	94%	18%	49%	28%	7%	14%	27%
1987	96%	4%	51%	26%	2%	41%	33%
1988	100%	91%	96%	97%	41%	100%	88%
1989	100%	79%	100%	100%	32%	100%	85%
1990	100%	92%	100%	100%	47%	100%	90%
1991	100%	23%	100%	100%	7%	100%	72%
1992	100%	31%	100%	97%	12%	100%	74%
1993	100%	22%	90%	80%	9%	100%	69%
1994	100%	18%	91%	79%	7%	100%	68%
1995	100%	39%	100%	89%	17%	100%	75%
1996	100%	41%	100%	100%	28%	100%	79%
1997	100%	51%	99%	100%	11%	100%	77%
1998	100%	31%	81%	100%	12%	100%	71%
1999	100%	9%	65%	52%	3%	100%	58%
2000	100%	29%	96%	77%	12%	100%	71%
2001	100%	3%	25%	56%	1%	36%	30%
2002	100%	53%	81%	77%	49%	33%	56%
2003	100%	37%	53%	41%	12%	32%	39%
2004	100%	53%	91%	92%	18%	59%	63%
2005	100%	5%	45%	60%	2%	48%	38%
2006	100%	39%	79%	64%	15%	94%	67%
2007	100%	29%	100%	100%	12%	97%	73%
Average	97%	35%	79%	74%	16%	76%	61%

Hence model results for the oases of Skoura and Toundout that prominently rely on groundwater for irrigation have to be considered as very uncertain. As depicted in Table 6-2 these oases cover only 35% (Toundout) and 16% (Skoura) of their irrigation demand by surface water. Heidecke (2006) emphasized the high importance of *khettaras*, traditional groundwater harvesting systems, in the oasis of Skoura (sections 3.1 and 5.1.2.2). These are either referred to as sources or groundwater in Table 5-2. Hence, it can be assumed that groundwater in larger quantities is available to these oases. Processes responsible for that are complex aquifer settings and groundwater divides that differ from surface catchment divides. A further implication is that if more water is available to these oases in reality, one of the loss terms incorporated in the model has to be overestimated. It can be assumed that this is the calibrated revaporation coefficient, accounting for revaporation losses of 60-105 Mm^3.

These model deficits can be overcome by a thorough analysis of groundwater hydrology in the region (flow paths, volumes etc.) and a dynamic coupling of SWAT with groundwater models (e.g. MODFLOW, as proposed by Kim et al. 2008; Sophocleous et al. 1999). Until now there is not enough data available to do so, hence the function of other loss terms acting as calibrated closure terms needs to be noted and kept in mind for a critical result analysis. As a consequence within the further result analysis the oases of Skoura and Toundout are not considered.

6.1.3 Reservoir Inflow

The model results concerning discharge to the reservoir, i.e. the outlet of the model domain, have been presented in the sections 5.4 and 5.5, so this section focusses on the associated uncertainties. The derived uncertainty bounds have been analyzed for annual and monthly discharge to the reservoir. Absolute uncertainty in annual discharge is particularly high in wet years (see Figure 6-5), whereas relative uncertainty is highest during dry periods. The average uncertainty to discharge ratio is 55% for dry years with discharge below measured median (1978-2007: 263 Mm³) and it is 31% for wet years with discharge above median.

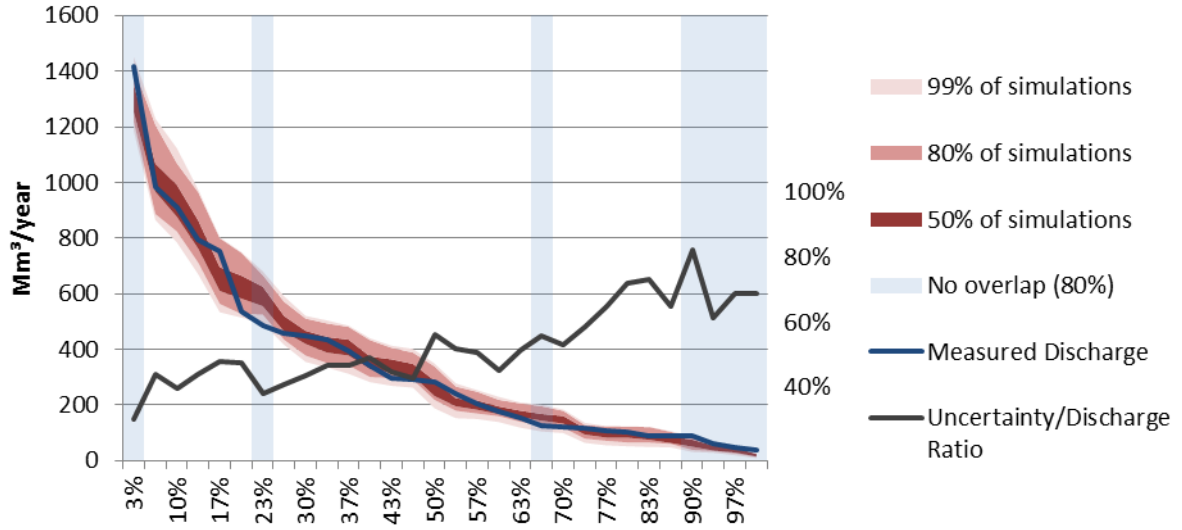

Figure 6-5: Annual flow duration curve including parameter uncertainty at the reservoir Mansour-Eddahbi (14,988 km²) indicating overlap between measured and simulated data (1978-2007). (Measured data: SE Ouarzazate)

Measured discharge is within the uncertainty bounds for 77% of the years. Relative uncertainty of annual model results can easily be estimated using the following exponential term:

$$\text{Uncertainty range [\%]} = 1.8841 * (\text{Discharge [Mm}^3/\text{a]})^{-0.29} \qquad (r^2 = 0.76)$$

The discharge required to sustain drinking water supply and irrigation in the Middle Drâa valley is 300 Mm³/year (see section 3.1), which is surpassed in 43% of the years, according to the measured data. Within the model, 300 Mm³ is surpassed in 41 to 52% of the years.

Within the annual time series only 47% of the measured values are bracketed by simulated values (Figure 6-6). It can be seen that uncertainty ranges are relatively high in 1988, a wet year following a long dry period. As it could be seen from the simple linear model outlined earlier (section 5.1), linear rainfall-runoff relationships come to their limits, as complex non-linear processes govern the system. In this cases different storage modules (soil,

groundwater), depleted to a vast extent in the previous years, are refilled, whereas in 1989, a year with less rainfall, a more direct reaction, i.e. immediate runoff is measured. Since many processes concerning storage or repartition are highly conceptualized and portrayed using uncertain parameters (Curve Number, Soil depth, Partition rate between aquifers), the runoff in 1989 is rather uncertain. Nevertheless, the linear relation mentioned earlier (section 5.1) is clearly outperformed by SWAT-MAROC.

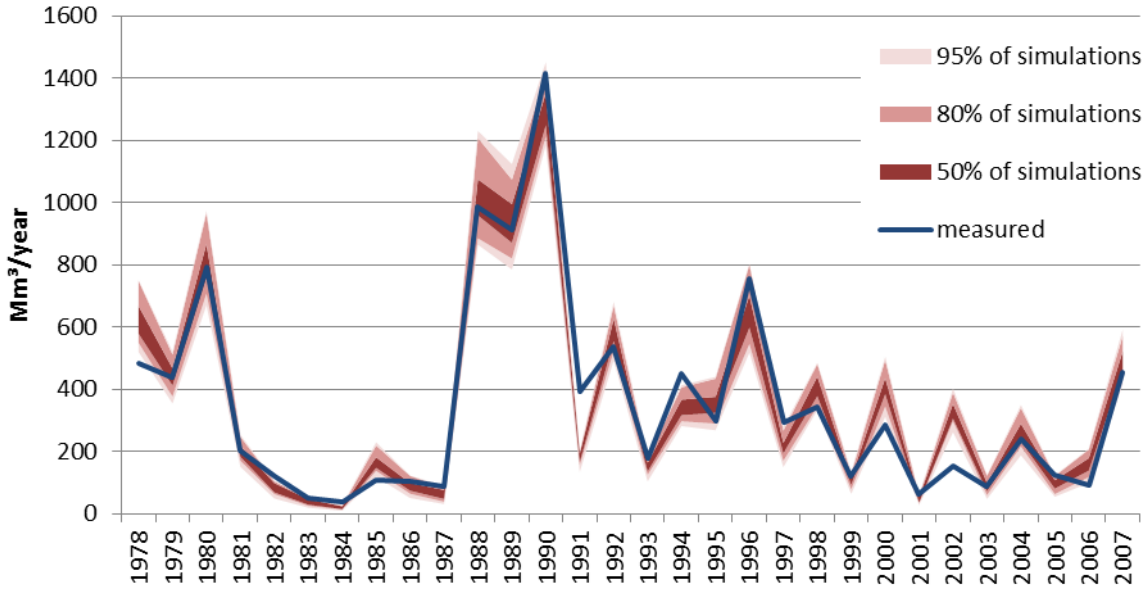

Figure 6-6: Annual discharge including parameter uncertainty at the reservoir Mansour-Eddahbi (1978-2007) (14,988 km²). (Measured data: SE Ouarzazate)

Especially the years 1991, 2000 and 2002 show large deviations between measured and simulated data that cannot be explained by parameter uncertainty, as uncertainty bounds are narrow for these years in particular. A general bias in the model structure cannot be excluded, but no particular trend towards under- or overestimation can be detected. Measurement errors of the precipitation and discharge gauges or a bad aerial representation of measured precipitation have been portrayed (see section 5.3.6.1) and might be the reasons for these mismatches. At least good input data would facilitate the detection of structural model errors.

Monthly values show similar performances (36% of measured values are bracketed in the time series, 98% in ranked form, see Appendix 14 and Appendix 15). Considering mean monthly discharge, again absolute uncertainty is higher during the wet season (see Figure 6-7), whereas relative uncertainty is highest during the dry season. In February the strongest deviations between measured and simulated data can be stated. Measured data is far from being bracketed by simulated data (~5-15 Mm³/month ≙ 0.33-1 mm/month). Therefore the deviation can hardly be explained by parameter uncertainty. Structural errors in the

simple snow routines of SWAT-MAROC or measurement/ extrapolation errors in the climate data might be responsible for these findings, as SWAT-MAROC's modeling of inter-seasonal snow-melt is also imperfect (see Validation section 5.5.3). Throughout the rest of the season measured data points are close to the centerline of the uncertainty bounds and the uncertainty band is narrower.

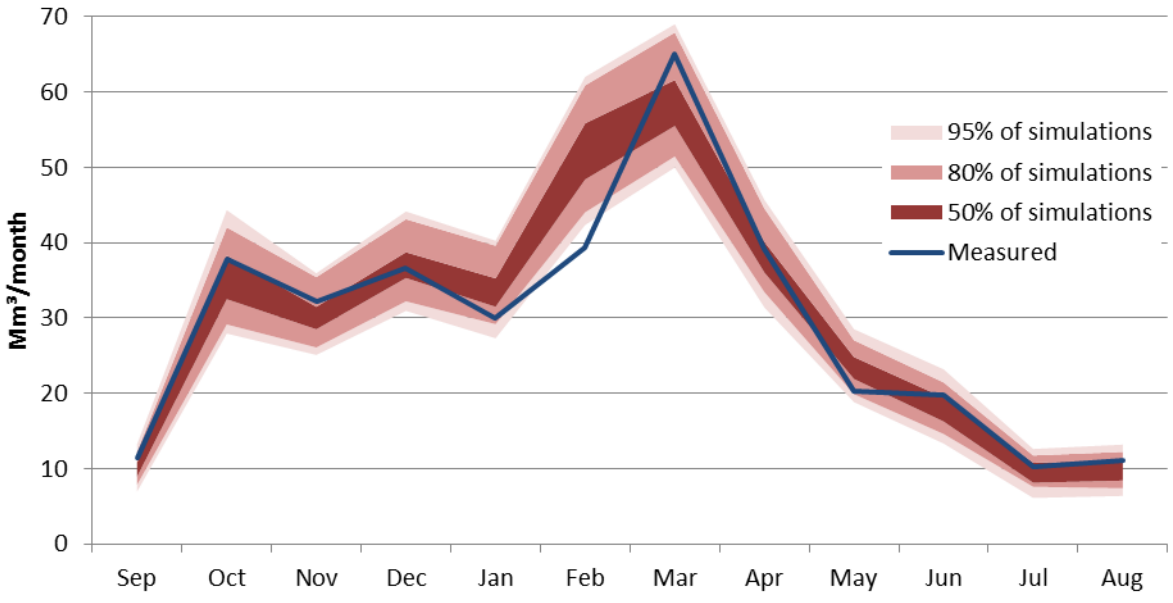

Figure 6-7: *Mean monthly discharge into the reservoir Mansour-Eddahbi (1978-2007) (14,988 km²). (Measured data: SE Ouarzazate)*

6.2 Scenario Results and Uncertainties

In this section the climate change scenario results are presented. Different sources of uncertainty are also quantified for the climate change scenario. Consequently selected rather certain results and trends of the model study are presented. Furthermore the impacts of changed water availability will be outlined, using the indicators introduced in section 4.2.2.

6.2.1 Water Balance

The signal-to-noise ratio determines the models suitability by comparing the "noise" from different sources of uncertainty to the signal of the "average" model result. Therefore the SNR_m provides valuable insight, whether the model can be used for scenario analysis and furthermore rank sources of uncertainty within the scenario analysis (see section 4.2.2.1). In this study al considered uncertainties, model uncertainties, downscaling uncertainties and ensemble uncertainty have been considered (Table 6-3).

Table 6-3: SNR_m-values for the scenarios 2010s and 2030s (green: $SNR_m>1$, sufficient suitability of model for scenario analysis; yellow: $0<SNR_m<1$, scenario effect larger than uncertainty; red: $SNR_m<0$, scenario effects not suitable to be assessed by model, thresholds are explained in detail in section 4.2.2.1)

Uncertainty considered	all considered uncertainties		Model uncertainty		Downscaling uncertainty		Ensemble uncertainty	
Scenario	**2010s**	**2030s**	**2010s**	**2030s**	**2010s**	**2030s**	**2010s**	**2030s**
Precipitation	0.4	4.6	-	-	10.5	24.4	0.6	4.6
Rain	0.1	4.0	-	-	7.9	18.1	0.3	4.0
Snow	2.6	4.7	-	-	48.6	80.8	2.6	4.8
Evapotranspiration	0.5	4.3	5.4	8.8	6.3	21.6	0.7	5.4
from snow	4.0	6.0	23.6	39.7	39.0	72.2	4.3	6.4
from GW	-0.6	-0.3	-0.5	-0.3	3.1	1.8	0.2	1.6
from soil/plants	0.8	4.3	5.2	7.6	7.1	17.8	1.1	6.6
from rivers	-0.8	-0.2	-0.7	0.1	0.4	0.8	-0.7	0.2
Local runoff	-0.3	0.6	0.0	1.0	4.1	2.5	0.0	2.3
Q_{surf}	-0.3	0.6	0.0	1.0	4.2	2.5	0.1	2.3
Q_{lat}	-0.4	-1.0	0.8	-1.0	5.3	-0.9	-0.2	-0.9
Recharge	0.0	1.0	0.9	2.0	6.2	3.3	0.4	2.1
direct	-0.4	0.2	-0.2	0.4	4.5	2.9	0.1	1.7
indirect	-0.1	0.6	0.3	0.9	6.1	3.2	0.5	2.4
evaporation	-0.6	-0.3	-0.5	-0.3	3.1	1.8	0.2	1.6
Baseflow	0.1	1.0	0.9	2.0	6.1	3.3	0.4	2.1
Aq1	-0.3	0.2	-0.2	0.3	4.9	2.9	0.3	2.0
Aq2	-0.5	-0.2	-0.5	-0.2	13.2	4.6	0.5	2.3
Discharge	-0.2	0.9	0.4	1.7	6.0	3.1	0.1	2.2
Irrigation	-0.3	0.1	-0.3	0.1	15.6	6.3	1.1	2.9
Reservoir Inflow	-0.3	0.7	0.2	1.4	5.1	2.7	0.0	2.0

The following conclusions can be drawn from the analysis of the SNR_m: The scenario 2030s provides a more profound signal and consequently a higher SNR_m than 2010s. In 2010s scenario effects can only be stated for snowfall and evaporation from snow and soil, thus temperature related effects. In 2030s strong scenario effects can be observed for precipitation and evapotranspiration, especially from snow and soil, as well as groundwater recharge and baseflow. Signal strength for local runoff, discharge and reservoir inflow is still greater than 0.5, i.e. the signal is by 50% stronger than the noise.

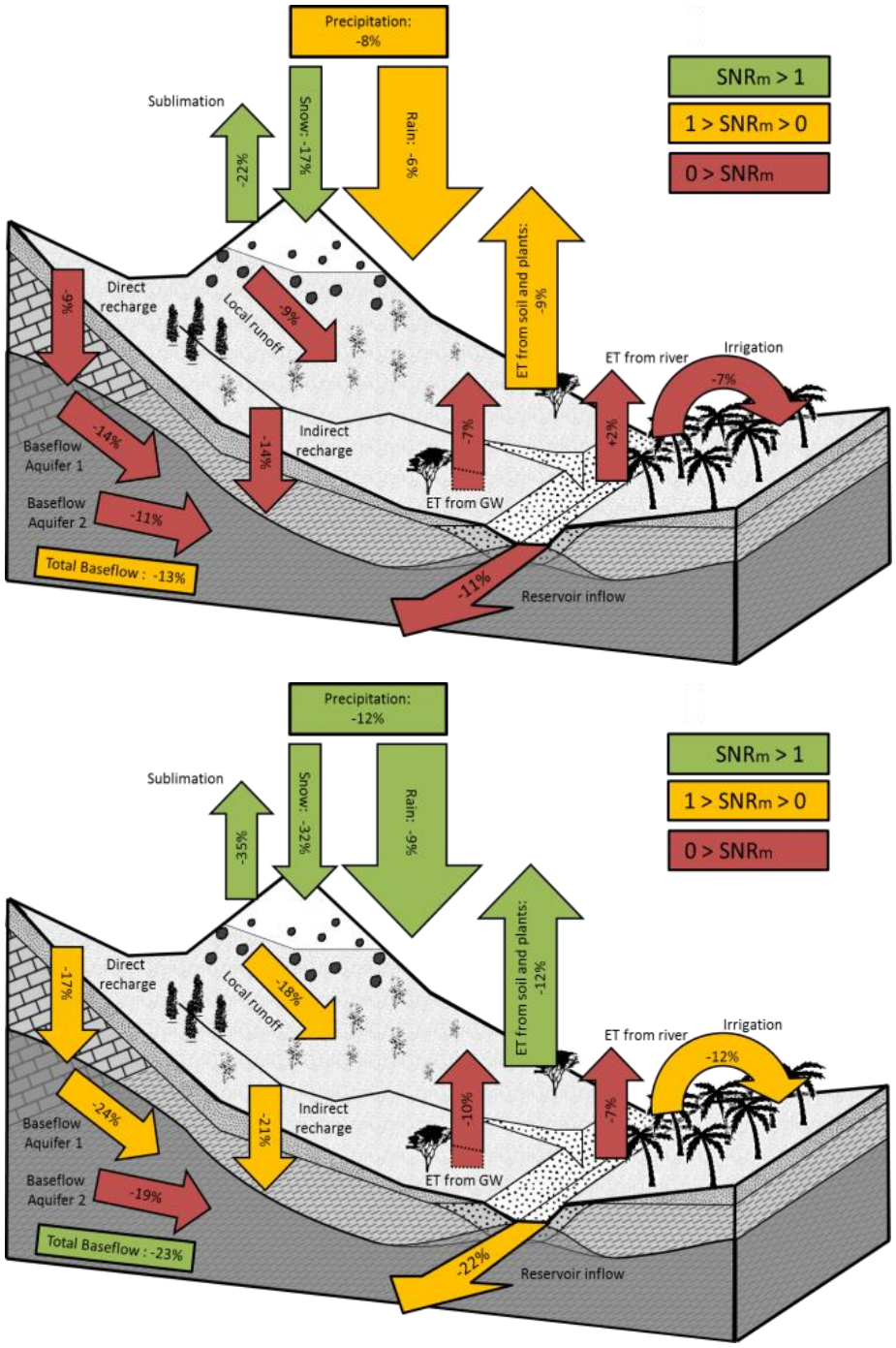

Figure 6-8: Median changes in water balance components due climate change. The color indicates signal to noise ratio (SNR_m) for all considered sources of uncertainty; 2010s (top); 2030s (bottom)

Comparing the scenarios 2010s and 2030s ensemble uncertainty, SNR_m-values increase for all water balance components except lateral flow, whereas SNR_m-values for downscaling increases for discharge, irrigation, lateral flow and groundwater related components. This can be interpreted as growing relative convergence of the climate change scenario ensembles on the one hand and diverging effects of downscaling techniques when applied to stronger climate change signals. In general downscaling and ensemble uncertainties are almost negligible but are superimposed by strong uncertainties of the hydrological model. Furthermore the SNR_m–values are generally higher for the 2030s scenario.

Beside significance of trends, magnitudes of projected changes in single water balance components are provided by Figure 6-8. It can be seen that any trends apart from climate forcing (including evaporation) and baseflow are covered by strong noises in the 2010s scenario. Therefore in this section primarily results from the 2030s scenario are presented. Further it can be seen that a decrease in precipitation is translated into a disproportionate decrease in runoff. In the baseline scenario the rainfall-runoff-coefficient was 13-17% (10-13% after subtraction of irrigation), whereas in the 2030s the rainfall-runoff-coefficient is 12-15% (8-11% after subtraction of irrigation). Irrigation decreases in the same order of magnitude as precipitation (12%).

Table 6-4: Likelihood and magnitude of changes in the hydrological cycle of the Upper Drâa Catchment in the 2030s scenario. The color indicates confidence in model result using the signal to noise ratio (SNR_m) for all considered sources of uncertainty: $SNR_m>1$ (green); $0<SNR_m<1$ (orange); $SNR_m<0$ (red)

		Virtually certain	Extremely likely	Very likely	Likely
Precipitation		-9%	-9%	-9%	-11%
	Rain	-6%	-6%	-7%	-8%
	Snow	-25%	-25%	-26%	-31%
Evapotranspiration		-7%	-8%	-8%	-10%
	from snow	-27%	-32%	-32%	-34%
	from GW				-7%
	from soil/plants	-8%	-8%	-9%	-11%
	from rivers				-3%
Local runoff				-2%	-13%
Direct Recharge					-13%
Indirect Recharge				-3%	-16%
Baseflow			-3%	-8%	-18%
	Aquifer 1				-18%
	Aquifer 2				-10%
Irrigation					-5%
Reservoir Inflow				-5%	-17%

Using the likelihood-terminology of the IPCC (section 4.2.2.2) the hydrological regime of the climate period 2020-2049 can be compared to that of the Baseline scenario (Table 6-4). The decrease in snowfall by one quarter is virtually certain, along with this goes a virtually certain slightly higher decrease in sublimation (27%). It can be assumed that the snow that still falls melts earlier and is therefore less prone to sublimation. A different picture is drawn for evapotranspiration that decreases less than precipitation, leading to drier conditions in the study area. In terms of likelihood the disproportionate decrease of reservoir inflow and irrigation outlined earlier is even more distinct. It is likely that the annual irrigation volume will decrease by at least 5%, whereas the reservoir inflow is likely to decrease by at least 17%. A pronounced decrease in baseflow is more likely to occur than a decrease in quick runoff components (surface runoff and lateral runoff, aggregated to local runoff). It can be assumed that these are perpetuated model uncertainties that were already evident in the Baseline scenario.

For the presentation of more complex model results, a representative scenario realization has been chosen to be compared to the baseline scenario. Therefore the calibrated model has been used. To determine the downscaling approach and the climate ensemble that are “closest” to the general trend, the RMSE of the average climate ensemble and downscaling realization in comparison to the average of all realizations for mean annual water balance components and mean monthly discharge to reservoir has been evaluated. In both cases the climate scenario B2, ensemble 1 (RMSE of ensemble B2.1 compared to general trend: 4.8 mm for water balance components and 0.5 mm for mean monthly discharge) and the downscaling approach “A” (RMSE of downscaling “A” compared to general trend: 1.6 mm for water balance components and 0.1 mm for mean monthly discharge) have been found to represent the general trend best (see section 5.6.1 for details on the downscaling).

The following model results are taken from this representative model only. The stated decrease of mean annual snowfall in the 2030s scenario is allocated differently in the altitudinal zones of the catchment, as the projected increase in temperature leads to decreased snowfall and increased snow melt predominantly in lower elevations, while the projected decrease in precipitation affects all elevation zones. In elevations above 3000 masl snowfall is reduced by only 12% compared to the baseline scenario, but due to average temperatures that are still below zero during most of the wintertime, large snowpacks establish during winter (Figure 6-9). A different situation arises in altitudes from 2500 to 3000 masl, where snowfall decreases by 25% and snow melts earlier so that the average snowpack is reduced considerably. According to these findings the relative importance of different subregions

shifts. Below 2000 masl only 4 instead of formerly 11% of total snow falls. The important snow buffer in the elevation zone of 2000-2500 masl receives only 31 instead of formerly 35% of snowfall, whereas the higher zones gain relative importance. Within the elevation zone of 2500-3000 masl fall 51 instead of 46% of the snow and in elevations above 3000 masl fall 11 instead of 9% of the snow.

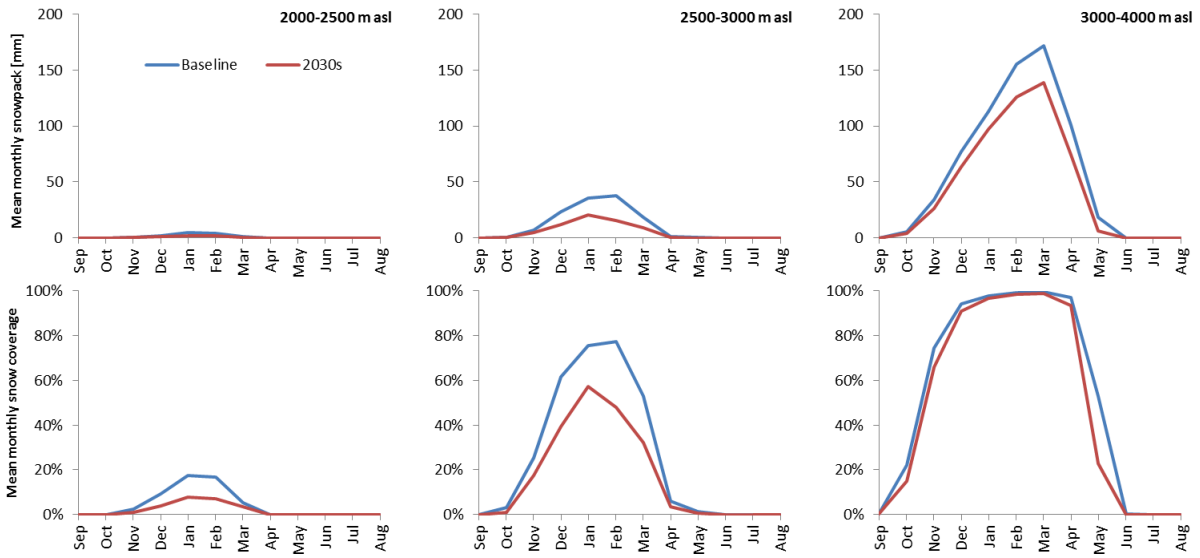

Figure 6-9: Climate change effects on the mean monthly snowpack and –cover in different elevation zones of the Upper Drâa catchment in the Baseline and 2030s Scenario.

Concluding the total decrease of snow buffers has implications on the effective precipitation in the catchment (Figure 6-10). The climate change scenarios prescribe already reduced precipitation in fall and spring. Since the snow melts share in effective precipitation is reduced from 24 to 14% in March, remains at 12% in April and is reduced from 7 to 5% in May, the diminished snow buffer eventually leads to a further substantial decrease in effective precipitation during spring.

While changes in precipitation are a key driver of the projected decrease in annual runoff, it can be seen that the projected warming produces strong decreases in winter snow accumulation and spring snowmelt regardless of precipitation change. This goes along with findings from many mid- to high-latitude areas where precipitation changes are either moderately positive or negative in the future projections (Adam et al. 2009).

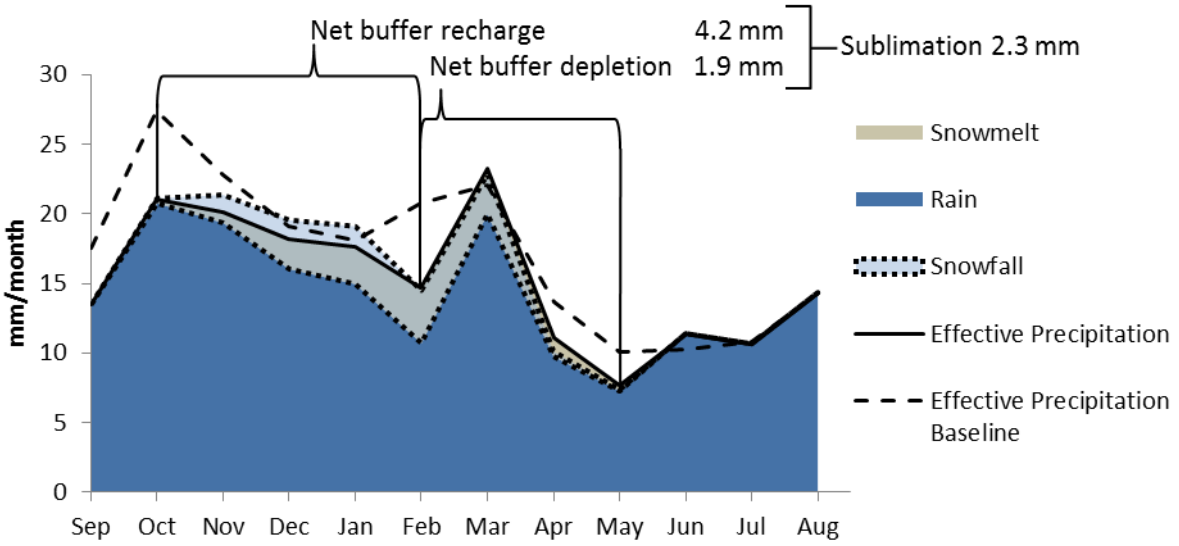

Figure 6-10: Mean monthly precipitation and buffering effect of snow in the Upper Drâa catchment (14,988 km²) for the 2030s scenario.

Most other changes in water balance components occur uniformly in the whole catchment. Therefore the relative importance of different tributaries to the reservoir does not change in comparison to the baseline scenario (values are given in Appendix 16). The only further difference that can be stated (compare Appendix 13 and Appendix 17) is a relative increase in direct groundwater recharge in the elevations above 2000 masl (60 to 64%), whereas in lower regions the relative share decreases from 40 to 36%. As pointed out, the absolute importance of direct recharge in the basin is small (section 2.5), and it can be assumed that due to a pronounced drying in the future this process is further losing importance.

6.2.2 Irrigation of Upstream Oases

The lumped model results presented so far do not reflect large changes of the water amount available for irrigation, despite the great decrease in reservoir inflow. But using a distributed model, results can be analyzed for single oases. In Figure 6-11 projected changes in surface water supply of the single oases can be seen.

Again the results are subject to considerable uncertainties, mainly model uncertainties. Consequently SNR_m-values for all trends are negative. Nevertheless the following key findings can be highlighted: In terms of irrigation water availability the upstream oasis of M'Semrir is not affected by climatic change, as sufficient water is available even in dry years and there are only little irrigated areas. These stable conditions are also reflected in narrow uncertainty bounds.

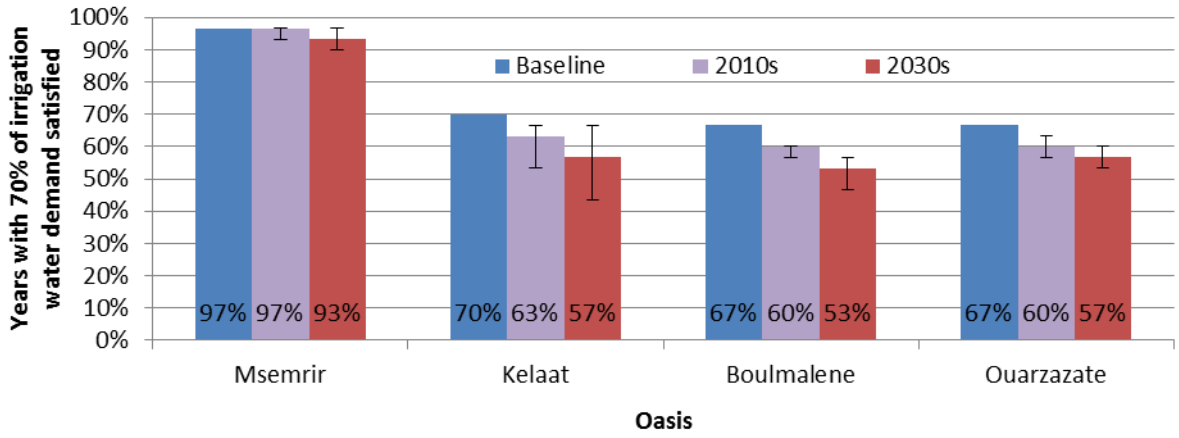

Figure 6-11: Fraction of years in which 70% of the irrigation demand of the Upper Drâa oases can be satisfied from surface water within the baseline and climate change scenarios. Bars represent median model results, error bars envelope the middle tercile of model results.

The decrease in irrigation water availability in the other oasis is similar according to the median model results, the upstream downstream riparian relationship of the oases of M'Semrir and Boulmalene does not seem to have an effect. Surface water availability at the oasis of Kelaat is subject to the highest uncertainties, as the drainage area of the Oued M'Goun at the oasis Kelaat (1305 km²) is smaller than that of the Oued Ouarzazate at the oasis of Ouarzazate (3887 km²) or the Oued Dades at the oasis of Boulmalene (1830 km²). Therefore model uncertainties in the field of snow or groundwater dynamics can hardly be averaged out.

It can be summarized for the oases of Boulmalene and Kelaat that, according to the IPCC-terminology, it is likely that one out of eight years that was above the irrigation threshold in the baseline scenario, falls below the threshold in the 2030s scenario. For the Oasis of Ouarzazate it is one out of ten years. Furthermore no riparian conflicts seem to arise in the surface water irrigated oases, as the oasis of Boulmalene does not experience above average reductions in irrigation volumes.

While the latter results consider interannual variability in water availability, inneranual changes go along with the findings presented in the last section 6.2.1. Especially the water availability at the oases of M'Semrir, Boulmalene and Kelaat reflect the decrease in spring rainfall and the decrease of snow melt (Figure 6-12). It can further be seen that the conditions for growing maize in summer become more unfavorable. The overall decrease in water availability at the oasis of Ouarzazate is not subject to pronounced seasonal trends.

Further aspects not addressed in this study include potential benefits of climate change on plant growth, as warmer temperatures and increased CO_2 availability. It is assumed that soil

moisture and irrigation deficits produced by a reduction in spring rainfall and melt water flows limit any increase in crop yields resulting from temperature increase (Bravo et al. 2008). Especially summer crops such as maize may suffer as a result. Equally, fruit trees require a specific chilling period that may not be met in a warmer environment (Luedeling et al. 2011; Luedeling & Brown 2010). Physically based agronomical modeling can provide further insight in the outlined processes. The developed model may provide the required boundary conditions to run these models.

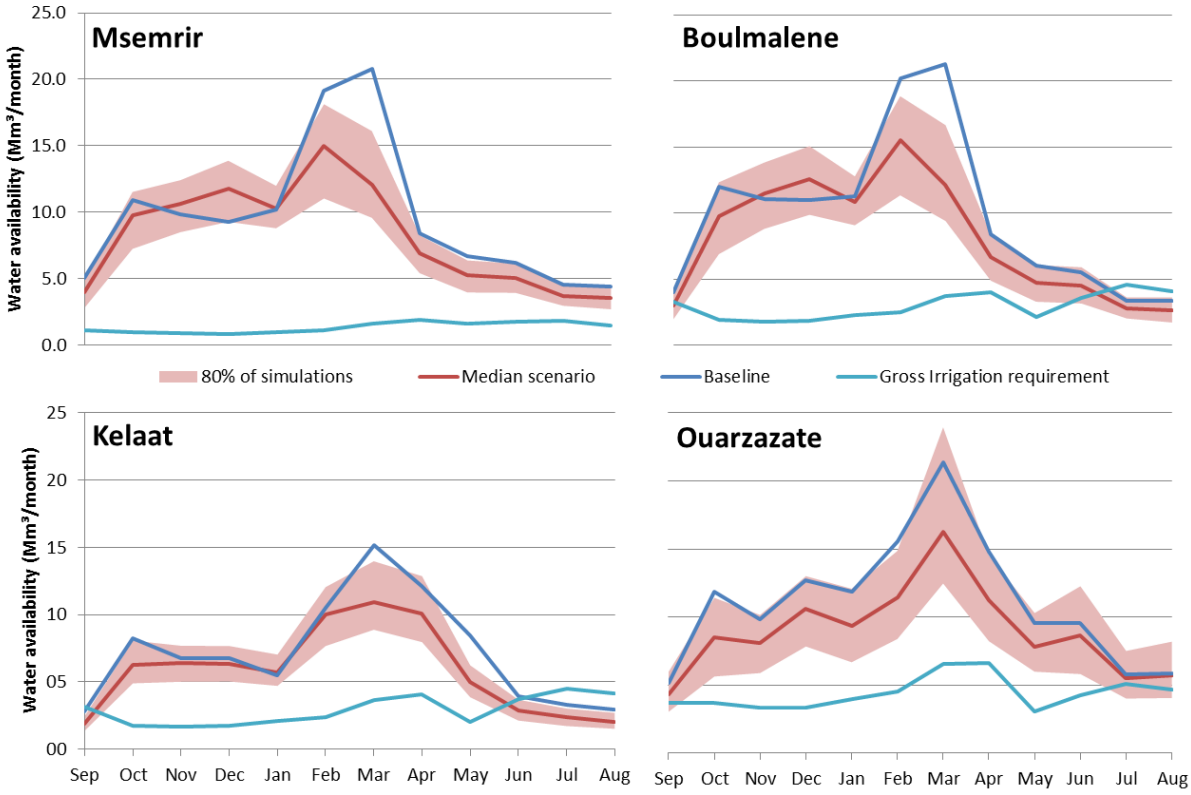

Figure 6-12: Mean monthly discharge at the surface water fed oases including all considered uncertainties during the scenario period 2030s

6.2.3 Reservoir Inflow

Implications of the outlined changes in the water balance involve a strong decrease in reservoir inflow for the 2030s scenario. Within the baseline scenario the threshold discharge of 300 Mm³/year is surpassed in 41 to 52% of the years (Figure 6-5).

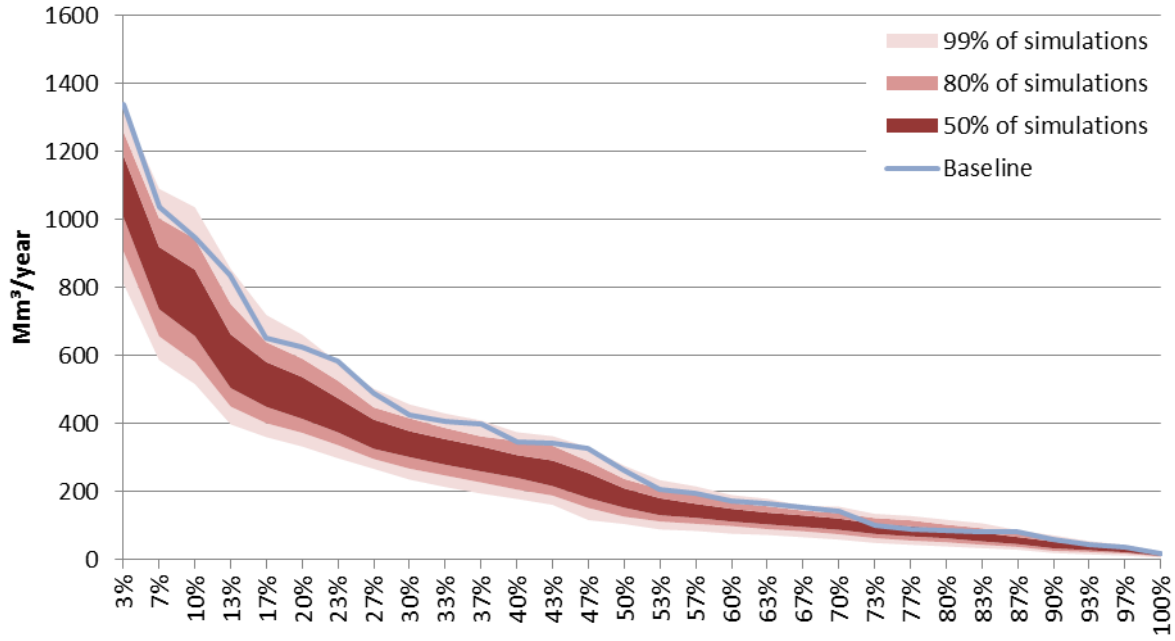

Figure 6-13: Annual flow duration curve including all considered uncertainties at the reservoir Mansour-Eddahbi (14,988 km²) during the scenario period 2030s

In the climate change scenario the threshold is surpassed in 27 to 46% of the years only (Figure 6-13). According to the IPCC terminology it is likely that 300 Mm³ annual discharge to the reservoir will be exceeded in 39% of the years.

Considering changes in mean monthly discharge, the largest decrease can be observed in March, despite considerable uncertainties (compare Figure 6-14a). To a large extent the uncertainties indicated by Figure 6-14 can be attributed to the uncertainty inherent to the hydrological model and the climate model ensembles. While the climate change signals seem to be consistent through most of the year or do barely affect discharge (e.g. in the early rainy season), different temperature and precipitation signals in the snow-melt period at the end of the rainy season have major effects on the discharge. The model uncertainty is not affected by seasonal variations and exhibits roughly the same dynamic as in the baseline scenario (see section 6.1.1). The effect of the different downscaling approaches is almost negligible, only during fall slight deviations between the different approaches can be stated. A similar, subordinate effect of downscaling approaches is reported from modeling studies in the Alps (Rößler 2011).

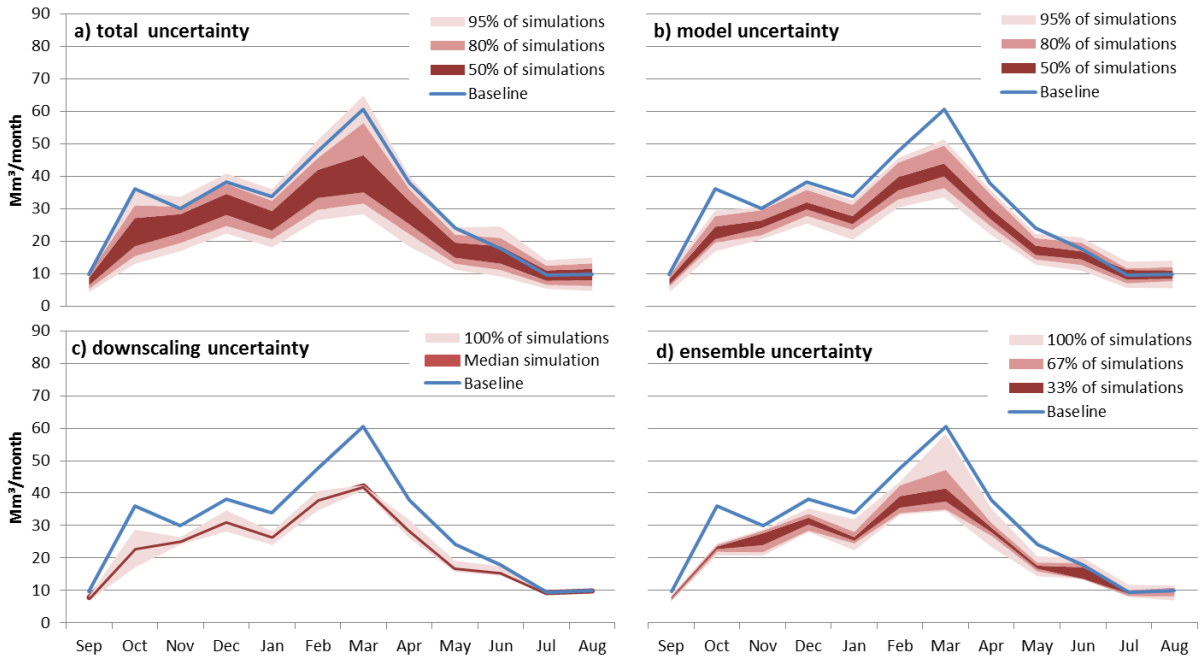

Figure 6-14: *Mean monthly discharge to reservoir Mansour-Eddahbi in the scenario 2030s, considering a) all considered uncertainties (378 varieties); b) model uncertainty (21 varieties); c) downscaling uncertainty (3 varieties) and d) ensemble uncertainty (6 varieties)*

The reservoir module results are highlighted in Table 6-5. The socio-economic scenarios lead to distinct changes in the reservoir management and in water availability for the Middle Drâa valley, despite the same inflow.

Under the assumptions of scenario **M1** it is likely that the reservoirs buffer function is exhausted in the period 2026-30, i.e. from that time on the reservoirs storage capacity is below the combined demand of the Ouarzazate region and the Middle Drâa valley. Within this scenario the highest sedimentation rate is assumed and accordingly the silting is happening sooner than in any other scenario. By the year 2050 the storage capacity is reduced to 39 to 89 Mm³, a volume that is negligible in terms of flood control and irrigation planning. The total volume of water that reaches the Middle Drâa valley is higher as in any other scenarios (205-256 Mm³/year) , as abstractions by the city of Ouarzazate are lower and evaporation losses in the reservoir are minimized due to the forced increase of direct releases.

Within the scenario **M2** it is likely that the reservoir stays operational until 2040-2042, with a final storage capacity of 245-260 Mm³, as siltation is assumed to slow down. Along with this goes a secure water supply of the city of Ouarzazate and higher evaporation losses. Consequently water release to the Middle Drâa Valley is lower than in the other scenarios. Due to the reservoirs buffer function that is maintained until the early 40ies, planned releases

(lâchers) can be provided to a higher extent as in the scenarios M1, but the total release is lower (190-236 Mm³/year).

The scenario **M3** is an intermediate between the more extreme assumptions of M1 and M2. The buffer function of the reservoir is likely to persist until 2033-37 and the final storage is 192-216 Mm³. The total water release to the Middle Drâa is 194-241 Mm³/year.

Table 6-5: Future operation of the reservoir Mansour-Eddahbi as derived from the reservoir water balance model assuming the climate change scenario 2030s and different socio-economic scenarios. The middle tercile of 2030s discharge time series is used as boundary condition. [1)] In the baseline scenario the Water supply of Ouarzazate is only given for the year 2010, as drinking water has not been abstracted from the reservoir until 1998, therefore an average would be distorting.

	Baseline (1978-2007)	**Socio-economic Scenario (2020-2049)**		
		M1	**M2**	**M3**
Reservoir operational until… (middle tercile)	-	2026-2030	2040-42	2033-37
Reservoir storage capacity in 2050 (min and max)	-	39-89 Mm³	245-260Mm³	192-216 Mm³
Annual Inflow (middle tercile)	356 Mm³	248-297 Mm³		
Evaporation Loss (min and max)	61 Mm³	31-33 Mm³	39-42 Mm³	38-40 Mm³
Average Water supply of Ouarzazate	8 Mm³ (2010)[1)]	14 Mm³	22 Mm³	19 Mm³
Total water release (min and max)	290 Mm³	205-256 Mm³	190-236 Mm³	194-241 Mm³

A common finding is that the buffer function of the reservoir will be exhausted between 2026 and 2042, dependent on the scenario. Policy responses have to be outlined in order to enable the farmers in the Middle Drâa Valley to cope with the discontinuation of more or less reliable surface water irrigation during the growing season within this period. The difference between the scenarios is only temporal but not qualitative.

6.2.4 Rangelands

The precipitation data for baseline and future scenarios indicate a spatiotemporal inhomogeneous drying for the Upper Drâa catchment. On the one hand a pronounced drying can be stated for the basin, i.e. the winter pastures; on the other hand the drying is more pronounced in spring and fall throughout the whole catchment. The pattern evolves more clearly in the 2030s scenario (Table 6-6). Within the whole time period and throughout the catchment the SPI does not fall below -0.5, which is the threshold for a mild drought.

Considering the 2030s scenario, the seasonal change of rangeland avoids the drought-prone regions in space and time. Only in spring, the transition pastures are subject to a more pronounced drying trend. Again it has to be added that the climate change scenarios do not contain any information about drought persistence, as they inherit the climatic variability from the baseline scenario. Furthermore the seasonal SPI might be a reasonable proxy for the availability of annual grasses, but to what extent perennial shrubs are affected by water stress experienced before the grazing season needs further consideration.

Table 6-6: Precipitation changes in different rangeland domains within the Upper Drâa catchment under climate change conditions (median results): 3-monthly SPI compared to the Baseline scenario (green: drying below scenario median; red: drying above scenario median). Black rectangles indicate the respective grazing seasons.

Scenario	2010s			2030s		
Rangeland	**summer**	**transition**	**winter**	**summer**	**transition**	**winter**
Sep	-0.12	-0.12	-0.22	-0.17	-0.22	-0.38
Oct	-0.03	-0.04	-0.15	-0.13	-0.16	-0.29
Nov	-0.02	-0.02	-0.10	-0.12	-0.13	-0.18
Dec	-0.03	-0.04	-0.11	-0.10	-0.11	-0.11
Jan	-0.10	-0.11	-0.16	-0.13	-0.14	-0.17
Feb	-0.09	-0.10	-0.13	-0.13	-0.13	-0.12
Mar	-0.05	-0.05	-0.06	-0.15	-0.15	-0.13
Apr	-0.12	-0.12	-0.12	-0.24	-0.26	-0.22
May	-0.16	-0.18	-0.24	-0.29	-0.36	-0.42
Jun	-0.09	-0.09	-0.14	-0.15	-0.19	-0.24
Jul	0.02	0.02	-0.01	-0.02	-0.05	-0.09
Aug	-0.04	-0.01	-0.07	-0.08	-0.11	-0.26

6.2.5 Scenario impacts on the Middle Drâa Valley

It has been shown that the decrease in annual water availability is disproportionally high compared to precipitation changes. Nevertheless irrigation water availability in the oases is only reduced in the magnitude of precipitation changes, as most of the irrigated perimeters benefit from above average precipitation in high altitudes and aquifer settings that provide discharge throughout the main irrigation season. Since no noteworthy upstream downstream relationships exist in the Upper Drâa valley, no water distribution conflicts among the upstream oases are expected. On the other hand, competition among water users in the Upper and Middle Drâa basin might increase. Figure 6-15 highlights the different development of water availability in the upstream areas and in the reservoir for both scenarios.

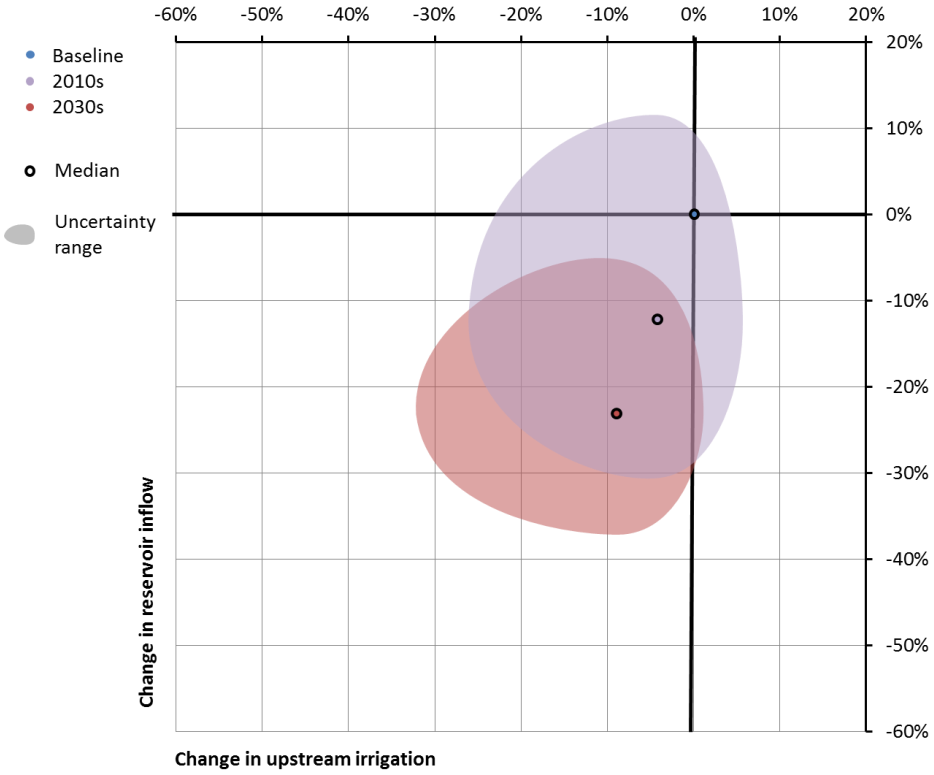

Figure 6-15: Relative changes in annual upstream irrigation and reservoir inflow under climatic change; bubbles envelope eight deciles of model results parallel to the axes.

The decrease of available irrigation water for downstream riparians is roughly twice as high as for upstream riparians. The situation further aggravates by a decreasing efficiency of the reservoir. On the one hand the buffering effect is reduced along with its volume; on the other hand evaporation losses from the reservoir increase as the surface to volume ratio becomes less favorable due to ongoing siltation. The tipping point of reservoir operation is likely to be reached between 2026 and 2042, depending on the socio-economic scenario. So within the coming decades the development of alternative water management schemes is required.

Managed aquifer recharge provides a management alternative to the surface water supply provided or planned today (Dillon 2005). This option becomes more and more feasible, as farmers in the Middle Drâa valley are already today increasingly relying on the use of motor pumps to supplement surface water irrigation (Heidecke 2009). Nevertheless institutional reforms and the technical support of farmers are required to establish such a system. Within the scenario M1, the functionality of the reservoir is likely to not go beyond 2030, but the same institutional and economical instabilities that lead to increased erosion rates in the Upper Drâa valley might inhibit a fast structural adaptation as outlined above in the Middle Drâa Valley within this period. Within the scenario M2, the reservoir is likely to remain operational until 2042, and the assumed political stability and economic prosperity create the surrounding in which structural adaptions can succeed.

The cessation of scheduled water supply to the Middle Drâa valley is becoming fact within the next 30 years. As upstream and downstream benefits and costs of dams are widely discussed (e.g. World Commission on Dams 2000), an unregulated Drâa would bear two consequences for the Middle Drâa valley. On the one hand the Middle Drâa's share of the Upper Drâa's discharge is likely to increase, as evaporation losses from the reservoir fall away. On the other hand the discharge might less often reach the oases further south and the timing of water availability might not coincide with plant water requirements.

7. Conclusions and Outlook

In this study the impact of climate change on a semi-arid mountainous catchment was addressed. Therefore a conceptual model has been adapted to the local conditions, focusing on the development of robust routines facing data scarcity and process complexity. The model calibrated and validated under recent conditions, has then been run using downscaled RCM climate data and socioeconomic scenarios. Uncertainties in every part of this approach have been quantified and results were interpreted in consideration of these uncertainties. In the introduction six objectives have been outlined and this chapter summarizes the key findings as well as the implications for further research.

Objective 1: Identification of relevant hydrological processes in a semi-arid mountainous catchment

From discharge data alone the discharge generating and delaying processes can hardly be identified. Within arid mountainous regions compensation effects in the soil, the groundwater and the snow are known and complicate model development. Within the IMPETUS project case studies on soil, snow and groundwater hydrology as well as surveys on agricultural water use have been conducted. Complemented by studies from local water authorities, a detailed picture of hydrological processes in the region could be drawn. The extensive measurement-network, established within the IMPETUS framework covers the strong altitudinal/aridity gradient of the catchment and allowed us to quantify climatic gradients within the catchment. Therefore a further operation of the elevated climate stations would be desirable to establish long time series and resilient climate gradients. The quality of the discharge measurements needs to be improved by more regular discharge measurements in order to establish robust stage-discharge relationships. Less error-prone discharge measurement equipment (e.g. ADCPs) could supplement the existing network and provide more accurate data to facilitate more detailed process knowledge (e.g. recession analysis) as well as more robust models (multi-site validation). However, the required funds exceed local capacities.

Further mapping of the complex aquifer settings and groundwater divides in the Upper Drâa catchment could augment the understanding of water availability in primarily groundwater-fed oases.

Objective 2: Development of an appropriate model structure that accounts for the relevant processes and provides the required results

The SWAT model has been extended to SWAT-MAROC, a model that suits the local conditions. Within the model, climate data are assigned not only to subcatchments, but spatially explicit to elevation-accounting HRUs within the subcatchments. Therefore the strong altitudinal climatic gradients prevailing in the study area are considered. A shortcoming of the model is the lumped snow parameterization that leads to faulty representation of snow covers, as the associated parameters cannot vary with elevation. It has been shown that the explicit consideration of elevation zones is a promising way to model elevation-dependent processes while maintaining a conceptual and computationally efficient approach. It has further been argued that the outlined approach could easily be integrated in the original SWAT model, making it more flexible. It has to be tested whether the lumped snow module parameterization could be improved by spatially distributed parameters (e.g. by relating snow cover thresholds to topographic features).

The second adaptation carried out within the SWAT-model is the second linear storage aquifer that allows modeling of complex groundwater settings, as detected in the Upper Drâa catchment. Since baseflow-fed discharge in the main irrigation season is the primary source of irrigation water, this adaptation was essential to assess water availability in wet as well as in dry periods. Nevertheless irrigation from groundwater could not be modeled satisfactorily. The dynamic coupling of more elaborate groundwater models with SWAT might be a way to overcome this problem, but is still inhibited by scarce data availability.

The loose coupling of SWAT with simple irrigation routines reflects the scarce data availability, which allows monthly estimations, but hardly physical based modeling on a daily timescale. The same is true for the simple reservoir routine. So far a model application as decision support tool is simplified, since agronomic scenarios can easily be conducted without recalculating the hydrological boundary conditions. Furthermore the model could serve as a basis for disciplinary studies that replace the above mentioned routines by more sophisticated approaches.

The most important aspect of model development is the improvement of the soil moisture component within SWAT, which works imperfect under the conditions in the research area. The reasons have to be identified and the routine has to be improved. Further optional aspects to reflect regional specifics are a reduced infiltration capacity during precipitation events due to soil crusting and variable streambed conductivities that reflect clogging effects.

Objective 3: Scenario Development

Climate change studies rely heavily on large-scale-model results that have to be processed in order to be used in impact assessments. This process is associated with various sources of uncertainty. To identify robust trends, two climate change scenarios (A1B and B1), each with three realizations, have been used. The regional climate model data has been statistically downscaled, in order to account for orographic effects. Nevertheless strong biases in comparison to measured data have been detected, so that only the change signals have been included in the climate change assessment. Three approaches have been developed to inflict the change signal on the measured time series. The effect of scenario choice, ensemble members and downscaling methods on model results has further been considered in the uncertainty analysis. The assessment of the new IPCC-scenarios, dependent on the availability of regional climate model results, is the next step. This would further enlighten uncertainty ranges associated with the climatic boundary conditions.

In this work rather simple assumptions concerning socioeconomic scenarios were made. Considering the persistence of irrigated areas within the catchment, socio-economic scenarios have only been imposed on the reservoir routine of the model. More elaborate socioeconomic scenarios as presented in this study can be applied by using the results of SWAT-MAROC as initial or boundary conditions for other models. In the Drâa catchment models such as WEAP (Szenasi 2011), IWEGS (Klose et al. 2008b) or MIVAD (Heidecke 2009) could exploit data provided by SWAT-MAROC.

Objective 4: Development of an uncertainty assessment scheme that allows quantifying and comparing uncertainties of different steps in the climate change impact assessment

In this study an uncertainty assessment scheme has been applied that accounts for the uncertainty cascade in the different steps of climate change impact assessment and the associated uncertainty propagation. The scheme comprehensively considers and quantifies uncertainties associated with the climate change scenarios, the climate model REMO, downscaling and the hydrological model. Further uncertainties associated with input data have either been discussed qualitatively or translated into parameter uncertainties and therefore been considered in the quantitative assessment. The developed SNR_m index allows the comparison and ranking of different of sources of uncertainty. Furthermore it can be used to identify research needs. The SNRm and the Likelihood terminology allowed assessing the confidence in the model structure and scenario trends as well as a relative probability of certain outcomes, and thereby complemented each other.

The use of multi-model climate data and multiple hydrological models could complete the comprehensive approach outlined in this study and provide further insight on uncertainty ranges in climate change impact studies.

Objective 5: Quantitative assessment of the catchments water budget and the respective uncertainties on a monthly timescale

Considering data availability and aim of the study, a monthly resolution of model results seemed adequate. In this study a detailed water balance for the Upper Drâa catchment was presented. The buffer effect of the snowpacks was quantified and it was found that a net amount of 63 Mm^3 of water is released from snow storage during the main irrigation season from March through May. The second finding is that baseflow driven discharge during spring is an important source for irrigation water, it sums up to 72-90 Mm^3, with roughly one third coming from the slow responding, hence more reliable second aquifer in the karstic regions. Oases that depend on these aquifers (M'Semrir, Boulmalene, Kelaat and partly Ouarzazate) can on average satisfy their irrigation demand to roughly three quarters from stream discharge. On the other hand the model has difficulties in representing the irrigation in the groundwater-dependent oases Toundout and Skoura. The hydrological model is characterized by relatively high uncertainties in its structure, input data and parameterization. The most sensitive model parameters are soil depth, Curve Number, and the recharge fraction of the second aquifer. All three parameters are highly uncertain as well; therefore further research should focus on the establishment of more robust data and/or the implementation of more physical based model routines.

Objective 6: Quantitative assessment of average climate change induced changes of the catchments water budget and the respective uncertainties on a monthly timescale

The uncertainties inherent to the hydrological model propagate in the climate change impact assessment. The developed SNR_m proved as very helpful in analyzing uncertainties deriving from different sources. While the different downscaling approaches do hardly affect model results and the different climate scenarios and ensembles converge at least for the 2030s period, uncertainties founded in the hydrological model limit the explanatory power of the scenario runs. Nevertheless, some robust findings can be stated for the period 2020-2049; it is likely that precipitation will be reduced by 11% and snowfall will be reduced by 31% compared to the baseline period (1978-2007). These changes propagate amplified through the hydrological system, a reduction of fast runoff components by 13% and of baseflow by 18% is likely. Since the drying is more pronounced in the rainy season, irrigation in the surface

water fed Upper Drâa oases is barely threatened. A reduction of irrigation volumes by only 5% is likely. A different situation arises in the Middle Drâa valley, as reservoir inflow is likely to decrease by 17%.

A further challenge to water managers is the siltation of the reservoir. Under climate change conditions and the business-as-usual-scenario the threshold of reasonable reservoir operation is likely to be exceeded by 2037. Assuming different pathways of development, this could already be the case in 2030 (scenario M1) or 2042 (scenario M2).

It has to be noted that the development of model routines that allow for the consideration of future reservoirs, for example by delineating required parameters from the DEM, is the next sensible step for developing this model into a decision support tool. The construction of several large scale reservoirs in Morocco is foreseen (El Maâroufi 2012). An example is the construction of an reservoir at the village of Tiouine, corresponding to the discharge gauge location of Tamdroust that has begun in 2010 and is foreseen to be completed in 2013/14 (Government of Morocco 2010). The reservoirs function is, besides flood control, to supply drinking water to the city of Ouarzazate. Further planning includes the irrigation of new agricultural perimeters at Timadline (1600 ha; Government of Morocco 2010; DRPE 1998), with an estimated mean annual irrigation demand of 10 Mm^3. Until now the inclusion of the reservoir into the hydrological model is fraught by several factors. The hydrological model performs very poor at the gauge of Tamdroust, as presented in section 5.5.2. Furthermore essential data on sedimentation rates and evaporation losses are not yet available.

Summary

A comprehensive climate change impact assessment study on the hydrological processes and specifically on surface water availability was successfully conducted at the regional scale (14,988 km^2) using a conceptual model adapted to the characteristics of a semi-arid mountainous environment. A wide-ranging uncertainty assessment scheme covering uncertainties from input data, the hydrological model, climate model data and downscaling methods has been developed and applied. It has been shown that climate change effects for the period 2000-2029 are subject to considerable uncertainties and no clear trends could be identified. Despite a significant decrease in snowfall and spring precipitation for the period 2020-2049, water availability in the surface water dependent oasis remains high enough to sustain agriculture to the current extent. Opposing, water availability at the reservoir is likely to decrease disproportionately high. Therefore the potential for riparian conflicts between the Upper Drâa and the Middle Drâa might augment. Robust metrics have been applied to quantify these future changes and their likelihood, to provide tools for local water managers.

Bibliography

Abbaspour, K.C., Johnson, C.A. & van Genuchten, M.T., 2004. Estimating Uncertain Flow and Transport Parameters Using a Sequential Uncertainty Fitting Procedure. *Vadose Zone J*, 3(4), p.1340–1352.

Abbaspour, K.C., Yang, J., Maximov, I., Siber, R., Bogner, K., Mieleitner, J., Zobrist, J. & Srinivasan, R., 2007. Modelling hydrology and water quality in the pre-alpine/alpine Thur watershed using SWAT. *Journal of Hydrology*, 333(2–4), p.413–430.

Abbaspour, K.C., Yang, J.J., Reichert, P., Vejdani, M., Haghighat, S. & Srinivasan, R., 2008. SWAT-CUP. SWAT Calibration and Uncertainty Programs. User Manual.

Abbott, M.B., Bathurst, J.C., Cunge, J.A., O'Connell, P.E. & Rasmussen, J., 1986a. An introduction to the European Hydrological System -- Systeme Hydrologique Europeen, "SHE", 1: History and philosophy of a physically-based, distributed modelling system. *Journal of Hydrology*, 87(1-2), p.45–59.

Abbott, M.B., Bathurst, J.C., Cunge, J.A., O'Connell, P.E. & Rasmussen, J., 1986b. An introduction to the European Hydrological System -- Systeme Hydrologique Europeen, "SHE", 2: Structure of a physically-based, distributed modelling system. *Journal of Hydrology*, 87(1-2), p.61–77.

Abbott, M.B. & Refsgaard, J.C., 1996. *Distributed hydrological modelling*, Dordrecht: Kluwer.

Abdalla, O.A.E., 2008. Groundwater discharge mechanism in semi-arid regions and the role of evapotranspiration. *Hydrological Processes*, 22(16), p.2993–3009.

Abrahams, A.D., Parsons, A.J. & Wainwright, J., 1994. Resistance to overland flow on semiarid grassland and shrubland hillslopes, Walnut Gulch, southern Arizona. *Journal of Hydrology*, 156(1-4), p.431–446.

Adam, J.C., Hamlet, A.F. & Lettenmaier, D.P., 2009. Implications of global climate change for snowmelt hydrology in the twenty-first century. *Hydrological Processes*, 23(7), p.962–972.

Allen, R.G., Jensen, M.E., Wright, J.L. & Burman, R.D., 1989a. Operational Estimates of Reference Evapotranspiration. *Agronomy Journal*, 81(4), p.650–662.

Allen, R.G., Pereira, L.S., Raes, S. & Smith, M., 1989b. *Crop evapotranspiration: guidelines for computing crop water requirements*, Rome: FAO.

Alley, W.M., Healy, R.W., LaBaugh, J.W. & Reilly, T.E., 2002. Flow and storage in groundwater systems. *Science*, 296(5575), p.1985–1990.

Amit, H., Lyakhovsky, V., Katz, A., Starinsky, A. & Burg, A., 2002. Interpretation of spring recession curves. *Ground Water*, 40(5), p.543–551.

Arboleya, M., Babault, J., Owen, L.A., Teixell, A. & Finkel, R.C., 2008. Timing and nature of Quaternary fluvial incision in the Ouarzazate foreland basin, Morocco. *Journal of the Geological Society*, 165(6), p.1059–1073.

Archer, N.A.L., Quinton, J.N. & Hess, T.M., 2002. Below-ground relationships of soil texture, roots and hydraulic conductivity in two-phase mosaic vegetation in South-east Spain. *Journal of Arid Environments*, 52(4), p.535–553.

Arnau-Rosalén, E., Calvo-Cases, A., Boix-Fayos, C., Lavee, H. & Sarah, P., 2008. Analysis of soil surface component patterns affecting runoff generation. An example of methods applied to Mediterranean hillslopes in Alicante (Spain). *Geomorphology*, 101(4), p.595–606.

Arnold, J.G., Allen, P.M. & Bernhardt, G., 1993. A Comprehensive Surface-Groundwater Flow Model. *Journal of Hydrology*, 142(1-4), p.47–69.

ASCE, 1993. Criteria for evaluation of watershed models. *Journal of Irrigation and Drainage Engineering*, 119, p.429–442.

Asner, G., Scurlock, J. & Hicke, J., 2003. Global synthesis of leaf area index observations: implications for ecological and remote sensing studies. *Global Ecology and Biogeography*, 12(3), p.191–205.

Atkinson, T.C., 1977. Diffuse flow and conduit flow in limestone terrain in the Mendip Hills, Somerset (Great Britain). *Journal of Hydrology*, 35(1-2), p.93–110.

Awad, H., 1963. Some Aspects of the Geomorphology of Morocco Related to the Quaternary Climate. *The Geographical Journal*, 129(2), p.129–139.

Di Baldassarre, G. & Montanari, A., 2009. Uncertainty in river discharge observations: a quantitative analysis. *Hydrol. Earth Syst. Sci.*, 13(6), p.913–921.

Baret, F., Hagolle, O., Geiger, B., Bicheron, P., Miras, B., Huc, M., Berthelot, B., Nino, F., Weiss, M., Samain, O., Roujean, J. & Leroy, M., 2007. LAI, fAPAR and fCover CYCLOPES global products derived from VEGETATION - Part 1: Principles of the algorithm. *Remote sensing of environment*, 110(3), p.275–286.

Barrow, C.. & Hicham, H., 2000. Two complimentary and integrated land uses of the western High Atlas Mountains, Morocco: the potential for sustainable rural livelihoods. *Applied Geography*, 20(4), p.369–394.

Bates, B.C., Kundzewicz, Z.W., Wu, S. & Palutikof, J.P., 2008. *Climate change and water*, Geneva: IPCC Secretariat.

Bates, P.D. & De Roo, A.P.J., 2000. A simple raster-based model for flood inundation simulation. *Journal of Hydrology*, 236(1-2), p.54–77.

Bathurst, J.C. & Cooley, K.R., 1996. Use of the SHE hydrological modelling system to investigate basin response to snowmelt at Reynolds Creek, Idaho. *Journal of Hydrology*, 175(1-4), p.181–211.

Baumann, G., 2009. *How to assess rangeland condition in semiarid ecosystems? The indicative value of vegetation in the High Atlas Mountains, Morocco*. PhD-Thesis. University of Cologne. Available at: http://kups.ub.uni-koeln.de/2869/ [Accessed June 4, 2012].

Bayard, D. & Stähli, M., 2005. Effects of frozen soil on the groundwater recharge in alpine areas. In C. de Jong, D. Collins, & R. Ranzi, eds. *Climate and hydrology in mountain areas*. pp. 73–83.

Becker, A. & Serban, P., 1990. *Hydrological models for water-resources system design and operation*, Geneva: World Meteorological Organization.

Beven, K., 2006. A manifesto for the equifinality thesis. *Journal of Hydrology*, 320(1-2), p.18–36.

Beven, K., 1989. Changing ideas in hydrology -- The case of physically-based models. *Journal of Hydrology*, 105(1-2), p.157–172.

Beven, K., 2008. *Environmental Modelling: An Uncertain Future?: An Introduction to Techniques for Uncertainty Estimation in Environmental Prediction* 1st ed., London: Taylor & Francis.

Beven, K., 1995. Linking parameters across scales: Subgrid parameterizations and scale dependent hydrological models. *Hydrological Processes*, 9(5-6), p.507–525.

Beven, K., 1993. Prophecy, reality and uncertainty in distributed hydrological modelling. *Advances in Water Resources*, 16, p.41–41.

Beven, K., 2003. *Rainfall Runoff Modelling: The Primer*, Chichester: Wiley.

Beven, K., 2002. Towards a coherent philosophy for modelling the environment. *Proceedings of the Royal Society of London. Series A: Mathematical, Physical and Engineering Sciences*, 458, p.2465–2484.

Beven, K. & Binley, A., 1992. The future of distrtributed models - Model calibration and uncertainty prediction. *Hydrological Processes*, 6(3), p.279–298.

Beven, K. & Freer, J., 2001. Equifinality, data assimilation, and uncertainty estimation in mechanistic modelling of complex environmental systems using the GLUE methodology. *Journal of Hydrology*, 249(1-4), p.11–29.

Beven, K.J. & Kirkby, M.J., 1979. A physically based, variable contributing area model of basin hydrology. *Hydrological Sciences Bulletin*, 24(1), p.43–69.

Blöschl, G. & Sivapalan, M., 1995. Scale issues in hydrological modelling: A review. *Hydrological Processes*, 9(3-4), p.251–290.

Bormann, H., 2005. Regional hydrological modelling in Benin (West Africa): Uncertainty issues versus scenarios of expected future environmental change. *Physics and Chemistry of the Earth, Parts A/B/C*, 30(8-10), p.472–484.

Born, K., Christoph, M., Fink, A.H., Knippertz, P., Paeth, H. & Speth, P., 2008. Moroccan Climate in the Present and Future: Combined View from Observational Data and Regional Climate Scenarios. In F. Zereini & H. Hötzl, eds. *Climatic Changes and Water Resources in the Middle East and in North Africa*. Wien: Springer, p. 552.

Boronina, A., Golubev, S. & Balderer, W., 2005. Estimation of actual evapotranspiration from an alluvial aquifer of the Kouris catchment (Cyprus) using continuous streamflow records. *Hydrological Processes*, 19, p.4055–4068.

Bos, M.G. & Nugteren, J., 1990. *On irrigation efficiencies*, Wageningen: ILRI.

Boussinesq, J., 1903. Recherches théoriques sur l'écoulement des nappes d'eau infiltrées dans le sol et sur le débit des sources. *Comptes Rendus Acad. Sci./J. Math. Pures Appl*, 10, p.5–78.

Box, G.E.P. & Draper, N.R., 1987. *Empirical Model-Building and Response Surfaces*, Chichester: Wiley.

Brakensiek, D.L. & Rawls, W.J., 1994. Soil containing rock fragments: effects on infiltration. *Catena*, 23(1-2), p.99–110.

Brancic, R., 1968. *Sols de la palmeraie Fezouata.*, Ouarzazate: Organistaion de mise en valeur agricole.

Bravo, D.N., Araújo, M.B., Lasanta, T. & Moreno, J.I.L., 2008. Climate Change in Mediterranean Mountains during the 21st Century. *AMBIO: A Journal of the Human Environment*, 37(4), p.280–285.

Breshears, D.D. & Barnes, F.J., 1999. Interrelationships between plant functional types and soil moisture heterogeneity for semiarid landscapes within the grassland/forest continuum: a unified conceptual model. *Landscape Ecology*, 14(5), p.465–478.

Brown, R.H., Konoplyanstev, A.A., Ineson, J. & Kovalevsky, V.S., 1972. *Groundwater Studies. An International Guide for Research and Practice*, Paris: Unesco.

Bryssine, G. & Billaux, P., 1967. Les sols du Maroc Ministère de l'Agriculture et de la Réforme Agraire, ed. *Cahiers de la recherche agronomique*, 24, p.59–101.

Busche, H., 2008a. Hydrology of the Drâa Basin. In O. Schulz & M. Judex, eds. *IMPETUS Atlas Morocco. Research Results 2000–2007*. Department of Geography, University of Bonn, Germany., pp. 43–44.

Busche, H., 2005. *Modellierung hydrologischer und erosiver Prozesse im Terou-Einzugsgebiet (Benin) unter der Annahme von Landnutzungs-und Klimaänderung*. Diploma Thesis. University of Bonn.

Busche, H., 2008b. The Reservoir Mansour Eddahbi and its Tributaries. In O. Schulz & M. Judex, eds. *IMPETUS Atlas Morocco. Research Results 2000–2007*. Department of Geography, University of Bonn, Germany., pp. 47–48.

Canadell, J., Jackson, R., Ehleringer, J., Mooney, H., Sala, O. & Schulze, E., 1996. Maximum rooting depth of vegetation types at the global scale. *OECOLOGIA*, 108(4), p.583–595.

Canadell, J., Le Quere, C., Raupach, M., Field, C., Buitenhuis, E., Ciais, P., Conway, T., Gillett, N., Houghton, R. & Marland, G., 2007. Contributions to accelerating atmospheric CO2 growth from economic activity, carbon intensity, and efficiency of natural sinks. *Proceedings of the National Academy of Sciences of the United States of America*, 104(47), p.18866–18870.

Cao, W.Z., Bowden, W.B., Davie, T. & Fenemor, A., 2006. Multi-variable and multi-site calibration and validation of SWAT in a large mountainous catchment with high spatial variability. *Hydrological Processes*, 20(5), p.1057–1073.

Cappy, S., 2006. *Hydrogeological Characterization of the Upper Drâa Catchment: Morocco*. PhD-Thesis. University of Bonn. Available at: http://hss.ulb.uni-bonn.de/2007/0963/0963.htm [Accessed June 4, 2012].

Carter, T.R., Hulme, M. & Lal, M., 1999. *Guidelines on the use of scenario data for climate impact and adaptation assessment*, IPCC, Task Group on Scenarios for Impact Assessment.

Casenave, A. & Valentin, C., 1992. A runoff capability classification system based on surface features criteria in semi-arid areas of West Africa. *Journal of Hydrology*, 130(1–4), p.231–249.

Castillo, V., Gómez-Plaza, A. & Martínez-Mena, M., 2003. The role of antecedent soil water content in the runoff response of semiarid catchments: a simulation approach. *Journal of Hydrology*, 284(1–4), p.114–130.

Cataldo, J., Behr, C. & Montalto, F., 2004. *A Summary of Published Reports of Transmission Losses in Ephemeral Streams in the U.S.*, National Center for Housing and the Environment.

Cavallar, W., 1950. *Esquisse Préliminaire de la Carte des Sols du Maroc. 1:1,500,000*, Rabat: Direction de l'Agriculture, du Commerce et des Forêts du Maroc. Division de l'Agriculture et de l'Elevage.

Cerdà, A., 1996. Seasonal variability of infiltration rates under contrasting slope conditions in southeast Spain. *Geoderma*, 69(3–4), p.217–232.

Chaponnière, A., Boulet, G., Chehbouni, A. & Aresmouk, M., 2008. Understanding hydrological processes with scarce data in a mountain environment. *Hydrological Processes*, 22, p.1908–1921.

Chen, X., Chen, D. & Chen, X., 2006. Simulation of baseflow accounting for the effect of bank storage and its implication in baseflow separation. *Journal of Hydrology*, 327(3-4), p.539–549.

Chen, X. & Chen, X., 2003. Stream water infiltration, bank storage, and storage zone changes due to stream-stage fluctuations. *Journal of Hydrology*, 280(1-4), p.246–264.

Childs, C., 2001. *The Secret Knowledge of Water: There Are Two Easy Ways to Die in the Desert: Thirst and Drowning*, New York: Back Bay Books.

Christmann, D. & Sonntag, C., 1987. Groundwater evaporation from East-Saharian depressions by means of deuterium and oxygen-18 in soil moisture. In *Isotope techniques in water resources development: proceedings of an International Symposium on the Use of Isotope Techniques in Water Resources Development*. pp. 189–204.

Christoph, M., Fink, A.H., Paeth, H., Born, K., Kerschgens, M. & Piecha, K., 2010a. Climate Scenarios. In P. Speth, M. Christoph, & B. Diekkrüger, eds. *Impacts of Global Change on the Hydrological Cycle in West and Northwest Africa*. Berlin: Springer, pp. 402–425.

Christoph, M., Reichert, B. & Jäger, A., 2010b. Scenarios. In P. Speth, M. Christoph, & B. Diekkrüger, eds. *Impacts of Global Change on the Hydrological Cycle in West and Northwest Africa*. Berlin: Springer, pp. 394–396.

CIA, 2009.The World Factbook Available at: https://www.cia.gov/library/publications/the-world-factbook/ [Accessed December 29, 2009].

Ciarapica, L. & Todini, E., 2002. TOPKAPI: a model for the representation of the rainfall-runoff process at different scales. *Hydrological Processes*, 16(2), p.207–229.

Cooke, R.U., Warren, A. & Goudie, A., 1993. *Desert geomorphology*, London: Taylor & Francis.

Coudrain-Ribstein, A., Pratx, B., Talbi, A. & Jusserand, C., 1998. L'evaporation des nappes phreatiques sous climat aride est-elle independante de la nature du sol? *Comptes Rendus de l'Académie des Sciences - Series II. Fascicule a-Sciences De La Terre Et Des Planetes*, 326, p.159–166.

Daniel, J.A. & Staricka, J.A., 2000. Frozen soil impact on ground water-surface water interaction. *Journal of the American Water Resources Association*, 36(1), p.151–160.

Davis, D.K., 2005. Indigenous knowledge and the desertification debate: problematising expert knowledge in North Africa. *Geoforum*, 36(4), p.509–524.

DGH, 1988. *Etude de la gestion de retenues de barrages - Rapport de synthese*, Rabat: Direction Generale Hydrologique.

Diekkrüger, B., 1996. SIMULAT-ein Modellsystem zur Berechnung der Wasser-und Stoffdynamik landwirtschaftlich genutzter Standorte. In O. Richter, D. Söndgerath, & B. Diekkrüger, eds. *Sonderforschungsbericht 179. Wasser- und Stoffdynamik in Agrarökosystemen. Abschlussbericht Band 1*. Landschaftsökologie und Umweltforschung. pp. 30–47.

Dillon, P., 2005. Future management of aquifer recharge. *Hydrogeology Journal*, 13(1), p.313–316.

Dodson, R. & Marks, D., 1997. Daily air temperature interpolated at high spatial resolution over a large mountainous region. *Climate Research*, 8(1), p.1–20.

Doukkali, M.R., 2005. Water institutional reforms in Morocco. *Water Policy*, 7(11), p.71–88.

Douma, M., Ouahid, Y., Campo, F.F. del, Loudiki, M., Mouhri, K. & Oudra, B., 2009. Identification and quantification of cyanobacterial toxins (microcystins) in two Moroccan drinking-water reservoirs (Mansour Eddahbi, Almassira). *Environmental Monitoring and Assessment*, 160(1-4), p.439–450.

Downer, C.W. & Ogden, F.L., 2004. Appropriate vertical discretization of Richards' equation for two-dimensional watershed-scale modelling. *Hydrological Processes*, 18(1), p.1–22.

DREF, 2007. *Elaboration du dossier de base pour le'etude d'amenagement en amont du barrage D'Mansour Eddahbi. Analyse du milieu biophysique. Rapport Principal.*, Rabat: Direction Regionale des eaux et forets du sud ouest.

DRPE, 1998. *Etude de plan Directeur De l'amenagement des eaux des bassins sud-atlasiques*, Rabat: Direction de la recherche et de la planification de l'eau.

Dunkerley, D., 2008. Bank permeability in an Australian ephemeral dry-land stream: variation with stage resulting from mud deposition and sediment clogging. *Earth Surface Processes and Landforms*, 33(2), p.226–243.

Easton, Z.M., Fuka, D.R., Walter, M.T., Cowan, D.M., Schneiderman, E.M. & Steenhuis, T.S., 2008. Re-conceptualizing the soil and water assessment tool (SWAT) model to predict runoff from variable source areas. *Journal of Hydrology*, 348(3–4), p.279–291.

Eckhardt, K., Haverkamp, S., Fohrer, N. & Frede, H.-G., 2002. SWAT-G, a version of SWAT99.2 modified for application to low mountain range catchments. *Physics and Chemistry of the Earth, Parts A/B/C*, 27(9–10), p.641–644.

EI-Hames, A.S. & Richards, K.S., 1994. Progress in arid-lands rainfall-runoff modelling. *Progress in Physical Geography*, 18(3), p.343–365.

El Harfi, A. El Harfi, Lang, J. Lang, Salomon, J. Salomon, Chellai & E. Chellai, 2001. Cenozoic sedimentary dynamics of the Ouarzazate foreland basin (Central High Atlas Mountains, Morocco). *International Journal of Earth Sciences*, 90(2), p.393–411.

El Maâroufi, M., 2012. Maroc : 130 barrages et 14 autres en cours de construction. *La vie éco 02.02.2012*.

Faiz, M.E. & Ruf, T., 2010. An Introduction to the Khettara in Morocco: Two Contrasting Cases. In G. Schneier-Madanes & M.-F. Courel, eds. *Water and Sustainability in Arid Regions*. Dordrecht: Springer Netherlands, pp. 151–163.

Falkenmark, M., 1989. The massive water scarcity now threatening Africa: why isn't it being addressed? *Ambio*, 18(2), p.112–118.

FAO, 2011.AQUASTAT Database Available at: http://www.fao.org/nr/water/aquastat/main/index.stm [Accessed August 16, 2011].

FAO, 2009. *Harmonized World Soil Database (version 1.1).*, Rom: FAO.

FAO, 1998. *World reference base for soil resources*, Rom: FAO.

Faramarzi, M., Abbaspour, K.C., Schulin, R. & Yang, H., 2009. Modelling blue and green water resources availability in Iran. *Hydrological Processes*, 23(3), p.486–501.

Farquharson, F.A.K., Meigh, J.R. & Sutcliffe, J.V., 1992. Regional flood frequency analysis in arid and semi-arid areas. *Journal of Hydrology*, 138(3-4), p.487–501.

Farr, T.G. & Kobrick, M., 2000. Shuttle Radar Topography Mission produces a wealth of data. *Eos*, 81(48), p.583–585.

Finckh, M., 2008. Vegetation map of the Drâa catchment. In O. Schulz & M. Judex, eds. *IMPETUS Atlas Morocco. Research Results 2000–2007*. Bonn: Department of Geography, University of Bonn, Germany., pp. 31–32.

Fink, A., Piech, K., Brücher, T. & Knippertz, P., 2008. Precipitation Variability in Northwest Africa. In O. Schulz & M. Judex, eds. *IMPETUS Atlas Morocco. Research Results 2000–2007*. Bonn: Department of Geography, University of Bonn, Germany., pp. 11–12.

Fink, A.H. & Knippertz, P., 2003. An extreme precipitation event in southern Morocco in spring 2002 and some hydrological implications. *Weather*, 58, p.377–392.

Flerchinger, G.N. & Cooley, K.R., 2000. A ten-year water balance of a mountainous semi-arid watershed. *Journal of Hydrology*, 237(1-2), p.86–99.

Flerchinger, G.N., Cooley, K.R. & Ralston, D.R., 1992. Groundwater response to snowmelt in a mountainous watershed. *Journal of Hydrology*, 133(3-4), p.293–300.

Fleury, P., Ladouche, B., Conroux, Y., Jourde, H. & Dörfliger, N., 2009. Modelling the hydrologic functions of a karst aquifer under active water management–The Lez spring. *Journal of Hydrology*, 365(3-4), p.235–243.

Fleury, P., Plagnes, V. & Bakalowicz, M., 2007. Modelling of the functioning of karst aquifers with a reservoir model: Application to Fontaine de Vaucluse (South of France). *Journal of Hydrology*, 345(1-2), p.38–49.

Flügel, W.-A., 1995. Delineating hydrological response units by geographical information system analyses for regional hydrological modelling using PRMS/MMS in the drainage basin of the River Bröl, Germany. *Hydrological Processes*, 9(3-4), p.423–436.

Foley, A.M., 2010. Uncertainty in regional climate modelling: A review. *Progress in Physical Geography*, 34(5), p.647 –670.

Fontaine, T.A., Cruickshank, T.S., Arnold, J.G. & Hotchkiss, R.H., 2002. Development of a snowfall-snowmelt routine for mountainous terrain for the soil water assessment tool (SWAT). *Journal of Hydrology*, 262(1-4), p.209–223.

Foody, G.M., Ghoneim, E.M. & Arnell, N.W., 2004. Predicting locations sensitive to flash flooding in an arid environment. *Journal of Hydrology*, 292(1-4), p.48–58.

Foster, S.S.. & Perry, C.J., 2010. Improving groundwater resource accounting in irrigated areas: a prerequisite for promoting sustainable use. *Hydrogeology Journal*, 18(1-4), p.291–294.

Freeze, A.R. & Cherry, J.A. eds., 1979. *Groundwater* 5th ed., Upper Saddle River: Prentice Hall.

Freier, K.P., Bruggemann, R., Scheffran, J., Finckh, M. & Schneider, U.A., 2012. Assessing the predictability of future livelihood strategies of pastoralists in semi-arid Morocco under climate change. *Technological Forecasting and Social Change*, 79(2), p.371–382.

Fritzsche, P., 2011. *Development of a satellite-based dynamic regional vegetation model for the Drâa catchment*. PhD-Thesis. University of Bonn. Available at: http://hss.ulb.uni-bonn.de/2011/2407/2407.htm [Accessed July 26, 2011].

Garen, D.C. & Moore, D.S., 2005. Curve Number hydrology in water quality modeling: uses, abuses and future directions. *JAWRA Journal of the American Water Resources Association*, 41(2), p.377–388.

Garratt, J.R., 1993. Sensitivity of Climate Simulations to Land-Surface and Atmospheric Boundary-Layer Treatments-A Review. *Journal of Climate*, 6(3), p.419–448.

Gee, G.W. & Hillel, D., 1988. Groundwater recharge in arid regions: Review and critique of estimation methods. *Hydrological Processes*, 2(3), p.255–266.

Gerrard, J., 1990. *Mountain environments*, Boston: MIT Press.

Gerrard, J., 1992. *Soil geomorphology*, Berlin: Springer.

Gheith, H. & Sultan, M., 2002. Construction of a hydrologic model for estimating Wadi runoff and groundwater recharge in the Eastern Desert, Egypt. *Journal of Hydrology*, 263(1-4), p.36–55.

Global Land Cover Facility, 2006.Schuttle Radar Topography Mission 3 Arc Second Scenes Available at: http://glcf.umiacs.umd.edu/data/srtm/ [Accessed July 13, 2009].

Goodrich, D.C., Faurès, J.-M., Woolhiser, D.A., Lane, L.J. & Sorooshian, S., 1995. Measurement and analysis of small-scale convective storm rainfall variability. *Journal of Hydrology*, 173(1-4), p.283–308.

Goodrich, D.C., Lane, L.J., Shillito, R.M. & Miller, S.N., 1997. Linearity of basin response as a function of scale in a semiarid watershed. *Water Resources Research*, 33(12), p.2951–2965.

Government of Morocco, 2010.Actualités du Maroc Available at: http://www.maroc.ma/PortailInst/An/Actualites/HM+the+King+chairs+in+Ouarzazate+signing+ceremony+of+agreements+finalizing+institutional+framework+o.htm [Accessed March 29, 2012].

Granger, R.J., Gray, D.M. & Dyck, G.E., 1984. Snowmelt infiltration to frozen prairie soils. *Canadian Journal of Earth Sciences*, 23(6), p.669–677.

Grayson, R. & Blöschl, G. eds., 2001. *Spatial patterns in catchment hydrology*, Cambridge: Cambridge University Press.

Green, C.H. & van Griensven, A., 2008. Autocalibration in hydrologic modeling: Using SWAT2005 in small-scale watersheds. *Environmental Modelling & Software*, 23(4), p.422–434.

Gresens, F., 2006. *Untersuchungen zum Wasserhaushalt ausgewählter Pflanzenarten im Draa-Tal - Südost Marokko*, University of Bonn.

van Griensven, A. & Meixner, T., 2007. A global and efficient multi-objective auto-calibration and uncertainty estimation method for water quality catchment models. *Journal of Hydroinformatics*, 9(4), p.277–291.

van Griensven, A., Meixner, T., Grunwald, S., Bishop, T., Diluzio, M. & Srinivasan, R., 2006. A global sensitivity analysis tool for the parameters of multi-variable catchment models. *Journal of Hydrology*, 324(1-4), p.10–23.

Griffiths, G.A. & Clausen, B., 1997. Streamflow recession in basins with multiple water storages. *Journal of Hydrology*, 190(1-2), p.60–74.

Güntner, A. & Bronstert, A., 2004. Representation of landscape variability and lateral redistribution processes for large-scale hydrological modelling in semi-arid areas. *Journal of Hydrology*, 297(1-4), p.136–161.

Güntner, A., Uhlenbrook, S., Seibert, J. & Leibundgut, C., 1999. Multi-criterial validation of TOPMODEL in a mountainous catchment. *Hydrological Processes*, 13(11), p.1603–1620.

Haase, P., Pugnaire, F., Fernandez, E., Puigdefabregas, J., Clark, S. & Incoll, L., 1996. An investigation of rooting depth of the semiarid shrub Retama sphaerocarpa (L) Boiss by labelling of ground water with a chemical tracer. *Journal of Hydrology*, 177(1-2), p.23–31.

Hák, T. & Moldan, B., 2007. *Sustainability indicators: a scientific assessment*, Washington: Island Press.

Harbaugh, A.W., Banta, E.R., Hill, M.C. & McDonald, M.G., 2000. *MODFLOW-2000, The U. S. Geological Survey Modular Ground-Water Model-User Guide to Modularization Concepts and the Ground-Water Flow Process*,

Hargreaves, G.H. & Samani, Z.A., 1985. Reference crop evapotranspiration from temperature. *Applied Engineering in Agriculture*, 1(2), p.96–99.

Harmel, R. & Smith, P., 2007. Consideration of measurement uncertainty in the evaluation of goodness-of-fit in hydrologic and water quality modeling. *Journal of Hydrology*, 337(3-4), p.326–336.

Harmel, R.D., Cooper, R.J., Slade, R.M., Haney, R.L. & Arnold, J.G., 2006. Cumulative uncertainty in measured streamflow and water quality data for small watersheds. *Transactions of the ASAE. American Society of Agricultural Engineers*, 49(3), p.689–701.

Hawkins, R.H., Ward, T.J., Woodward, D.E. & Mullem, J.A.V. eds., 2009. *Curve number hydrology: state of the practice*, Reston: ASCE Publications.

Hazell, P.B.R., Oram, P. & Chaherli, N., 2001. *Managing droughts in the low-rainfall areas of the Middle East and North Africa*, Washington: International Food Policy Research Institute.

Healy, R. & Cook, P., 2002. Using groundwater levels to estimate recharge. *Hydrogeology Journal*, 10(1), p.91–109.

Heidecke, C., 2009. *Economic analysis of water use and management in the Middle Draa valley in Morocco*. PhD-Thesis. University of Bonn. Available at: http://hss.ulb.uni-bonn.de/2010/2022/2022.htm [Accessed June 4, 2012].

Heidecke, C., 2006. *Production agricole dans la vallée du Dadès. Evaluation d'une enquête agro économique*, unpublished working paper.

Heim, R.R., 2002. A review of twentieth-century drought indices used in the United States. *Bulletin of the American Meteorological Society*, 83(8), p.1149–1166.

Henderson-Sellers, A., 1993. An antipodean climate of uncertainty? *Climatic Change*, 25(3), p.203–224.

Hennig, H. & Schwarze, R., 2001. Geohydraulische Interpretation des Konzeptmodells Einzellinearspeicher und Konsequenzen für die Modellierung des Grundwasserabflusses. *Wasserwirtschaft*, 90(1), p.42–48.

Herbst, M., Diekkrüger, B. & Vanderborght, J., 2006. Numerical experiments on the sensitivity of runoff generation to the spatial variation of soil hydraulic properties. *Journal of Hydrology*, 326(1–4), p.43–58.

Hernandez, M., Miller, S.N., Goodrich, D.C., Goff, B.F., Kepner, W.G., Edmonds, C.M. & Jones, K.B., 2000. Modeling Runoff Response to Land Cover and Rainfall Spatial Variability in Semi-Arid Watersheds. *Environmental Monitoring and Assessment*, 64, p.285–298.

Hiepe, C., 2008. *Soil degradation by water erosion in a sub-humid West-African catchment: a modelling approach considering land use and climate change in Benin*. PhD-Thesis. University of Bonn. Available at: http://hss.ulb.uni-bonn.de/2008/1628/1628.htm [Accessed June 4, 2012].

Hock, R., 2003. Temperature index melt modelling in mountain areas. *Journal of Hydrology*, 282(1-4), p.104–115.

Hofmann, H., 2002. *Geologische Kartierung und hydrogeologische Bewertung der IMPETUS-Testfläche Ameskar, Region MGoun, südlicher Hoher Atlas, Marokko. Unveröffentlicht*. Diploma Thesis. University of Bonn.

Horton, R.E., 1933. The role of infiltration in the hydrologic cycle. *Trans. Am. Geophys. Union*, 14, p.446–460.

Le Houérou, H., 2001. Biogeography of the arid steppeland north of the Sahara. *Journal of Arid Environments*, 48(2), p.103–128.

Le Houérou, H., 1996. Climate change, drought and desertification. *Journal of Arid Environments*, 34(2), p.133–185.

Hughes, D.A., 1995. Monthly rainfall-runoff models applied to arid and semiarid catchments for water resource estimation purposes. *Hydrological Sciences Journal-Journal Des Sciences Hydrologiques*, 40(6), p.751–770.

Hughes, D.A., 1994. Soil moisture and runoff simulations using four catchment rainfall-runoff models. *Journal of Hydrology*, 158(3-4), p.381–404.

Hughes, P., Woodward, J. & Gibbard, P., 2006. Quaternary glacial history of the Mediterranean mountains. *Progress in Physical Geography*, 30(3), p.334–364.

Hulme, M., Doherty, R., Ngara, T., New, M. & Lister, D., 2001. African climate change: 1900-2100. *Climate Research*, 17(2), p.145–168.

Ilahiane, H., 1999. The Berber Agdal Institution: Indigenous Range Management in the Atlas Mountains. *Ethnology*, 38(1), p.21–45.

Jackson, S.I. & Prowse, T.D., 2009. Spatial variation of snowmelt and sublimation in a high-elevation semi-desert basin of western Canada. *Hydrological Processes*, 23(18), p.2611–2627.

Janssen, P.H.M. & Heuberger, P.S.C., 1995. Calibration of process-oriented models. *Ecological Modelling*, 83(1-2), p.55–66.

Jarvis, A., Rubiano, J., Nelson, A., Farrow, A. & Mulligan, M., 2004. Practical use of SRTM data in the tropics: comparisons with digital elevation models generated from cartographic data. *CIAT Working document*, 198, p.32.

Jenny, H., 1941. *Factors of Soil Formation, A System of Quantitative Pedology, 281 pp*, New York: McGraw-Hill.

Jones, R.N., 2000. Managing uncertainty in climate change projections–issues for impact assessment. *Climatic Change*, 45(3), p.403–419.

de Jong, C., Cappy, S., Finckh, M. & Funk, D., 2008. A transdisciplinary Analysis of water problems in the mountainous karst areas of Morocco. *Engineering Geology*, 99, p.228–238.

de Jong, C., Collins, D.N. & Ranzi, R., 2005. *Climate and hydrology in mountain areas*, Chichester: Wiley.

de Jong, C., Machauer, R., Reichert, B., Cappy, S., Viger, R. & Leavesley, G., 2004. An integrated geomorphological and hydrogeological MMS modelling framework for a semi-arid mountain basin in the High Atlas, southern Morocco. In *Complexity and Integrated Resources Management*. 2nd Biennial Meeting of the International Environmental Modelling and Software Society. Manno, pp. 88–900787.

de Jong, C., Makroum, K. & Leavesley, G., 2006. *Developing an oasis-based irrigation management tool for a large semi-arid mountainous catchment in Morocco*,

Jothityangkoon, C., Sivapalan, M. & Farmer, D.L., 2001. Process controls of water balance variability in a large semi-arid catchment: downward approach to hydrological model development. *Journal of Hydrology*, 254(1-4), p.174–198.

Jun, K.S., Chung, E.-S., Sung, J.-Y. & Lee, K.S., 2011. Development of spatial water resources vulnerability index considering climate change impacts. *Science of The Total Environment*, 409(24), p.5228–5242.

Kalma, J. & Franks, S., 2003. Rainfall in arid and semi-arid regions. In I. Simmers, ed. *Understanding water in a dry environment*. London: Taylor & Francis, pp. 15–64.

Kemp, P.R., Reynolds, J.F., Pachepsky, Y. & Chen, J., 1997. A comparative study of soil water dynamics in a desert ecosystem. *Water Resources Research 33: 73*, 33(1), p.73–90.

Kim, N.W., Chung, I.M., Won, Y.S. & Arnold, J.G., 2008. Development and application of the integrated SWAT-MODFLOW model. *Journal of Hydrology*, 356(1-2), p.1–16.

Kite, G.W. & Droogers, P., 2000. Comparing evapotranspiration estimates from satellites, hydrological models and field data. *Journal of Hydrology*, 229(1-2), p.3–18.

Klemeš, V., 1990. Foreword L. Molnár, ed. *Hydrology of mountainous areas. Proceedings of the Rome Symposium*, 190, p.vii.

Klose, A., 2009. *Soil characteristics and soil erosion by water in a semi-arid catchment (Wadi Drâa, South Morocco) under the pressure of global change*. PhD-Thesis. University of Bonn. Available at: http://hss.ulb.uni-bonn.de/2009/1959/1959.htm [Accessed June 4, 2012].

Klose, A., 2008a. Soil properties in the Drâa catchment. In O. Schulz & M. Judex, eds. *IMPETUS Atlas Morocco. Research Results 2000–2007*. Bonn: Department of Geography, University of Bonn, Germany., pp. 33–36.

Klose, A., Busche, H., Klose, S., Schulz, O., Diekkrüger, B., Reichert, B. & Winiger, M., 2010a. Hydrological processes and soil degradation in Southern Morocco. In P. Speth, M. Christoph, & B. Diekkrüger, eds. *Impacts of Global Change on the Hydrological Cycle in West and Northwest Africa*. Springer, Berlin, pp. 198–253.

Klose, S., 2008b. Hydrogeological Map of the Drâa Basin. In O. Schulz & M. Judex, eds. *IMPETUS Atlas Morocco. Research Results 2000–2007*. Bonn: Department of Geography, University of Bonn, Germany., pp. 33–36.

Klose, S., Busche, H., Klose, A., Schulz, O., Diekkrüger, B., Reichert, B. & Winiger, M., 2010b. Impacts of Global Change on water resources and soil salinity in Southern Morocco. In P. Speth, M. Christoph, & B. Diekkrüger, eds. *Impacts of Global Change on the Hydrological Cycle in West and Northwest Africa*. Springer, Berlin, pp. 592–611.

Klose, S., Rademacher, C., Klose, A. & Roth, A., 2008a. Wechselwirkungen zwischen Wassernutzungsstrategien und den Grundwasser- und Bodenverhältnissen im mittleren Drâa-Tal. In M. Christoph, ed. *Achter IMPETUS-Zwischenbericht*. Cologne, pp. 243–253.

Klose, S., Reichert, B. & Lahmouri, A., 2008b. Management options for a sustainable groundwater use in the Middle Drâa Oases under the pressure of climatic changes. In *Climatic Changes and Water Resources in the Middle East and North Africa*. Berlin: Springer, pp. 179–195.

Knighton, A.D. & Nanson, G.C., 2001. An event-based approach to the hydrology of arid zone rivers in the Channel Country of Australia. *Journal of Hydrology*, 254(1-4), p.102–123.

Knippertz, P., Christoph, M. & Speth, P., 2003. Long-term precipitation variability in Morocco and the link to the large-scale circulation in recent and future climates. *Meteorology and Atmosphere Physics*, 83, p.67–88.

Knippertz, P. & Fink, A.H., 2006. Tropische Wolkenfahnen: Ein sichtbares Zeichen von tropisch-extratropischen Wechselwirkungen. *Promet*, 32(3), p.144–153.

Konikow, L.F. & Bredehoeft, J.D., 1992. Ground-water models cannot be validated. *Advances in Water Resources*, 15(1), p.75–83.

Kottek, M., Grieser, J., Beck, C., Rudolf, B. & Rubel, F., 2006. World Map of the Koppen-Geiger climate classification updated. *Meteorologische Zeitschrift*, 15(3), p.259–263.

Kovalevsky, V.S., Kruseman, G.P. & Rushton, K.R., 2004. *Groundwater studies: an international guide for hydrogeological investigations*, Parsi: IHP.

Kristensen, P., 2004. The DPSIR framework. In *Workshop on a comprehensive/detailed assessment of the vulnerability of water resources to environmental change in Africa using river basin approach.* Nairobi: UNEP, p. 10.

Kuczera, G. & Parent, E., 1998. Monte Carlo assessment of parameter uncertainty in conceptual catchment models: the Metropolis algorithm. *Journal of Hydrology*, 211(1-4), p.69–85.

Kutsch, U., 2008. *Modellierung des Wasserhaushaltes in einem semi-ariden Einzugsgebiet im Süden Marokkos*. Unpublished Diploma Thesis. University of Bonn.

Lahlou, A., 1988. The silting of Moroccan Dams. *IN: Sediment Budgets. IAHS Publication*, (174), p.71–78.

Lamb, P.J. & Peppler, R.A., 1987. North Atlantic Oscillation: Concept and an Application. *Bulletin of the American Meteorological Society*, 68(10), p.1218–1225.

Lane, L.J., 1983. Chapter 19: Transmission Losses. In SCS, ed. *National Engineering Handbook, Section 4: Hydrology*. Des Moines: Soil Conservation Service.

Lange, J., 1999. *A non-calibrated rainfall-runoff model for large arid catchments, Nahal Zin, Israel*,

Lange, J., 2005. Dynamics of transmission losses in a large arid stream channel. *Journal of Hydrology*, 306(1-4), p.112–126.

Lange, J., Liebundgut, C. & Schick, A.-P., 2000. The importance of single events in arid zone rainfall-runoff modelling. *Physics and Chemistry of the Earth, Part B: Hydrology, Oceans and Atmosphere*, 25(7-8), p.673–677.

Laville, E., Pique, A., Amrhar, M. & Charroud, M., 2004. A restatement of the Mesozoic Atlasic Rifting (Morocco). *Journal of African Earth Sciences*, 38(2), p.145–153.

Law, J. & Dijk, D.V., 1994. Sublimation as a geomorphic process: A review. *Permafrost and Periglacial Processes*, 5(4), p.237–249.

Legates, D.R. & McCabe, G.J., 1999. Evaluating the Use of "Goodness-of-Fit" Measures in Hydrologic and Hydroclimatic Model Validation. *Water Resources Research*, 35(1), p.233–241.

Lerner, D.N., Issar, A.S. & Simmers, I., 1990. *Groundwater recharge: a guide to understanding and estimating natural recharge*, Hannover: Heise.

Li, M., Ma, Z. & Du, J., 2010. Regional soil moisture simulation for Shaanxi Province using SWAT model validation and trend analysis. *Science China Earth Sciences*, 53(4), p.575–590.

van Liew, M., Arnold, J. & Bosch, D., 2005. Problems and Potential of Autocalibrating a Hydrologic Model. *Transactions of the ASAE*, 48(3), p.1025–1040.

Lightfoot, D.R., 1996. Moroccan khettara: Traditional irrigation and progressive desiccation. *Geoforum*, 27(2), p.261–273.

Lindstrom, G., Johansson, B., Persson, M., Gardelin, M. & Bergstrom, S., 1997. Development and test of the distributed HBV-96 hydrological model. *Journal of Hydrology*, 201(1-4), p.272–288.

Luedeling, E. & Brown, P.H., 2010. A global analysis of the comparability of winter chill models for fruit and nut trees. *International Journal of Biometeorology*, 55(3), p.411–421.

Luedeling, E., Girvetz, E.H., Semenov, M.A. & Brown, P.H., 2011. Climate Change Affects Winter Chill for Temperate Fruit and Nut Trees. *PLoS ONE*, 6(5), p.1–13.

Lundberg, A., 1993. Evaporation of intercepted snow -- Review of existing and new measurement methods. *Journal of Hydrology*, 151(2-4), p.267–290.

Luo, Y., He, C., Sophocleous, M., Yin, Z., Hongui, R. & Quyang, Z., 2008. Assessment of crop growth and soil water modules in SWAT2000 using extensive field experiment data in an irrigation district of the Yellow River Basin. *Journal of Hydrology*, 352(1-4), p.139–156.

Di Luzio, M., Srinivasan, R. & Arnold, J.G., 2004. A GIS-coupled hydrological model system for the watershed assessment of agricultural nonpoint and point sources of pollution. *Transactions in GIS*, 8(1), p.113–136.

Lybbert, T.J., Kusunose, Y., Magnan, N. & Fadlaoui, A., 2009. Drought Risk and Drought Response in Morocco: Vulnerability, Risk Perceptions and Drought Coping Among Rainfed Cereal Farmers. In *Agricultural & Applied Economics Association Meeting*. pp. 26–29.

Magier, J. & Ravina, I., 1983. Hydraulic Conductivity and Water Retention of Clay Soils Containing Coarse Fragments. *Soil Science Society of America Journal*, 48(4), p.736–740.

Male, D.H. & Gray, D.M., 1981. *Handbook of Snow: Principles, Processes, Management and Use*, Caldwell: Blackburn Press.

Maneta, M.P., Schnabel, S., Wallender, W.W., Panday, S. & Jetten, V., 2008. Calibration of an evapotranspiration model to simulate soil water dynamics in a semiarid rangeland. *Hydrological Processes*, 22(24), p.4655–4669.

Margat, J. & Treyer, S., 2004. L'eau des Méditerranéens: situation et perspectives. *UNEP-MAP (Mediterranean Action Plan) Technical Report*, 158, p.366.

Marks, D., Winstral, A. & Seyfried, M., 2002. Simulation of terrain and forest shelter effects on patterns of snow deposition, snowmelt and runoff over a semi-arid mountain catchment. *Hydrological Processes*, 16(18), p.3605–3626.

McCuen, R.H., 1973. The role of sensitivity analysis in hydrologic modeling. *Journal of Hydrology*, 18(1), p.37–53.

McKay, M.D., Beckman, R.J. & Conover, W.J., 1979. A Comparison of Three Methods for Selecting Values of Input Variables in the Analysis of Output from a Computer Code. *Technometrics*, 21(2), p.239–245.

McKee, T.B., Doesken, N.J. & Kleist, J., 1993. The relationship of drought frequency and duration to time scales. In *Proceedings of the 8th Conference on Applied Climatology*.

McMichael, C., Hope, A. & Loaiciga, H., 2006. Distributed hydrological modelling in California semi-arid shrublands: MIKE SHE model calibration and uncertainty estimation. *Journal of Hydrology*, 317(3-4), p.307–324.

McMillan, H., Krueger, T. & Freer, J., 2012. Benchmarking observational uncertainties for hydrology: rainfall, river discharge and water quality. *Hydrological Processes*, p.online.

ME, 1959. *Geological Map of Morocco, Sheet Ouarzazate. 1:500000*, Rabat: Ministère de la economie.

Mearns, L.O., Giorgi, F., McDaniel, L. & Shields, C., 1995. Analysis of daily variability of precipitation in a nested regional climate model: comparison with observations and doubled CO2 results. *Global and Planetary Change*, 10(1-4), p.55–78.

Menking, K.M., Syed, K.H., Anderson, R.Y., Shafike, N.G. & Arnold, J.G., 2003. Model estimates of runoff in the closed, semiarid Estancia basin, central New Mexico, USA. *Hydrological Sciences Journal-Journal Des Sciences Hydrologiques*, 48(6), p.953–970.

Mero, F., 1964. Application of the groundwater depletion curves in analyzing and forecasting spring discharges influenced by well fields. Publication no. 63 of the IASH. In *Symposium on Surface Waters*. pp. 107–117.

Messouli, M., Salem, A.B., Ghallabi, B., Yacoubi-Khebiza, M., Boughrous, A.A., El Filali, A.E.A., Rochdane, S. & Hammadi, F.E., 2009. Ecohydrology and groundwater resources management under global change: A pilot study in the pre-Saharan basins of southern Morocco. In *Options Méditerranéennes*. Technological Perspectives for Rational Use of Water Resources in the Mediterranean Region. Marakech, pp. 255–264.

Michard, A., Saddiqi, O. & Lamotte, D.F. de eds., 2008. *Continental Evolution: The Geology of Morocco: Structure, Stratigraphy, and Tectonics of the Africa-Atlantic-Mediterranean Triple Junction* 1st ed., Springer, Berlin.

Middleton, N.J. & Thomas, D.S.G., 1992. *World Atlas of Desertification*, London: Hodder Arnold.

Mishra, A.K. & Coulibaly, P., 2009. Developments in hydrometric network design: A review. *Reviews of Geophysics*, 47(2), p.published online.

Mishra, A.K. & Singh, V.P., 2010. A review of drought concepts. *Journal of Hydrology*, 391(1–2), p.202–216.

Montanari, A., Shoemaker, C.A. & Giesen, N. van de, 2009. Introduction to special section on Uncertainty Assessment in Surface and Subsurface Hydrology: An overview of issues and challenges. *Water Resources Research*, 45, p.published online.

Monteith, J.L., 1965. Evaporation and environment. In *Symposia of the Society for Experimental Biology*. pp. 205–234.

Moore, R., 1997. Storage-outflow modelling of streamflow recessions, with application to a shallow-soil forested catchment. *Journal of Hydrology*, 198(1-4), p.260–270.

Moriasi, D.N., Arnold, J.G., Van Liew, M.W., Bingner, R.L., Harmel, R.D. & Veith, T.L., 2007. Model evaluation guidelines for systematic quantification of accuracy in watershed simulations. *Transactions of the ASAE*, 50(3), p.885–900.

Morin, E., Grodek, T., Dahan, O., Benito, G., Kulls, C., Jacoby, Y., Langenhove, G.V., Seely, M. & Enzel, Y., 2009. Flood routing and alluvial aquifer recharge along the ephemeral arid Kuiseb River, Namibia. *Journal of Hydrology*, 368(1-4), p.262–275.

Moss, R.H., Edmonds, J.A., Hibbard, K.A., Manning, M.R., Rose, S.K., Vuuren, D.P. van, Carter, T.R., Emori, S., Kainuma, M., Kram, T., Meehl, G.A., Mitchell, J.F.B., Nakicenovic, N., Riahi, K., Smith, S.J., Stouffer, R.J., Thomson, A.M., Weyant, J.P. & Wilbanks, T.J., 2010. The next generation of scenarios for climate change research and assessment. *Nature*, 463(7282), p.747–756.

Motovilov, Y.G., Gottschalk, L. & Engeland, K., 1999. *Ecomag—a physically based hydrological model—application to the NOPEX region*, University of Oslo: Department of Geophysics.

MTP ed., 1998. *Etude du plan directeur de l'aménagement des eaux des bassins sud-atlasiques, Misssion 3: Etude des schemas d'aménagement. 4: Unites du Drâa*, Rabat: Ministère des travaux publics.

Müller-Hohenstein, K. & Popp, H., 1990. *Marokko: ein islamisches Entwicklungsland mit kolonialer Vergangenheit*, Stuttgart: Klett.

NASA, 2003.Landsat ETM+ scene Available at: http://glcf.umiacs.umd.edu/data/landsat/ [Accessed July 14, 2009].

Nash, J.E. & Sutcliffe, J.V., 1970. River flow forecasting through conceptual models part I -- A discussion of principles. *Journal of Hydrology*, 10(3), p.282–290.

Neitsch, S.L., Arnold, J.G., Kiniry, J.R., Srinivasan, R. & Williams, J.R., 2004. *Soil Water Assesment Tool. Input/Output File Documentation*, Temple: USDA-ARS.

Neitsch, S.L., Arnold, J.G. & Williams, J.R., 1999. *Soil and Water Assessment Tool - User Manual*, Temple: USDA-ARS.

Nicholson, S., 2001. Climatic and environmental change in Africa during the last two centuries. *Climate Research*, 17(2), p.123–144.

Nicholson, S.E. & Kim, J., 1997. The Relationship of the El Nino-Southern Oscillation to African Rainfall. *International Journal of Climatology*, 17, p.117–136.

NRCS, 1999. *Soil Taxonomy. A basic System of Soil Classification for Making and Interpreting Soil Surveys*, Des Moines: National Resource Conservation Service.

NRCS, 1986. *Urban Hydrology for Small Watersheds*, Des Moines: National Resource Conservation Service.

Oke, T.R., 1987. *Boundary layer climates*, London: Routledge.

Oreskes, N., Shrader-Frechette, K. & Belitz, K., 1994. Verification, Validation, and Confirmation of Numerical Models in the Earth Sciences. *Science*, 263(5147), p.641–646.

ORMVAO, 1995. *Étude d'amélioration de l'exploitation des systèmes d'irrigation et de drainage del' ORMVAO: Phase 1 Diagnostique de la situation actuelle*, Ouarzazate: Organistaion de mise en valeur agricole.

Ouassou, A., Ameziane, T., Belghiti, M., Ziyad, A. & Belhamd, A., 2005. Morocco. In *Drought Preparedness and Mitigation in the Mediterranean: Analysis of the Organizations and Institutions*. Options Méditerranéennes, Series B. pp. 105–130.

Paeth, H., Born, K., Girmes, R., Podzun, R. & Jacob, D., 2009. Regional Climate Change in Tropical and Northern Africa due to Greenhouse Forcing and Land Use Changes. *Journal of Climate*, 22(1), p.114–132.

Palmer, W.C., 1965. *Meteorological drought*, Washington: US Dept. of Commerce, Weather Bureau.

Parish, R. & Funnell, D.C., 1999. Climate change in mountain regions: some possible consequences in the Moroccan High Atlas. *Global Environmental Change*, 9(1), p.45–58.

Penman, H.L., 1956. Evaporation: an introductory survey. *Netherlands Journal of Agricultural Science*, 4(1), p.9–29.

Peterson, D.M. & Wilson, J.L., 1989. *Variably saturated flow between streams and aquifers*, Socorro: New Mexico Institute of Mining and Technology.

Peterson, T.C. & Vose, R.S., 1997. An overview of the Global Historical Climatology Network temperature database. *Bulletin of the American Meteorological Society*, 78(12), p.2837–2849.

Petros, M., 2009. *Simulation of the hydrological processes in the Upper Drâa catchment, Morocco: an application of the SWAT model using globally available data.* Unpublished Master Thesis. University of Bonn.

Peyron, M., 1995. Middle Atlas Berber Poetry. *Alpine Journal*, 100(1), p.96–99.

Phillips, W.S., 1963. Depth of roots in soil. *Ecology*, 44(2), p.424–424.

Piecha, K., 2009. *Statistisch-dynamische Regionalisierung von Niederschlag und Evapotranspiration für den Hohen Atlas in Marokko*. University of Cologne. Available at: http://kups.ub.uni-koeln.de/2923/ [Accessed July 13, 2012].

Piqué, A., Tricart, P., Guiraud, R., Laville, E., Bouaziz, S., Amrhar, M. & Ait Ouali, R., 2002. The Mesozoic-Cenozoic Atlas belt (North Africa): an overview. *Geodinamica Acta*, 15(3), p.185–208.

Pittock, A.B. & Jones, R.N., 2000. Adaptation to what and why? *Environmental Monitoring and Assessment*, 61(1), p.9–35.

Platt, S., 2008a. Current Development of the Population in the Provinces of Ouarzazate and Zagora. In O. Schulz & M. Judex, eds. *IMPETUS Atlas Morocco. Research Results 2000–2007*. Bonn: Department of Geography, University of Bonn, Germany., pp. 33–36.

Platt, S., 2008b. Development of the Urbanized Regions in the Provinces of Ouarzazate and Zagora until 2020. In O. Schulz & M. Judex, eds. *IMPETUS Atlas Morocco. Research Results 2000–2007*. Department of Geography, University of Bonn, Germany., pp. 61–62.

Poesen, J. & Lavee, H., 1994. Rock fragments in top soils: significance and processes. *Catena*, 23(1-2), p.1–28.

Potchter, O., Goldman, D., Kadish, D. & Iluz, D., 2008. The oasis effect in an extremely hot and arid climate: The case of southern Israel. *Journal of Arid Environments*, 72, p.1721–33.

Priestley, C.H.B. & Taylor, R.J., 1972. On the assessment of surface heat flux and evaporation using large-scale parameters. *Monthly weather review*, 100(2), p.81–92.

Radanovic, R., 1968. *Sols de la palmeraie Mezguita.*, Ouarzazate: Organistaion de mise en valeur agricole.

Rademacher, C., 2010. *Gehen, damit andere bleiben können? Migration, Geschlecht und sozio-ökonomischer Wandel in einem südmarokkanischen Oasendorf*. PhD-Thesis. University of Cologne. Available at: http://kups.ub.uni-koeln.de/3095/ [Accessed June 4, 2012].

Rao, C.X. & Maurer, E.P., 1996. A simplified model for predicting daily transmission losses in a stream channel. *Water Resources Bulletin*, 32(6), p.1139–1146.

Raskin, P.D., 2005. Global scenarios: background review for the Millennium Ecosystem Assessment. *Ecosystems*, 8(2), p.133–142.

Rauh, W., 1952. Vegetationsstudien im Hohen Atlas und dessen Vorland. *Sitzungsberichte der Heidelberger Akademie der Wissenschaften*, 1952(1).

Rawls, W.J., Brakensiek, D.L. & Saxton, K.E., 1982. Estimation of Soil-Water Properties. *Transactions of the Asae*, 25(5), p.1316–1328.

Refsgaard, J.C., 1997. Parameterisation, calibration and validation of distributed hydrological models. *Journal of Hydrology*, 198(1-4), p.69–97.

Refsgaard, J.C. & Henriksen, H.J., 2004. Modelling guidelines–terminology and guiding principles. *Advances in Water Resources*, 27(1), p.71–82.

Refsgaard, J.C., Van der Sluijs, J.P., Brown, J. & Van der Keur, P., 2006. A framework for dealing with uncertainty due to model structure error. *Advances in Water Resources*, 29(11), p.1586–1597.

Reggiani, P., Sivapalan, M. & Hassanizadeh, S.M., 1998. A unifying framework for watershed thermodynamics: balance equations for mass, momentum, energy and entropy, and the second law of thermodynamics. *Advances in Water Resources*, 22(4), p.367–398.

RGPH, 2004. *Recensement Général de la Population et de l'Habitat*, Rabat.

RGPH, 1994. *Recensement Général de la Population et de l'Habitat*, Rabat.

Richardson, C.W. & Wright, D.A., 1984. WGEN: A Model for Generating Daily Weather Variables. *Agricultural Research Service Report*, 8, p.83.

Risbey, J.S. & Kandlikar, M., 2007. Expressions of likelihood and confidence in the IPCC uncertainty assessment process. *Climatic Change*, 85(1), p.19–31.

Rödiger, T., Sauter, M. & Büchel, G., 2009. Infiltration und Grundwasserströmung in geklüftet-porösen Buntsandsteingrundwasserleitern im Osten des Thüringer Beckens. *Grundwasser*, 14(1), p.21–32.

Rodriguez, E., Morris, C.S. & Belz, J.E., 2006. A global assessment of the SRTM performance. *Photogrammetric Engineering and Remote Sensing*, 72(3), p.249–260.

Roe, G., 2005. Orographic precipitation. *Annual Review of Earth and Planetary Sciences*, 33, p.645–671.

Roeckner, E., Arpe, K., Bengtsson, L., Christoph, M., Dümenil, L., Esch, M., Giorgetta, M., Schulzweida, U., Claussen, M. & Schlese, U., 1996. *The atmospheric general circulation model ECHAM-4: Model description and simulation of present-day climate*, Hamburg: Max Planck Institut.

Rößler, O., 2011. *A Climate Change Impact Assessment Study on Mountain Soil Moisture with Emphasis on Epistemic Uncertainties*. PhD-Thesis. University of Bonn. Available at: http://hss.ulb.uni-bonn.de/2011/2600/2600.htm [Accessed June 4, 2012].

Rößler, O. & Löffler, J., 2009. Analyzing Spatio-Temporal Hydrological Processes and Related Gradients to Improve Hydrological Modeling in High Mountains. In J.-C. Otto & R. Dikau, eds. *Landform - Structure, Evolution, Process Control*. Berlin, Heidelberg: Springer, pp. 243–256.

Rostamian, R., Jaleh, A., Afyuni, M., Mousavi, A.F., Heidarpour, M., Jalalian, A. & Abbaspour, K.C., 2008. Application of a SWAT model for estimating runoff and sediment in two mountainous basins in central Iran. *Hydrological Sciences*, 53(5), p.977–988.

Roth, A., 2009. *Impact of climate change and stocking rates on pasture systems in SE Morocco–An Application of the SAVANNA Ecosystem Model*. PhD-Thesis. University of Bonn. Available at: http://hss.ulb.uni-bonn.de/2010/2337/2337.htm [Accessed June 4, 2012].

Royaume du Maroc : Administration du Tourisme, 2011.Vision 2010 et avenir Available at: http://www.tourisme.gov.ma/francais/2-Vision2010-Avenir/2-chantiers/2-Produit/produit.htm [Accessed March 27, 2012].

Sadani, M., Ouazzani, N. & Mandi, L., 2004. Impact de la sécheresse sur l'évolution de la qualité des eaux du lac Mansour Eddahbi (Ouarzazate, Maroc). *Revue des sciences de l'eau, Journal of Water Science*, 17(1), p.69–90.

Sadek, M.F., Shahin, M.M. & Stigter, C.J., 1997. Evaporation from the reservoir of the High Aswan Dam, Egypt: A new comparison of relevant methods with limited data. *Theoretical and Applied Climatology*, 56(1), p.57–66.

Salomonson, V. & Appel, I., 2004. Estimating fractional snow cover from MODIS using the normalized difference snow index. *Remote sensing of environment*, 89(3), p.351–360.

Saltelli, A. & Annoni, P., 2010. How to avoid a perfunctory sensitivity analysis. *Environmental Modelling & Software*, 25(12), p.1508–1517.

Saltelli, A., Ratto, M., Tarantola, S. & Campolongo, F., 2006. Sensitivity analysis practices: Strategies for model-based inference. *Reliability Engineering & System Safety*, 91(10–11), p.1109–1125.

Scanlon, B., Keese, K., Flint, A., Flint, L., Gaye, C., Edmunds, W. & Simmers, I., 2006. Global synthesis of groundwater recharge in semiarid and arid regions. *Hydrological Processes*, 20(15), p.3335–3370.

Schulz, O., 2007. *Analyse schneehydrologischer Prozesse und Schneekartierung im Einzugsgebiet des Oued M'Goun, Zentraler Hoher Atlas (Marokko)*. PhD-Thesis. University of Bonn. Available at: http://hss.ulb.uni-bonn.de/2007/1128/1128.htm [Accessed June 4, 2012].

Schulz, O., 2008. The IMPETUS climate monitoring network. In O. Schulz & M. Judex, eds. *IMPETUS Atlas Morocco. Research Results 2000–2007*. Department of Geography, University of Bonn, Germany., pp. 17–18.

Schulz, O., Busche, H. & Benbouziane, A., 2008. Decadal Precipitation Variances and Reservoir Inflow in the Semi-Arid Upper Drâa basin (South-Eastern Morocco). In F. Zereini & H. Hoetzl, eds. *Climatic Changes and Water Resources in the Middle East and in North Africa*. Wien: Springer, pp. 165–178.

Schulz, O. & de Jong, C., 2004. Snowmelt and sublimation: field experiments and modelling in the High Atlas Mountains of Morocco. *Hydrology and Earth System Sciences*, 8(6), p.1076–1089.

Schuol, J., Abbaspour, K., Srinivasan, R. & Yang, H., 2008. Estimation of freshwater availability in the West African sub-continent using the SWAT hydrologic model. *Journal of Hydrology*, 352(1-2), p.30–49.

Schwarze, R., 1999. Skalenwechsel über Parameter: Grundwasser. In H. Kleeberg, W. Mauser, G. Peschke, & U. Streit, eds. *Hydrologie und Regionalisierung. DFG Research Report.* Weinheim: Wiley, p. 477.

Schwarze, R., Grünewald, U., Becker, A. & FRÜHLICH, W., 1989. Computer-aided analyses of flow recessions and coupled basin water balance investigations. *IAHS-AISH publication*, (187), p.75–83.

Schwarze, R., Herbert, D. & Opherden, K., 1995. On the residence time of runoff from small catchment areas in the Erzgebirge region. *Isotopes in Enviromental and Health Studies*, 31(1), p.15–28.

Sebrier, M., Siame, L., Zouine, E., Winter, T., Missenard, Y. & Leturmy, P., 2006. Active tectonics in the Moroccan High Atlas. *COMPTES RENDUS GEOSCIENCE*, 338(1-2), p.65–79.

Seyfried, M.S. & Wilcox, B.P., 1995. Scale and the nature of spatial variability: field examples having implications for hydrologic modeling. *Water Resources Research*, 31(1), p.173–184.

Sharma, K.D. & Murthy, J.S.R., 1994. Estimating Transmission Losses in an Arid Region. *Journal of Arid Environments*, 26(3), p.209–219.

Shukla, S. & Wood, A.W., 2008. Use of a standardized runoff index for characterizing hydrologic drought. *Geophysical Research Letters*, 35, p.published online.

Siebert, S., Nagieb, M. & Buerkert, A., 2007. Climate and irrigation water use of a mountain oasis in northern Oman. *Agricultural Water Management*, 89(1-2), p.1–14.

Simanton, J.R., Hawkins, R.H., Mohseni-Saravi, M., Renard, K.G. & USDA, A., 1996. Runoff curve number variation with drainage area Walnut Gulch, Arizona. *Transactions of the ASAE*, 39(4), p.1391–1394.

Simmers, I., 2003. *Understanding water in a dry environment*, London: Taylor & Francis.

Singer, M., 1991. Physical properties of arid region soils. In J. Skujiņš, ed. *Semiarid Lands and Deserts*. London: CRC Press, pp. 81–110.

Singh, J., Knapp, H.V., Arnold, J.G. & Demissie, M., 2005. Hydrological Modeling of the Iroquois River Watershed Using HSPF and SWAT. *Journal of the Astronomical Society of Western Australia*, 41, p.343–360.

Sloan, P.G. & Moore, I.D., 1984. Modeling subsurface stormflow on steeply sloping forested watersheds. *Water Resources Research*, 20(12), p.1815–1822.

Smakhtin, V.U., 2001. Low flow hydrology: A review. *Journal of Hydrology*, 240(1-4), p.147–186.

Smedema, L.K. & Rycroft, D.W., 1983. *Land drainage: planning and design of agricultural drainage system*, Cornell University.

Smith, D. & Vivekananda, J., 2007. *A climate of conflict: The links between climate change, peace and war*, London: International Alert.

Solomon, S., Qin, D., Manning, M., Alley, R.B., Berntsen, T., Bindoff, N.L., Chen, Z., Chithaisong, A., Gregory, J.M. & Hegerl, G.C., 2007. *Climate change 2007: the physical science basis*, Cambrige: Intergovernmental Panel on Climate Change.

Sophocleous, M., 2002. Interactions between groundwater and surface water: the state of the science. *Hydrogeology Journal*, 10(1), p.52–67.

Sophocleous, M.., Koelliker, J.., Govindaraju, R.., Birdie, T., Ramireddygari, S.. & Perkins, S.., 1999. Integrated numerical modeling for basin-wide water management: The case of the Rattlesnake Creek basin in south-central Kansas. *Journal of Hydrology*, 214(1–4), p.179–196.

Sorooshian, S. & Gupta, V.K., 1995. Model calibration. In V. Singh, ed. *Computer models of watershed hydrology*. pp. 23–68.

Speth, P., Christoph, M. & Diekkrüger, B. eds., 2010. *Impacts of Global Change on the Hydrological Cycle in West and Northwest Africa* 1st ed., Springer, Berlin.

Stäblein, G., 1988. Geomorphological aspects of the quaternary evolution of the Ouarzazate Basin, Southern Morocco. In *The Atlas System of Morocco*. pp. 433–444.

Stachowiak, H., 1973. *Allgemeine Modelltheorie*, Berlin: Springer.

Stanners, D. & Bourdeau, P., 1995. *Europe's environment: the Dobrís assessment*, Luxemburg: European Environmental Agency.

Staudinger, M. & Finckh, M., 2005. Räumliche Vegetationsmuster in ariden Gebieten Südmarokkos - Klassifizierung zugrundeliegender Mechanismen. *UFZ-Berichte*, 1, p.41–53.

Stets, J. & Wurster, P., 1981. On the stuctural history of the High Atlas of Marocco. *Geologische Rundschau*, 70(3), p.801–841.

Strzepek, K. & Boehlert, B., 2010. Competition for water for the food system. *Philosophical Transactions of the Royal Society B: Biological Sciences*, 365(1554), p.2927 –2940.

Swart, R.J., Raskin, P. & Robinson, J., 2004. The problem of the future: sustainability science and scenario analysis. *Global Environmental Change, Part A: Human and Policy Dimensions*, 14(2), p.137–146.

Swearingen, W.D., 1992. Drought hazard in Morocco. *Geographical Review*, 82(4), p.401–412.

Szenasi, Z., 2011. *Analyse der Wasserverfügbarkeit und des Wasserbedarfs im Drâa-Tal, Marokko, mit Hilfe des Entscheidungsunterstützungsmodells WEAP*. Unpublished Diploma Thesis. University of Bonn.

Tallaksen, L.M., 1995. A review of baseflow recession analysis. *Journal of Hydrology*, 165(1-4), p.349–370.

Tarboton, D.G., Chowdhury, T.G. & Jackson, T.H., 1995. A spatially distributed energy balance snowmelt model. *IAHS Publications*, 228, p.141–156.

Thieken, A.H., Lücke, A., Diekkrüger, B. & Richter, O., 1999. Scaling input data by GIS for hydrological modelling. *Hydrological Processes*, 13(4), p.611–630.

Tilmant, A., Faouzi, E.H. & Vanclooster, M., 2002. Optimal operation of multipurpose reservoirs using flexible stochastic dynamic programming. *Applied Soft Computing*, 2(1), p.61–74.

Tooth, S., 2000. Process, form and change in dryland rivers: a review of recent research. *Earth-Science Reviews*, 51(1-4), p.67–107.

Topping, J., 1972. *Errors of Observation and their Treatment*, London: Chapman and Hall.

Troll, C., 1973. The Upper Timberlines in Different Climatic Zones. *Arctic and Alpine Research*, 5(3), p.3–18.

UN, 2011. *The Millennium Development Goals Report 2011*, New York: United Nations.

UN, 2009.United Nations Data Division Available at: http://data.un.org/Default.aspx [Accessed December 28, 2009].

USACE, 1997. *Hydrologic Engineering Requirements for Reservoirs*, Washington: US Army Corps of Engineers.

Veith, T., Van Liew, M., Bosch, D. & Arnold, J., 2010. Parameter Sensitivity and Uncertainty in SWAT: A Comparison Across Five USDA-ARS Watersheds. *Transactions of the ASABE*, 53(5), p.1477–1486.

Vertessy, R.A., Hatton, T.J., O'Shaughnessy, P.J. & Jayasuriya, M.D.A., 1993. Predicting water yield from a mountain ash forest catchment using a terrain analysis based catchment model. *Journal of Hydrology*, 150(2-4), p.665–700.

Villeneuve, M. & Cornée, J.J., 1994. Structure, evolution and palaeogeography of the West African craton and bordering belts during the Neoproterozoic. *Precambrian Research*, 69(1-4), p.307–326.

Viviroli, D., Weingartner, R. & Messerli, B., 2003. Assessing the hydrological significance of the world's mountains. *Mountain Research and Development*, 23(1), p.32–40.

Vivoni, E.R., Valeriy Y. Ivanov, Rafael L. Bras & Dara Entekhabi, 2005. On the effects of triangulated terrain resolution on distributed hydrologic model response. *Hydrological Processes*, 19(11), p.2101–2122.

Vörösmarty, C.J., Green, P., Salisbury, J. & Lammers, R.B., 2000. Global Water Resources: Vulnerability from Climate Change and Population Growth. *Science*, 289(5477), p.284 –288.

de Vries, J. & Simmers, I., 2002. Groundwater recharge: an overview of processes and challenges. *Hydrogeology Journal*, 10(1), p.5–17.

Vrugt, J.A., Gupta, H.V., Bouten, W. & Sorooshian, S., 2003. A Shuffled Complex Evolution Metropolis algorithm for optimization and uncertainty assessment of hydrologic model parameters. *Water Resources Research*, 39(8), p.1201–1217.

Wahi, A., Hogan, J., Ekwurzel, B., Baillie, M. & Eastoe, C., 2008. Geochemical quantification of semiarid mountain recharge. *Ground Water*, 46(3), p.414–425.

Walker, J.D. & Geissman, J.W., 2009. 2009 GSA Geologic Time Scale. *GSA Today*, 19(4), p.60–61.

Weber, B., 2004. *Untersuchungen zum Bodenwasserhaushalt und Modellierung der Bodenwasserflüsse entlang eines Höhen- und Ariditätsgradienten (SE Marokko)*. PhD-Thesis. University of Bonn. Available at: http://hss.ulb.uni-bonn.de/2004/0523/0523.htm [Accessed June 4, 2012].

Weingartner, R., Barben, M. & Spreafico, M., 2003. Floods in mountain areas - An overview based on examples from Switzerland. *Journal of Hydrology*, 282(1-4), p.10–24.

Weiß, M. & Menzel, L., 2008. A global comparison of four potential evapotranspiration equations and their relevance to stream flow modelling in semi-arid environments. *Advances in Geosciences*, 18, p.15–23.

Wheater, H., 2002. Hydrological processes in arid and semi-arid regions. In R. A. Al-Weshah & H. Wheater, eds. *Hydrology of Wadi systems. IHP Regional Network on Wadi Hydrology in the Arab region*. pp. 5–22.

Wheater, H. & Al-Weshah, R.A., 2002. Hydrology of Wadi systems. IHP Regional Network on Wadi Hydrology in the Arab region. *Technical Documents in Hydrology*, (55).

White, J.D., Gutzwiller, K.J., Barrow, W.C., Randall, L.J. & Swint, P., 2008. Modeling mechanisms of vegetation change due to fire in a semi-arid ecosystem. *Ecological Modelling*, 214(2-4), p.181–200.

White, W.B., 2002. Karst hydrology: recent developments and open questions. *Engineering Geology*, 65, p.85–105.

Wilcox, B.P., 2002. Shrub Control and Streamflow on Rangelands: A Process Based Viewpoint. *Journal of Range Management*, 55(4), p.318–326.

Wilhite, D.A., 1996. A methodology for drought preparedness. *Natural Hazards*, 13(3), p.229–252.

Wilhite, D.A. & Glantz, M.H., 1985. Understanding: the Drought Phenomenon: The Role of Definitions. *Water International*, 10(3), p.111–120.

Wilks, D.., 1999. Interannual variability and extreme-value characteristics of several stochastic daily precipitation models. *Agricultural and Forest Meteorology*, 93(3), p.153–169.

Williams, J.R., 1969. Flood routing with variable travel time or variable storage coefficients. *Transactions of the Asae*, 12(1), p.100–103.

Willmott, C.J., 1981. On the validation of models. *Physical geography*, 2(2), p.184–194.

Wilson, J.L. & Guan, H., 2004. Mountain-block hydrology and mountain-front recharge. *Groundwater Recharge in a Desert Environment: The Southwestern United States, Water Sci. Appl. Ser*, 9, p.113–137.

Wilson, K.B., Hanson, P.J., Mulholland, P.J., Baldocchi, D.D. & Wullschleger, S.D., 2001. A comparison of methods for determining forest evapotranspiration and its components: sap-flow, soil water budget, eddy covariance and catchment water balance. *Agricultural and Forest Meteorology*, 106(2), p.153–168.

Winchell, M., Srinivasan, R., Di Luzio, M. & Arnold, J., 2007. *ArcSWAT Interface for SWAT User's Guide*, Blackland Research Center, Texas Agricultural Experiment station and USDA Agricultural Research Service.

Winstral, A. & Marks, D., 2002. Simulating wind fields and snow redistribution using terrain-based parameters to model snow accumulation and melt over a semi-arid mountain catchment. *Hydrological Processes*, 16(18), p.3585–3603.

WMO, 1994. *Guide to Hydrometeorological Practices*, Geneva: World Meteorological Organization.

Wood, E.F., Sivapalan, M., Beven, K. & Band, L., 1988. Effects of spatial variability and scale with implications to hydrologic modeling. *Journal of Hydrology*, 102(1-4), p.29–47.

World Bank, 2004. *Kingdom of Morocco. Recent Economic Developments in Infrastructure (REDI).Water Supply and Sanitation Sector*, Washington: World Bank.

World Commission on Dams, 2000. *Dams and Development: A New Framework for Decision-making : the Report of the World Commission on Dams*, London: Earthscan.

Xu, C., 1999. From GCMs to river flow: a review of downscaling methods and hydrologic modelling approaches. *Progress in Physical Geography*, 23(2), p.229.

Yair, A. & Lavee, H., 1976. Runoff generative process and runoff yield from arid talus mantled slopes. *Earth Surface Processes*, 1(3), p.235–247.

Youbi, L., 1990. *Hydrologie du bassin du Dadés*, Ouarzazate: Office Regional de Mise en Valeur Agricole.

Zhang, J., 2007. *Modeling considerations for vadose zone soil moisture dynamics*. University of South Florida. Available at: http://scholarcommons.usf.edu/etd/2429/.

Appendix A

Appendix 1: Climate data available for the Upper Drâa catchment: Long-term data (SE Ouarzazate, ORMVAO) and IMPETUS climate stations. Locations of the gauges are given in Figure 3-4. Measured variables used in this study: PCP=Precipitation, TMP=Temperature, WND=Wind speed, RH=Relative humidity, RAD=Radiation 205
Appendix 2: Subcatchments of the Upper Drâa catchments and discharge data available provided by SE Ouarzazate and DRPE 206
Appendix 3: Model parameters used in the sensitivity and uncertainty analysis or adapted during calibration. For details on parameter functions and plausible ranges see the respective sub-sections of section 5.3 or the SWAT-Manuals (Neitsch et al. 1999; Neitsch et al. 2004) 207
Appendix 4: Soil properties used in SWAT-MAROC 208
Appendix 5: Vegetation parameters used in SWAT-MAROC 209
Appendix 6: Cultivated Area in the different oases (MTP 1998). The exceedance of the oases size by the cultivated area is due to the double use of fields by growing Maize as a spring grain and by intercropping practices. 210
Appendix 7: Spatial extent (km²) of different soil types in the soil map and in the EHRUs after the model discretization. See Appendix 4 for details on the soil types. ... 211
Appendix 8: Altitudinal dependence of measured climate data; given is the linear relationship and the associated r²; x is elevation (km above sea level) 212
Appendix 9: Polynomial approximation of reservoir volume dependent on reservoir stage level 213
Appendix 10: Modeled discharge compared to measured discharge for the stream gauges Agouillal, Assaka, Ait-Mouted and Tinouar (bars represent measurement uncertainty). See Figure 3-13 for gauge locations. (Measured data: SE Ouarzazate) 214
Appendix 11: Behavioral set of 20 models considered within the uncertainty analysis, including the associated parameter values, model efficiency and average annual discharge to the reservoir Mansour-Eddahbi. 215
Appendix 12: Absolute mean annual water balance of Sub-regions in Baseline Scenario. Values are given in mm. 216
Appendix 13: Relative mean annual water balance of Sub-regions (Baseline Scenario): Fraction of total process volume that occurs in the specific Sub-region. 217
Appendix 14: Monthly discharge including parameter uncertainty at the reservoir Mansour-Eddahbi (1978-2007) (14,988 km²) 218
Appendix 15: Monthly flow duration curve including parameter uncertainty at the reservoir Mansour-Eddahbi (1978-2007) (14,988 km²) 219
Appendix 16: Absolute mean annual water balance of Sub-regions in the representative 2030s Scenario. Values are given in mm. 220
Appendix 17: Relative mean annual water balance of Sub-regions (representative 2030s scenario): Fraction of total process volume that occurs in the specific Sub-region. 221

Operator	Gauge	Coordinates Decimal Degrees		Elevation [masl]	Measured Variable	Time Series available
		x	y			
Regional Authorities (SE, ORMVAO)	**Agouillal**	-7.10	31.01	1220	PCP TMP	01/1976-10/2008 01/1975-12/2002
	Agouim	-7.46	31.16	1647	PCP TMP	01/1975-10/2008 01/1975-12/2001
	Ait-Mouted	-6.00	31.42	1545	PCP TMP	01/1975-10/2008 01/1975-12/2001
	Amane-n-Tini	-7.05	30.94	1170	PCP	12/1982-10/2008
	Assaka-Tafounante	-7.14	30.59	1380	PCP TMP	09/1975-04/2008 01/1984-05/2006
	Ifre	-6.18	31.33	1500	PCP TMP	01/1975-10/2008 01/1975-12/2001
	Imdghar	-7.36	30.60	1502	PCP	05/1975-09/2008
	Mansour-Eddahbi reservoir	-6.76	30.91	1100	PCP TMP	01/1975-10/2008 02/1975-05/2006
	M'Semrir	-5.82	31.71	1942	PCP	01/1975-05/2006
	Tahrbilte	-7.15	30.98	1226	PCP	01/1975-10/2008
	Tamdroust	-7.19	30.95	1245	PCP	06/1977-10/2008
	Tinouar	-6.61	31.01	1136	PCP	01/1975-09/2008
IMPETUS	**Bou Skour**	-6.33	30.95	1420	PCP, TMP, WND, RH, RAD	11/2001-03/2008
	Imeskar	-6.25	31.50	2250	PCP, TMP, WND RH, RAD	04/2001-03/2008
	M'Goun	-6.45	31.50	3850	PCP, TMP, WND, RH, RAD	10/2001-03/2008
	Taoujgalt	-6.32	31.38	1870	PCP, TMP, WND, RH, RAD	11/2001-03/2008
	Tichki	-6.30	31.53	3260	PCP, TMP, WND, RH, RAD	04/2001-03/2008
	Tizi'n'Tounza	-6.30	31.57	2960	PCP, TMP, WND, RH, RAD	10/2001-03/2008
	Trab Labied	-6.58	31.17	1380	PCP, TMP, WND, RH, RAD	04/2001-03/2008

Appendix 1: Climate data available for the Upper Drâa catchment: Long-term data (SE Ouarzazate, ORMVAO) and IMPETUS climate stations. Locations of the gauges are given in Figure 3-4. Measured variables used in this study: PCP=Precipitation, TMP=Temperature, WND=Wind speed, RH=Relative humidity, RAD=Radiation

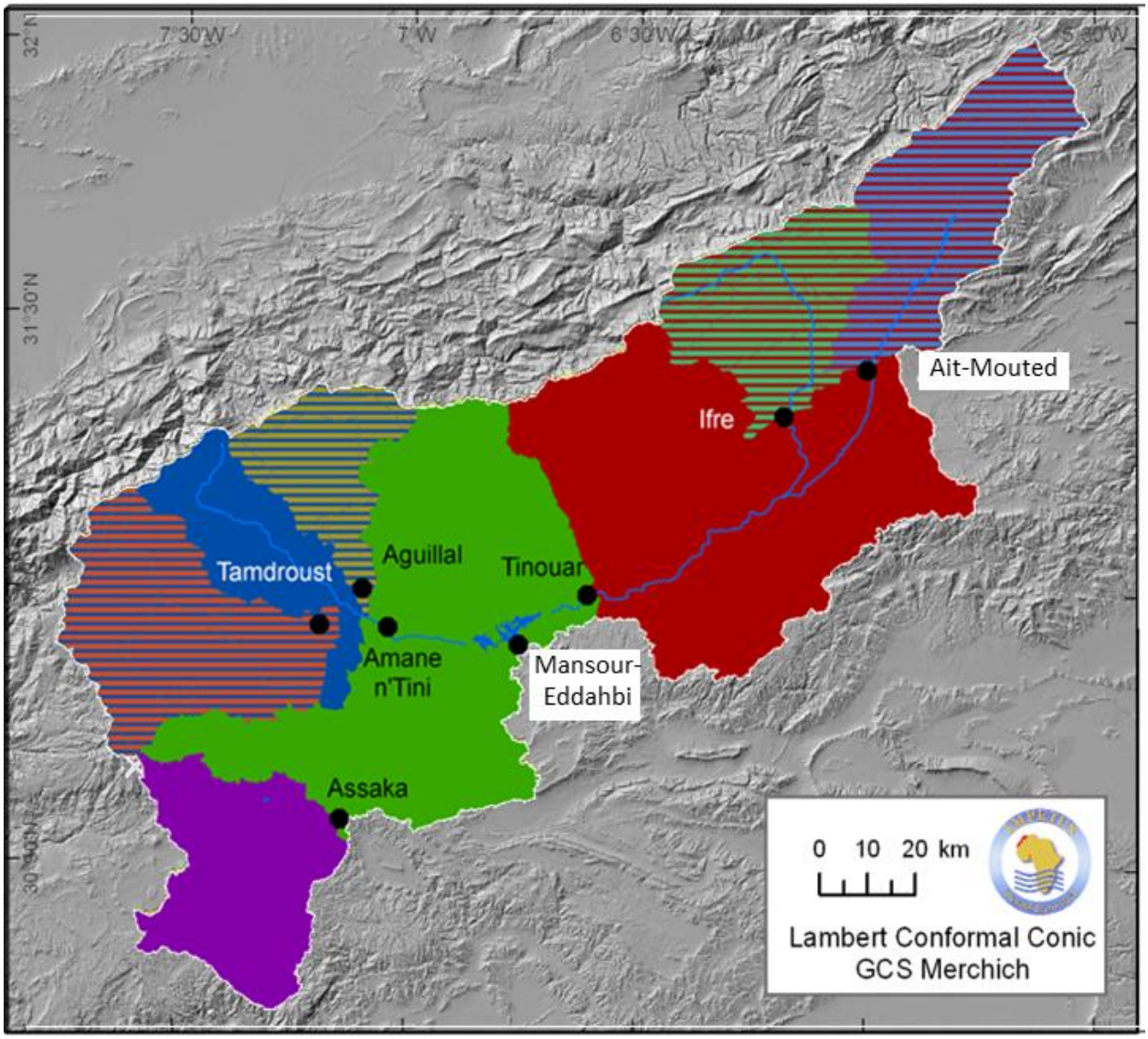

Gauge	Catchment Size [km²]	Coordinates Decimal Degrees		Elevation [masl]	Measured Variable	Time Series available
		x	y			
Agouillal	791	-7.10	31.01	1220	Water level	1976-1997
Ait-Mouted	1484	-6.00	31.42	1545	Water level	1963-2003
Amane-n-Tini	3427	-7.05	30.94	1170	Water level	1982-2002
Assaka-Tafounante	1389	-7.14	30.59	1380	Water level	1975-2000
Ifre	1234	-6.18	31.33	1500	Water level	1963-2005
Tamdroust	1724	-7.19	30.95	1245	Water level	1975-2003
Tinouar	6447	-6.61	31.01	1136	Water level	1972-1995
Mansour-Eddahbi reservoir	14737	-6.76	30.91	1100	Water level	1973-2006

Appendix 2: Subcatchments of the Upper Drâa catchments and discharge data available provided by SE Ouarzazate and DRPE

Parameter	Explanation	Unit	Model file
ALAI	Maximum LAI	[m²/m²]	crop
ALPHA_BF	Baseflow recession coefficient	[1/d]	gw
ALPHA_BNK	Baseflow recession coefficient of the alluvial aquifer	[1/d]	rte
BLAI	Minimum LAI	[m²/m²]	crop
CH_N	Mannings n for channel routing	[-]	rte
CH_K1	Effective hydraulic conductivity of tributary channels	[mm/h]	sub
CH_K2	Effective hydraulic conductivity of main channels	[mm/h]	rte
CH_L	Channel length	[m]	rte/sub
CHTMX	Canopy Height	[m]	crop
CN2	Curve number	[-]	mgt
CH_W	Channel Width	[m]	rte/sub
ESCO[-]	Evaporation from soil compensation factor	[-]	bsn
HRU_SLOPE	Slope	[m/m]	hru
HYDGRP	Hydrological soil Group	A-D	sol
GSI	Stomatal conductance	[m/s]	crop
GW_DELAY	Exponent of an exponential delay function for direct groundwater recharge	[days]	gw
GW_REVAP	Fraction of PET that can be satisfied from shallow groundwater (revaporation)	[%]	gw
IRR_EFF	Irrigation efficiency	[%]	cw
IRR_FRAC	Fraction of streamflow, available for irrigation	[%]	cw
RDMAX	Rooting depth of plant	[mm]	crop
RCHRG_DP	Fraction of recharge diverted to aquifer 2	[%]	gw
SFTMP	Temperature below which snowfall occurs	[°C]	bsn
SLSOIL	Slope length	[m]	hru
SMFMN	Snow melt factor (degree-day approach)	[mm/°C*day]	bsn
SMTMP	Temperature below which snowmelt occurs	[°C]	bsn
SNO50COV	Percentage of SNOCOVMX, corresponding to 50% of snow cover	[%]	bsn
SNOCOVMX	Amount of snow, corresponding with 100% of snow cover	[mm]	bsn
SOL_ALB	Soil Albedo	[%]	sol
SOL_AWC	Available water capacity of the soil	[%]	sol
SOL_BD	Soil bulk density	[t/m³]	sol
SOL_CLAY, SOL_SILT, SOL_SAND, SOL_ROCK	Volumetric fraction of different particle classes within the soil	[%]	sol
SOL_K	Saturated hydraulic conductivity	[mm/h]	sol
SOL_Z	Soil depth	[mm]	sol
SOL_ZMAX	Maximum rooting depth within soil	[mm]	sol
T_BASE	Minimum growing Temperature	[°C]	crop
T_OPT	Optimal growing temperature	[°C]	crop

Appendix 3: Model parameters used in the sensitivity and uncertainty analysis or adapted during calibration. For details on parameter functions and plausible ranges see the respective sub-sections of section 5.3 or the SWAT-Manuals (Neitsch et al. 1999; Neitsch et al. 2004)

Soil Unit	Soil Hydrological Group	Soil Layer 1										Soil Layer 2								
		Depth [mm] r^2=0.42	Bulk Density [g/cm³]	Available Soil water capacity [mm]	Saturated Hydraulic conductivity [mm/h]	Organic Carbon [%] r^2=0.56	Clay [%] r^2=0.69	Silt [%] r^2=0.47	Sand[%] r^2=0.57	Rock [%] r^2=0.79	USLE k factor [-]	Depth [mm] r^2=0.52	Bulk Density [g/cm³]	Available Soil water capacity [mm]	Saturated Hydraulic conductivity [mm/h]	Organic Carbon [%] r^2=0.84	Clay [%] r^2=0.56	Silt [%] r^2=0.56	Sand[%] r^2=0.55	Rock [%] r^2=0.54
111	D	158 ± 15	1.15	14 ± 12	2 ± 2	0.6 ± 0.6	32 ± 13	51 ± 17	17 ± 17	65 ± 20	0.20	33 ± 21	1.31	16 ± 10	1 ± 2	0.4 ± 0.6	28 ± 15	36 ± 19	36 ± 20	78 ± 16
112	D	96 ± 12	1.11	10 ± 10	3 ± 2	0.9 ± 0.9	31 ± 16	58 ± 20	12 ± 15	54 ± 24	0.23	28 ± 18	1.45	21 ± 12	47 ± 81	1.7 ± 1.3	22 ± 13	25 ± 17	53 ± 16	64 ± 23
121	D	153 ± 14	1.38	13 ± 11	14 ± 5	0.6 ± 0.6	20 ± 8	35 ± 13	44 ± 11	63 ± 21	0.17	33 ± 20	1.33	17 ± 10	1 ± 2	0.4 ± 0.6	28 ± 15	33 ± 18	38 ± 19	75 ± 18
122	C	127 ± 12	1.35	12 ± 10	15 ± 5	0.8 ± 1	18 ± 9	41 ± 18	40 ± 15	58 ± 23	0.17	26 ± 16	1.46	19 ± 11	47 ± 84	1.7 ± 1.3	24 ± 12	22 ± 17	53 ± 15	63 ± 24
131	D	137 ± 12	1.44	15 ± 11	34 ± 6	0.7 ± 0.7	17 ± 6	32 ± 10	51 ± 8	50 ± 21	0.17	29 ± 19	1.33	15 ± 9	2 ± 2	0.5 ± 0.7	29 ± 15	32 ± 18	38 ± 19	74 ± 19
132	C	114 ± 10	1.42	14 ± 11	35 ± 6	0.8 ± 0.8	15 ± 7	36 ± 11	49 ± 9	45 ± 20	0.17	21 ± 14	1.45	17 ± 11	46 ± 80	1.7 ± 1.3	24 ± 12	24 ± 17	52 ± 15	62 ± 24
141	D	92 ± 10	1.49	12 ± 12	100 ± 68	1.1 ± 1.1	14 ± 7	28 ± 11	58 ± 9	35 ± 21	0.16	28 ± 19	1.31	15 ± 10	2 ± 2	0.7 ± 1	28 ± 16	36 ± 20	36 ± 20	72 ± 23
142	A	67 ± 8	1.51	10 ± 11	126 ± 89	1.6 ± 1.5	13 ± 7	28 ± 10	60 ± 10	32 ± 17	0.14	19 ± 15	1.47	17 ± 12	113 ± 179	2 ± 1.3	23 ± 15	22 ± 18	55 ± 18	53 ± 30
211	D	287 ± 21	1.15	31 ± 20	3 ± 2	0.7 ± 0.8	32 ± 13	51 ± 17	17 ± 16	61 ± 21	0.20	35 ± 27	1.26	28 ± 20	2 ± 2	0.6 ± 0.9	28 ± 14	42 ± 19	30 ± 20	65 ± 24
212	D	189 ± 17	1.10	25 ± 19	3 ± 2	1 ± 0.9	34 ± 17	55 ± 19	11 ± 14	51 ± 23	0.23	32 ± 20	1.41	36 ± 19	54 ± 96	1.9 ± 1.3	20 ± 12	32 ± 18	48 ± 16	55 ± 24
221	D	255 ± 18	1.37	27 ± 18	15 ± 5	0.6 ± 0.7	21 ± 8	36 ± 12	43 ± 10	59 ± 21	0.17	40 ± 24	1.31	33 ± 19	2 ± 2	0.4 ± 0.7	27 ± 14	37 ± 18	36 ± 19	62 ± 21
222	C	204 ± 14	1.33	25 ± 17	15 ± 5	1 ± 1.3	19 ± 9	43 ± 17	38 ± 15	54 ± 23	0.16	33 ± 19	1.42	36 ± 18	58 ± 102	1.7 ± 1.3	22 ± 12	29 ± 18	49 ± 16	54 ± 23
231	D	238 ± 14	1.43	30 ± 15	34 ± 6	0.5 ± 0.6	17 ± 6	32 ± 8	51 ± 7	45 ± 20	0.17	36 ± 20	1.34	30 ± 16	2 ± 2	0.4 ± 0.6	26 ± 13	35 ± 16	39 ± 18	60 ± 22
232	C	191 ± 12	1.41	27 ± 16	35 ± 6	0.8 ± 0.9	16 ± 7	36 ± 11	48 ± 9	41 ± 20	0.17	29 ± 16	1.43	33 ± 17	56 ± 99	1.6 ± 1.3	22 ± 11	28 ± 18	50 ± 16	52 ± 24
241	D	217 ± 14	1.49	32 ± 17	90 ± 62	0.8 ± 0.8	15 ± 7	27 ± 9	57 ± 8	30 ± 21	0.17	34 ± 21	1.32	28 ± 18	2 ± 2	0.5 ± 0.8	26 ± 15	36 ± 18	38 ± 19	62 ± 22
242	B	151 ± 12	1.48	25 ± 18	100 ± 71	1.3 ± 1.3	14 ± 7	30 ± 10	56 ± 10	28 ± 18	0.15	29 ± 16	1.43	35 ± 19	85 ± 148	1.8 ± 1.3	21 ± 12	29 ± 18	50 ± 17	50 ± 25
311	D	365 ± 29	1.15	46 ± 32	3 ± 2	0.8 ± 0.9	31 ± 14	51 ± 18	17 ± 16	55 ± 23	0.20	50 ± 33	1.26	52 ± 33	2 ± 2	0.6 ± 0.8	27 ± 14	43 ± 20	30 ± 21	56 ± 24
312	D	261 ± 21	1.12	38 ± 28	3 ± 2	0.8 ± 0.8	31 ± 16	55 ± 18	14 ± 15	48 ± 25	0.22	41 ± 25	1.38	59 ± 29	59 ± 90	2 ± 1.4	19 ± 11	37 ± 19	44 ± 17	44 ± 25
321	D	348 ± 26	1.34	43 ± 28	15 ± 5	0.7 ± 0.8	20 ± 8	40 ± 14	40 ± 12	51 ± 20	0.17	56 ± 29	1.30	57 ± 28	2 ± 2	0.4 ± 0.7	26 ± 12	39 ± 18	35 ± 19	55 ± 20
322	C	268 ± 20	1.33	36 ± 25	15 ± 5	0.9 ± 1.1	18 ± 9	43 ± 16	39 ± 14	50 ± 24	0.17	46 ± 25	1.39	63 ± 26	54 ± 86	1.8 ± 1.3	20 ± 11	35 ± 18	45 ± 15	48 ± 20
331	D	322 ± 19	1.42	46 ± 22	35 ± 6	0.5 ± 0.6	17 ± 6	34 ± 9	49 ± 7	39 ± 18	0.17	55 ± 24	1.35	56 ± 23	2 ± 2	0.4 ± 0.6	23 ± 10	37 ± 16	40 ± 18	53 ± 16
332	C	250 ± 18	1.39	39 ± 25	35 ± 6	0.9 ± 0.9	16 ± 7	38 ± 11	46 ± 9	34 ± 21	0.17	43 ± 22	1.39	60 ± 25	56 ± 93	1.7 ± 1.2	20 ± 10	35 ± 17	45 ± 15	46 ± 21
341	D	277 ± 18	1.47	44 ± 25	84 ± 70	0.9 ± 0.9	14 ± 7	31 ± 9	55 ± 9	24 ± 19	0.17	51 ± 24	1.32	58 ± 27	3 ± 2	0.6 ± 0.9	22 ± 12	40 ± 17	38 ± 19	50 ± 18
342	B	217 ± 17	1.45	38 ± 27	87 ± 65	1.2 ± 1.2	14 ± 7	34 ± 11	53 ± 10	22 ± 19	0.16	41 ± 20	1.38	61 ± 28	64 ± 108	1.9 ± 1.3	19 ± 12	36 ± 20	44 ± 18	45 ± 22
411	D	748 ± 68	1.15	106 ± 86	3 ± 2	0.8 ± 0.9	30 ± 12	53 ± 17	17 ± 15	50 ± 22	0.20	89 ± 85	1.25	99 ± 100	2 ± 2	0.7 ± 1	28 ± 13	43 ± 23	28 ± 22	54 ± 23
412	D	509 ± 56	1.13	78 ± 86	3 ± 2	1 ± 1	26 ± 14	59 ± 18	15 ± 14	49 ± 26	0.22	111 ± 102	1.36	172 ± 164	56 ± 87	2 ± 1.3	21 ± 13	36 ± 21	42 ± 18	41 ± 22
421	D	672 ± 61	1.34	91 ± 77	15 ± 5	0.6 ± 0.7	19 ± 8	41 ± 13	40 ± 10	47 ± 21	0.18	95 ± 76	1.29	105 ± 87	2 ± 2	0.5 ± 0.7	26 ± 12	40 ± 19	34 ± 19	50 ± 22
422	C	497 ± 53	1.32	71 ± 74	16 ± 5	0.9 ± 1	16 ± 8	46 ± 14	38 ± 12	46 ± 24	0.17	104 ± 86	1.36	160 ± 135	51 ± 70	1.8 ± 1.2	20 ± 11	37 ± 19	42 ± 15	42 ± 20
431	D	575 ± 49	1.42	84 ± 66	35 ± 6	0.5 ± 0.5	16 ± 6	34 ± 8	49 ± 6	36 ± 17	0.18	91 ± 64	1.35	100 ± 73	3 ± 2	0.4 ± 0.6	22 ± 10	37 ± 15	41 ± 17	47 ± 17
432	C	537 ± 53	1.39	88 ± 86	34 ± 6	0.9 ± 1	15 ± 7	39 ± 10	46 ± 8	34 ± 22	0.17	97 ± 83	1.38	149 ± 129	57 ± 76	1.7 ± 1.2	20 ± 11	36 ± 17	44 ± 14	40 ± 21
441	D	550 ± 49	1.47	91 ± 77	72 ± 31	0.7 ± 0.8	14 ± 6	31 ± 7	55 ± 6	22 ± 18	0.17	89 ± 66	1.36	103 ± 79	3 ± 2	0.4 ± 0.6	21 ± 10	37 ± 15	43 ± 16	42 ± 19
442	B	542 ± 56	1.45	97 ± 100	82 ± 43	1.1 ± 1.1	13 ± 7	33 ± 9	53 ± 8	22 ± 19	0.16	90 ± 82	1.40	144 ± 131	69 ± 97	1.7 ± 1.3	19 ± 11	34 ± 17	46 ± 15	36 ± 21

Appendix 4: Soil properties used in SWAT-MAROC

		Vegetation Type						
		Mountainous vegetation		Brush steppe		Hamada steppe		
Parameter	**Unit**	**Dense**	**Degraded**	**Dense**	**Degraded**	**Dense**	**Degraded**	**Source**
Dominant plant type	-	Perennial thorny cushion shrubs *(Bupleurum spinosum*)		Perennial dwarf shrubs *(Artemisia herba-alba)*		dwarf shrubs and annual grasses		Baumann, personal communication, 2009
Maximum leaf area index	m^2/m^2	0.8	0.4	0.3	0.1	0.1	0.05	see Table 5-8 (page 107)
Minimum leaf area index	m^2/m^2	0.6	0.3	0.225	0.75	0	0	
Plant height	m	0.5		0.3		0.3		Estimated, not accounting for dispersed trees
Optimal growing temperature	°C	22		27		27		(White et al. 2008)
Minimum growing temperature	°C	5		5		5		(White et al. 2008)
Maximum stomata conductance	m/s	0.004		0.002		0.005		(White et al. 2008)
Rooting depth	m	generally higher than soil depth						e.g. (Haase et al. 1996)

Appendix 5: Vegetation parameters used in SWAT-MAROC

Oasis		Toundout	M'Semrir	Boulmalene	Kelaat	Skoura	Ouarzazate
Size (km²)		26.4	12.0	25.5	26.7	17.3	52.2
Cultivated Area (km²)		36.1	16.1	41.7	43.7	29.5	62.0
Cultivated Area (km²)	Wheat	9.7	5.3	17.1	18.1	3.2	20.2
	Barley	8.8	1.0	0.8	0.8	0.8	13.5
	Maize	5.0	0.5	11.4	12.0	2.4	9.5
	Pulses	1.2	0.0	0.2	0.5	2.0	0.0
	Alfalfa	4.5	1.5	5.9	5.8	4.0	9.5
	Vegetables	2.6	3.3	1.4	1.3	4.2	1.0
Orchards (Trees/km²)	Date palms	2000	0	0	0	130000	150000
		0.1	0.0	0.0	0.0	4.3	5.0
	Fruits	150000	183420	150000	160000	210000	0
		3.8	4.6	3.8	4.0	5.2	0.0
	Olives	20000	0	50000	55000	140000	130000
		0.5	0.0	1.2	1.4	3.5	3.3

Appendix 6: Cultivated Area in the different oases (MTP 1998). The exceedance of the oases size by the cultivated area is due to the double use of fields by growing Maize as a spring grain and by intercropping practices.

Soil type	Soil map	EHRU
Soil 111	1146	3203
Soil 112	213	0
Soil 121	921	902
Soil 122	187	0
Soil 131	425	192
Soil 132	123	0
Soil 141	603	1037
Soil 142	267	198
Soil 211	952	1773
Soil 212	287	0
Soil 221	941	1119
Soil 222	274	26
Soil 231	494	328
Soil 232	178	33
Soil 241	496	166
Soil 242	256	67
Soil 311	584	122
Soil 312	159	0
Soil 321	933	924
Soil 322	242	0
Soil 331	650	511
Soil 332	177	26
Soil 341	568	745
Soil 342	216	38
Soil 411	510	276
Soil 412	138	0
Soil 421	873	962
Soil 422	321	34
Soil 431	685	540
Soil 432	220	100
Soil 441	632	633
Soil 442	297	871

Appendix 7: Spatial extent (km²) of different soil types in the soil map and in the EHRUs after the model discretization. See Appendix 4 for details on the soil types.

	Maximum Temperature		Minimum Temperature		Precipitation									
lin.	Average (°C)	Standard Deviation (°C)	Average (°C)	Standard Deviation (°C)	Average (mm)	Standard Deviation (mm)	Skewness	Probability of a wet day following a dry day	Probability of a wet day following a wet day	Precipitation days	Maximum rainfall intensity (mm/30 min)	Solar Radiation (MJ/m²/day)	Dew Point (°C)	Average Wind Speed (m/s)
JAN	-6.39*x +0.61	-4.24*x +0.69	-0.51*x +0.16	-0.55*x +0.15	18.64*x +1.88	0.88*x +0.14	1.84*x +1.21	0.02*x +0.01	0.01*x +0.01	4.82*x +1.4	1.29*x +0.27	0.84*x +0.27	-3.08*x +0.50	-6.39*x +0.61
	0.92	0.79	0.50	0.58	0.91	0.80	0.19	0.49	0.13	0.54	0.70	0.49	0.79	0.92
FEB	-6.97*x +0.54	-4.90*x +0.70	-0.27*x +0.16	-0.29*x +0.12	21.26*x +1.82	1.47*x +0.23	0.06*x +1.03	0.04*x +0.01	0.01*x +0.01	4.38*x +1.27	1.56*x +0.67	0.32*x +0.15	-3.03*x +0.41	-6.97*x +0.54
	0.94	0.83	0.23	0.38	0.93	0.81	<0.01	0.88	0.11	0.54	0.35	0.30	0.85	0.94
MAR	-7.91*x +0.21	-5.67*x +0.66	-0.10*x +0.13	-0.02*x +0.13	26.2*x +2.61	2.59*x +0.41	0.54*x +0.59	0.03*x +0.01	0.01*x +0.01	4.54*x +1.22	-0.01*x +0.74	-0.22*x +0.04	-2.56*x +0.47	-7.91*x +0.21
	0.99	0.88	0.06	<0.01	0.91	0.80	0.08	0.64	0.20	0.58	<0.01	0.80	0.75	0.99
APR	-8.51*x +0.10	-6.3*x +0.69	0.09*x +0.09	0.18*x +0.14	17.17*x +1.58	0.18*x +0.36	-1.97*x +0.81	0.06*x +0.01	0.01*x +0.01	4.57*x +1.25	-0.72*x +0.58	-0.66*x +0.17	-2.62*x +0.43	-8.51*x +0.10
	>0.99	0.89	0.10	0.14	0.92	0.03	0.38	0.70	0.06	0.57	0.14	0.59	0.79	>0.99
MAY	-8.82*x +0.20	-6.68*x +0.81	-0.15*x +0.10	-0.17*x +0.12	22.17*x +1.91	1.29*x +0.21	1.28*x +1.13	0.12*x +0.02	-0.01*x +0.01	5.28*x +1.30	0.74*x +0.52	-0.88*x +0.23	-2.42*x +0.35	-8.82*x +0.20
	0.99	0.87	0.16	0.16	0.93	0.78	0.11	0.73	0.13	0.62	0.16	0.60	0.83	0.99
JUN	-8.94*x +0.39	-6.71*x +1.00	-0.44*x +0.10	-0.47*x +0.12	18.2*x +1.25	0.44*x +0.11	-1.52*x +0.62	0.05*x +0.01	0.01*x +0.01	4.69*x +1.13	0.76*x +0.62	-0.72*x +0.21	-2.42*x +0.32	-8.94*x +0.39
	0.98	0.82	0.64	0.61	0.95	0.63	0.38	0.88	0.09	0.63	0.13	0.55	0.85	0.98
JUL	-9.20*x +0.48	-7.02*x +1.13	-0.55*x +0.13	-0.62*x +0.13	17.78*x +1.45	0.27*x +0.05	-2.61*x +0.66	0.06*x +0.02	0.01*x +0.01	4.75*x +1.10	1.65*x +0.79	-0.40*x +0.13	-2.3*x +0.31	-9.20*x +0.48
	0.97	0.79	0.65	0.71	0.94	0.72	0.61	0.58	0.12	0.65	0.30	0.46	0.85	0.97
AUG	-9.05*x +0.43	-6.82*x +1.07	-0.51*x +0.12	-0.55*x +0.10	20.83*x +1.49	0.67*x +0.08	-0.83*x +0.66	0.05*x +0.01	0.01*x +0.01	4.59*x +1.05	0.73*x +0.84	-0.52*x +0.08	-2.48*x +0.27	-9.05*x +0.43
	0.98	0.80	0.65	0.75	0.95	0.88	0.14	0.69	0.20	0.66	0.07	0.81	0.89	0.98
SEP	-8.63*x +0.27	-6.52*x +0.90	-0.39*x +0.08	-0.47*x +0.08	17.33*x +1.15	0.4*x +0.09	-2.11*x +0.57	0.06*x +0.01	0.004*x +0.01	4.34*x +0.94	0.11*x +0.9	-0.12*x +0.08	-2.79*x +0.22	-8.63*x +0.27
	0.99	0.84	0.70	0.79	0.96	0.66	0.58	0.88	0.03	0.68	<0.01	0.18	0.94	0.99
OCT	-8.27*x +0.13	-6.23*x +0.75	-0.29*x +0.10	-0.38*x +0.09	18.64*x +2.00	0.03*x +0.25	-1.46*x +0.51	0.07*x +0.01	0.01*x +0.01	4.39*x +0.95	-0.28*x +0.49	0*x +0.19	-3.11*x +0.21	-8.27*x +0.13
	>0.99	0.87	0.47	0.63	0.90	<0.01	0.45	0.84	0.11	0.68	0.03	<0.01	0.96	<0.99
NOV	-7.20*x +0.37	-5.27*x +0.68	-0.21*x +0.10	-0.21*x +0.08	21.37*x +1.60	0.78*x +0.22	0.04*x +0.34	0.06*x +0.01	0.03*x +0.01	5.63*x +1.05	0.28*x +0.32	0.64*x +0.27	-3.6*x +0.26	-7.2*x +0.37
	0.97	0.86	0.33	0.43	0.95	0.55	<0.01	0.84	0.25	0.74	0.07	0.36	0.95	0.97
DEC	-6.36*x +0.57	-4.45*x +0.69	-0.61*x +0.16	-0.56*x +0.13	18.88*x +1.59	0.30*x +0.23	0.33*x +0.73	0.02*x +0.01	0.03*x +0.01	5.66*x +1.22	-0.2*x +0.45	0.85*x +0.32	-3.79*x +0.34	-6.36*x +0.57
	0.93	0.81	0.60	0.66	0.93	0.15	0.02	0.50	0.35	0.68	0.02	0.41	0.92	0.93

Appendix 8: Altitudinal dependence of measured climate data; given is the linear relationship and the associated r^2; x is elevation (km above sea level)

$$1972: \quad V_r = 0.016562283049902 * x^3 - 53.3708055693780 * x^2 + 57332.011430458 * x - 20530523.8155266$$

$$1982: \quad V_r = 0.014001970528829 * x^3 - 44.9838882092434 * x^2 + 48173.9355278963 * x - 17197062.7297383$$

$$1988: \quad V_r = 0.012480462015234 * x^3 - 40.0055525588767 * x^2 + 42744.4675789356 * x - 15223320.8054422$$

$$1994: \quad V_r = 0.018872501198838 * x^3 - 60.9312747555396 * x^2 + 65576.111564162 * x - 23525852.5606701$$

$$1998: \quad V_r = 0.032412884845751 * x^3 - 105.374087324454 * x^2 + 114196.397332581 * x - 41254663.4931467$$

with

V_r = Reservoir volume [m^3]

x = Reservoir stage level volume [m. asl] with $1072 < x < 1104$

Appendix 9: Polynomial approximation of reservoir volume dependent on reservoir stage level

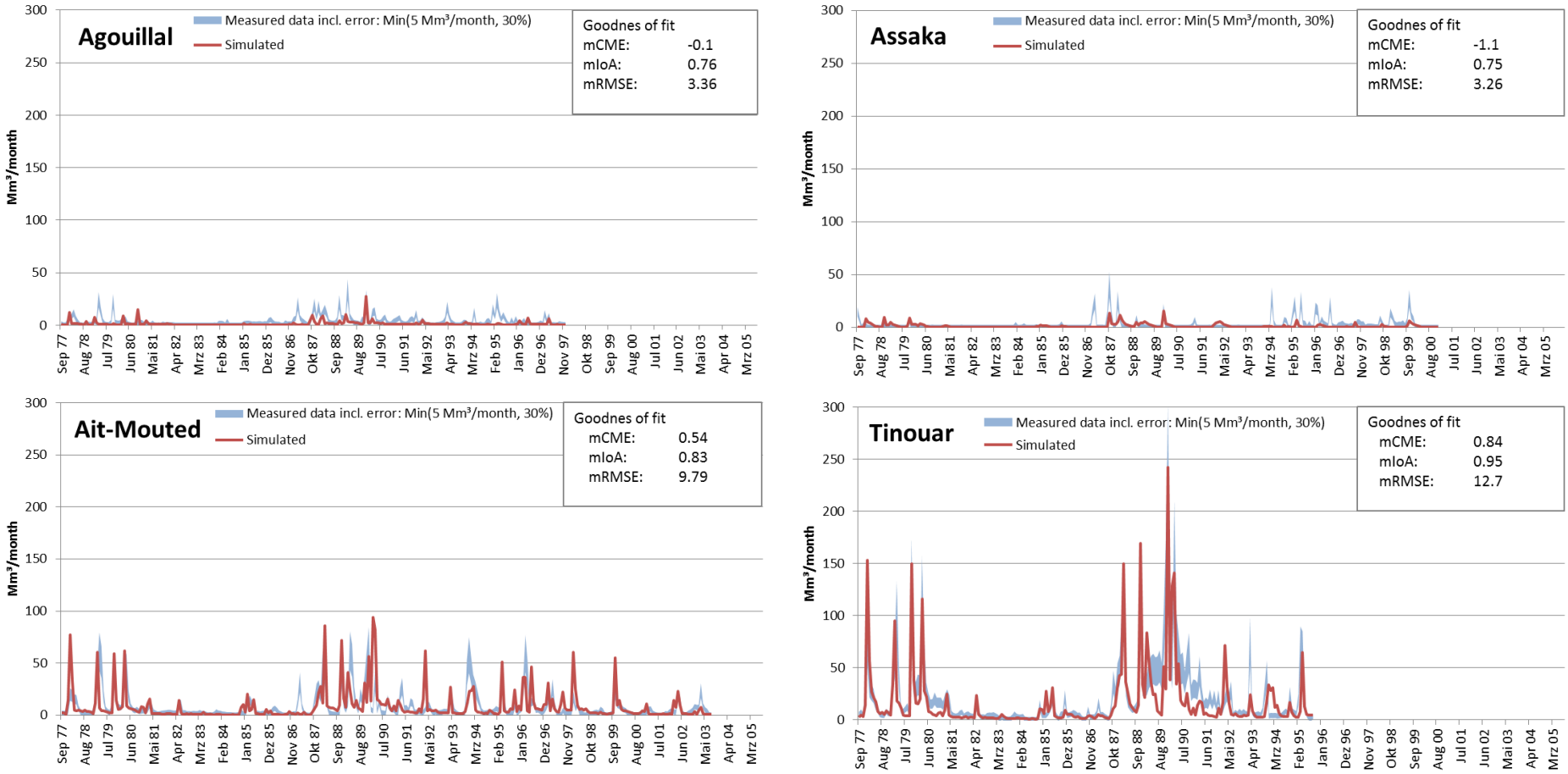

Appendix 10: Modeled discharge compared to measured discharge for the stream gauges Agouillal, Assaka, Ait-Mouted and Tinouar (bars represent measurement uncertainty). See Figure 3-13 for gauge locations. (Measured data: SE Ouarzazate)

Simulation	CN2 (absolute change)	GW_REVAP [%]	RCHRG_DP [%]	SOL_Z [%] (relative change)	ESCO [-]	IRR_FRAC[%]	IRR_EFF [%]	Nash-Sutcliffe Model Efficiency	Discharge to reservoir [Mm³]
Measured									**356**
Calibrated model	**0**	**0.5%**	**50%**	**0%**	**0.78**	**0.50**	**0.75**	**0.89**	**345**
1	0.5	0.5%	39%	-9%	0.79	0.61	0.75	0.86	366
2	-1.5	0.6%	71%	-7%	0.84	0.69	0.80	0.87	339
3	-1.3	0.7%	26%	-15%	0.71	0.46	0.78	0.86	334
4	-1.7	0.5%	51%	15%	0.78	0.29	0.73	0.85	307
5	1.5	0.7%	44%	-19%	0.80	0.41	0.72	0.82	416
6	-0.1	0.4%	41%	1%	0.73	0.44	0.71	0.88	336
7	0.9	0.3%	59%	7%	0.80	0.56	0.71	0.88	359
8	-1.9	0.4%	61%	11%	0.82	0.64	0.73	0.86	294
9	1.3	0.4%	66%	19%	0.81	0.71	0.78	0.88	343
10	0.1	0.6%	74%	3%	0.76	0.66	0.72	0.88	317
11	-0.9	0.6%	46%	17%	0.76	0.74	0.79	0.86	272
12	-0.3	0.6%	29%	-13%	0.74	0.36	0.75	0.86	365
13	0.3	0.4%	49%	-1%	0.73	0.31	0.76	0.87	371
14	1.7	0.7%	64%	-3%	0.78	0.51	0.74	0.86	374
15	-0.7	0.5%	56%	-17%	0.75	0.59	0.79	0.86	358
16	1.1	0.3%	34%	5%	0.72	0.54	0.76	0.87	359
17	-0.5	0.5%	69%	9%	0.77	0.49	0.70	0.87	310
18	0.7	0.4%	36%	-11%	0.85	0.39	0.74	0.84	419
19	-1.1	0.5%	54%	13%	0.83	0.26	0.77	0.87	341
20	1.9	0.6%	31%	-5%	0.83	0.34	0.77	0.83	424
							Max	0.89	424
							Mean	0.86	350
							Min	0.82	272

Appendix 11: Behavioral set of 20 models considered within the uncertainty analysis, including the associated parameter values, model efficiency and average annual discharge to the reservoir Mansour-Eddahbi.

Region	Fraction of watershed (%)	**Precipitation**	- Rain	- Snow	**ET**	- from snow	- from GW	- from soil/plants	**Local runoff**	- Qsurf	- Qlat	direct recharge	indirect recharge	**Baseflow**	- Aquifer 1	- Aquifer 2	**Discharge**
Basin	40%	142	141	<1	130	<1	5	125	16	16	<1	1	9	5	4	<1	12
High Atlas	54%	267	219	48	225	6	5	213	38	35	3	15	11	21	13	8	48
Anti-Atlas	6%	210	206	4	178	1	6	172	28	18	10	11	6	10	10	<1	32
Aquifer																	
karstic	28%	299	229	69	241	9	5	227	52	47	5	19	13	26	11	15	65
porous	23%	158	155	2	147	<1	4	142	14	13	1	1	7	4	4	<1	11
fractured	50%	189	176	13	167	2	5	159	22	20	2	7	9	11	11	<1	24
Elevation Zone																	
1000-1500	35%	138	137	<1	127	<1	5	122	15	15	<1	<1	9	5	4	<1	11
1500-2000	39%	205	198	7	179	1	5	173	23	20	3	9	9	13	9	4	27
2000-2500	17%	298	245	53	255	8	6	241	33	29	5	23	11	28	18	10	50
2500-3000	8%	365	222	143	280	17	5	258	88	84	4	19	10	24	11	12	102
>3000	1%	463	184	279	294	22	5	268	181	181	1	14	14	23	13	10	191
Subcatchment																	
Reservoir direct	24%	155	154	1	140	<1	5	135	17	17	<1	3	9	7	7	<1	15
Assaka	9%	179	175	3	158	1	5	152	21	21	<1	6	8	9	9	<1	22
Tamdroust	12%	249	210	39	216	5	6	204	27	27	1	18	12	23	20	4	39
Amane-n-Tini	6%	243	212	31	197	4	6	187	37	37	<1	18	14	26	12	13	49
Amane-n-Tini (total)	23%	245	212	33	212	5	5	202	28	28	1	15	11	21	14	7	37
Agouillal	5%	239	217	22	221	4	3	214	20	20	1	5	8	9	3	6	21
Tinouar	25%	180	172	8	162	1	5	156	20	17	3	4	8	7	7	<1	19
Tinouar (total)	44%	155	154	1	140	<1	5	135	17	17	<1	3	9	7	7	<1	15
Ifre	8%	299	216	83	239	10	5	224	58	55	4	16	13	24	10	14	69
Ait-Mouted	10%	316	228	88	247	11	5	231	62	51	11	21	10	26	11	15	78

Appendix 12: Absolute mean annual water balance of Sub-regions in Baseline Scenario. Values are given in mm.

Region	Fraction of watershed (%)	**Precipitation**	- Rain	- Snow	**ET**	- from snow	- from GW	- from soil/plants	**Local runoff**	- Qsurf	- Qlat	direct recharge	indirect recharge	**Baseflow**	- Aquifer 1	- Aquifer 2	**Discharge**
Basin	40%	26%	30%	1%	28%	<1%	37%	28%	22%	24%	6%	3%	36%	14%	19%	3%	15%
High Atlas	54%	68%	63%	98%	66%	99%	55%	66%	72%	72%	69%	90%	60%	82%	74%	97%	79%
Anti-Atlas	6%	6%	7%	1%	6%	1%	8%	6%	6%	4%	25%	7%	4%	5%	7%	<1%	6%
Aquifer																	
karstic	28%	39%	34%	75%	37%	72%	28%	36%	51%	50%	55%	58%	38%	54%	33%	100%	56%
porous	23%	17%	19%	2%	18%	2%	18%	19%	11%	11%	10%	2%	16%	6%	9%	<1%	8%
fractured	50%	44%	47%	24%	45%	26%	53%	45%	38%	38%	34%	40%	45%	39%	58%	<1%	36%
Elevation Zone																	
1000-1500	35%	23%	26%	<1%	24%	<1%	33%	24%	19%	20%	6%	1%	34%	12%	17%	3%	11%
1500-2000	39%	38%	42%	11%	38%	11%	39%	39%	31%	30%	45%	39%	36%	37%	39%	32%	32%
2000-2500	17%	24%	22%	35%	23%	42%	19%	23%	20%	18%	33%	42%	20%	35%	33%	40%	26%
2500-3000	8%	14%	10%	46%	13%	42%	9%	12%	26%	27%	15%	17%	9%	15%	10%	24%	26%
>3000	1%	2%	1%	9%	1%	5%	1%	1%	5%	6%	<1%	1%	1%	1%	1%	2%	5%
Subcatchment																	
Reservoir direct	24%	18%	20%	1%	18%	2%	24%	19%	14%	15%	5%	7%	22%	12%	17%	<1%	11%
Assaka	9%	8%	9%	1%	8%	1%	10%	8%	7%	7%	1%	6%	8%	6%	9%	<1%	6%
Tamdroust	12%	14%	13%	18%	14%	18%	14%	14%	11%	12%	3%	22%	14%	20%	25%	10%	14%
Amane-n-Tini	6%	7%	7%	7%	7%	7%	7%	7%	8%	9%	1%	12%	9%	12%	8%	19%	9%
Amane-n-Tini (total)	23%	27%	26%	30%	27%	31%	25%	27%	23%	25%	5%	38%	28%	35%	35%	36%	27%
Agouillal	5%	6%	6%	5%	6%	6%	4%	7%	4%	4%	1%	3%	5%	4%	2%	7%	3%
Tinouar	25%	21%	23%	8%	22%	9%	24%	22%	17%	16%	31%	12%	20%	13%	18%	1%	15%
Tinouar (total)	44%	48%	45%	68%	47%	66%	42%	46%	56%	53%	89%	49%	42%	47%	39%	64%	56%
Ifre	8%	12%	10%	27%	11%	23%	8%	11%	17%	17%	13%	14%	12%	15%	9%	27%	18%
Ait-Mouted	10%	15%	12%	34%	14%	34%	9%	13%	22%	19%	45%	23%	11%	19%	12%	35%	24%

Appendix 13: Relative mean annual water balance of Sub-regions (Baseline Scenario): Fraction of total process volume that occurs in the specific Sub-region.

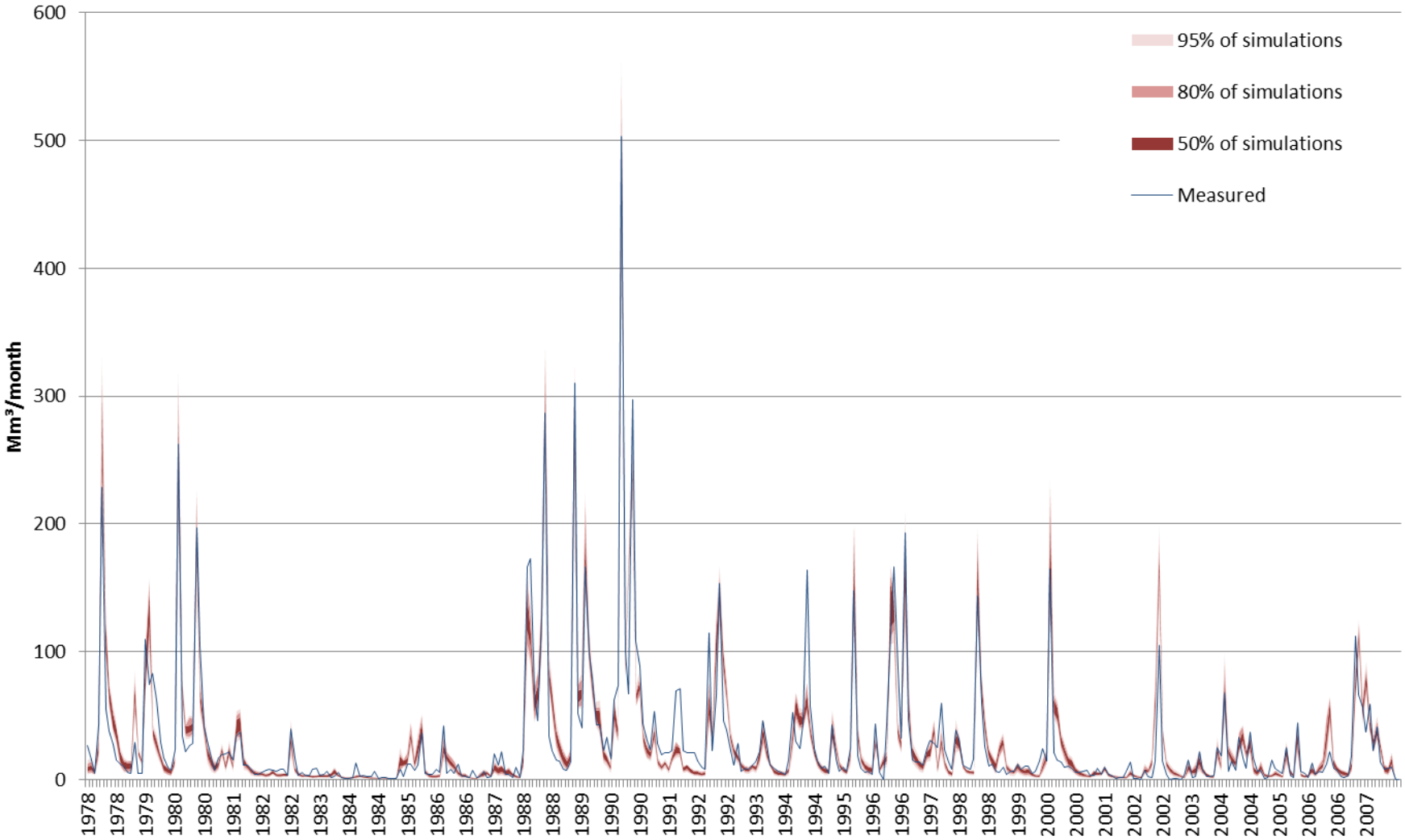

Appendix 14: Monthly discharge including parameter uncertainty at the reservoir Mansour-Eddahbi (1978-2007) (14,988 km²)

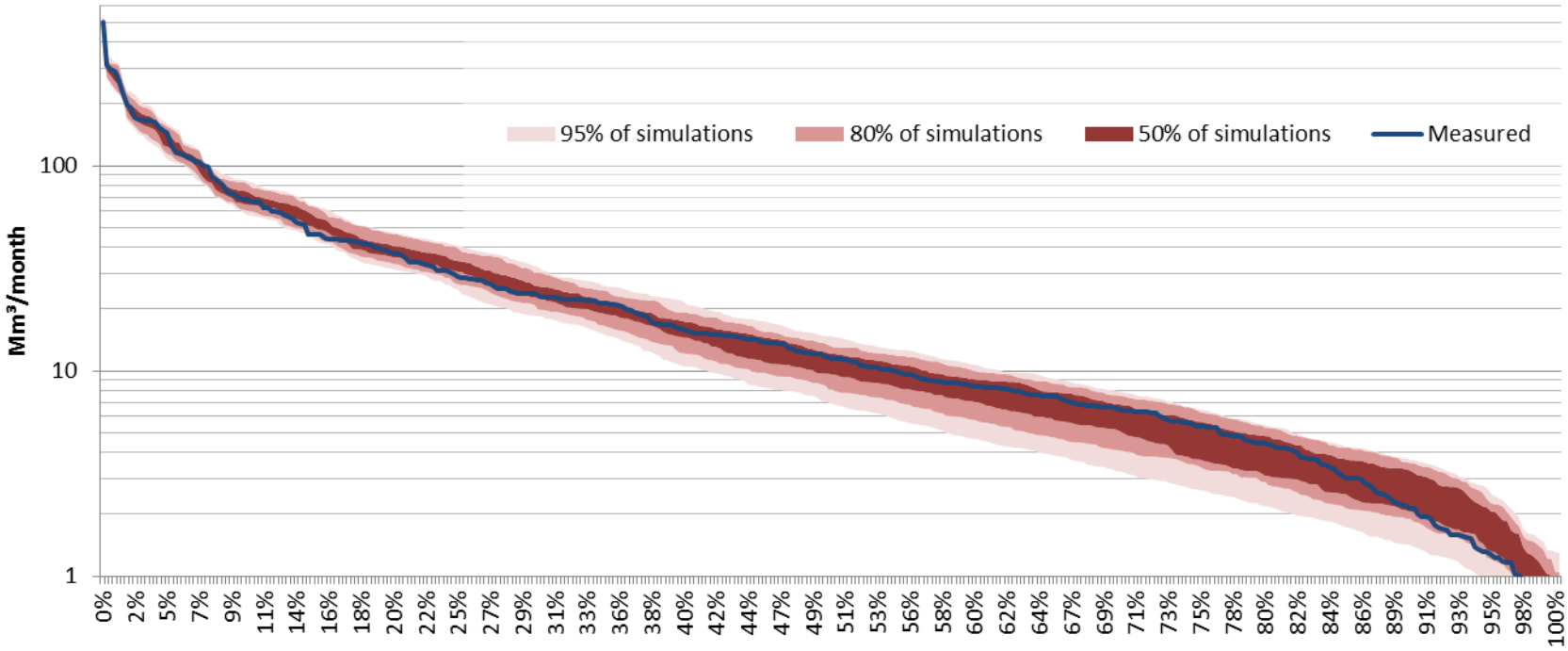

Appendix 15: Monthly flow duration curve including parameter uncertainty at the reservoir Mansour-Eddahbi (1978-2007) (14,988 km²)

Region	Fraction of watershed (%)	**Precipitation**	- Rain	- Snow	**ET**	- from snow	- from GW	- from soil/plants	**Local runoff**	- Qsurf	- Qlat	direct recharge	indirect recharge	**Baseflow**	- Aquifer 1	- Aquifer 2	**Discharge**
Basin	40%	118	118	<1	109	<1	4	105	13	12	<1	1	7	3	3	<1	9
High Atlas	54%	242	210	32	208	4	5	199	31	28	3	12	8	15	9	6	38
Anti-Atlas	6%	182	180	2	157	<1	5	152	23	15	8	8	5	7	7	<1	25
Aquifer																	
karstic	28%	273	226	47	226	6	5	215	43	38	5	14	10	19	8	12	52
porous	23%	132	132	<1	125	<1	3	121	10	9	1	<1	5	2	2	<1	7
fractured	50%	165	157	8	148	1	5	142	18	16	1	6	7	8	8	<1	19
Elevation Zone																	
1000-1500	35%	114	113	<1	106	<1	4	102	12	11	<1	<1	7	3	3	<1	8
1500-2000	39%	180	177	3	159	<1	4	155	19	16	2	6	7	9	6	3	20
2000-2500	17%	275	243	32	238	5	5	228	28	23	5	18	8	21	13	8	41
2500-3000	8%	340	233	107	273	14	5	254	70	66	5	16	8	19	9	10	81
>3000	1%	436	191	245	298	20	4	274	153	152	1	9	13	18	10	7	157
Subcatchment																	
Reservoir direct	24%	131	130	1	120	<1	4	116	13	12	<1	2	7	4	4	<1	11
Assaka	9%	151	150	2	135	<1	5	131	17	17	<1	4	6	5	5	<1	16
Tamdroust	12%	231	205	25	203	3	6	194	23	22	1	14	9	18	15	3	31
Amane-n-Tini	6%	220	201	18	181	2	5	174	32	32	<1	14	11	19	9	10	40
Amane-n-Tini (total)	23%	225	204	21	197	3	5	189	24	23	1	12	9	16	10	5	30
Agouillal	5%	220	205	15	203	2	3	198	18	17	1	4	7	7	2	5	18
Tinouar	25%	154	150	4	140	1	4	135	16	13	3	3	6	5	4	<1	14
Tinouar (total)	44%	208	180	28	178	4	4	170	30	25	5	8	7	10	6	5	33
Ifre	8%	270	209	61	224	7	4	212	47	44	3	10	11	16	6	10	53
Ait-Mouted	10%	291	231	60	234	8	4	222	51	40	11	18	7	20	8	12	64

Appendix 16: Absolute mean annual water balance of Sub-regions in the representative 2030s Scenario. Values are given in mm.

Region	Fraction of watershed (%)	**Precipitation**	- Rain	- Snow	**ET**	- from snow	- from GW	- from soil/plants	**Local runoff**	- Qsurf	- Qlat	direct recharge	indirect recharge	**Baseflow**	- Aquifer 1	- Aquifer 2	**Discharge**
Basin	40%	25%	27%	<1%	26%	<1%	36%	26%	22%	23%	6%	3%	36%	13%	18%	3%	14%
High Atlas	54%	69%	66%	99%	68%	99%	56%	68%	72%	72%	71%	90%	60%	83%	75%	97%	80%
Anti-Atlas	6%	6%	7%	1%	6%	1%	7%	6%	6%	4%	23%	7%	4%	5%	7%	<1%	6%
Aquifer																	
karstic	28%	41%	37%	77%	38%	75%	29%	38%	52%	52%	58%	58%	39%	56%	33%	100%	58%
porous	23%	16%	18%	1%	17%	<1%	17%	17%	10%	10%	9%	1%	16%	5%	8%	<1%	7%
fractured	50%	43%	45%	23%	44%	25%	54%	44%	38%	38%	32%	41%	46%	39%	59%	<1%	36%
Elevation Zone																	
1000-1500	35%	21%	23%	<1%	22%	<1%	32%	23%	18%	19%	5%	1%	34%	11%	16%	3%	11%
1500-2000	39%	37%	41%	6%	38%	6%	38%	38%	31%	30%	42%	36%	36%	35%	37%	31%	31%
2000-2500	17%	25%	24%	31%	24%	37%	20%	24%	20%	19%	36%	44%	19%	36%	35%	39%	27%
2500-3000	8%	15%	11%	51%	14%	50%	9%	13%	25%	26%	17%	19%	9%	16%	11%	25%	26%
>3000	1%	2%	1%	11%	1%	7%	1%	1%	5%	6%	<1%	1%	1%	1%	1%	2%	5%
Subcatchment																	
Reservoir direct	24%	17%	18%	1%	18%	1%	23%	18%	13%	14%	4%	7%	21%	11%	16%	<1%	10%
Assaka	9%	8%	8%	1%	8%	1%	10%	8%	7%	7%	1%	5%	8%	5%	8%	<1%	6%
Tamdroust	12%	14%	14%	17%	14%	17%	15%	14%	11%	12%	3%	24%	15%	21%	27%	10%	14%
Amane-n-Tini	6%	7%	7%	7%	7%	6%	7%	7%	8%	9%	1%	12%	10%	12%	9%	19%	10%
Amane-n-Tini (total)	23%	28%	28%	28%	28%	29%	26%	28%	24%	26%	5%	39%	29%	37%	38%	37%	28%
Agouillal	5%	6%	6%	5%	7%	5%	4%	7%	4%	4%	1%	3%	5%	4%	2%	8%	4%
Tinouar	25%	21%	22%	6%	21%	7%	24%	22%	17%	16%	28%	10%	20%	12%	17%	1%	14%
Tinouar (total)	44%	48%	46%	70%	47%	69%	42%	47%	56%	52%	90%	49%	42%	47%	38%	63%	56%
Ifre	8%	12%	10%	29%	11%	26%	8%	11%	17%	17%	12%	12%	12%	14%	8%	25%	17%
Ait-Mouted	10%	16%	14%	35%	14%	36%	9%	14%	22%	19%	49%	26%	10%	21%	13%	37%	25%

Appendix 17: Relative mean annual water balance of Sub-regions (representative 2030s scenario): Fraction of total process volume that occurs in the specific Sub-region.

Appendix B

The attached CD contains:

Model files: contains the model files

TxtInOut_Cal: contains the model files of the calibrated model, execute _run.bat to run the model including the irrigation procedure. Consider: the model executable is called swat2005.exe, but it is the modified version SWAT_MAROC!

Model_DB: Microsoft ACCESS database that contains all the model-files to build the model. It can be run using the SWAT-Editor

Programs: contains adapted or new model routines and programs used in this study

Irrigation_postprocessing: Programs required for the loosely coupled Irrigation postprocessing

- irri: Irrigation postprocessing, subtracts pre-calculated irrigation amounts from specified reach segments in output.rch
- irr_changepar: Changes the irrigation-related parameters (IRR_EFF and IRR_FRAC) within the sensitivity-, autocalibration- and uncertainty analysis of SUFI2

SUFI_bat: Adapted batch files of the SUFI2 sensitivity-, autocalibration- and uncertainty analysis

SWAT: Original and modified SWAT source code and executable

- SWAT-MAROC_source: The source code of the model used in this study
- swat-maroc.exe: The executable SWAT-MAROC, build using the Fortran-files contained in SWAT-MAROC_source
- SWAT2005_source: The original source code from SWAT Version 2005 Available at: http://swatmodel.tamu.edu/software/swat-model/ (accessed: 12.07.2012)
- swat2005.exe: The executable SWAT2005, build using the Fortran-files contained in SWAT2005_source

Input data (climate data), calibration and validation data (discharge) from Moroccan Partner Institutions are not published in the Appendix, since the author does not have the rights to do so.

All other data that has been used can be assessed at the IMPETUS-Geonetwork: http://geonetwork.impetus.uni-koeln.de/srv/en/main.home (Accessed: 13.07.2012)